NASA Technical Memorandum 4087

Toward Improved Durability in Advanced Aircraft Engine Hot Sections

APRIL 1989

NASA

DISCLAIMER NOTICE

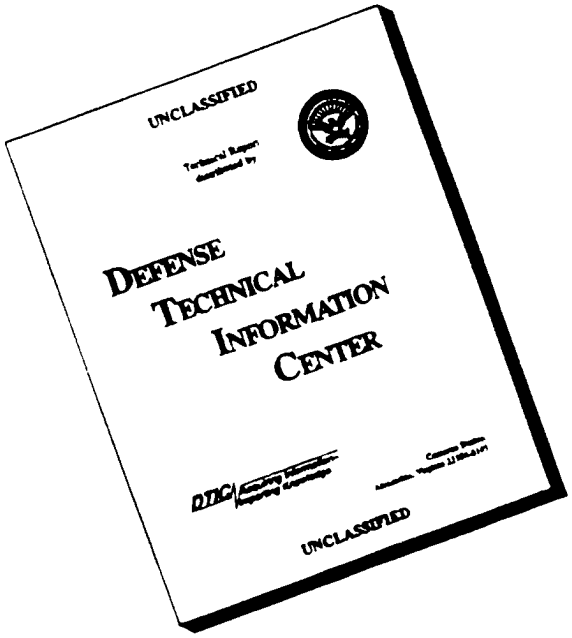

THIS DOCUMENT IS BEST QUALITY AVAILABLE. THE COPY FURNISHED TO DTIC CONTAINED A SIGNIFICANT NUMBER OF PAGES WHICH DO NOT REPRODUCE LEGIBLY.

NASA Technical Memorandum 4087

Toward Improved Durability in Advanced Aircraft Engine Hot Sections

D. E. Sokolowski, *Editor*
Lewis Research Center
Cleveland, Ohio

National Aeronautics and
Space Administration
Office of Management
Scientific and Technical
Information Division

1989

CONTENTS

NASA HOST PROJECT OVERVIEW

D. E. Sokolowski
National Aeronautics and Space Administration
Lewis Research Center
Cleveland, Ohio

INTRODUCTION

Since introduction of the gas turbine engine to aircraft propulsion, the quest for greater performance has resulted in a continuing upward trend in overall pressure ratio for the engine core. Associated with this trend are increasing temperatures of gases flowing from the compressor and combustor and through the turbine. For commercial aircraft engines in the foreseeable future, compressor discharge temperature will exceed 922 K (1200 °F), while turbine inlet temperature will be approximately 1755 K (2700 °F). Military aircraft engines will significantly exceed these values.

Increasing fuel prices, especially since 1973, have created the demand for energy conservation and more fuel efficient aircraft engines. In response to this demand, engine manufacturers continually increased the performance of the current generation of gas turbine engines. Soon afterward, the airline industry began to experience a notable decrease in durability or useful life of critical parts in the engine core hot section -- the combustor and turbine. This was due primarily to cracking in the combustor liners, turbine vanes, and turbine blades. In addition, spalling of thermal barrier coatings that protect some combustor liners was evident.

For the airlines reduced durability for in-service engines was measured by a dramatic increase in maintenance costs, primarily for high bypass ratio engines. Higher maintenance costs were especially evident in the hot section. As shown by Dennis and Cruse (1979), hot section maintenance costs account for almost 60 percent of the engine total. Widespread concern about such soaring maintenance costs led to a new demand -- to improve hot section durability.

Durability can be improved in hot section components by using any combination of the following four approaches. They are the use of (1) materials having higher use temperatures, (2) more effective cooling techniques to reduce material temperatures, (3) advanced structural design concepts to reduce stresses, and (4) more accurate analytical models and computer codes in the design analysis process to identify hot spots, high stresses, etc.

High temperature metallic materials currently include nickel- and cobalt-based superalloys. Certain elements of these alloys, such as cobalt, are in short supply and are expensive. Ways for reducing these alloying elements were presented by Stephans (1982). In addition, advanced high temperature superalloy components also include directionally solidified, single crystal, and oxide-dispersion-strengthened materials. Development time for new materials is lengthy, fabrication is sometimes difficult, and again costs are high. Thus, successful use of these materials requires a balance among design requirements, fabrication possibilities, and total costs.

Current cooling techniques tend to be sophisticated; fabrication is moderately difficult. In higher performance engines, cooling capability may be improved by increasing the amount of coolant. There is a penalty for doing this, however, in the reduction of thermodynamic cycle performance of the engine system. In addition, the coolant temperature of such advanced engines is higher than that for current in-service engines. Consequently, more effective cooling techniques are being investigated. They are generally more complex in design, demand new fabrication methods, and may require a multitude of small film-cooling holes, each of which introduces potential life-limiting high stress concentrations. Acceptable use of the advanced cooling techniques requires accurate models for design analysis.

The introduction of advanced structural design concepts usually begins with a preliminary concept that then must be proven, must be developed, and -- most critically -- must be far superior to entrenched standard designs. Acceptance certainly is time consuming, and benefits must be significant. For improved durability in high performance combustors, an excellent example of an advanced structural design concept is the segmented liner as discussed by Tanrikut et al. (1981). The life-limiting problems associated with high hoop stresses were eliminated by dividing the standard full-hoop liners into segments. At the same time, designers realized increased flexibility in the choice of advanced cooling techniques and materials, including ceramic composites.

Finally, the design analysis of hot section component parts, such as combustor liners or turbine vanes and blades, involves the use of analytical or empirical models. Such models often are put into the form of computer codes for predicting and analyzing the aerothermal environment, the thermomechanical loads, and material and structural responses to such loading. When the parts are exposed to cyclic high temperature operation as in a turbine engine, the repetitive straining of the materials leads to crack initiation and propagation until failure or break-away occurs. The useful life or durability of a part is usually defined as the number of mission cycles that can be accumulated before initiation and propagation of significant cracks. Thus, designers need to predict useful "life" so they can design a part to meet requirements.

Efforts to predict the life of a part generally follow the flow of analyses portrayed in Fig. 1. In practice, designing of a part such as a turbine blade to meet a specified life goal may require a number of iterations through the "Life Prediction System" of Fig. 1, varying the blade geometry, material, or cooling effectiveness in each pass, until a satisfactory life goal is predicted.

Analysis models and codes have frequently predicted physical behavior qualitatively but have exhibited unacceptable quantitative accuracy. To improve predictive capability, researchers generally need (1) to understand and model more accurately the basic physics of the phenomena related to durability, (2) to emphasize local as well as global conditions and responses, (3) to accommodate nonlinear and inelastic behavior, and (4) to expand some models from two to three dimensions.

Fortunately, at the time of demands for improved hot section durability dramatic increases were occurring in mathematical solution techniques, electronic computer memory, and computer computational speed. The time was ripe for significant improvements in analytical predictive capability.

OVERVIEW OF THE HOST PROJECT

To meet the needs for improved analytical design and life prediction tools, especially those used for analysis of cyclic high temperature operation in advanced combustors and turbines, the NASA Lewis Research Center sponsored the Turbine Engine Hot Section Technology (HOST) Project. The project was initiated in October 1980 and completed in late 1987.

Objective

The HOST Project developed improved analytical models for the aerothermal environment, the thermomechanical loads, material behavior, structural response, and life prediction, along with sophisticated computer codes, which can be used in design analyses of critical parts in advanced turbine engine combustors and turbines. More accurate analytical tools better ensure -- during the design process -- improved durability of future hot section engine components.

Approach

Addressing the complex durability problem in high temperature cyclically operated turbine engine components requires research efforts in numerous technical disciplines. In the HOST Project six disciplines were involved: instrumentation, combustion, turbine heat transfer, structural analysis, fatigue and fracture, and surface protection. This involvement was not only through focused research but was sometimes interdisciplinary and integrated.

Most disciplines in the HOST Project followed a common approach to research. First, phenomena related to durability were investigated, often using benchmark quality experiments. With known boundary conditions and proper instrumentation, these experiments resulted in a characterization and better understanding of such phenomena as the aerothermal environment, the material and structural behavior during thermomechanical loading, and crack initiation and propagation. Second, state-of-the-art analytical models were identified, evaluated, and then improved by more inclusive physical considerations and/or more advanced computer code development. When no state-of-the-art models existed, researchers developed new models. Finally, predictions using the improved analytical tools were validated by comparison to experimental results, especially the benchmark quality data.

Programs

Fulfillment of the HOST Project objective was accomplished through numerous research and technology programs. HOST management issued contracts for 40 separate activities with private industry, most of which were multiyear and multiphased. In several activities, more than one contractor was involved because of the nature of the research and each contractor's unique qualifications. Thirteen more separate activities were conducted through grants with universities. Finally, at the NASA Lewis Research Center, 17 major efforts were supported by the project. Table I lists all the technical activities conducted in the project.

TECHNOLOGY TRANSFER

The HOST Project research activities were usually organized, conducted, and reported along the above discipline lines. This report is organized accordingly and summarizes research results accomplished in the project.

Numerous publications provide further details about research results from the HOST Project. Six annual workshops were conducted with conference proceedings (Turbine Engine Hot Section Technology, 1982 through 1987) being provided for each one. Each of the proceedings generally covers research results for the preceding year. The last two proceedings also included a bibliography of definitive research reports. Progress in the development of advanced instrumentation and in the improvement of combustor aerothermal and turbine heat transfer models was reported by Sokolowski and Ensign (1986). Finally, a comprehensive bibliography of the HOST Project is being prepared and is scheduled for publication later this year (Sokolowski, 1988).

REFERENCES

Dennis, A.J. and Cruse, T.A., 1979, "Cost Benefits from Improved Hot Section Life Prediction Technology - for Aircraft Engine Combustor and Turbine Parts," AIAA Paper 79-1154.

Sokolowski, D.E. and Ensign, C.R., 1986, "Toward Improved Durability in Advanced Combustors and Turbines -- Progress in the Prediction of Thermomechanical Loads", NASA TM-88932.

Sokolowski, D.E., 1988, "Comprehensive Bibliography of the Turbine Engine Hot Section Technology (HOST) Project," NASA TM-100275, to be published.

Stephans, J.R., 1982, "COSAM Program Overview," COSAM (Conservation of Strategic Aerospace Materials, Program Overview, NASA TM-83006, pp. 1-11.

Tanrikut, S., Marshall, R.L., and Sokolowski, D.E., 1981, "Improved Combustor Durability - Segmented Approach with Advanced Cooling Techniques," AIAA Paper 81-1354.

Turbine Engine Hot Section Technology (HOST) 1982, NASA TM-83022.

Turbine Engine Hot Section Technology (HOST) 1983, NASA CP-2289.

Turbine Engine Hot Section Technology (HOST) 1984, NASA CP-2339.

Turbine Engine Hot Section Technology (HOST) 1985, NASA CP-2405.

Turbine Engine Hot Section Technology (HOST) 1986, NASA CP-2444.

Turbine Engine Hot Section Technology (HOST) 1987, NASA CP-2493.

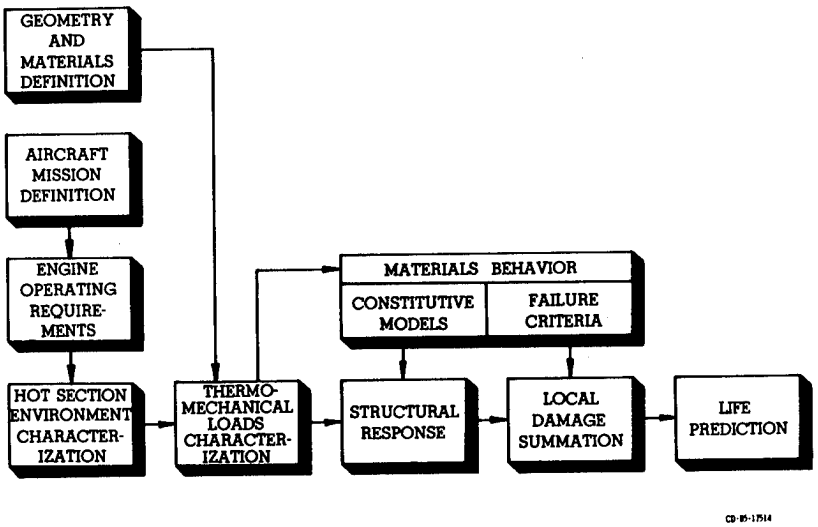

FIGURE 1. - INTEGRATION OF ANALYSES LEADS TO LIFE PREDICTION OF HOT SECTION PARTS.

TABLE I. - HOST Project Activities

	Contract (C), Grant (G), or NASA Organization (N)	Number
Instrumentation		
Hot Section Viewing System	C	NAS3-23156
Dynamic Gas Temperature Measurement System - A	C	NAS3-23154
Dynamic Gas Temperature Measurement System - B	C	NAS3-24228
Turbine Static Strain Gage - A	C	NAS3-23169
Turbine Static Strain Gage - B	C	NAS3-23722
Turbine Heat Flux Sensors	C	NAS3-23529
Laser Speckle Strain Measurement	C	NAS3-26615
High Temperature Strain Gage Materials	G	NAG3-501
Hot Section Sensors	N	2510
Laser Anemometry for Hot Section Applications	N	2520/2530
HOST Instrument Applications	N	2510
Combustion		
Assessment of Combustor Aerothermal Models - I	C	NAS3-23523
Assessment of Combustor Aerothermal Models - II	C	NAS3-23524
Assessment of Combustor Aerothermal Models - III	C	NAS3-23525
Improved Numerical Methods - I	C	NAS3-24351
Improved Numerical Methods - II	C	NAS3-24350
Improved Numerical Methods - III	G	NAG3-596
Flow Interaction Experiment	C	NAS3-24350
Fuel Swirl Characterization - I	C	NAS3-24350
Fuel Swirl Characterization - II	C	NAS3-24352
Mass and Momenta Transfer	C	NAS3-22771
Diffuser/Combustor Interaction	C	F33615-84-C-2427
Dilution Jet Mixing Studies	C	NAS3-22110
Lateral Jet Injection into Typical Combustor Flowfields	G	NAG3-549
Flame Radiation Studies	N	2650
Turbine Heat Transfer		
Mainstream Turbulence Influence on Flow in a Turning Duct - A	C	NAS3-23278
Mainstream Turbulence Influence on Flow in a Turning Duct - B	G	NAG3-617
2-D Heat Transfer without Film Cooling	C	NAS3-22761
2-D Heat Transfer with Leading Edge Film Cooling	C	NAS3-23695
2-D Heat Transfer with Downstream Film Cooling	C	NAS3-24619
Measurement of Blade and Vane Heat Transfer Coefficient in a Turbine Rotor	C	NAS3-23717
Assessment of 3-D Boundary Layer Code	C	NAS3-23716
Coolant Side Heat Transfer with Rotation	C	NAS3-23691
Analytic Flow and Heat Transfer	C	NAS3-24358
Effects of Turbulence on Heat Transfer	G	NAG3-522
Tip Region Heat Transfer	G	NAG3-623
Impingement Cooling	G	NSG3-075
Computation of Turbine Blade Heat Transfer	G	NAG3-579
Advanced Instrumentation Development	N	2640
Warm Turbine Flow Mapping with Laser Anemometry	N	2620
Real Engine-Type Turbine Aerothermal Testing	N	2640
Structural Analysis		
Thermal/Structural Load Transfer Code	C	NAS3-23272
3-D Inelastic Analysis Methods - I	C	NAS3-23697
3-D Inelastic Analysis Methods - II	C	NAS3-23698
Component Specific Modeling	C	NAS3-23687
Liner Cyclic Life Determination	N	5210
Structural Components Response Program	N	5210
High Temperature Structures Research Laboratory	N	5210
Constitutive Model Development	N	5210
Constitutive Modeling for Isotropic Materials - I	C	NAS3-23925
Constitutive Modeling for Isotropic Materials - II	C	NAS3-23927
Theoretical Constitutive Models for Single Crystal Alloys	G	NAG3-511
Biaxial Constitutive Equation Development for Single Crystals and Directionally Solidified Alloys	G	NAG3-512
Fatigue and Fracture		
Creep-Fatigue Life Prediction for Isotropic Materials	C	NAS3-23288
Elevated Temperature Crack Propagation	C	NAS3-23940
Life Prediction and Material Constitutive Behavior for Anisotropic Materials	C	NAS3-23939
Analysis of Fatigue Crack Growth Mechanism	G	NAG3-348
Vitalization of High Temperature Fatigue and Structures Laboratory	N	5220
Surface Protection		
Effects of Surface Chemistry on Hot Corrosion	C	NAS3-23926
Thermal Barrier Coating Life Prediction - I	C	NAS3-23943
Thermal Barrier Coating Life Prediction - II	C	NAS3-23944
Thermal Barrier Coating Life Prediction - III	C	NAS3-23945
Airfoil Deposition Model	G	NAG3-201
Mechanical Behavior of Thermal Barrier Coatings	G	NCC3-27
Coating Oxidation/Diffusion Prediction	N	5160
Deposition Model Verification	N	5160
Dual Cycle Attack	N	5160
Rig/Engine Correlation	N	5160
Burner Rig Modernization	N	5160

Notes: A, B — Activities in series
I, II, III — Activities in parallel

ADVANCED HIGH TEMPERATURE INSTRUMENTATION FOR HOT SECTION RESEARCH APPLICATIONS

D. R. Englund and R. G. Seasholtz
National Aeronautics and Space Administration
Lewis Research Center
Cleveland, Ohio

ABSTRACT

Programs to develop research instrumentation for use in turbine engine hot sections are described. These programs were initiated to provide improved measurements capability as support for a multidisciplinary effort to establish technology leading to improved hot section durability. Specific measurement systems described here include heat flux sensors, a dynamic gas temperature measuring systems, laser anemometry for hot section applications, an optical system for viewing the interior of a combustor during operation, thin film sensors for surface temperature and strain measurements, and high temperature strain measuring systems. The paper will describe the state of development of these sensors and measuring systems and, in some cases, will show examples of measurements made with this instrumentation. The paper covers work done at the NASA Lewis Research Center and at various contract and grant facilities.

INTRODUCTION

The Turbine Engine Hot Section Technology (HOST) Program was started by NASA in the late 1970's in order to develop technology leading to improved hot section durability. The program was a multidisciplinary effort involving structures, surface protection, fatigue, combustion, heat transfer, and instrumentation. The objective of the instrumentation portion of the program was to develop improved measurements capability to measure the environment within the hot section and measure the response of hot section components to that imposed environment. Instrument development programs that resulted included the following:

(1) Development of sensors for measuring the heat flux on combustor liners and turbine airfoils.

(2) Development of a system to measure the fluctuating component of combustor exit temperature with a frequency response to 1000 Hz.

(3) Development of laser anemometer techniques for applications in hot sections.

(4) Development of an optical system for viewing the interior of a combustor during operation.

(5) Development of high temperature strain measuring systems.

In addition to this, a major effort was started just prior to the start of HOST to develop thin film sensors for applications in hot sections, particularly for the measurement of turbine airfoil surface temperature.

This paper will describe the state of development of these sensors and measuring systems and, in some cases, will show examples of measurements made with this new instrumentation. The work described was done at the NASA Lewis Research Center and at various contract and grant facilities.

HEAT FLUX SENSORS

One of the important environmental parameters in the hot section is heat flux. The heat flux is one of the variables in the heat balance equation which establishes the cooling requirements and the anticipated surface temperature of a hot section component. There is not sufficient knowledge of heat transfer coefficients under engine operating condition to permit prediction of surface temperatures to within acceptable accuracy. This is especially true as heat fluxes approach 1 MW/m^2. Initial work was directed at developing sensors for use in combustor liners (Atkinson et al., 1983; Atkinson and Strange, 1982; Atkinson et al., 1985a). In later work sensors were mounted into air cooled blades and vanes (Atkinson et al., 1984; Atkinson et al., 1985b).

Sensor designs followed conventional concepts in which the temperature difference proportional to heat conduction through the sensor body is measured. Differential thermocouples using the sensor body material as part of the circuit were used to measure the temperature differences. Calibrations (Holanda, 1984) were made of the thermoelectric potential of a number of engineering alloys and these established the validity of this approach, which considerably simplified fabrication.

Figures 1 and 2 show the sensors that were developed for combustor liners. The sensor is built into a Hastelloy X disk 0.8 cm in diameter and the same thickness as the liner. After calibration of the sensor

the disk is welded into a hole cut in the liner. Figure 1 shows the embedded thermocouple sensor. The disk is grooved so that 0.25 mm outside diameter sheathed, single conductor thermocouple wire can be laid into the grooves and covered with weld material. The thermocouple wires are ISA Type K, Chromel-Alumel, and single conductor leads are used so as to maintain good insulation resistance between the wire and the external metal sheath. Grounded Alumel junctions are located on the hot and cold side of the sensor body and a Chromel junction is added to the cold side. A voltage measurement between the Alumel leadwires (i.e., using the Alumel-Hastelloy X-Alumel differential thermocouple) provides the hot-to-cold side temperature difference proportional to the one-dimensional heat flow through the sensor body at that point. A measurement using the conventional Chromel-Alumel thermocouple provides the cold side temperature of the sensor.

Figure 2 shows a Gardon Gage sensor. In this case the sensor body has a 1.5 mm diameter cylindrical cavity on the cold side so that a thin membrane of material is left on the hot side. Alumel wires are positioned so the junctions are formed with the Hastelloy X at the center of the membrane and halfway up the sidewall of the cavity. A Chromel wire junction is also made on the sidewall of the cavity. After the thermocouples are installed, the cavity is filled with ceramic cement.

Sensors of the embedded thermocouple and Gardon Gage types have also been built into air cooled blades and vanes. In the case of turbine blades, two-piece blades were used and the sensors were installed from the cooling passage side of the blade. The two blade halves were then joined by brazing. In the case of vanes, sections of the vane wall opposite to the desired sensor sites were removed and the sensors were installed through these "windows." Figure 3 depicts the installation process on a turbine vane.

The heat flux sensors were calibrated over a heat flux range up to 1.7 MW/m^2 and a temperature range to 1250 K. The calibrations were accomplished by imposing a known radiant heat flux on the hot side surface of the sensor and flowing cooling air over the cold side surface. The hot side surface was coated with a high temperature black paint with a measured absorptance and emittance of 0.89 over the test temperature range. In all cases the reference temperature was measured and used to estimate the hot side surface temperature so that energy being radiated away from the hot surface could be calculated and taken into account. Estimates of the convective heat flow from the hot surface were also made and used in the heat balance.

The heat flux sensor calibration systems used banks of tungsten filament lamps enclosed in quartz tubes as heat flux sources; the most powerful of these systems provided heat fluxes up to 1.7 MW/m^2. The quartz lamp rigs were capable of long time and cyclic operation at reduced heat fluxes. Thermal cycling and drift tests were run on these sensors using this capability.

Calibration and performance tests on heat flux sensors have indicated that measurements can be achieved fairly readily on combustor liners, but that accurate measurements on airfoils are difficult to achieve. Combustor liner measurements have been made both at a contractor facility and at NASA Lewis using sensors whose calibration uncertainty is within ± 5 percent of a nominal full scale heat flux of 1 MW/m^2. Figure 4 shows an instrumented combustor liner segment. Figure 5 compares measured values of heat flux conducted through a combustor liner and radiant flux incident on the liner at different combustor pressure levels. The radiant heat flux was measured with a commercial radiometer. The combustor liner in this test was the type with louver lips and bleed holes to provide film cooling of the hot side surface. The data of Fig. 5 indicate that there is significant convective cooling of the hot side surface of the combustor.

Test results from sensors mounted in turbine airfoils indicate that these sensors are sufficiently sensitive to transverse gradients in heat flux and temperature that applications in blades and vanes must be carefully evaluated. The greater complexity of the airfoils (e.g., high surface curvature and cooling passage structure) causes more severe gradients than were encountered in combustor liners. Sensitivity to transverse gradients is especially apparent in the Gardon gage sensor because of its lack of symmetry.

DYNAMIC GAS TEMPERATURE MEASURING SYSTEM

Another important environmental parameter in the hot section of a turbine engine is the gas temperature. In general, most attention has been directed at the time-average value of gas temperature rather than the fluctuating component of gas temperature. It is generally agreed that there may be significant temperature fluctuation in the gas exiting a combustor due to incomplete mixing of the combustion and dilution gas streams. It is also agreed that thermal cycling of the surfaces of turbine airfoils can result in spalling of oxide films used for corrosion projection and thus shorten the life of the airfoils. Development of a system to measure gas temperature fluctuations was undertaken to aid in modeling combustor flow and in studying the thermal cycling of airfoil surfaces. Combustor modeling requirements set the frequency response goal at 1000 Hz.

The approach used in this work was to devise a way to determine in situ the compensation spectrum required to correct for the limited frequency response of a thermocouple probe located in the gas stream. Frequency compensation has often been used, especially with hot wire anemometers, in the measurement of dynamic flow phenomena. The problem with this technique when applied to a thermal element in a flow stream is that the required compensation spectrum is a function of both the thermal mass of the thermocouple and the coefficient for heat transfer between the gas and the thermocouple. This heat transfer coefficient is a function of the gas flow conditions. Each time the flow conditions change, the compensation spectrum must be redetermined. In some cases estimates of the compensation spectrum may be sufficient; in this case it was important to be able to make in situ determinations of the compensation spectrum.

The system that was developed (Elmore et al., 1984; Elmore et al., 1983; Elmore et al., 1986a and b; Stocks and Elmore, 1986) uses a dual element thermocouple probe such as shown in Fig. 6. Thermocouples are formed with carefully butt welded junctions so that there is no variation in diameter in the region of the junction. These thermocouples are each supported across a pair of support posts so that they are parallel cylinders in cross flow and are in close enough proximity (approx 1 mm) so that they are measuring the same temperature. The thermocouple wires and the support posts are made from Pt-30Rh/Pt-6Rh. The thermocouple junctions are midway between the support posts. The two thermocouples have different diameters, commonly 75 and 250 μm. Neither of these thermocouples have the desired frequency response, but a comparison of their dynamic signals can lead to the needed compensation spectrum. The technique is based on the use of the ratio of the Fourier coefficients of the dynamic signals for frequencies in the range where the signals

become attenuated. In the system which has been developed, the signals are recorded on magnetic tape and processed in a general purpose digital computer at a later time. The data reduction process takes approximately 5 min for each flow condition for which a new compensation spectrum must be calculated.

Elmore et al. (1986 a and b) describe experiments to demonstrate the frequency response of the system. Measurements were made in a specially designed test rig and in the exhaust of an atmospheric burner. Comparisons were made between the dynamic gas temperature system and very fine wire resistance thermometers (6 and 12 μm wire diameters). At low frequencies (below 250 Hz) with reasonable temperature fluctuations agreements within ±23 percent were obtained. Poorer results were obtained at higher frequencies but here the temperature fluctuations were so small as to make the data questionable.

This system has been used to measure fluctuating temperature in both turbine engines and in combustor test rigs. A sample of data from a turbine engine test is shown in Fig. 7. In this test the probe was located between first-stage turbine vanes. For the data shown in Fig. 7, the engine was operating at an intermediate power level and the average gas temperature was 1200 K. Figure 7 shows four plots of fluctuating temperature versus time. Figures 7(a) and (b) shown the uncompensated signals from the 75 and 250 μm thermocouples. Note that the temperature scales on these plots have been adjusted so as to show the waveforms. Also note that the rms temperature fluctuation is listed on each plot. Figure 7(c) shows the compensated temperature fluctuation from the 75 μm thermocouple, and Fig. 7(d) show an expanded time segment of the compensated signal. The rms value of the compensated temperature fluctuation is 218 K and the peak-to-peak fluctuation is approximately ±500 K.

LASER ANEMOMETRY

The laser anemometer (LA) has become a valuable tool in turbine engine research, providing data that would be almost impossible to gather using conventional instrumentation. However, the use of LA in turbomachinery has proven to be one of its more difficult applications. Turbomachinery components are typified by small passages and highly accelerated, high-velocity flows. This leads to the need for small seed particles that will faithfully follow the flow. Unfortunately, small particles are weak light scatterers, which result in low signal levels. In addition, measurements in small passages require great care in the design of the optics to minimize the amount of detected surface-scattered laser light (flare). All these considerations must be included in the design of an LA to obtain the maximum amount of accurate data in minimum experimental run times.

HOST experiments where researchers planned to use LA were studied to determine critical technology areas. Research programs were then conducted in several of these areas including optical design, seed generation, signal processing, and data acquisition. An ambient pressure, laboratory-type combustor was used to evaluate optical systems and signal processors.

Modeling of Fringe-Type LA

The fringe-type LA was analyzed (Seasholtz et al., 1984) using the Cramer-Rao lower bound for the variance of the estimate of the Doppler frequency as a figure of merit. Mie scattering theory was used to calculate the Doppler signal with both the amplitude and phase of the scattered light taken into account. The noise due to wall scatter (flare) was calculated using the wall bi-directional reflectance distribution function (BRDF) and the irradiance of the incident beams. A procedure was developed to find the optimum aperture stop shape for the probe volume located a given distance from a wall. Figure 8 shows SNR as a function of probe volume to wall distance for two optical systems with optimum aperture masks.

The BRDF was measured for a number of uncoated materials, finishes, and surface coating. Data were obtained for "as machined" surfaces, polished surfaces, glossy black coatings, and flat back coatings. Based on these data, the best surface for LA applications appears to be a glossy black coating. Although a black glossy surface has a relatively large specular reflection, the diffusely reflected light, which is usually of greatest concern in LA systems, is substantially less than the diffusely reflected light from a flat black coating.

Seeding

Particle characteristics necessary for hot section LA are primarily the same as low temperature LA, with the exception that the particles must retain those characteristics at high temperatures. Based on a survey of available materials, a particular grade of aluminum oxide (nominal 1 μm diam) was selected. A commercial, high-volume fluidized bed was chosen to disperse the seed particles.

An experiment was also conducted to determine the feasibility of using chemically formed seed for hot flows. Titanium tetrachloride vapor was injected into the flow where it reacted with the water vapor to form titanium dioxide and hydrochloric acid (HCl). The titanium dioxide is a suitable high temperature seed material; it has a sub-micron size, and it is produced in large quantities. However, the HCl, if not neutralized, can cause corrosion, which limits the application of this seeding technique.

Preprocessor for Fringe-Type LA

The quality of data from an LA is critically dependent on a number of control settings of the signal processor. These typically include the optical detection system gain (determined by the photomultiplier tube high voltage and amplifier gain) and the electrical filters used to remove the low frequency pedestal component and to reduce shot noise. A study was made to quantify the effect of filters on measurement accuracy (Oberle and Seasholtz, 1985). Several common filter designs were examined. It was shown that both the filter type and the cutoff frequencies must be carefully selected to avoid filter-induced errors in counter-type processors. It was shown that these errors are particularly significant for probe volumes containing a small number of fringes and for highly turbulent flow.

Experiments in turbomachinery test facilities usually have high operational costs, so it is necessary to acquire the desired data in a minimum time. Extensive operator interaction with the instrumentation during a test run is usually not desirable. To provide for efficient data acquisition and correct processor settings, a computer-controlled interface (called a preprocessor) was designed, fabricated, and tested (Oberle, 1987). The preprocessor (Fig. 9) amplifies the signal from the photodetector, filters it using both low- and high-pass filters, and then routes it to the counter processor.

The chief virtue of the preprocessor is that it provides direct computer control of the PMT high voltage, the rf gain (50 dB of amplification and a programmable attenuator are used to provide control over the range -77 dB to +50 dB in 1 dB steps), and selection

of the low- and high-pass filters (8 low-pass and 8 high-pass). In addition, the preprocessor provides computer control of the seed generator and allows computer monitoring of the PMT dc current. With proper software, the preprocessor will allow the researcher to preprogram the various processor settings based on the expected flow conditions. It will also be possible to use "smart" adaptive software to select the proper settings based current measurement parameters such as the frequency, turbulence intensity, and noise level.

Four-Spot LA

The conventional fringe-type LA has a large acceptance angle (i.e., it can measure velocities having a wide range of flow angles), but it has a relatively large probe volume. This large probe volume limits the closest measurements to about 1 mm from surfaces. The conventional time-of-flight LA (aka two-spot or transit LA) has a much smaller probe volume, which allows it to measure much closer to surfaces. However, the two-spot LA has a very limited acceptance angle, which greatly reduces its capabilities in highly turbulent flows.

The need for an anemometer incorporating the large acceptance angle of the fringe LA and the ability of the two-spot LA to measure close to walls led to the development of a new type of time-of-flight LA (Lading, 1983; Wernet and Edwards, 1986). The new Four-Spot LA, shown in Fig. 10, incorporates two features. One is the use of elliptical rather than circular spots to give a large acceptance angle. (This use of two elliptical spots is also called a two-dash or two-sheet time-of-flight LA.) The other feature, which is unique, is the use of four beams arranged to form two pairs of orthogonally polarized, partially overlapping spots. This allows the use of an optical method to accurately determine the start and stop timing signals. Previously, delay-and-subtract techniques were used to generate the timing signals. The optical method, unlike delay and subtract, is independent of the velocity. This is advantageous in highly turbulent flow or in other flows with a wide range of velocities.

The Four-Spot LA was designed, fabricated, and successfully tested. Measurements were obtained as close as 75 μm from a normal surface (Wernet, 1987). Comparison measurements were also made using the four-spot LA, a two-spot LA, and a fringe-type LA in the vicinity of a single turbine vane mounted in the exhaust of the open jet burner (Wernet and Oberle, 1987).

Windows and Correction Optics

In turbomachinery studies it is highly desirable to obtain measurements without altering the flow being studied. With optical techniques this means that the window contour should match the internal flow passage contour. One Lewis HOST facility was a 508 mm diameter, single stage, axial flow turbine facility. Two cylindrical windows were designed to allow measurements within the stator and rotor passages. These windows, however, act as cylindrical lenses that introduce aberrations into the LA optical system. If not corrected, these aberrations can greatly degrade the measurements or even prevent any measurements. A monochromatic correction optic (Fig. 11) was designed for this application (Wernet and Seasholtz, 1987). The addition of the correction optic restores the diffraction limited performance of the optical system.

COMBUSTOR VIEWING SYSTEM

Another way to determine the response of a component to the hot section environment is to monitor visual images of the component during operation. This is not likely to produce quantitative data but, in some cases, qualitative data are sufficient or even preferable. A case in point is the Combustor Viewing System (Morey, 1984; Morey, 1985). This system was designed to provide recorded images of the interior of a combustor during operation; the objective was to produce a visual record of some of the causes of premature hot section failure.

The Combustor Viewing System consists of a water cooled optical probe, a probe actuator, an optical interface unit that couples the probe to cameras and to an illumination source, and system controls. The probe with its actuator is designed to mount directly on an engine or a combustor. The probe is 12.7 mm in diameter, small enough to fit into an igniter port. The actuator provides a rotational motion of ±180° and radial insertion to a maximum depth of 7.6 cm. Two probes were built to use with the system. The wide field-of-view probe can be fitted with lenses for 90° and 60° fields-of-view, with the viewing axis oriented 45° to the axis of the probe. The narrow field-of-view probe has lenses for 35° and 13° fields-of-view that are oriented 60° relative to the probe axis. Both probes are water cooled and gas purged and are capable of operating within the primary combustion zone of a combustor.

Figures 12(a) and (b) show cross section views of the two probes. In each case an image conduit is used to transfer the image through the length of the probe. The image conduit is a fused bundle of fibers 3 mm in diameter and consists of about 75 000 fibers 10 μm in diameter. Each of these fibers corresponds to a picture element. The image conduit is 33 cm long and is coupled to a flexible fiber bundle which connects the probe to the optical interface unit. Each probe is also equipped with two 1 mm diameter plastic clad fused quartz fibers used for illumination when required.

The optical interface unit contains cameras, filters, and an illumination source. Either film or video cameras can be remotely selected and up to eight filters can be inserted into the viewing path. The illumination source is a mercury arc lamp which is focused on the ends of the illumination fibers.

This system has been used in both combustor and full scale engine tests. Although the original use for the system was in combustor liner durability studies, the system also has capability as a flowpath diagnostic device. It has been used to examine light off and blowout characteristics and appears to have considerable potential for other time dependent phenomena and for flame radiometry. Subsequent to the initial development program, additional systems were built and put into service in aircraft engine development work and in testing turbine engines used to generate electrical power.

HIGH TEMPERATURE STRAIN MEASURING SYSTEMS

The most ambitious instrumentation development effort in this program is the development of high-temperature strain measuring systems. The target goal for this work is to measure strain (approx 2000 microstrain, maximum) at temperatures up to 1250 K with an uncertainty of ±10 percent. This requirement is for relatively short term testing; a 50 hr sensor life is considered sufficient. Spatial resolution of the order of 3 mm is desired and where measurements are required on blades or vanes, large temperature gradients are anticipated. In general, the requirement is for steady-state measurements as differentiated from dynamic (fluctuating component only) measurements.

The principal candidate for making such measurements under similar but lower temperature conditions (less than approx 700 K) is the resistance strain gage. However, at the higher temperatures, strain measurements become increasingly difficult and the commonly used strain gages are marginal at best. As the required temperature range increases, the magnitude of the correction for apparent strain becomes substantially larger than the strain signal and the uncertainty of the correction is excessive. To meet the goals listed above, the uncertainty of the apparent strain correction must be less than ±200 microstrain. This requirement translates to a repeatability of the resistance versus temperature for the mounted strain gage to be well within ±400 parts per million (ppm), based on a gage factor of two.

We made an extensive study of potentially useful high-temperature static strain measurement techniques (Hulse et al., 1987a). As a result of this study, we are pursuing the following to improve our high temperature strain measuring capability:

(1) developing improved high temperature strain gages
(2) learning how better to use available strain gages
(3) developing optical strain measuring systems as alternatives to strain gages

The following section will discuss these three areas of work.

Development of Improved High Temperature Strain Gages

In attempting to develop improved high temperature strain gages, we are emphasizing development of alloys with very repeatable resistance versus temperature characteristics (Hulse et al., 1985; Hulse et al., 1987b). We tested a number of alloy compositions from five alloy families. These alloy families are FeCrAl, NiCrSi (Nicrosil), PtPdMo, PdCr, and PtW. In all cases except for the thermocouple alloy Nicrosil, we looked at a range of compositions. Alloy sample were cast into rods and then machined into suitable test samples. Measurements were made of resistance versus temperature over a number of cycles in which cooling rates were varied from 50 to 250 K/minute. Additional tests included oxidation (weight gain method) and resistance drift for up to 3 hr in air at 1250 K. The results of these tests indicated that two alloys, one in the FeCrAl family and one in the PdCr family, had the best potential for high temperature strain gage applications.

The FeCrAl alloy was designated as "Mod 3." The fractional resistance change with temperature for this alloy at temperatures up to 1250 K is compared with the commercial Kanthal A-1 (also FeCrAl) alloy in Fig. 13. In this case both alloys were annealed for 2 hr at 1150 K prior to testing. The resistance change of the Mod 3 alloy is much less than that of the Kanthal A-1 alloy and shows comparatively little change for different cooling rates. This alloy does, however, exhibit different resistance versus temperature characteristics, depending on previous thermal history. Figure 14 illustrates this effect for exposure to 1250 K air for times ranging from 10 to 105 hr. Because of this effect, work on this alloy has been de-emphasized in favor of the PdCr alloy.

The PdCr alloy has a resistance versus temperature curve which is characteristic of a solid solution alloy with no phase or internal structure changes being evident. The resistance is essentially linear with temperature and not affected by changes in cooling rate or previous thermal history. Cycle-to-cycle repeatability of the fractional change in resistance with temperature is excellent. Tests over four thermal cycles showed an average (over the temperature range) standard deviation of 130 ppm. The greatest variation was at approximately 700 K with a standard deviation of 245 ppm. The long term drift of cast samples of this alloy at 1100 and 1250 K in air and in argon is shown in Fig. 15. It should be noted that these data imply a repeatability in resistance measurement to the order of 100 ppm; it is likely that some of the fluctuation in these curves is attributable to the measuring system rather than the resistance of the alloy samples.

The repeatability of the PdCr alloy is the property that we feel is essential for high-temperature strain gage work. However, there are other properties required for good strain gages and the PdCr alloy may not be ideal considering these properties. The temperature coefficient of resistance is high enough that temperature compensation will be required; the added complication and the larger gage size required for this will have to be accommodated. Other potential problems such as oxidation resistance of high surface-to-volume ratio thin films and fine wires, gage factor changes with temperature, and the elastic/plastic strain properties are still under investigation.

Work With Available Strain Gages

Learning how best to use available strain gages in high-temperature applications requires that considerable experimental work be done to explore strain gage characteristics and devise optimum procedures for specific applications. Such work is very time consuming, especially when tests at many different temperatures are required. Consequently, one of our objectives in this work was to establish a computer controlled testing capability at NASA Lewis so that testing could be accomplished with minimal operator attention.

The automated strain gage test laboratory has the capability to measure apparent strain and gage factor over a range of temperatures from 300 to 1370 K. The laboratory has two ovens (one of which contains a test fixture for a constant strain beam), a computer controlled actuator for deflecting the beam, strain gage and temperature instrumentation, and a personal computer for controlling the tests and collecting the data. Communication between various parts of the system is accomplished using both an IEEE-488 data bus and an RS-232 serial interface. A very versatile control program was developed that allows us to construct a variety of test profiles by entering a series of temperatures and command statements into a data set. Figure 16 shows a block diagram of the system.

One approach to better utilization of available strain gages is outlined by Stetson (1984). In this work using Kanthal A-1 alloy, it was determined that the apparent strain of the gage was strongly affected by the rate at which the gage was cooled from the highest use temperature. Further, the apparent strain for the next thermal cycle followed that established by the cooling part of the previous cycle; a repeatable apparent strain could be obtained if the cooling rate could be reproduced during each thermal cycle. This implies that an accurate apparent strain correction could be obtained by matching the cooling rate during calibration to that which would be impressed on the strain gage during use. It is necessary, of course, that the cooling rates be controllable during use and that is not always possible. But for the work of Stetson (1984), the cooling rates could be matched and, although it took considerable effort, the result was usable static strain measurements at temperatures up to 950 K.

Work based on controlled cooling rates has also been undertaken at NASA Lewis. Hastelloy X plates 13

by 20 cm were instrumented with Kanthal A-1 and Chinese FeCRAl 700 °C (Wu et al., 1981) strain gages. A plate holding fixture was made that permitted cooling gas to flow over the plate uniformly so as to get controlled cooling rates. The Kanthal A-1 gages were mounted using a flame sprayed alumina and ceramic cement process and the Chinese gages were mounted with a Chinese ceramic cement using directions supplied with the gages. The plates were also instrumented with 10 thermocouples so as to measure the temperature distribution at the strain gages. Apparent strain measurements were made over a temperature range from 300 to 950 K with cooling rates controlled at 0.1, 1.0, and 5.6 K/sec. Figure 17 shows the resulting resistance versus temperature data. Plotted here are fractional changes in resistance for one each of the Kanthal A-1 and Chinese gages for the three different cooling rates. The data show the Kanthal gage to be strongly dependent on cooling rate but repeatable in resistance at the maximum temperature. The resistance of the Chinese gage is independent of cooling rate at both 300 and 950 K, but at intermediate temperatures the curves deviate depending on cooling rate. The maximum deviations in these curves occur in the temperature range from 650 to 800 K, roughly the same region for which high drift rates have been reported for the Chinese gages (Hobart, 1985).

Optical Strain Measurement

Optical systems may not provide exact alternatives to resistance strain gages for all turbine engine applications, but they appear to have high potential for providing high temperature, noncontact, two-dimensional strain measuring systems with virtually unlimited strain range. An optical technique that requires no modification to the surface under test uses laser speckle patterns. These patterns are formed by constructive and destructive interference of laser light reflected from a diffuse surface. The source of the pattern is the irregularities in the surface; when the surface is distorted, for example by strain in the plane of the surface, the speckle pattern changes. Precise measurements of changes in recorded speckle patterns can provide information on the strain imposed on the surface. A practical implementation of this technique is a laser speckle photogrammetric system in which speckle patterns are recorded on photographic film (Stetson, 1983). Speckle pattern photographs (called specklegrams) are made at different increments of loading of the test sample and then pairs of specklegrams are examined in an automated interferometric photocomparator. The system uses heterodyne techniques to achieve accurate measurements to a fraction of an interference fringe. No attempt will be made here to describe this system in detail; it has been thoroughly described in the open literature (Stetson, 1983).

The laser speckle photogrammetric system has successfully measured high-temperature surface deformation. Stetson (1983) describes an experiment to measure the thermal expansion of an unrestrained plate of Hastelloy X at temperatures up to 1150 K. The plate was heated in a laboratory furnace to 1150 K and then allowed to cool to 500 K over a period of several hours. Specklegrams were recorded at roughly 200 K intervals during the heating and cooling and succeeding specklegram pairs were used to determine the thermal expansion of the plate. Measured thermal expanison agreed with values calculated from the measured temperature and the thermal expansion coefficient to within 3 percent.

We have attempted to use the laser speckle photogrammetric system in test cell environments. In one attempt we recorded specklegrams of a combustor liner in a high-temperature, high-pressure combustor test rig (Stetson, 1984). The specklegrams were taken through a viewing port in the pressure vessel of the test rig as combustor pressure and temperature were varied. A potential problem in this application is that the high-pressure cooling air flowing over the exterior surface of the combustor liner is in the optical viewing path, and turbulence in the gas flow may cause sufficient optical distortion to prevent correlation of succeeding pairs of specklegrams. Examples of undistorted and distorted specklegrams are shown in Figs. 18(a) and (b). This effect proved to be a fundamental limitation for the measuring system in this application when combustor pressure was higher than approximately 3 atm. We intend to explore further high temperature applications of optical strain measuring systems.

THIN FILM SENSORS

One of the fundamental precepts of experimentation is that the sensors used to get experimental data must not perturb the subject of the experiment from its condition prior to the introduction of the sensors. In turbine engine testing there are many situations in which this precept may be violated. A prime example is the measurement of turbine airfoil surface temperature. Conventional technology involves laying sheathed thermocouple wire into grooves cut into the surface of the airfoil, then covering the installation and smoothing the airfoil contour. Although the airfoil contour is restored, the thermocouple disturbs the temperature distribution, does not give a true measure of the outside surface temperature, and threatens the integrity of the structure of thin walled blades and vanes.

The thin film thermocouple shown in Fig. 19 appears to be an ideal solution for blade and vane surface temperature measurement (Grant and Przybyszewski, 1980; Grant et al., 1981; Grant et al., 1982). As seen in the cross-sectional sketch of the sensor in Fig. 20, the sensor has minimal intrusiveness. In this case the blade or vane, coated with an MCrAlY anticorrosion coating, is polished and then oxidized to form an adherent surface coating of aluminum oxide. Additional aluminum oxide is deposited over this film to form an electrically insulating film of roughly 2 μm thickness. Films of thermocouple alloy (Pt and Pt10%Rh) are sputter deposited through appropriate masks so that the films overlap at one point to form the thermocouple junction. The thermocouple films extend to the root of the vane where connections to conventional leadwires are made. Film-to-leadwire connections are made by parallel-gap welding. The complete installation of insulating film and thermocouple alloy films has a thickness of less than 20 μm. The installation has not changed the contour or the strength of the component and the greatest thermal changes apparent are the different absorptance and emittance of the thermocouple films compared to the oxidized MCrAlY surface. The technology for thin film thermocouples and turbine airfoils has been developed to the extent that instrumented vanes and blades are being used in turbine engine tests at temperatures up to 1250 K.

Thin film sensor development work is going on both at contractor facilities and at NASA Lewis. Figure 21 shows the thin film sensor laboratory at NASA Lewis. The laboratory is housed in a clean room in which both temperature and humidity are controlled. On the left in the photograph are three vacuum sputtering machines for deposition of both insulator and sensor films. In the right-hand corner of the room is equipment for photolithography of sensors; conventional photo-resist

techniques are used. At the far right edge of the photograph is a welder for connecting leadwires to sensor films.

CONCLUDING REMARKS

This paper has reviewed the state of development of a number of advanced instrumentation projects applicable to the hot sections of turbine engines. Most of these projects are complete and the instrumentation is in use. This is the case for the Combustor Viewing System, the Dynamic Gas Temperature Measuring System, total heat flux sensors, the laser anemometry projects described here, and thin film thermocouples. Work in the general area of thin film sensors is continuing in order to further improve the technology and expand sensor types and applications. The work to improve our high-temperature strain measuring capability is still in progress.

REFERENCES

Atkinson, W.H., and Strange, R.R., 1982, "Development of Advanced High-Temperature Heat Flux Sensors," NASA CR-165618.

Atkinson, W.H., Hobart, H.F., and Strange, R.R., 1983, "Advanced High Temperature Heat Flux Sensors," Proceedings of the 38th Instrument Society of America Conference, Advances in Instrumentation, Vol. 38, Part 2, Instrument Society of America, pp. 1457-1479.

Atkinson, W.H., Cyr, M.A., and Strange, R.R., 1984, "Turbine Blade and Vane Heat Flux Sensor Development, Phase I," NASA CR-168297.

Atkinson, W.H., Cyr, M.A., and Strange, R.R., 1985a, "Development of High-Temperature Heat Flux Sensors, Phase II - Verification Testing," NASA CR-174973.

Atkinson, W.H., Cyr, M.A., and Strange, R.R., 1985b, "Turbine Blade and Vane Heat Flux Sensor Development, Phase II," NASA CR-174995.

Elmore, D.L., Robinson, W.W., and Watkins, W.B., 1983, "Dynamic Gas Temperature Measurement System Final Report, Volume I Technical Efforts," NASA CR-168267.

Elmore, D.L., Robinson, W.W., and Watkins, W.B., 1984, "Dynamic Gas Temperature Measurement System," Proceedings of the 30th International Instrumentation Symposium, Instrumentation in the Aerospace Industry, Vol. 30, Advances in Test Measurements, Vol. 21, Instrument Society of America, pp. 289-302.

Elmore, D.L., Robinson, W.W., and Watkins, W.B., 1986a, "Further Development of the Dynamic Gas Temperature Measurement System, Vol. I Technical Efforts," NASA CR-179513.

Elmore, D.L., Robinson, W.W., and Watkins, W.B., 1986b, "Further Development of the Dynamic Gas Temperature Measurement System," AIAA Paper 86-1648.

Grant, H.P., and Przybyszewski, J.S., 1980, "Thin Film Temperature Sensor," NASA CR-159782.

Grant, H.P., Przybyszewski, J.S., and Claing, R.G., 1981, "Turbine Blade Temperature Measurements Using Thin Film Temperature Sensors," NASA CR-165201.

Grant, H.P., Przybyszewski, J.S., Claing, R.G., and Anderson, W.L., 1982, "Thin Film Temperature Sensors, Phase III," NASA CR-165476.

Hobart, H.F., 1985, "Evaluation Results of the 700°C Chinese Strain Gages," NASA TM-86973.

Holanda, R., 1984, "Analysis of Thermoelectric Properties of High-Temperature Complex Alloys of Nickel-Base, Iron-Base, and Cobalt-Base Groups," NASA TP-2278.

Hulse, C.O., Bailey, R.S., and Lemkey, F.D., 1985, "High Temperature Static Strain Gage Alloy Development Program," NASA CR-174833.

Hulse, C.O., et al., 1986, "Advanced High Temperature Static Strain Sensor Development," NASA CR-179520.

Hulse, C.O., Bailey, R.S., Grant, H.P., and Przybyszewski, J.S., 1987, "High Temperature Static Strain Gage Development Contract," NASA CR-180811.

Lading, L., 1983, "Estimating Time and Time-Lag in Time-of-Flight Velocimetry," Applied Optics, Vol. 22, No. 22, pp. 3637-3643.

Morey, W.W., 1984, "Hot Section Viewing System," NASA CR-174773.

Morey, W.W., 1985, "Jet Engine Combustor Viewing System," Conference on Lasers and Electro-Optics, IEEE, New York, p. 298.

Oberle, L.G., and Seasholtz, R.G., 1985, "Filter Induced Errors in Laser Anemometry Using Counter-Processor," International Symposium on Laser Anemometry, ASME FED Vol. 33, A. Dybbs and P.A. Pfund, eds., ASME, New York, pp. 221-230.

Oberle, L.G., 1987, "A Computer Controlled Signal Preprocessor for Laser Fringe Anemometer Applications," NASA TM-88982.

Seasholtz, R.G., Oberle, L.G., and Weikle, D.H., 1984, "Optimization of Fringe-Type Laser Anemometers for Turbine Engine Component Testing," AIAA Paper 84-1459. (NASA TM-83658).

Stetson, K.A., 1983, "The Use of Heterodyne Speckle Photogrammetry to Measure High-Temperature Strain Distributions," Holographic Data Nondestrutive Testing, D. Vukicevic, ed., Proc. SPIE-370, SPIE, Bellingham, WA, pp. 46-55.

Stetson, K.A., 1984, "Demonstration Test of Burner Liner Strain Measuring System," NASA CR-174743.

Stocks, D.R., and Elmore, D.L., 1986, "Further Development of the Dynamic Gas Temperature Measurement System, Vol. II - Computer Program User's Manual," NASA CR-179513-VOL-2.

Wernet, M.P., and Edwards, R.V., 1986, "Implementation of a New Type of Time-of-Flight Laser Anemometer," Applied Optics, Vol. 25, No. 5, pp. 644-648.

Wernet, M.P., 1987a, "Four Spot Laser Anemometer and Optical Access Techniques for Turbine Engine Applications," ICIASF '87, International Congress on Instrumentation in Aerospace Simulation Facilities, IEEE, New York, pp. 245-254. (NASA TM-88972).

Wernet, M.P., and Oberle, L.G., 1987b, "Laser Anemometry Techniques for Turbine Applications," ASME Paper 87-GT-241. (NASA TM-88953).

Wernet, M.P., and Seasholtz, R.G., 1987c, "Zoom Lens Compensator for a Cylindrical Window in Laser Anemometer Uses," Applied Optics, Vol. 26, No. 21, pp. 4603-4611.

Wu, T.T., Ma, L.C., and Zhao, L.B., 1981, "Development of Temperature Compensated Resistance Strain Gages for Use to 700°C," Experimental Mechanics, Vol. 21, No. 3, pp. 117-123.

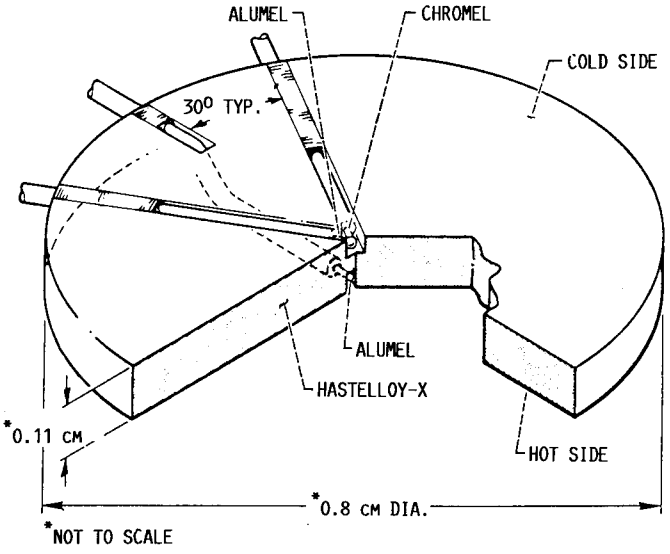

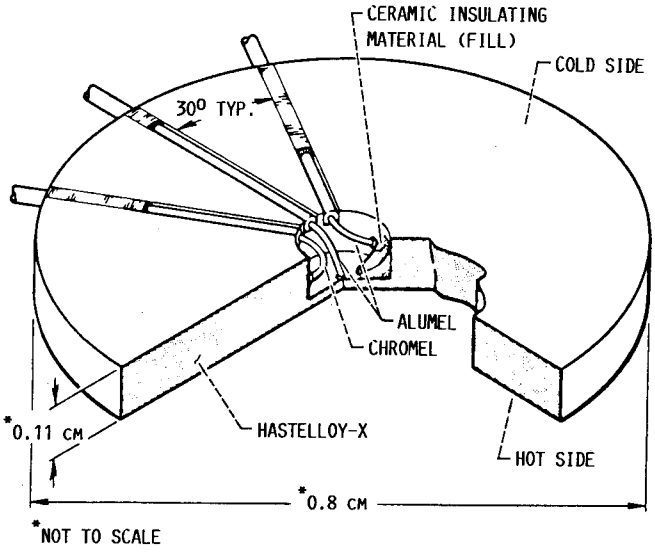

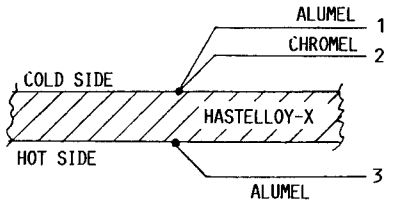

FIGURE 1. - EMBEDDED THERMOCOUPLE HEAT FLUX SENSOR.

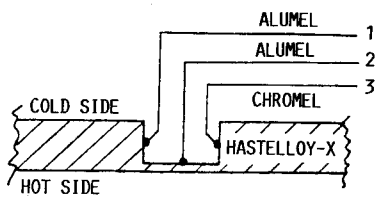

FIGURE 2. - GARDON GAGE HEAT FLUX SENSOR.

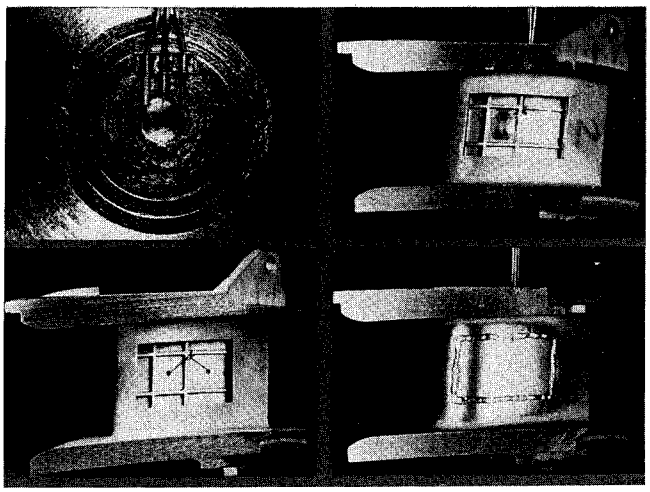

FIGURE 3. - HEAT FLUX SENSORS INSTALLED IN TURBINE VANE.

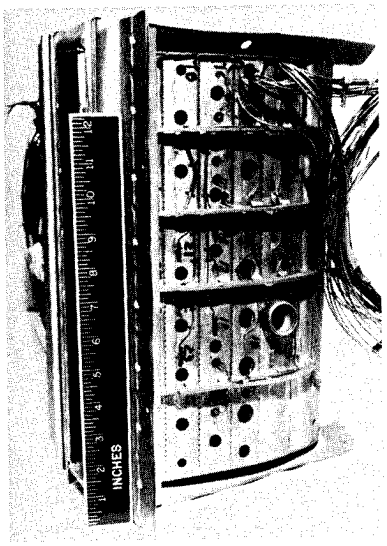

FIGURE 4. - COMBUSTOR SEGMENT INSTRUMENTED WITH HEAT FLUX SENSORS.

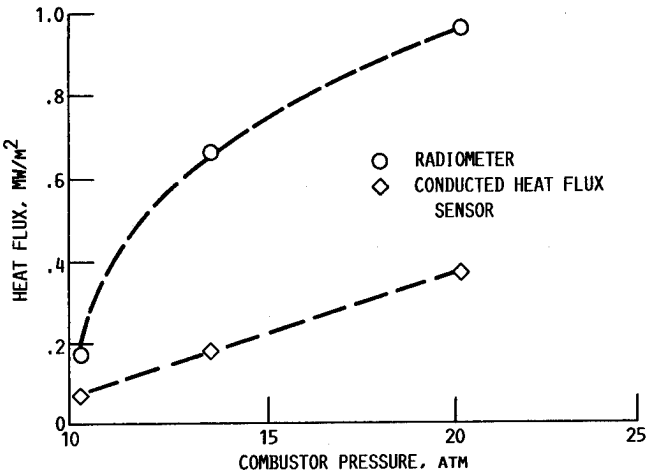

FIGURE 5. - COMPARISON OF HEAT FLUX CONDUCTED THROUGH THE COMBUSTOR LINER AND INCIDENT RADIANT HEAT FLUX FOR VARIOUS LEVELS OF COMBUSTOR PRESSURE. RADIANT HEAT FLUX WAS MEASURED WITH A COMMERCIAL RADIOMETER.

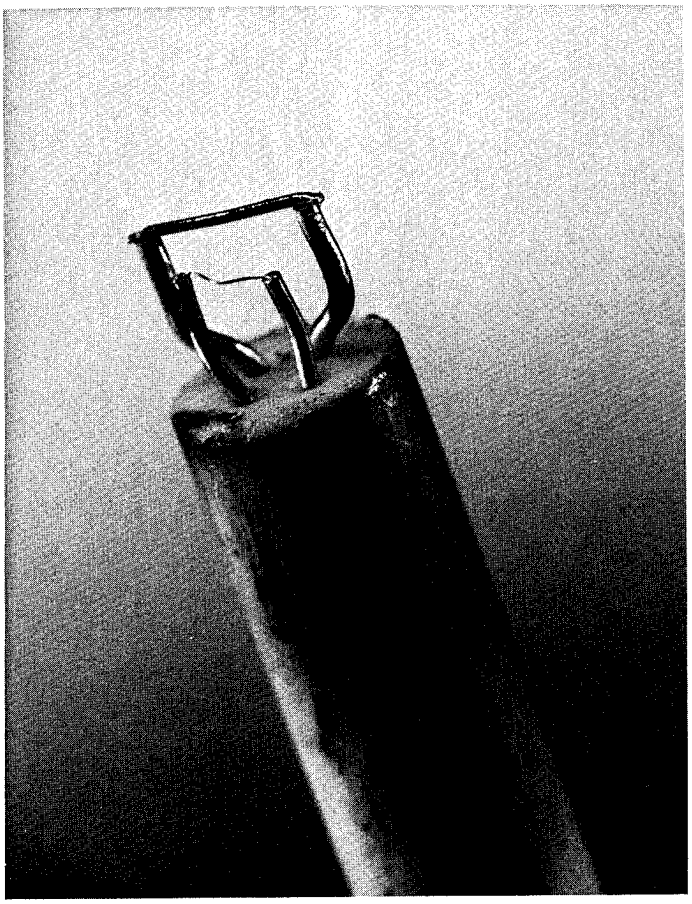

FIGURE 6. - DUAL ELEMENT THERMOCOUPLE PROBE FOR MEASURING FLUCTUATING GAS TEMPERATURE.

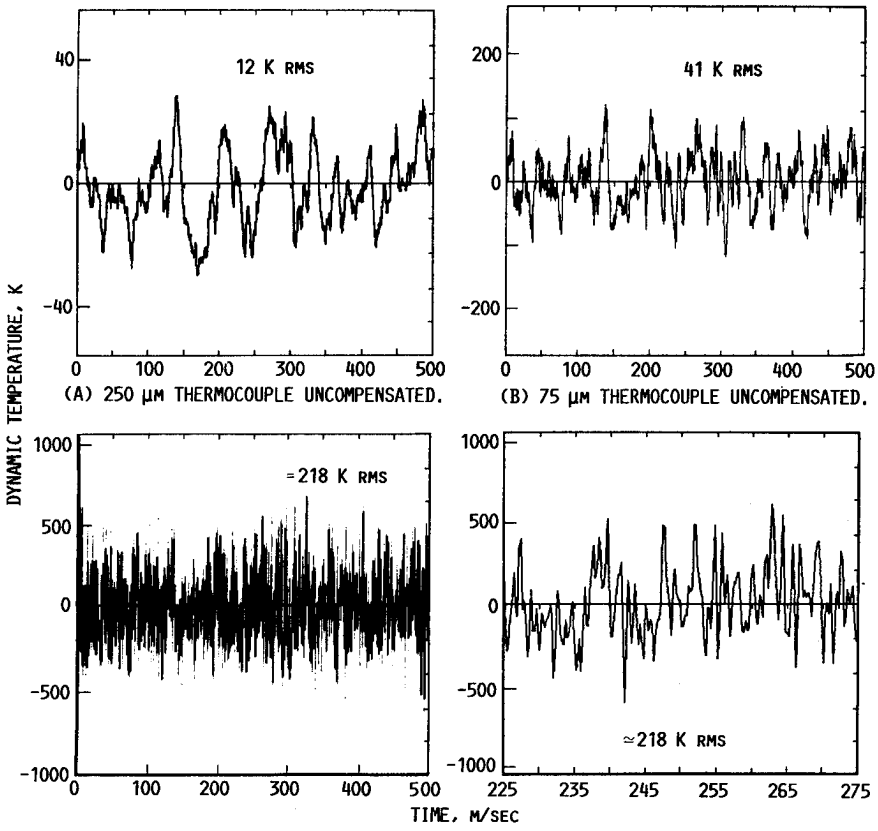

(A) 250 μM THERMOCOUPLE UNCOMPENSATED. (B) 75 μM THERMOCOUPLE UNCOMPENSATED.

(C) 75 μM THERMOCOUPLE COMPENSATED. (D) 75 μM THERMOCOUPLE COMPENSATED.

FIGURE 7. - DYNAMIC GAS TEMPERATURE SIGNALS FROM AN ENGINE TEST.

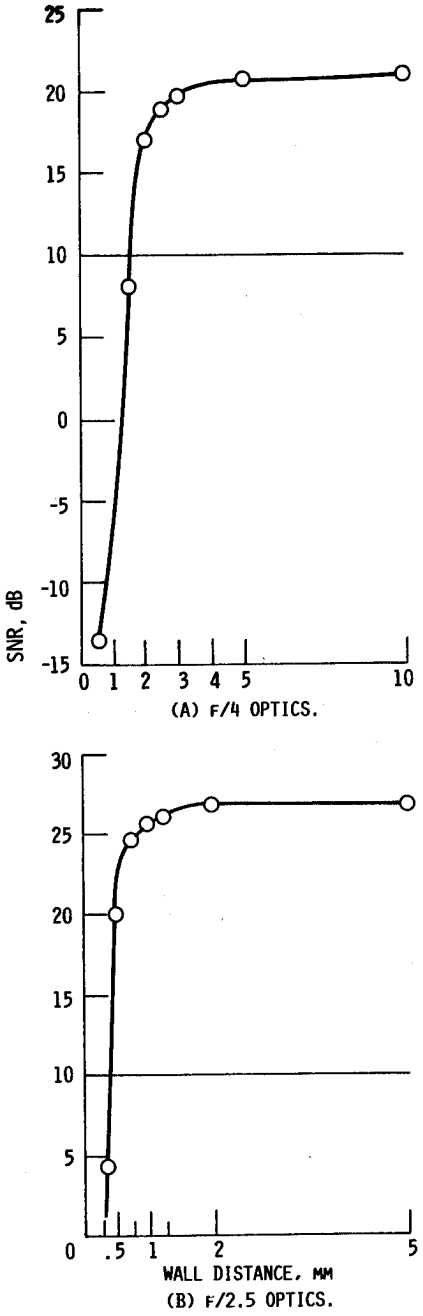

FIGURE 8. - SIGNAL-TO-NOISE RATIO (SNR) FOR OPTIMUM MASK VERSUS DISTANCE OF PROBE VOLUME FROM WALL.

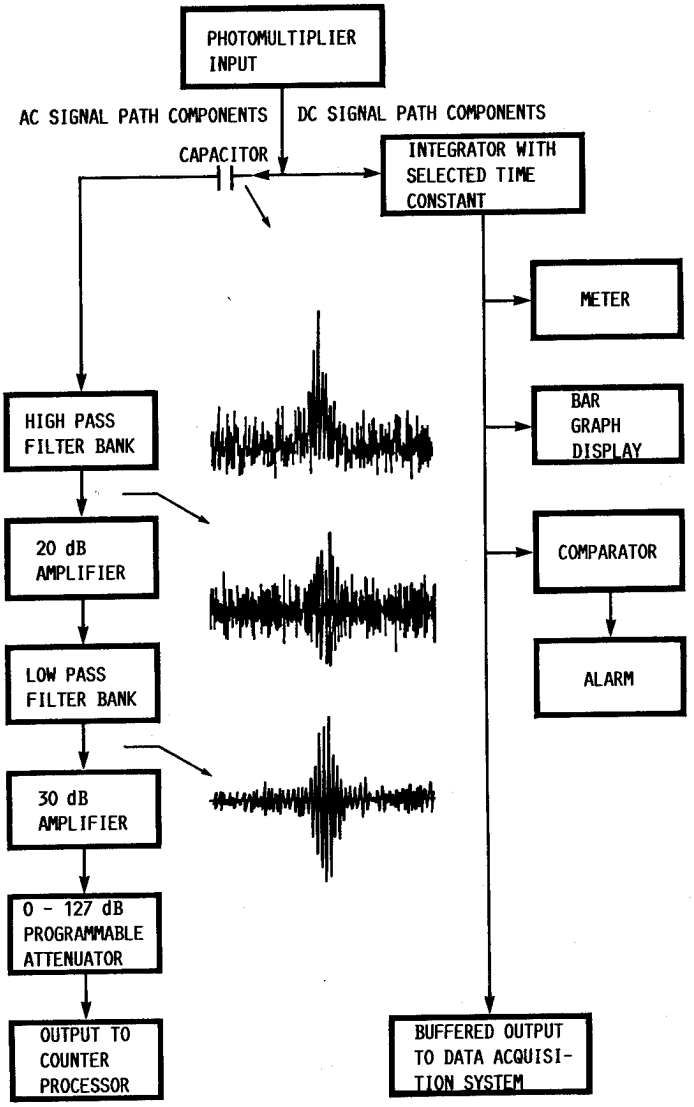

FIGURE 9. - LASER FRINGE ANEMOMETER PRE-PROCESSOR SIGNAL FLOW DIAGRAM SHOWING THE DOPPLER SIGNAL IN THE TIME DOMAIN AT THREE POINTS IN THE SIGNAL FLOW.

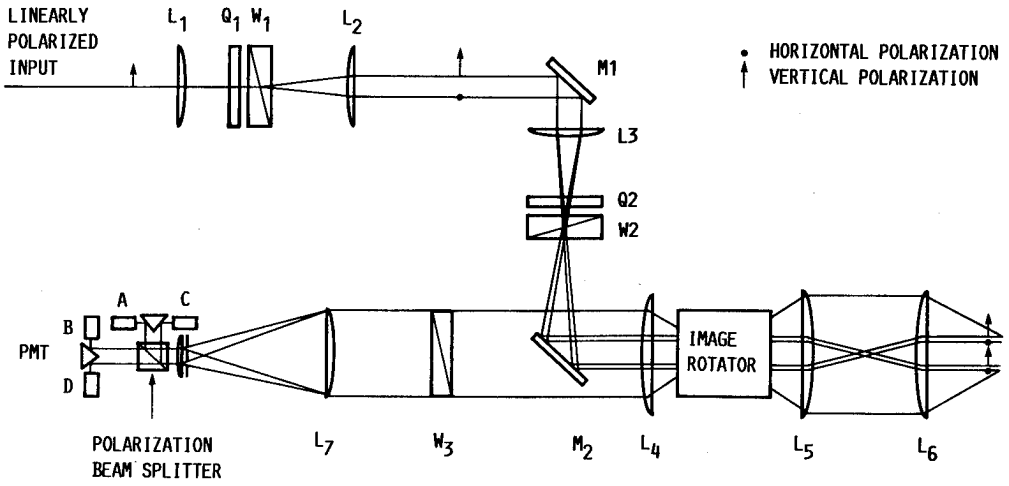

FIGURE 10. - SCHEMATIC VIEW OF THE TRANSMITTING AND RECEIVING OPTICS.

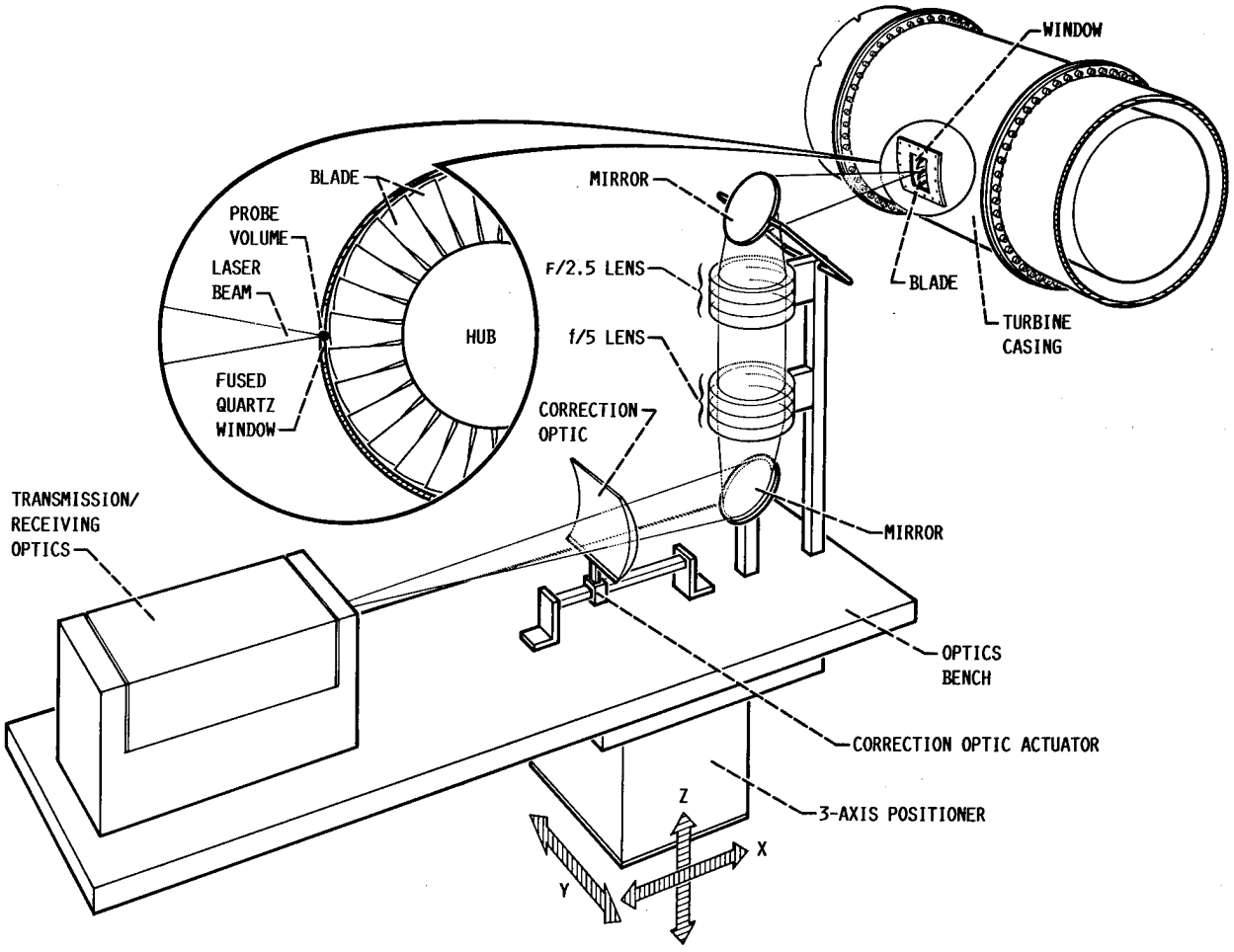

FIGURE 11. - SCHEMATIC VIEW OF A LASER ANEMOMETER SYSTEM APPLIED TO A TURBINE RIG INCORPORATING A CURVE CASING WINDOW. THE ABERRATIONS INDUCED BY THE TURBINE WINDOW ARE COMPENSATED FOR BY THE CORRECTION OPTIC. AS THE 3-AXIS TABLE SCANS THE PROBE VOLUME THROUGH THE BLADE PASSAGE, THE CORRECTION OPTIC POSITION IS ADJUSTED BY ANOTHER ACTUATOR. IN THIS POSITION, THE PROBE VOLUME IS JUST INSIDE THE TURBINE WINDOW, AND THE ACTUATOR IS AT ITS FURTHEST POSITION FROM THE F/5 LENS.

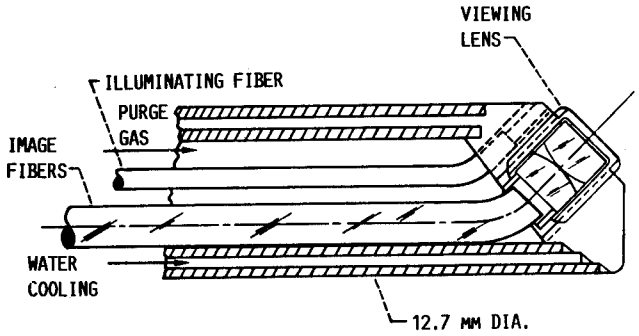

FIGURE 12(A). - CROSS SECTION OF WIDE FIELD OF VIEW COMBUSTOR VIEWING PROBE.

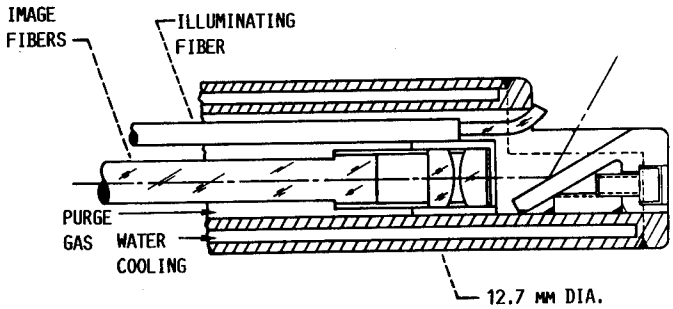

FIGURE 12(B). - CROSS SECTION OF NARROW FIELD OF VIEW COMBUSTOR VIEWING PROBE.

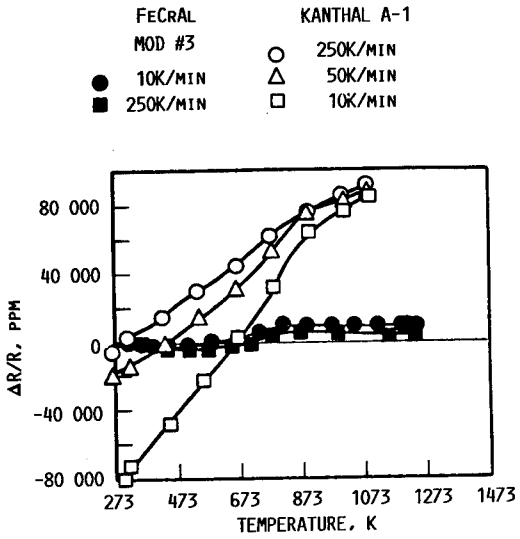

FIGURE 13. - FRACTIONAL RESISTANCE CHANGE OF KANTHAL A-1 AND FECRAL MOD #3 AS A FUNCTION OF TEMPERATURE.

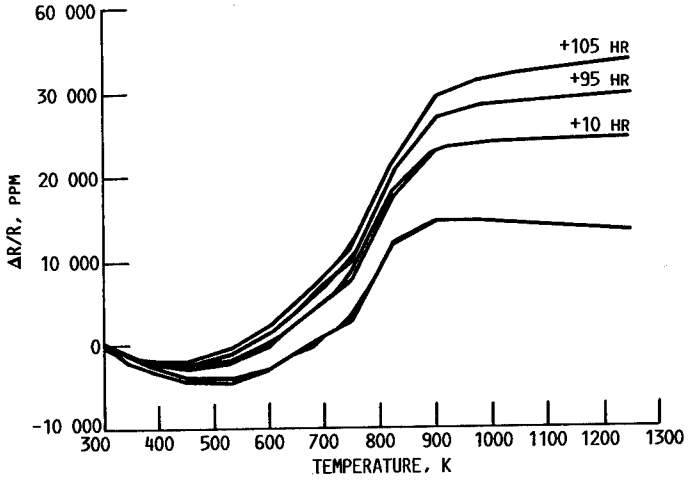

FIGURE 14. - EFFECT OF SOAK TIME AT 1250 K ON THE RESISTANCE VERSUS TEMPERATURE CHARACTERISTIC OF FECRAL MOD #3.

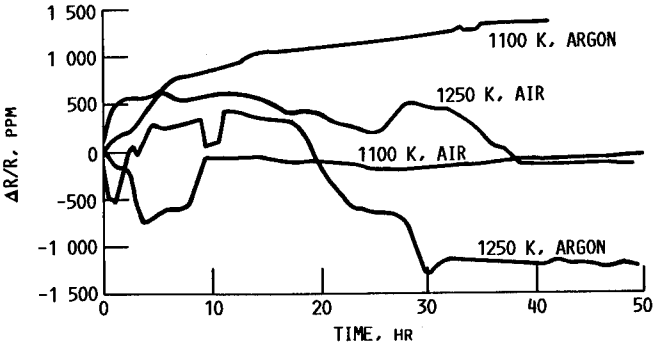

FIGURE 15. - LONG-TERM RESISTANCE DRIFT OF PDCR ALLOY IN ARGON AND AIR.

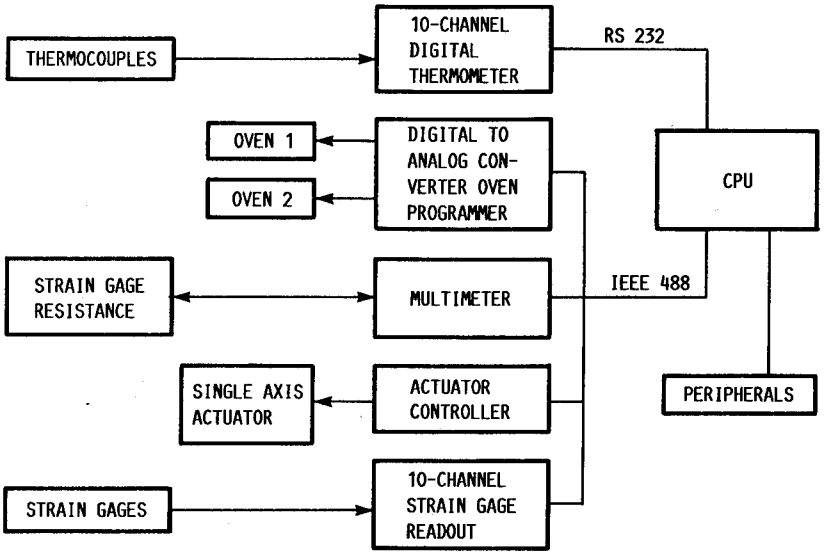

FIGURE 16. - BLOCK DIAGRAM OF THE HIGH TEMPERATURE STRAIN GAGE TESTING SYSTEM.

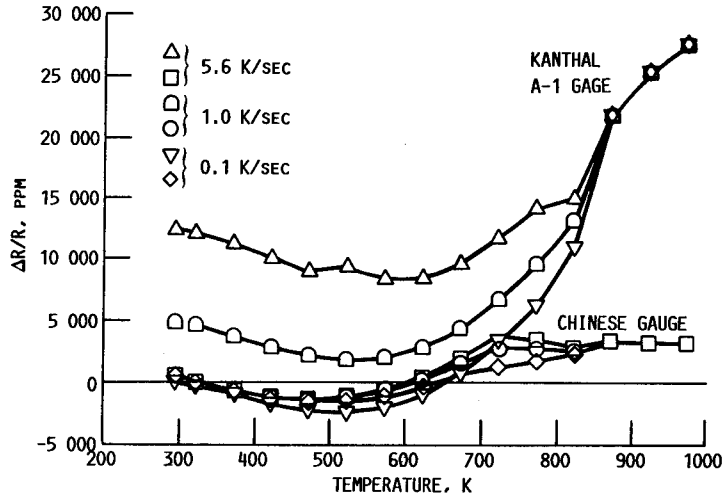

FIGURE 17. - FRACTIONAL RESISTANCE CHANGE VERSUS TEMPERATURE FOR KANTHAL A-1 AND 700 ^{o}C CHINESE GAGES WITH THREE DIFFERENT COOLING RATES.

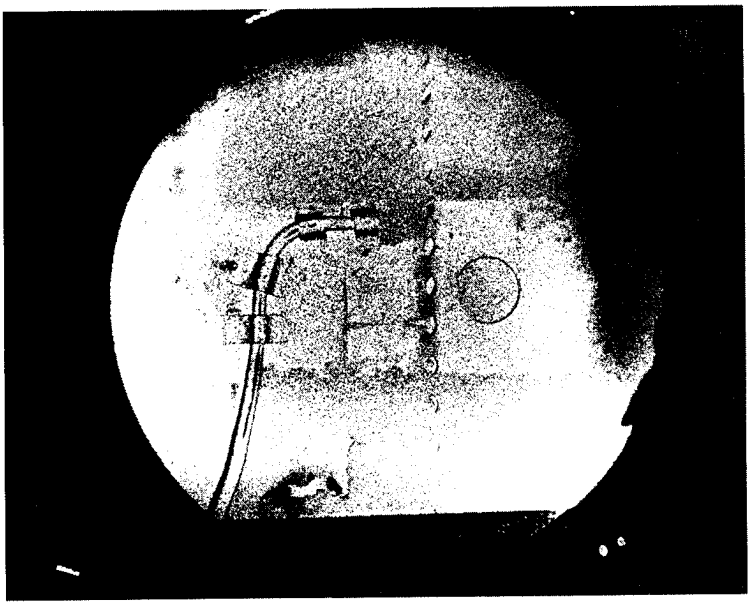

FIGURE 18(A). - SPECKLEGRAM OF COMBUSTOR LINER WITH NO DISTORTION DUE TO FLOW.

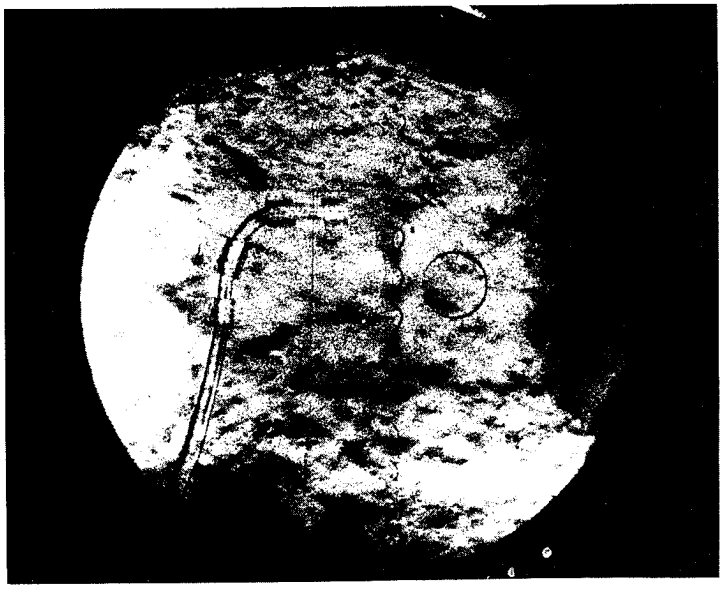

FIGURE 18(B). - SPECKLEGRAM OF COMBUSTOR LINER WITH DISTORTION FROM TURBULENT GAS FLOW.

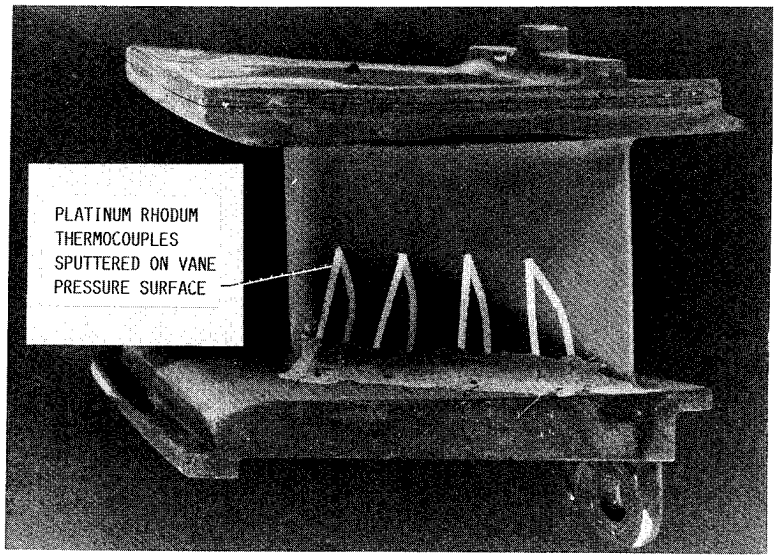

FIGURE 19. - A TURBINE VANE INSTRUMENTED WITH THIN FILM THERMOCOUPLES.

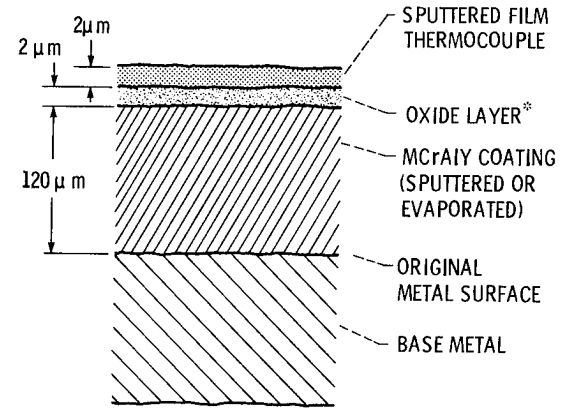

* THE STABLE ADHERENT Al_2O_3 INSULATING LAYER IS OBTAINED BY AT LEAST 50-hr OXIDATION (AT 1300 K) OF THE COATING, FOLLOWED BY Al_2O_3 SPUTTERING.

FIGURE 20. - THIN FILM THERMOCOUPLE CROSS SECTION.

FIGURE 21. - THIN FILM SENSOR LABORATORY AT THE LEWIS RESEARCH CENTER.

ASSESSMENT, DEVELOPMENT, AND APPLICATION OF COMBUSTOR AEROTHERMAL MODELS

J. D. Holdeman
National Aeronautics and Space Administration
Lewis Research Center
Cleveland, Ohio

H. C. Mongia
Allison Gas Turbine Division
General Motors Corporation
Indianapolis, Indiana

E. J. Mularz
Propulsion Directorate
U.S. Army Aviation and Technology Activity – AVSCOM
NASA Lewis Research Center
Cleveland, Ohio

ABSTRACT

The gas turbine combustion system design and development effort is an engineering exercise to obtain an acceptable solution to the conflicting design trade-offs between: combustion efficiency, gaseous emissions, smoke, ignition, restart, lean blowout, burner exit temperature quality, structural durability, and life cycle cost. For many years, these combustor design trade-offs have been carried out with the help of fundamental reasoning and extensive component and bench testing, backed by empirical and experience correlations.

Recent advances in the capability of computational fluid dynamics (CFD) codes have led to their application to complex three-dimensional flows such as those in the gas turbine combustor. A number of U.S. Government and industry sponsored programs have made significant contributions to the formulation, development, and verification of an analytical combustor design methodology which will better define the aerothermal loads in a combustor, and be a valuable tool for design of future combustion systems. The contributions made by NASA Hot Section Technology (HOST) sponsored Aerothermal Modeling and supporting programs are described in this paper.

INTRODUCTION

The goal of gas turbine combustion system design and development is to obtain an acceptable solution to the conflicting design trade-offs between combustion efficiency, gaseous emissions, smoke, ignition, restart, lean blowout, burner exit temperature quality, structural durability, and life cycle cost. For many years, these combustor design trade-offs have been carried out with the help of fundamental reasoning and extensive component and bench testing, backed by empirical and experience correlations. The ultimate goal has been to develop a reliable combustor design system that can provide quantitatively accurate predictions of the complex combustion flow field characteristics (Fig. 1) so that an optimum combustion system design can be achieved within reasonable cost and schedule constraints.

Empirically based procedures have led to successful evolutionary combustor improvements. However, as these methods are experience-based, they are not well suited when combustor design requirement are significantly different from that of current technology engines. The rapidly developing CFD (Computational Fluid Dynamics) capability is providing an additional tool in the design process which can have a powerful positive influence on future design capability. In these codes, combustion system subcomponents including diffusers, fuel injectors, and combustor liners, in addition to the complex internal flow, need to be accurately modelled. To achieve this, physical sub-models and accurate numerical schemes must be developed to describe the various aerothermochemical processes occurring within the combustion chamber.

A number of U.S. Government and company sponsored programs have made significant contributions to the formulation, development, and verification of an analytical combustor design methodology. These have included: U.S. Army Combustor Design Criteria Validation (Bruce et al., 1979; Mongia et al., 1979, Mongia and Reynolds, 1979), NASA Swirling Recirculating Flow (Srinivasan and Mongia, 1980), NASA Soot and NOx Emissions Prediction (Srivatsa, 1980), NASA Primary Zone Study (Sullivan et al., 1983), NASA Mass and Momentum Transfer (Johnson and Bennett, 1981; Roback and Johnson, 1983; Johnson et al., 1984), NASA Lateral Jet Injection (Lilley, 1986; Ferrell and Lilley, 1985; McMurray and Lilley, 1986; Ong and Lilley, 1986), NASA Dilution Jet Mixing (Srinivasan et al., 1982, 1984, 1985; Srinivasan and White, 1986; Holdeman et al., 1984; Holdeman and Srinivasan, 1986; Holdeman et al., 1987a), NASA Transition Mixing Study (Reynolds and White, 1986; Holdeman et al., 1987b), NASA HOST Aerothermal Modeling (Kenworthy et al., 1983; Sturgess, 1983; Srinivasan et al., 1983a, 1983b), NASA Error Reduction (Syed et al., 1985), industry IR & D programs, and advanced combustor development programs.

The NASA Hot Section Technology (HOST) Combustion Program has supported several of these programs. The overall objective of the HOST Combustion Project is to develop and verify advanced analytical methods to improve the capability to design combustion systems

for advanced aircraft gas turbine engines. This objective is being approached both computationally and experimentally.

Computationally, HOST first sponsored studies to assess and evaluate the capabilities of existing aerothermal models (circa 1982). Based on the results of these assessments and other studies in the literature, HOST supported several studies to develop new and improved numerical methods for the analysis of turbulent viscous recirculating flows, with emphasis on accuracy and speed of solution.

The objectives of HOST sponsored experimental studies were to improve understanding of the flow physics and chemistry in constituent flows, and to obtain fully-specified, benchmark-quality experimental data suitable for the assessment of the capabilities of advanced computational codes.

This paper reviews the advances in the state-of-the-art in combustor aerothermal modeling, while highlighting the programs supported by the HOST Project (Turbine Engine Hot Section Technology, 1982, 1983, 1984, 1985, 1986, 1987). Due to length limitations not all programs that received HOST support are included, and, for completeness, some programs that made a significant contribution, but which did not draw their primary support from HOST are discussed.

AEROTHERMAL MODELING ASSESSMENT

Gas turbine combustion models include submodels of turbulence, chemical kinetics, turbulence/chemistry interaction, spray dynamics, evaporation/combustion, radiation, and soot formation and oxidation. A very extensive assessment of numerics, physical submodels, and the suitability of the available data was made by three contractors under Phase 1 of the HOST Aerothermal Modeling program (Kenworthy et al., 1983; Sturgess, 1983; Srinivasan et al., 1983a, 1983b). These investigations surveyed and assessed current models and identified model deficiencies through comparison between calculated and measured quantities. Results of the assessment by Srinivasan et al., (1983a, 1983b) are summarized by Mongia et al. (1986). The constituent flows examined included: (1) simple flows with no streamline curvature, (2) complex flows without swirl, and (3) complex flows with swirl. Geometries for several test cases from each of these categories are shown in Fig. 2.

k-ε Turbulence Model

The k-ε model is the simplest turbulence model that is suitable for recirculating flow calculations. This model achieves closure by using a gradient transport model for Reynolds stress with an isotropic eddy viscosity. For flows where the isotropic eddy viscosity assumption is not valid, the k-ε model may be either modified (e.g. low Reynolds number correction, Richardson number correction) or replaced with an algebraic or differential Reynolds stress model.

Assessment of the k-ε model(s) of turbulence showed that these models:

(1) require low Reynolds Number correction for predicting wall shear flows, and streamline curvature modifications for accurately predicting curved boundary layers
(2) give quantitatively good correlation with data for simple flows and non-recirculating swirling flows
(3) give quantitatively reasonable results for nonswirling recirculating flows
(4) give quantitatively unsatisfactory correlation with data for complex swirling flows with recirculation zones
(5) give quantitatively unsatisfactory correlation, but predict trends correctly, for complex three-dimensional flows.

Algebraic Stress Model and Its Modifications

Mean flow predictions with this model agreed with the data as well as the k-ε model results, therefore the conclusions above also apply to this model. In addition, the Algebraic Stress Model gives reasonable predictions for the Reynolds stress components, consistent with the strengths and limitations of the k-ε models (Mongia et al., 1986).

The results of standard k-ε and algebraic and differential Reynolds stress turbulence models, have been compared in several continuing assessment studies. An example comparison (Mongia, 1987) of data and calculations using a hybrid/SIMPLE numerical scheme is shown in Fig. 3. This flow is that of co-annular turbulent jets flowing into an axisymmetric sudden expansion (Roback and Johnson, 1983). In this figure, velocity profiles are shown at downstream, distance from 0.11 to 2.5 pipe diameters from the expansion.

Scalar Transport Model

Mongia et al., (1986) reported that the k-ε model with specified Prandtl number predicts scalar fluxes reasonably well for flow where the gradient diffusion approximation is valid. An alternative, the algebraic scalar transport model, has the capability to improve predictions over the k-ε approach, but further work is needed to establish its validity for swirling recirculating flows.

Turbulence/Chemistry Interaction Models

It was also concluded by Mongia et al., (1986) that both 2- and 4-step reaction schemes showed promise for application in gas turbine combustors, but need to be further validated against data from simple flames. The modified eddy breakup model predicted trends well, and it was recommended that it should be pursued because this approach could be easily extended to multistep kinetic schemes.

Numerical Accuracy

A significant deficiency identified in the assessments was that for many flows of interest the accuracy of the calculation was limited by the numerical approximations, wherein the false diffusion is of the same order of magnitude as the turbulent diffusion. This masked the differences between turbulence models such that very different models gave essentially the same result, and sometimes resulted in undeservedly good agreement between data and predictions.

If false diffusion is present, the numerical solution obtained for any given flow depends on the grid density and distribution. An example of the comparisons made in the assessment program is given by the comparison in Figs. 4 and 5 between measured and calculated temperature distributions downstream from a row of jets entering a confined crossflow. This flow is a constituent flow in most gas turbine combustors, and has been treated extensively in the literature, including the recently completed NASA Dilution Jet Mixing program, from which data were compared with three-dimensional calculations in the Phase I assessment study by Srinivasan et al., (1983).

The calculated and experimental results shown are for a single row of jets with an orifice spacing to diameter ratio, S/D, = 2 injected into a ducted mainstream with a duct height to orifice diameter ratio H/D, = 8. The jet-to-mainstream momentum flux ratio, J, for this test was 25.32. Calculations for this case made with 45x26x17 (19890) nodes, are shown in Fig. 4. The parameter plotted in these figures is the dimensionless mean temperature difference ratio, THETA, where THETA = (Tm - T)/(Tm - Tj). The predicted jet penetration and mixing are less than that shown by the data.

The calculation shown in Fig. 4 used 49 nodes to simulate each jet. It is generally not possible to use this many grid points in such a small region; as few as four may be used in practice for each jet. To simulate the accuracy of this approximation, calculations were performed for the same flow and geometric conditions, but with a 27x26x8 (5615) grid. These coarse-grid calculations (Fig. 5) are in much better agreement with the data than the fine-grid calculations. These and other calculations in Srinivasan et al., (1983b) clearly demonstrated that the three-dimensional calculations were not grid independent.

Conclusions from the Assessments

The major conclusion in the HOST Aerothermal Modeling Phase I assessment studies by Kenworthy et al. (1983), Sturgess (1983), and Srinivasan et al. (1983a, 1983b) was that the available computational fluid dynamics (CFD) codes provided a useful combustor design tool. Although significant advances have been made in the development and validation of multidimensional gas turbine combustion calculation procedures, the codes assessed were only qualitatively accurate, especially for complex three-dimensional flows, and further work was needed. It was concluded that both a significantly improved numerical scheme and fully-specified experimental data (i.e. both mean and turbulence flowfield quantities, with measured boundary conditions) for complex non-reacting and reacting constituent flows were needed before various emerging physical sub-models of turbulence, chemistry, sprays, turbulence/chemistry interactions, soot formation/oxidation, radiation, and heat transfer could be properly assessed.

A SECOND GENERATION MODEL

The first generation combustor design procedure outlined by Mongia and Smith (1978) has been very useful for developing several combustors (Mongia et al., 1986) that exhibited significant technology advances. However, in addition to the model deficiencies identified in the assessments, there were several parameters of importance in gas turbine combustor design that the analytical models could not predict; e.g. gaseous emissions, soot formation, flame blow-out limits, combustor pattern factor, and liner heat transfer. These parameters were, however, successfully predicted by well-established semi-analytical correlations developed by Plee and Mellor (1980), Lebfevre (1985), and their associates. Therefore, a combustor design procedure that could be applied to current and future gas turbine engines was implemented that makes use of empirical design concepts and employs analytical modeling tools to represent various combustion processes (Rizk and Mongia, 1986; Mongia, 1987).

This method makes use of multidimensional models to establish liner flowfield features and combustion characteristics. The analytical results are then integrated with semi-empirical correlations for performance parameters of interest. That is, flow field and geometric parameters that are needed in the empirical equations, such as combustion volume and the fraction of air participating in the primary combustion reaction, are provided by the analytical calculations.

Satisfactory agreement with experimental data has been shown (Rizk and Mongia, 1986) for emissions, performance and heat transfer. The combustor for which data were available, and for which calculations were performed, is shown schematically in Fig. 6. A typical comparison between data and predictions for CO, unburned hydrocarbons, NOx, soot emissions, combustion efficiency, pattern factor, and lean blowout are shown in Figs. 7(a) to (g) respectively. The model is in good agreement with the data over the entire sea-level engine operating range. Calculated liner wall temperatures for both the inner and outer walls of this combustor are shown in Fig. 8 for three typical z-planes along k = 5, 14, and 23. Here k denotes nodal planes along the combustor circumferential direction. Although no direct comparison with liner wall temperature data was made, the predictions look reasonable.

AEROTHERMAL MODELING PHASE II

Based on the recommendations of the Phase I assessment studies, activities in Phase II of the HOST Aerothermal Modeling program concentrated on developing improved numerical schemes, and collecting completely-specified data for nonreacting single and two-phase swirling and nonswirling flows. The programs initiated were: Improved Numerical Methods; Flow Interaction Experiment; and Fuel Injector/Air Swirl Characterization. The first of these is a prerequisite to further model development, and the data obtained in the latter two studies will be used to validate advanced models being developed independently.

Improved Numerical Methods

The hybrid finite differencing scheme employed in generally available combustor codes gives excessive numerical diffusion errors which preclude accurate quantitative calculations. In response to this deficiency, HOST supported three programs with the primary objective to identify, assess, and implement improved solution algorithms applicable to analysis of turbulent viscous recirculating flows. Both solution accuracy and solution efficiency were addressed (Turbine Engine Hot Section Technology, 1985, 1986, 1987; Turan and VanDoormal, 1987).

For most practical problems, a central differencing scheme would be ideally suited if it were unconditionally stable. Central differencing is a simple second-order scheme which is easy and straightforward to implement. However, for grid Peclet numbers larger than 2, central differencing can lead to over- and under-shoots and is unstable. The hybrid (central/upwind) scheme is stable for all Peclet numbers, but suffers from excessive false diffusion. An alternative scheme, named CONDIF (Controlled Numerical Diffusion with Internal Feedback) (Runchal et al., 1986) has unconditionally positive coefficients and still maintains the essential features of central differencing and its second-order accuracy.

CONDIF uses central differencing when Pe < 2. Where Pe > 2 and the dependent variable varies monotonically, a modified central differencing scheme is used, otherwise upwind differencing is used. CONDIF employs just enough numerical diffusion to ensure stability based internally on the field distribution of

the variable, rather than switching to upwind differencing whenever Pe exceeds 2. Since upwinding is done at relatively few grid points, CONDIF essentially maintains the second-order accuracy of central differencing, and false diffusion is substantially reduced.

Another advanced numerical scheme, called flux-spline (Patankar et al., 1987), is based on a linear variation of total flux (convection + diffusion between two grid points. This is an improvement over the assumption of uniform flux used in hybrid schemes, and leads to reduced numerical diffusion.

Both of these schemes have been used to solve a variety of analytical, two-dimensional laminar and turbulent flows (Runchal et al., 1987; Patankar et al., 1987). As an example, results for a laminar flow (Re = 400) in a square driven cavity are shown in Fig. 9. This flow, shown schematically in part a), is characterized by a strong recirculation zone typical of many physical situations. The problem was solved with both CONDIF and flux-spine schemes on a uniform 22x22 grid and compared with the exact analytical solution and a hybrid solution on an extremely fine 82x82 grid. Velocity profiles at the midsection of the cavity are shown in Fig. 9(b). Both advanced schemes show improvement over the hybrid calculation.

An attractive feature of both CONDIF and flux-spline schemes is that their extension to three dimensions is relatively straight-forward. The resulting linear differential equations involve only seven points as opposed to 27 points needed in many skewed-upwind schemes (Syed et al., 1985).

In addition to the need for improved numerical accuracy, there is a need for improved computational efficiency for a given level of accuracy. Typically the continuity and momentum equations are solved separately, and then linked through iteration of the pressure term; e.g. SIMPLE (Semi-Implicit Method for Pressure Linked Equations). Modifications, such as SIMPLER and PISO, have been shown to improve computational efficiency. Other advanced schemes (Turbine Engine Hot Section Technology, 1985, 1986, 1987; Vanka, 1987), such as block correction techniques and direct solution of the coupled equations have been proposed. Calculations with the latter coupled with the flux-spine technique have shown a speed increase by a factor of 15 for a calculation of turbulent flow over a backward-facing step (Mongia, 1987).

Gas Phase Experiments

An experimental study of the interactions between the combustor and diffuser systems (Srinivasan and Thorp, 1987) is in progress to:

(1) Identify the mechanisms and magnitude of aerodynamic losses in various sections of an annular combustor-diffuser system
(2) Determine the effects of geometric changes in the prediffuser, dome, and shroud on these losses
(3) Obtain a data base to assess current and advanced aerodynamic computer models for predicting these complex flowfields
(4) Upgrade the analytical models based on the experimental data
(5) Design and test advanced diffuser systems to verify the accuracy of the upgraded analytical model

Another study in progress will obtain comprehensive mean and turbulence measurements of velocity and species concentration in a three-dimensional flow model of the primary zone of gas turbine combustion chambers (Turbine Engine Hot Section Technology, 1985, 1986, 1987). The flowfield of interest is the interaction between swirling flow and lateral jets in a rectangular channel (Fig. 10). The mainstreams flow enters through 5 swirlers with the transverse jets injected from both the top and bottom duct walls with either 2 or 4 jets per swirler at 1/2 or 1 channel height downstream from the swirler.

These experiments are being conducted on both air and water multiple-swirler rigs, as well as single swirler and swirling jet rigs. Fifteen cases (combinations of swirl and jet strength and location) are under test using laser sheet light and dye water flow visualization, and detailed velocity and scalar mean and turbulence LDV measurements are being made in the air rig.

A key feature of this program is comparison of model calculations against the data obtained to ensure that the data are complete and consistent, and satisfy the boundary condition input requirements of current three-dimensional codes. Calculations were performed using a three-dimensional code (Srivasta, 1980) for all test cases before the experiments were begun. Data and both previous and advanced model calculations are being compared as data are obtained.

Fuel-Injector/Air-Swirl Characterization

The objective of this study is to obtain fully-specified mean and turbulence measurements of both gas and droplet phases downstream of a fuel injector and air swirler typical of those used in gas turbine combustion chambers.

The flowfield of interest is an axisymmetric particle-laden jet flow with and without confinement and co-annular swirling air flow. Approximately 30 cases are under test with both glass-bead particle-laden jets and liquid sprays, with various combination of swirl strengths and confinement (Turbine Engine Hot Section Technology, 1985, 1986, 1987). Measurements of mean and turbulence quantities, for both gas and solid phases are being made using a 2-component Phase/Doppler LDV particle analyzer (McDonell et al., 1987).

Calculations were performed for all test cases with a two-dimensional TEACH-type nonreacting turbulent viscous two-phase flow code before the experiments were begun. Data and both previous and advanced model calculations are being compared as data are obtained (Mostafa et al., 1987, 1988; Nikjooy et al., 1988).

In the first series of tests, the developing regions of unconfined single and two-phase flows, with 105 μm glass beads, have been examined experimentally and analytically for particle-to-gas mass loadings of 0.2 and 1.0. Data and calculations for the latter are shown in Fig. 11. A two-component Phase/Doppler system was used to map the flowfield, including particle number density, and two orthogonal components of velocity for both phases.

Calculations are shown for both deterministic and stochastic treatments of the particles, using a two-phase k-ε model. Both treatments of the particles give the same gas-phase axial velocity profiles, however, the stochastic approach, which attempts to model particle/gas phase interactions, gives better agreement for particle quantities than the deterministic approach which ignores turbulence interactions.

Another experimental program was conducted to obtain information on the characteristics of the spray produced by a gas turbine fuel injector (McVey et al., 1988a, 1988b). The objective of this study was to obtain spatially-resolved information on both the liquid and gaseous phases of the spray flow field under conditions of high-flow, high velocity, and high swirl that are typical of engine operation. Measurements

were made with a high-resolution spray patternator, a two-component laser velocimeter, and a single-component Phase/Doppler particle analyzer.

The comprehensive experimental data generated in these programs will be used to validate advanced models of turbulence, scalar, and spray transport, including two-equation turbulence models, algebraic and differential Reynolds stress models, scalar and scalar-velocity transport models, and Eulerian and Lagrangian deterministic and stochastic spray models.

SUMMARY

Although significant progress has been made in the development of three-dimensional analytical CFD codes and their application in future gas turbine combustor design, these codes are neither sufficiently comprehensive nor quantitatively accurate enough to permit a complete design alone. They are, however, a valuable component in an evolving combustor design methodology in which their capability is integrated with the substantial base of empirical experience and one-dimensional flow modeling.

CONCLUDING REMARKS

The NASA HOST sponsored Aerothermal Modeling Phase II programs will lead to significant improvements in our technical ability to predict nonreacting gas turbine combustor flow fields with and without spray injection. Significantly enhanced capabilities for accurately predicting combustor aerothermal performance and wall temperature levels and gradients will require further improvements in numerical schemes and physical submodels. It is equally important to collect fully-specified reacting flow data, similar to what is being done for nonreacting flows under HOST Phase II, for both complex constituent flows, and generic gas turbine combustors.

In parallel, work should continue in the formulation and systematic validation of turbulent combustion models for reacting sprays and multidimensional heat transfer models. These capabilities will provide the tools needed to analytically conduct the combustion trade-off studies so that optimum future combustion systems can be designed, fabricated, and developed within acceptable cost and schedule constraints.

REFERENCES

Bruce, T.W., Mongia, H.C., and Reynolds, R.S., 1979, "Combustor Design Criteria Validation, Vol. I - Element Tests and Model Validation," USARTL-TR-78-55I, (Avail. NITS, AD-A067657).

Ferrell, G.B., and Lilley, D.G., 1985, "Deflected Jet Experiments in a Turbulent Combustor Flowfield," NASA CR-174863.

Holdeman, J.E., Srinivasan, R., and Berenfeld, A., 1984, "Experiments in Dilution Jet Mixing," AIAA Journal, Vol. 22, no. 10, pp. 1436-1443.

Holdeman, J.D., and Srinivasan, R., 1986, "Modeling Dilution Jet Flowfields," Journal of Propulsion and Power, Vol. 2, No. 1, pp. 4-10.

Holdeman, J.D., Srinivasan, R., Coleman, E.B., Meyers, G.D., and White, C.D., 1987, "Effects of Multiple Rows and Noncircular Orifices on Dilution Jet Mixing," Journal of Propulsion and Power, Vol. 3, No. 3, pp. 219-226.

Holdeman, J.D., Reynolds, R., and White, C., 1987, "A Numerical Study of the Effects of Curvature and Convergence on Dilution Jet Mixing," AIAA Paper 87-1953.

Johnson, B.V., and Bennett, J.C., 1981, "Mass and Momentum Turbulent Transport Experiments with Confined Coaxial Jets," NASA CR-165574.

Johnson, B.V., Roback, R., and Bennett, J.C., 1984, "Scalar and Momentum Turbulent Transport Experiments with Swirling and Nonswirling Flows," Experimental Measurements and Techniques in Turbulent Reactive and Non-Reactive Flows, R.M.C. So, J.H. Whitlaw, and M. Sapp, eds., ASME, New York, pp. 107-119.

Kenworthy, M.J., Correa, S.M., and Burrus, D.L., 1983, "Aerothermal Modeling: Phase I Final Report - Volume 1 Model Assessment," NASA CR-168296.

Lebfevre, A.H., 1985, "Influence of Fuel Properties of Gas Turbine Combustor Performance," AFWAL-TR-84-1104, (Avail. NTIS, AD-A151464).

Lilley, D.G., 1986, "Lateral Jet Injection into Typical Combustor Flowfields," NASA CR-3997.

McDonell, V.G., Cameron, C.D., and Samuelsen, G.S., 1987, "Symmetry Assessment of a Gas Turbine Air-Blast Atomizer," AIAA Paper 87-2136.

McMurry, C.B., and Lilley, D.B., 1986, "Experiments on Two Opposed Lateral Jets Injected Into Swirling Crossflow," NASA CR-175041.

McVey, J.B., Kennedy, J.B., Russell, S., 1988, "Fuel-Injector/Air-Swirl Characterization Final Report," United Technologies Research Laboratories, United Technologies Research Center, NASA CR-180864.

McVey, J.B., Kennedy, J.B., Russell, S., 1988, "Application of Advanced Diagnostics to Airblast Injector Flows," to be presented at the 33rd International Aeroengine and Gas Turbine Congress, Amsterdam, the Netherlands.

Mongia, H.C., and Smith, K.G., 1978, "An Empirical/Analytical Design Methodology for Gas Turbine Combustors," AIAA Paper 78-998.

Mongia, H.C., Reynolds, R.S., Coleman, E., and Bruce, T.W., 1979, "Combustor Design Criteria Validation, Volume II - Development Testing of Two Full-Scale Annular Gas Turbine Combustors," USARTL-TR-78-55B-VOL-2. (Avail. NTIS, AD-A067689).

Mongia, H.C., and Reynolds, R.S., 1979, "Combustor Design Criteria Validation," Volume III - User's Manual," USARTL-TR-8-55C-VOL-3. (Avail. NTIS, AD-A066793).

Mongia, H.C., Reynolds, R.S., and Srinivasan, R., 1986, "Multidimensional Gas Turbine Combustion Modeling: Applications and Limitations," AIAA Journal, Vol. 24, no. 6, pp. 890-904.

Mongia, H., C., 1987, "A Status Report on Gas Turbine Combustor Modeling," presented at the AGARD Combustion and Fuels in Gas Turbine Engines Meeting, Crete, Oct. 12-16.

Mostafa, A.A., Mongia, H.C., McDonell, V.G., and Samuelsen, G.S., 1987, "On the Evolution of Particle-Laden Jet Flows: A Theoretical and Experimental Study," AIAA Paper 87-2181.

Mostafa, A.A., Mongia, H.C., McDonell, V.G., and Samuelsen, G.S., 1988, "On the Evolution of Particle-Laden Coaxial Jet Flows: A Theoretical and Experimental Study," AIAA Paper 88-0239.

Nikjooy, M., Karki, K.C., Mongia, H.C., McDonell, V.G., and Samuelsen, G.S. 1988, "K-E Turbulence Model Assessment with Reduced Numerical Diffusion for Coaxial Jets," AIAA Paper 88-0342.

Ong, L.H., and Lilley, D.G., 1986, "Measurements of a Single Lateral Jet Injected into Swirling Crossflow," NASA CR-175040.

Patankar, S.W., Karki, K.C., and Mongia, H.C., 1987, "Development and Evaluation of Improved Numerical Schemes for Recirculating Flows, AIAA Paper 87-0061.

Plee, S.L., and Mellor, A.M., 1979, "Characteristics Time Correlation for Lean Blowoff of Bluff-body Stabilized Flames," Combustion and Flame, Vol. 35, pp. 61-80.

Reynolds, R., and White, C., 1986, "Transition Mixing Study Final Report," NASA CR-175062.

Rizk, N.K., and Mongia, H.C., 1986, "Gas Turbine Design Methodology," AIAA Paper 86-1513.

Roback, R., and Johnson, B.V., 1983, "Mass and Momentum Turbulent Transport Experiments with Confined Coaxial Jets," NASA CR-168252.

Runchal, Aksai, K., Anand, M.S., and Mongia, H.C., 1987, "An Unconditionally-Stable Central Differencing Scheme for High Reynolds Number Flows. AIAA Paper 87-0060.

Sokolowski, D. E., and Ensign, C. R., 1986, "Toward Improved Durability in Advanced Combustors and Turbines - Progress in the Prediction of Aerothermal Loads," ASME Paper 86-GT-172. (NASA TM-88932),

Srinivasan, R., and Mongia, H.C., 1980, "Numerical Computations of Swirling Recirculating Flow Final Report," NASA CR-165196.

Srinivasan, R., Berenfeld, A., and Mongia, H.C., 1982, "Dilution Jet Mixing Program: Phase I Report," NASA CR-168031.

Srinivasan, R., Reynolds, R., Ball, I., Berry, R., Johnson, K., and Mongia, H., 1983, "Aerothermal Modeling Program: Phase I Final Report - Volume I," NASA CR-168243.

Srinivasan, R., Reynolds, R., Ball, I., Berry, R., Johnson, K., and Mongia, H., 1983, "Aerothermal Modeling Program: Phase I Final Report - Volume II," NASA CR-168243.

Srinivasan, R., Coleman, E., and Johnson, K., 1984, "Dilution Jet Mixing Program: Phase II Report," NASA CR-174624.

Srinivasan, R., Meyers, G., Coleman, E., and White, C., 1985, "Dilution Jet Mixing Program: Phase III Report." NASA CR-174884.

Srinivasan, R., and White, C., 1986, "Dilution Jet Mixing Program: Supplementary Report," NASA CR-175043.

Srinivasan, R., and Thorp, D.J., 1987, "Combustor Diffuser Interaction Program," AFWAL-TR-86-2093, Air Force Wright Aeronautical Labs, Wright Patterson AFB, OH.

Srivatsa, S.K., 1982, "Computations of Soot and NO_x Emissions from Gas Turbine Combustors," NASA CR-165196.

Sturgess, Geoffrey J., 1983, "Aerothermal Modeling: Phase I Final Report," NASA CR-168202.

Sullivan, R.E., Young, E.R., Miles, G.A., Williams, J.R., 1983, "Small Gas Turbine Combustor Primary Zone Study," NASA CR-168122.

Syed, S.A., Chiappetta, L.M., and Gosman, A.D., 1985, "Error Reduction Program," NASA CR-174776.

Turan, A., and VanDoormal, J.P., 1987, "Improved Numerical Methods for Turbulent Viscous Recirculation Flows," NASA CR-180852.

Turbine Engine Hot Section Technology (HOST) 1982 NASA TM-83022.

Turbine Engine Hot Section Technology 1983, NASA CP-2289.

Turbine Engine Hot Section Technology 1984, NASA CP-2339.

Turbine Engine Hot Section Technology 1985, NASA CP-2405.

Turbine Engine Hot Section Technology 1986, NASA CP-2444.

Turbine Engine Hot Section Technology 1987, NASA CP-2493.

Vanka, S.P., 1987, "Block-Implicit Computation of Viscous Internal Flows - Recent Results," AIAA Paper 87-0058.

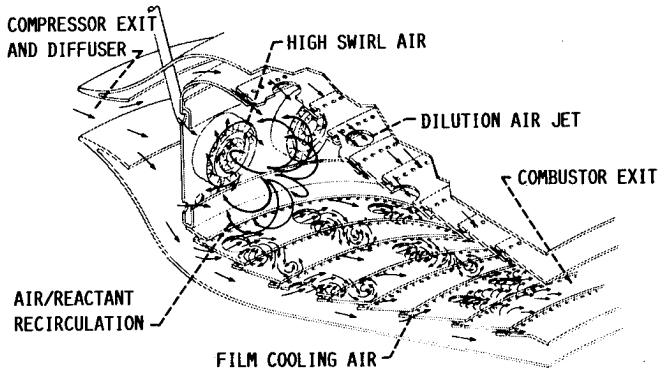

- FULLY 3-DIMENSIONAL FLOW
- HIGH TURBULENCE LEVELS
- CHEMICAL REACTION/HEAT RELEASE
- 2 PHASE WITH VAPORIZATION

FIGURE 1. - COMBUSTOR FLOW PHENOMENA.

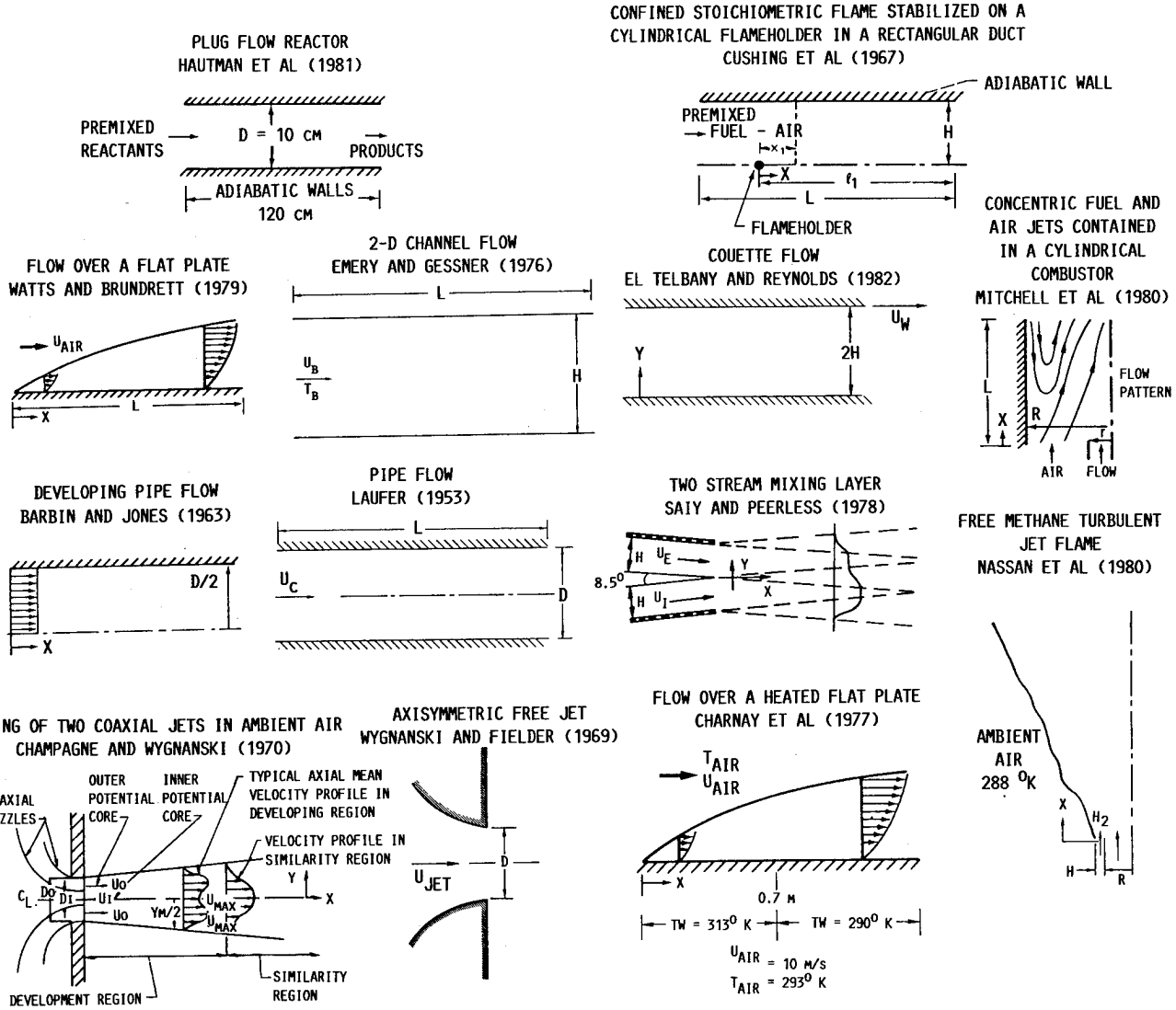

(A) SIMPLE FLOWS.

FIGURE 2. - FLOWS FOR WHICH ANALYTICAL MODEL CALCULATIONS WERE PERFORMED IN SRINIVASAN ET AL. (1983)

APL COMBUSTION TUNNEL

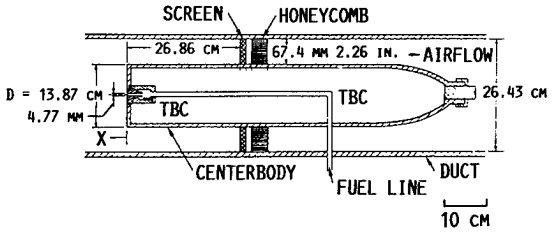

FLOW IN A CURVED CHANNEL
SHIVA PRASAD AND RAMA PRIYAN (1978)

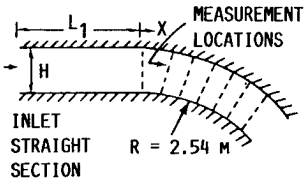

FLOW OVER A BACKWARD FACING PLANE STEP
KIM, KLINE, AND JOHNSTON (1978) AND EATON AND JOHNSTON (1980)

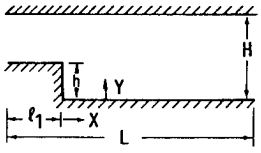

WEDGE-SHAPED FLAMEHOLDER

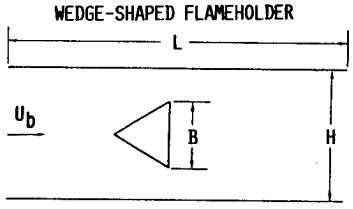

FLOW OVER A RING IN A PIPE
PHATARAPHRUK AND LOGAN (1979)

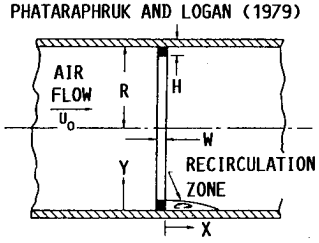

SUDDEN PIPE-EXPANSION
MOON AND RUDINGER (1977)

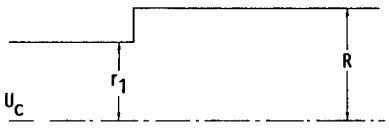

FLOW THROUGH A SUDDEN EXPANSION IN A PIPE
JOHNSON AND BENNETT (1981)

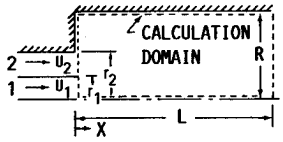

OPPOSED JET COMBUSTOR
SCHEFFER AND SAWYER (1976)

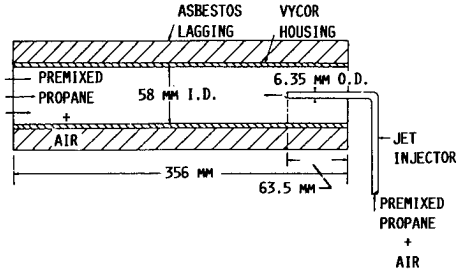

AXISYMMETRIC COMBUSTOR WITH
COAXIAL FUEL AND AIR JETS
LEWIS AND SMOOT (1973)

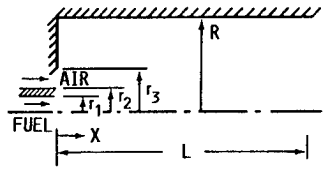

FLOW BEHIND A BACKWARD FACING STEP
PITZ AND DAILY (1981)

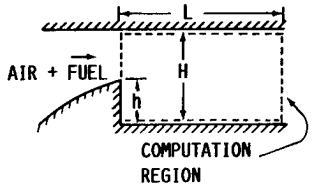

(B) COMPLEX NONSWIRLING FLOWS.

FIGURE 2. - CONTINUED.

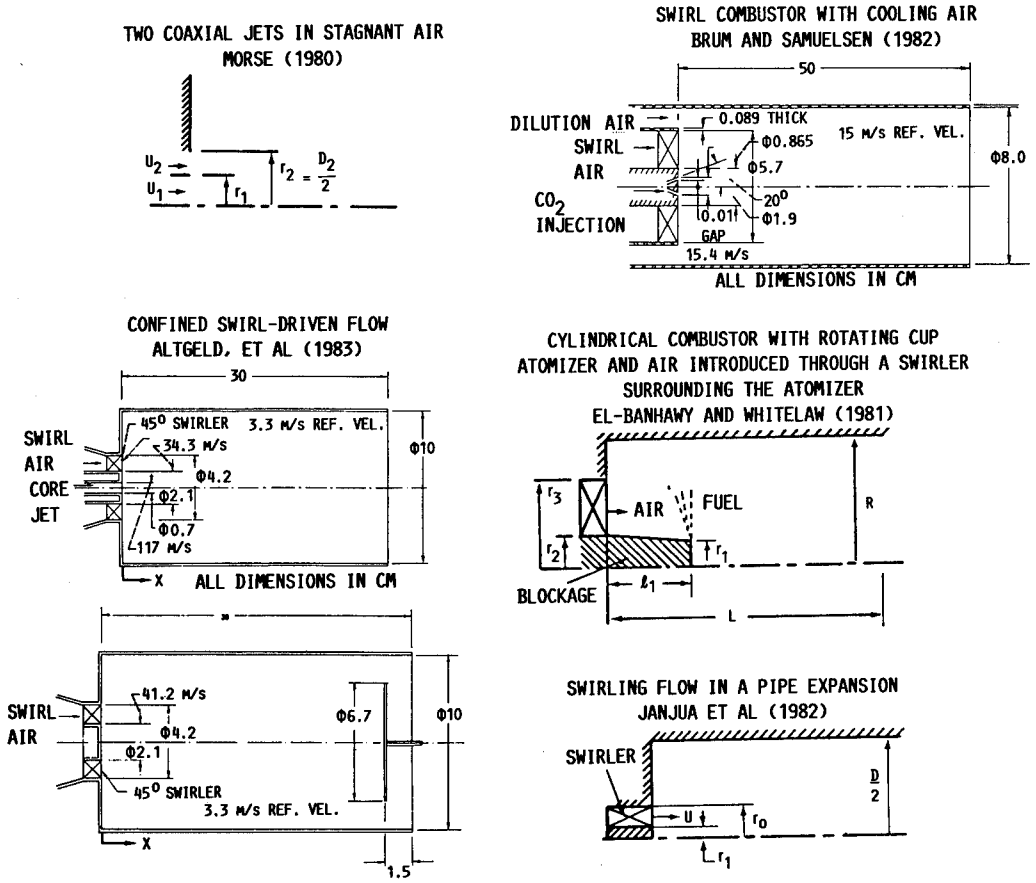

(C) SWIRLING FLOWS.

FIGURE 2. - CONCLUDED.

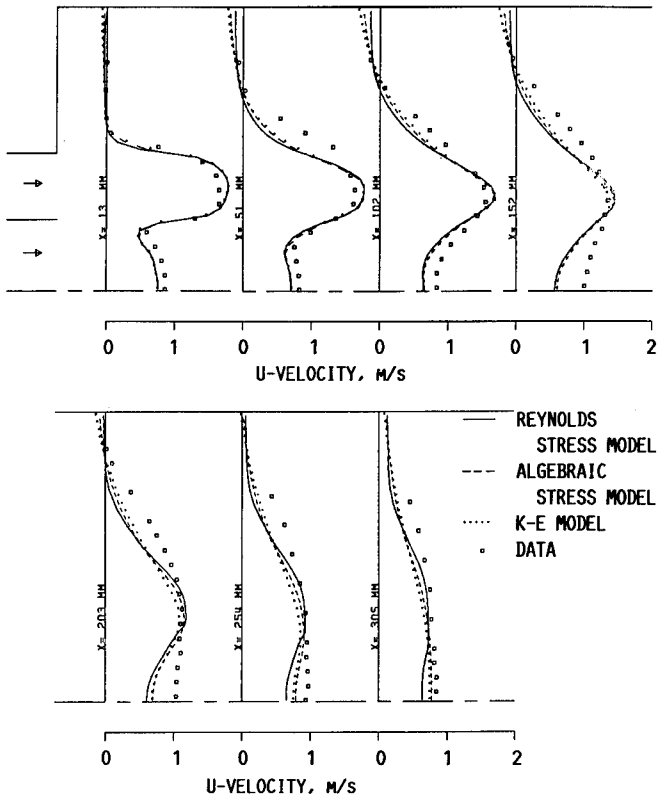

FIGURE 3. - COMPARISON OF MEASURED MEAN AXIAL VELOCITY PROFILES FOR COANNULAR JETS DOWNSTREAM OF AN AXISYMMETRIC SUDDEN EXPANSION, WITH CALCULATIONS MADE USING THREE TURBULENCE MODELS.

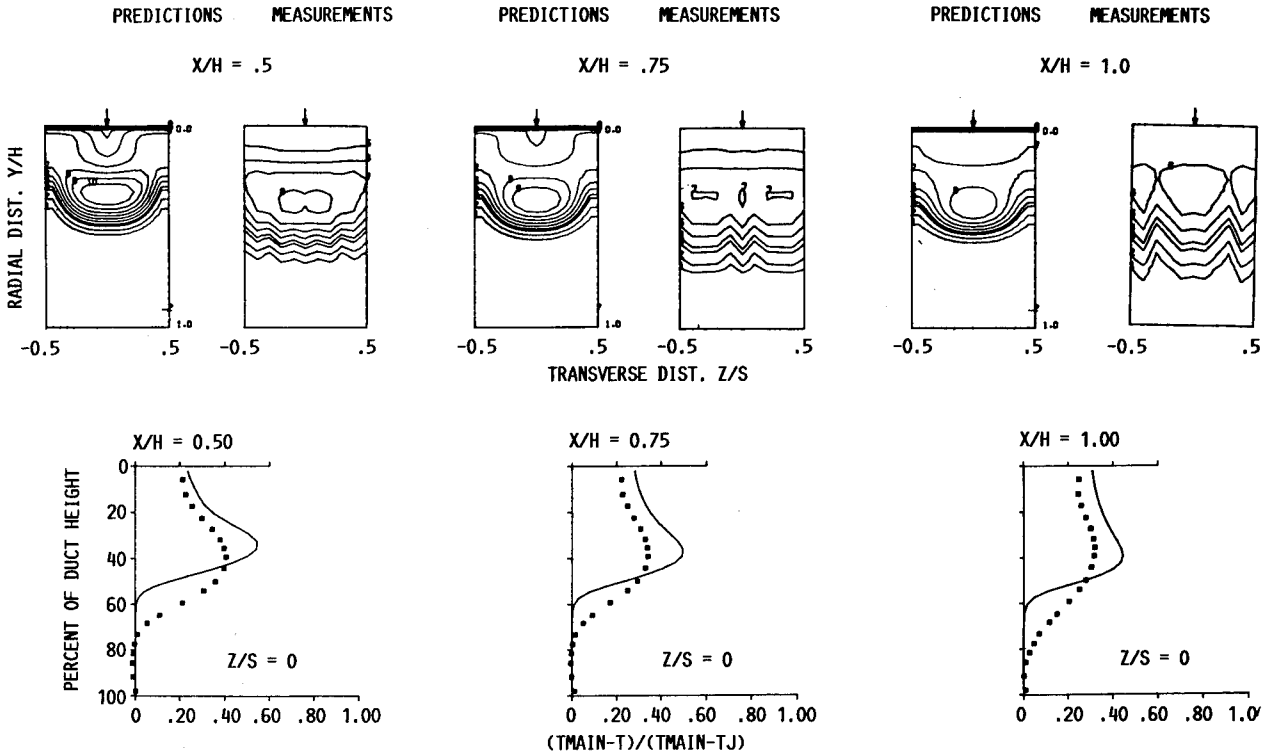

FIGURE 4. - COMPARISON BETWEEN MEASURED AND CALCULATED DIMENSIONLESS TEMPERATURE DIFFERENCE RATIOS DOWNSTREAM FROM A ROW OF COOL JETS INJECTED INTO A CONSTANT-TEMPERATURE CROSS FLOW FROM THE UPPER WALL OF A CONSTANT AREA DUCT (J = 25.32, S/H = 0.25, H/D = 8, 19 890 NODES.

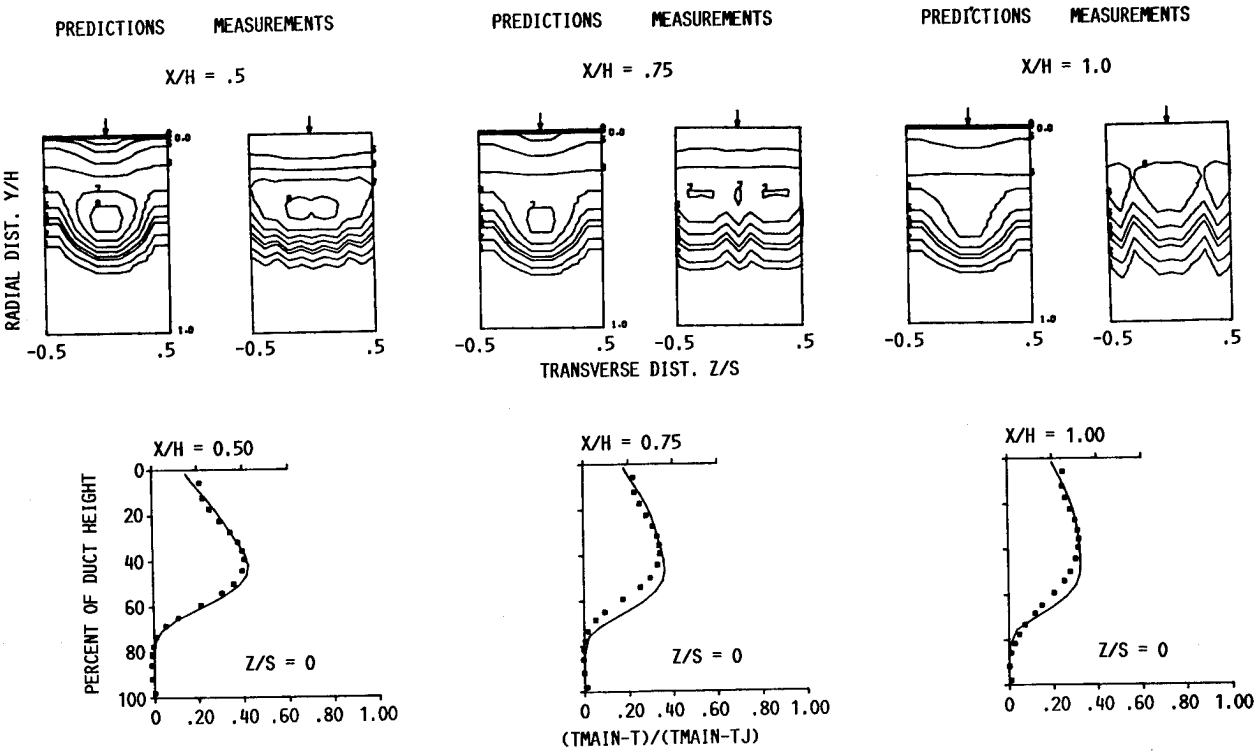

FIGURE 5. - COMPARISON BETWEEN MEASURED AND CALCULATED DIMENSIONLESS TEMPERATURE DIFFERENCE RATIOS DOWNSTREAM FROM A ROW OF COOL JETS INJECTED INTO A CONSTANT-TEMPERATURE CROSS FLOW FROM THE UPPER WALL OF A CONSTANT AREA DUCT (J = 25.32, S/H = 0.25, H/D = 8, 5615 NODES).

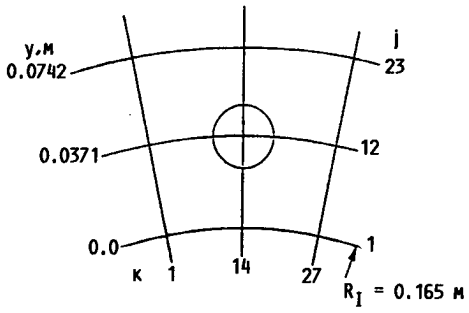

COMBUSTOR SECTOR END VIEW

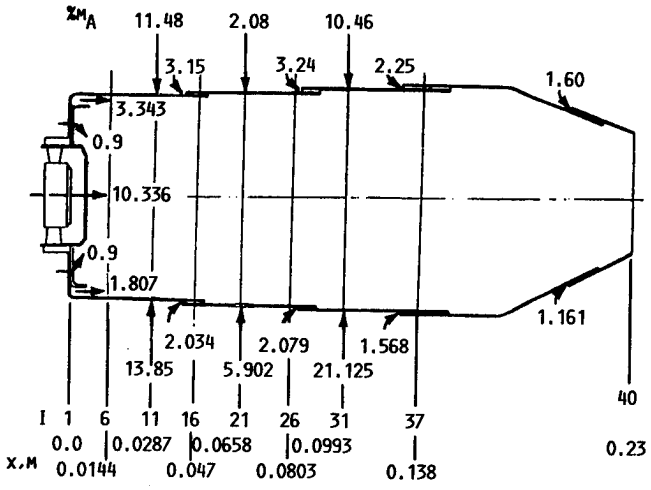

MAXIMUM POWER

$\dot{M}_A$ = 15.768 KG/S
P_3 = 1085.3 KPA
T_3 = 609.4 K
FAR = 0.0225

FIGURE 6. - ANNULAR COMBUSTOR SCHEMATIC AND CALCULATION GRID CONFIGURATION.

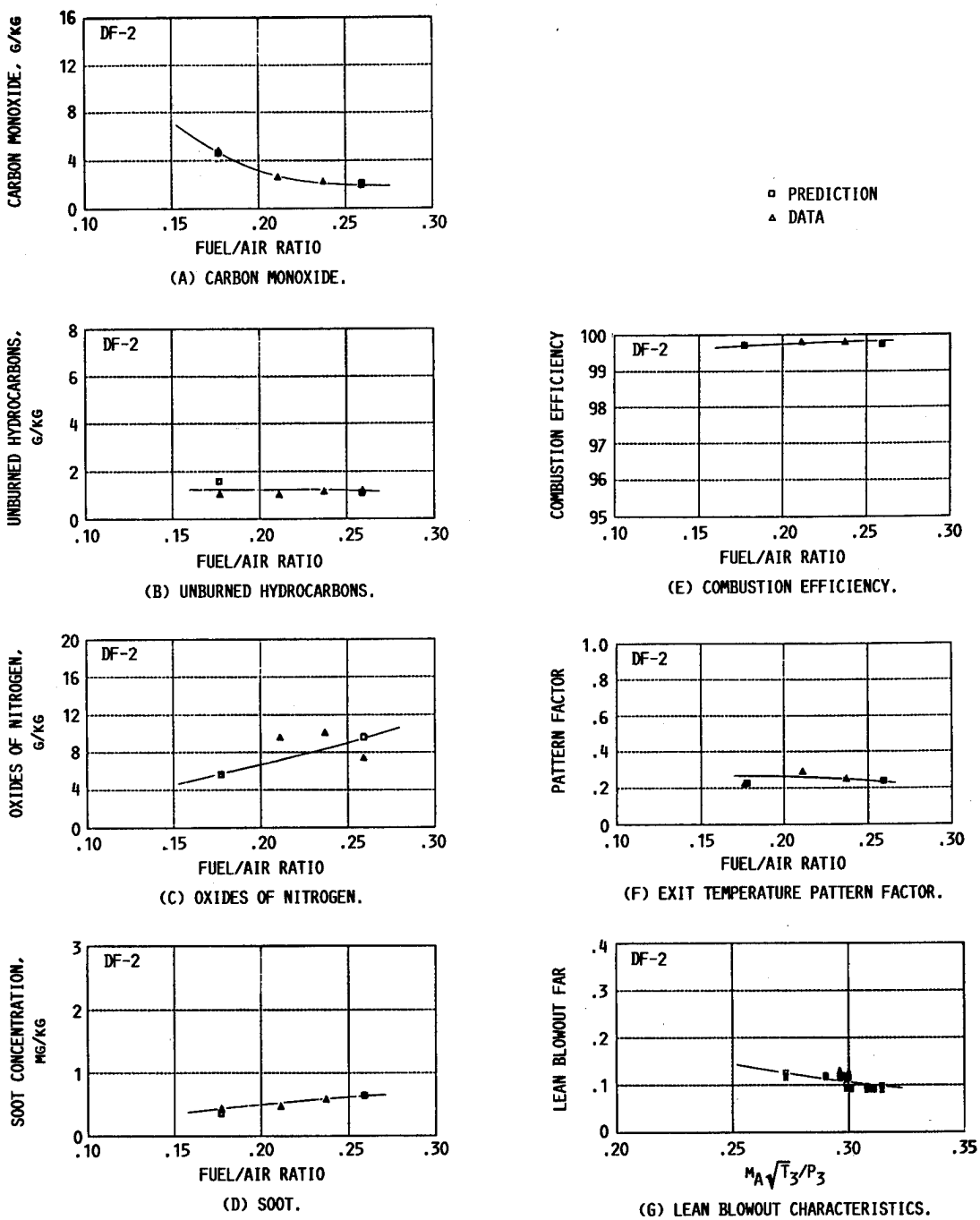

FIGURE 7. - COMPARISON OF MEASURED AND PREDICTED PERFORMANCE AND EMISSIONS FOR COMBUSTOR IN FIG. 6.

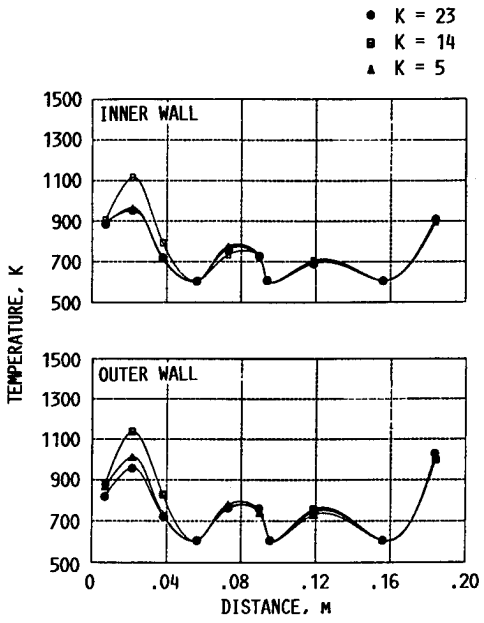

FIGURE 8. - CALCULATED LINER WALL TEMPERATURES AT MAXIMUM POWER CONDITION FOR COMBUSTOR IN FIG. 6.

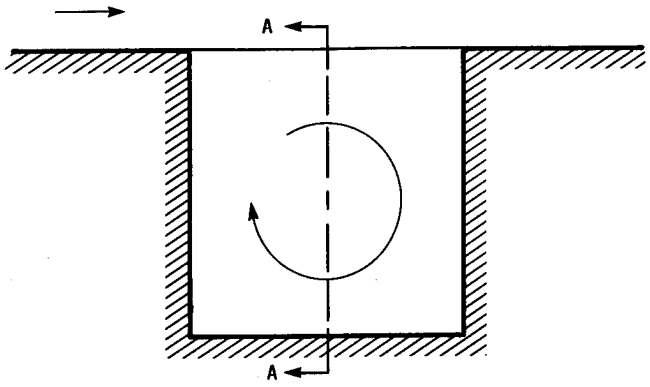

(A) FLOW SCHEMATIC.

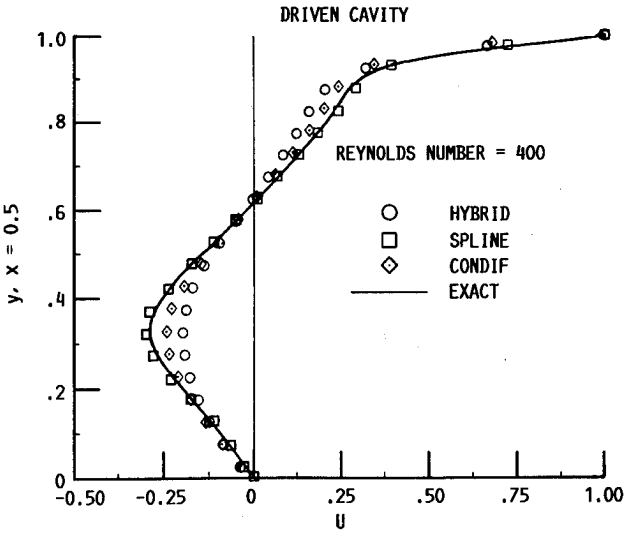

(B) VELOCITY PROFILES AT SECTION A-A.

FIGURE 9. - CALCULATIONS OF LAMINAR FLOW IN A SQUARE (2-D) DRIVEN CAVITY.

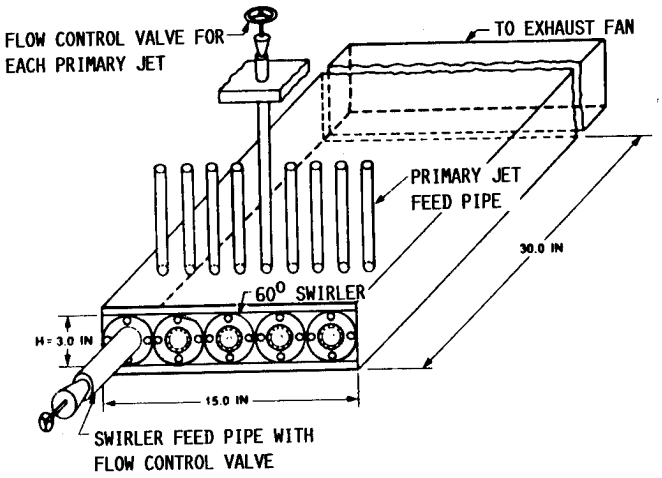

FIGURE 10. - TEST SECTION GEOMETRY FOR EXPERIMENTAL STUDY OF INTERACTION BETWEEN FLOW FROM MULTIPLE SWIRLERS AND TRANSVERSE JETS.

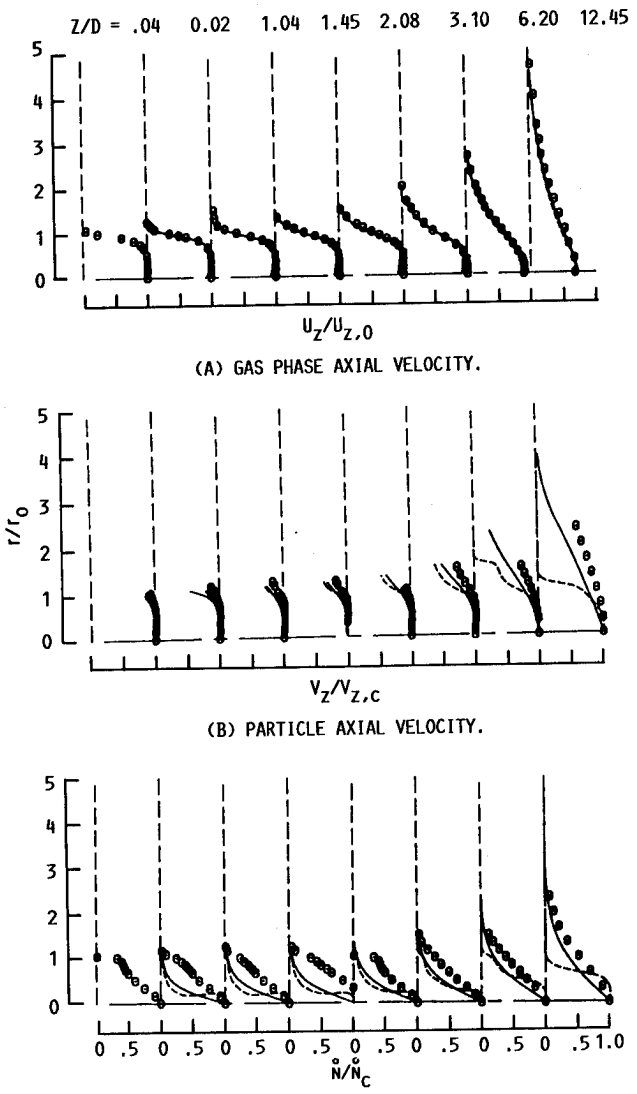

FIGURE 11. - RADIAL PROFILES OF GAS-AND SOLID-PHASE MEAN FLOW COMPONENTS AND PARTICLE NUMBER DENSITY AT A PARTICLE NUMBER DENSITY AT A PARTICLE-TO-GAS MASS LOADING RATIO OF 1.0.

REVIEW AND ASSESSMENT OF THE DATABASE AND NUMERICAL MODELING FOR TURBINE HEAT TRANSFER

H. J. Gladden and R. J. Simoneau
National Aeronautics and Space Administration
Lewis Research Center
Cleveland, Ohio

ABSTRACT

The objectives of the HOST Turbine Heat Transfer subproject were to obtain a better understanding of the physics of the aerothermodynamic phenomena and to assess and improve the analytical methods used to predict the flow and heat transfer in high-temperature gas turbines. At the time the HOST project was initiated, an across-the-board improvement in turbine design technology was needed. A building-block approach was utilized and the research ranged from the study of fundamental phenomena and modeling to experiments in simulated real engine environments. Experimental research accounted for approximately 75 percent of the funding while the analytical efforts were approximately 25 percent. A healthy government/industry/university partnership, with industry providing almost half of the research, was created to advance the turbine heat transfer design technology base.

NOMENCLATURE

B_x	airfoil axial chord
C	blade tip gap
C_x	axial flow speed
D	jet diameter/blade tip cavity depth
d	coolant channel hydraulic diameter
H	heat transfer coefficient
Ho	reference heat transfer coefficient
M_2	stator exit Mach number
Nu	Nusselt number
Nu_o	reference Nusselt number
P_c	coolant pressure
P_t	gas stream pressure
R	radius
Re_2	stator exit Reynolds number
Re_x	local Reynolds number
T_c	coolant temperature
T_G	gas stream temperature
T_w	airfoil temperature
Tu	turbulence intensity
S	surface distance
St	Stanton number
St_o	reference Stanton number
U	gas stream velocity
U_m	rotor wheel speed
U_w	moving surface velocity
u'	instantaneous velocity
V	coolant velocity
W	blade tip cavity width
X	axial length
θ	angle between mean velocity and major tip cavity axis
λ	length scale
Ω	rotational velocity

INTRODUCTION

Improved performance of aircraft gas turbine engines is typically accompanied by increased cycle pressure ratio and combustor exit gas temperature. The hot-section components of these turbojet/turbofan engines are subjected to severe aerothermal loads during the mission flight profile. Meeting the design goals of high cycle efficiency, increased durability of the hot-section components, and lower operating costs requires a multidisciplinary approach. Turbine Heat Transfer was one of the six disciplines addressed in the multidisciplinary Hot Section Technology (HOST) Project.

When the HOST Project was originally being planned, Stepka (1980), one of the originators of the project, performed an uncertainty analysis on the ability to predict turbine airfoil temperatures. He estimated that the then current ability to predict metal temperature in an operating engine was within 100 K and that by testing prototypes this could be refined to within 50 K. He also suggested that the uncertainty in heat flux was on the external or the hot gas side surface of the airfoil was a principle contributor to the inability to predict metal temperatures; however, both internal and external surface heat transfer were important. These levels of uncertainty in metal temperature can contribute to an order of magnitude uncertainty in component life.

A typical cooled aircraft gas turbine blade is illustrated in Fig. 1, showing the intricate internal flow passages and the variety of heat transfer mechanisms at work. These include: impingement cooling, serpentine passages with turbulator surfaces, and pin fins, all in very short (i.e., entrance length) distances and subject to strong rotational forces. In addition, since most blades are film cooled, the internal mass balance is a variable. The complexity of the external flow field over the turbine blade is illustrated in Fig. 2. Heat transfer in the external flow field is characterized by: high Reynolds number forced convection with rotation, high free-stream turbulence, strong pressure and temperature gradients, surface curvature, and an unsteady flow field. In addition, and most important, the internal and external surface heat transfer coefficients are coupled through the metal walls. In fact, the turbine airfoil is a very compact, very complex, and very efficient heat exchanger. This feature is particularly important in a durability program, such as HOST, where the real focus is on the thermal stress and fatigue of the structural elements.

Thus, in the HOST Turbine Heat Transfer Subproject it was important to direct research attention to both the internal and external surfaces of the turbine airfoil.

In the multidisciplinary HOST Project each participating discipline selected its own objective based on the greatest need in that particular area, rather than some common interdisciplinary goal. In Turbine Heat Transfer it was decided, based on evaluations of the type performed by Stepka (1980), that an across-the-board improvement in turbine heat transfer technology was needed. A ratcheting up of the overall technology; a moving from a correlation base to a more analytical base was identified as the Turbine Heat Transfer Subproject goal. It was also identified that the existing data base was insufficient to support this movement and increasing both the size and quality of the data base was essential. It was further recognized that HOST alone could not achieve this goal. It was hoped that HOST could be a sufficient catalyst and provide a sufficient forum to make this goal one that all of the partners; government, industry and universities; would find obtainable and worth pursuing.

This paper outlines the program directed at these goals. The paper will delineate progress towards the goals by reporting example results from each of the various research activities. It will summarize the major accomplishments and will make some observations on future needs.

TURBINE HEAT TRANSFER SUBPROJECT

The research program of the Turbine Heat Transfer Subproject was based on the idea that an across-the-board improvement in turbine design was needed. It was also based on an overall philosophy at NASA Lewis Research Center of taking a building block approach to turbine heat transfer, as shown in Fig. 3. The research ranged from the study of fundamental phenomena and modeling to experiments in real engine environments. Both experimental and analytical research were conducted.

Returning to Figs. 1 and 2, the range of phenomena addressed in the Turbine Heat Transfer Subproject are identified by numbers and arrows on these figures. The corresponding research programs are identified in Tables 1 and 2. One can see from these figures that the Turbine Heat Transfer Subproject covered most of the key heat transfer points on the turbine airfoil: film cooled airfoils, passage curvature, endwall flows, transitioning blade boundary layers, tip regions, and free-stream turbulence on the external surfaces. The subproject included impingement and turbulated serpentine passages on the internal surfaces. The program broke some new ground. An experiment was conducted, which obtained heat transfer data on the surfaces of the airfoils in a one and one-half stage large low speed rotating turbine. Another experiment acquired data on the internal turbulated serpentine passages subject to rotation at engine condition levels. Finally, vane heat transfer data were acquired in a real engine type environment behind an actual operating combustor.

Over the life of the HOST Project a little less than 5.5 million net research dollars were invested in the Turbine Heat Transfer Subproject. As shown in Fig. 4(a), there was a healthy government/industry/university partnership with industry providing almost half the research effort. Approximately three-fourths of the effort was experimental, as shown in Fig. 4(b). The majority of effort established a large number of major experimental datasets. These datasets have been well received and are expected to provide benchmarks for turbine heat transfer for many years to come. The analyses covered a wide range, including a three-dimensional Navier-Stokes effort; however, most of the analytic effort was focused on modeling local phenomena of key importance. The scope and range of the program is best seen by examining representative results.

EXPERIMENTAL DATABASE

The experimental part of the Turbine Heat Transfer Subproject consisted of six (6) large experiments and three (3) of somewhat more modest scope and was structured to address the phenomena identified in Figs. 1 and 2. Three (3) of the large experiments were conducted in a stationary frame of reference and three (3) were conducted in a rotating frame of reference.

Stationary Reference

One of the initial research efforts was the stator airfoil heat transfer program performed at the Allison Gas Turbine Division (Nealy et al., 1983; Hylton et al., 1983; Nealy et al., 1984; Turner et al., 1985; Yang et al., 1985). This research consisted of determining the effects of Reynolds number, turbulence level, Mach

number, temperature ratio, acceleration, and boundary layer transition on heat transfer coefficients for various airfoil geometries at simulated engine conditions. This research was conducted for nonfilm-cooled airfoils, showerhead film-cooled designs and showerhead/gill-region film cooling concepts. Typical results of this research are shown in Fig. 5. A typical cascade configuration is shown in the photograph (Fig. 5(a)). Two-dimensional midspan heat transfer coefficients and static pressure distributions were measured on the central airfoil of the three vane cascade. Nonfilm-cooled data are shown in Fig. 5(b) where the boundary layer transition is clearly identified as a function of Reynolds number on the suction surface. Figure 5(c) shows the effect on heat transfer in the downstream recovery region to the addition of showerhead film cooling. Data are presented as a Stanton number reduction. A detrimental effect is noted in the boundary layer transition region of the suction surface to the addition mass at the leading edge. Figure 5(d) shows a strong dependence on "gill-region" film cooling which is consistent with experience. However, when combining showerhead with gill-region film cooling more mass addition is not always better as indicated by the Stanton number reduction data on the pressure surface. This is a very extensive dataset which systematically shows the important effects of modern film cooling schemes on modern airfoils. It went beyond the traditional effectiveness correlations to provide actual heat transfer data. It should provide a valuable baseline for emerging analysis codes.

An investigation of secondary flow phenomena in a 90° curved duct was conducted at the University of Tennessee Space Institute (Crawford et al, 1985). The curved duct was utilized to represent airfoil passage curvature without the complexity of the horseshoe vortex. These data consist of simultaneous three-dimensional mean value and fluctuating components of velocity through the duct and compliment similar data in the literature. A schematic of the test facility and the three-dimensional laser velocimeter are shown in Fig. 6. The first phase of the research examined flows with a relatively thin inlet boundary layer and low free-stream turbulence. The second phase studied a thicker inlet boundary layer and higher free-stream turbulence. Typical experimental results of this research are shown in Fig. 6. The vector plot of cross-flow velocities clearly shows the development of a vortex in the duct corner near the low pressure surface. The analytical results will be mentioned in the Viscous Flow Analysis section. These data provide a comprehensive benchmark to verify codes at realistic flow conditions.

Two experiments were also conducted at NASA Lewis in the high-pressure facility (Gladden et al., 1985a; Gladden et al., 1985b; Gladden et al., 1987; Hippensteele et al., 1985). This facility was capable of testing a full-sized single-stage turbine at simulated real engine conditions. The tests, however, were limited to combined combustor/stator experiments. One experiment examined full-coverage film-cooled stator airfoils, while the second experiment utilized some of the advanced instrumentation developed under the instrumentation subproject. A comparison of experimental airfoil temperatures with temperatures obtained from a typical design system showed substantial differences for the full-coverage, film-cooled airfoils and suggests that models derived from low-temperature experiments are inadequate for "real-engine" conditions. The advanced instrumentation tests demonstrated the capability and the challenges of measuring heat flux and time-resolved gas temperature fluctuation in a real-engine environment.

Typical results are shown in Fig. 7 for thin film thermocouples and the dynamic gas temperature probe tested a simulated real engine condition. A comparison is made between steady state heat flux measurements and those determined from dynamic signal analysis techniques.

Stanford University has conducted a systematic study of the physical phenomena that affect heat transfer in turbine airfoil passages. Their recent experimental research has been concerned with high free-stream turbulence intensity and large turbulence scale that might be representative of combustor exit phenomena. A schematic of their free jet test facility and typical results are shown in Fig. 8. Data are measured on a constant temperature flat plate located at a specified radial and axial distance from the jet exit centerline. These data, presented as Stanton number ratios, indicate that heat transfer augmentation can be as high as 5X at a high value of free-stream turbulence intensity but only 3X if the length scale is changed. These results suggest that the designer must know a great deal more about the aerodynamic behavior of the flow field in order to successfully predict the thermal performance of the turbine components.

Prior to the advent of the HOST program, Arizona State University was pursuing a systematic study of impingement heat transfer with cross-flow characteristic of turbine airfoil cooling schemes. The work was initially sponsored by a NASA Lewis grant but was subsequently funded by the HOST program. The results of this research are summarized in Florschuetz et al. (1982a), Florschuetz et al. (1982b), Florschuetz et al. (1982c), Florschuetz et al. (1983), Richards et al. (1984), Florschuetz et al (1984), Florschuetz et al. (1987), Florschuetz et al. (1985), Florschuetz et al. (1984). In addition to the many geometry variations, this research also investigated the effects of various jet-flow to crossflow ratios and differences between the jet-flow and the cross-flow temperature. Correlations were developed for both inline rows of impingement jets and staggered arrays of jets but without an initial cross-flow. The effects of cross-flow and temperature differences were then determined relative to the base correlations.

Rotating Reference

In the rotating reference frame, experimental aerodynamic and heat transfer measurements were made in the large, low-speed turbine at the United Technologies Research Center (Dring et al., 1987; Dring et al., 1986a; Dring et al., 1986b; Dring et al., 1986c; Blair et al., 1988; Blair et al., 1988). Single-stage data with both high and low-inlet turbulence were taken in phase I. The second phase examined a one and one-half stage turbine and focused on the second vane row. Under phase III aerodynamic quantities such as interrow time-averaged and rms values of velocity, flow angle, inlet turbulence, and surface pressure distributions were measured. A photograph of the test facility is shown in Fig. 9. Typical heat transfer data for both the first stator and rotor are also shown. These data show that an increase of inlet turbulence has a substantial impact on the first stator heat transfer. However, the impact on the rotor heat transfer is minimal. These data are also compared with Stanton numbers calculated by a boundary layer code and the assumption that the boundary layer was either laminar (LAM) or fully turbulent (TURB). These assumptions generally bracketed the data on the suction surface of both the stator and the rotor. However, the heat transfer on the pressure surface, especially for the high turbulence case, was generally above even fully turbulent levels on both airfoils. Pressure surfaces have traditionally received less

attention than suction surfaces. The high heat transfer on the pressure surface is not readily explainable and calls for additional research, especially modeling, on pressure surfaces.

The tip region of rotor blades is often a critical region and an area that suffers substantial damage from the high temperature environment. Arizona State University has experimentally modeled the blade tip cavity region and determined heat transfer rates by a mass transfer analogy with naphthylene (Chyu et al., 1987). A schematic of the test is shown in Fig. 10.

The blade tip cavity is a stationary model and the relative velocity of the shroud is represented by a moving surface at a specified "gap" spacing from the blade. Stanton number results for two different cavity aspect ratios are also shown in Fig. 10. The heat transfer on the surfaces next to the shroud are little changed by the aspect ratio which is not surprising. However, the heat transfer to the floor of the cavity is increased significantly on the downstream portion at the lower aspect ratio. Also shown in the figure is the flow angle effect on heat transfer. Because of the airfoil turning at the tip the cavity will be at different angles of attack to the mean crossflow direction. The data shows a minimal effect at an aspect ratio of 0.9 and a substantial effect at an aspect ratio of 0.23. This dataset is really quite a new addition to a traditionally neglected area and shows that with careful datasets and analyses one can obtain an optimal design for tip cavities.

The preceeding studies were focused on the hot-gas side phenomena. Since the heat transfer phenomena is driven by the hot-gas side conditions, it is appropriate to concentrate resources on this area. However, the coolant-side heat transfer is also important. Therefore, coolant passage heat-transfer and flow measurements in a rotating reference frame were also obtained at Pratt & Whitney Aircraft/United Technologies Research Center (Kopper, 1984; Sturgess et al., 1987; Lord et al., 1987). Experimental data were obtained for smooth-wall serpentine passages and for serpentine passages with skewed and normal turbulators. The flow and rotation conditions were typical of those found in actual engines. This was a very realistic experiment. Data for both the smooth-wall and skewed turbulator passages are shown in Fig. 11 for radial outflow, representing only a tiny fraction of the total data involved in this very complex flow. Both datasets are shown correlated with the rotation number except for high rotation numbers on the high pressure surface. This is an area that requires additional research to understand and model the physical phenomena occurring in these passages.

ANALYTICAL TOOLS

The analytic parts of the turbine heat transfer subproject are characterized by efforts to adapt existing codes and analyses to turbine heat transfer. In general, these codes and analyses were well established before HOST became involved; however, the applications were not for turbine heat transfer, and extensive revision has often been required. In some cases the analytic and experimental work were part of the same contract.

Boundary Layer Analysis

The STAN5 boundary-layer code (Crawford et al., 1976) (which was developed on NASA contract at Stanford University in the mid-1970's) was modified by Allison Gas Turbine Division to define starting points and transition length of turbulent flow to accommodate their data, with and without film cooling, as well as data in the literature. Specific recommendations are made to improve turbine airfoil heat transfer modeling utilizing a boundary layer analysis. These recommendations address the boundary conditions, the initial condition specification, including both velocity and thermal profiles, and modifications of conventional zero order turbulence models. The results of these improvements are shown in Fig. 12 where the start of transition and its extent on the suction surface are reasonably well characterized. For the case of showerhead film cooling, two empirical coefficients were utilized to modify the free-stream turbulence intensity and the gas stream enthalpy boundary conditions and permit a representative prediction of the Stanton number reduction in the recovery region. Boundary layer methods can be used for midspan analysis, however they require a realistic data base to provide the coefficients needed for proper reference.

In another boundary layer code effort United Technologies Research Center assessed the applicability of its three-dimensional boundary layer code to calculate heat transfer total pressure loss and streamline flow patterns in turbine passages. The results indicate a strong three-dimensional effect on a turbine blade, and agrees qualitatively with experimental data. The same code was modified for use as a two-dimensional unsteady code in order to analyze the rotor-stator interaction phenomena (Vatsa, 1985; Anderson et al., 1985a; Anderson et al., 1985b; Anderson, 1985c). These codes also needed data as input.

Finally, a fundamental study on numerical turbulence modeling, directed specifically at the airfoil in the turbine environment, was conducted at the University of Minnesota. A modified form of the Lam-Bremhorst low-Reynolds-number k-e turbulence model was developed to predict transitional boundary layer flows under conditions characteristic of gas turbine blades (Schmidt et al., 1987) including both free-stream turbulence and pressure gradient.

The purpose was to extend previous work on turbulence modeling to apply the model to transitional flows with both free-stream turbulence and pressure gradients. The results of the effort are compared with the experimental data of Allison Gas Turbine Division in Fig. 13. The augmentation of heat transfer on the pressure surface over the fully turbulent value is predicted reasonably well. In addition, when an adverse pressure gradient correction is utilized, the suction surface heat transfer data is also predicted reasonably well.

This was a reasonably good beginning to establishing a methodology for moving away from the heavy dependence on empirical constants. Although boundary layer methods will never solve the whole problem, they will always remain important analytic tools.

Viscous Flow Analysis

The three-dimensional Navier-Stokes TEACH code has been modified by Pratt & Whitney for application to internal passages and to incorporate rotational terms. The modified code has been delivered to NASA Lewis and tested on some simple geometric cases. The results of this effort indicate that the code is qualitatively adequate for simple geometries. For geometries of practical interest, much work remains to be done to bring the internal passage computational codes up to the level of proficiency of the free-stream codes. For the external airfoil surface important analytic progress is being made. By contrast, the work on internal passages is still primitive. The internal problem is substantially more complex.

A fully elliptic three-dimensional Navier-Stokes code has been under development at Scientific Research

Associates (SRA) for many years. This code was primarily directed at inlets and nozzles. SRA, Inc., has modified the code for turbine applications (Weinberg et al., 1985). This includes grid work for turbine airfoils, adding an energy equation and turbulence modeling, and improved user friendliness. The heat transfer predictions from the MINT code are shown in Fig. 14 compared to the data from the Allison Gas Turbine research. The analytical/experimental data comparison is good, however, the location of boundary layer transition was specified for the analytical solution.

The University of Tennessee Space Institute also developed a three-dimensional viscous flow analysis capability for the curved duct experiment utilizing the P.D. Thomas code (Thomas, 1979) as a base. Some analytical results from this code are shown in Fig. 6 where a vector plot of the cross-flow velocities are compared with the experiment. In addition, a stream sheet is shown as it propagates through the duct and is twisted and stretched. Additional comparisons of analysis and experiment show that the thin turbulent boundary layer results of this experiment are difficult to calculate with current turbulence models.

CONCLUDING REMARKS

Since this paper is an overview of the Turbine Heat Transfer aspects of the HOST program it has been presented as a cataloging and summarizing of the various activities. More importantly, the HOST program should be viewed as a catalyst bringing together the gas turbine community and building a technology momentum to carry advanced propulsion systems into the future. Specifically, the HOST Turbine Heat Transfer Subproject can point to the following accomplishments.

1. The impact of axial spacing and inlet turbulence on heat transfer and aerodynamics throughout the stator-rotor-stator of a stage and one-half axial turbine was measured. High-turbulence and post-transitional effects on the pressure surface of both stator and rotor can cause the Stanton number to be greater than the fully turbulent value.

2. Reynolds number, Mach number, curvature, and wall-to-gas temperature effects on boundary layer transition and heat transfer were determined for a stator airfoil.

3. Showerhead and "gill-region" film-cooling were shown to have both beneficial and adverse effects on the recovery region heat transfer at simulated engine conditions which depended on specific operating conditions.

4. Heat Transfer in both smooth-wall and turbulated-wall serpentine rotating coolant passages were correlated with a rotation number for the low-pressure surface. The high-pressure surface heat transfer was not well correlated.

5. Blade tip cavity heat transfer was shown to be strongly dependent on the cavity aspect ratio and angle-of-attack to blade tip flow direction.

6. Heat transfer measurements in high-turbulence intensity flow fields, simulating combustor exit phenomena, shows augmentation rates of 3X to 5X depending on the length scale of the turbulence.

7. Improved definition of the initial conditions and boundary conditions which are applicable to turbine airfoils was successful in improving the prediction of airfoil heat transfer for a wide range of geometries using the STAN5 boundary layer code.

8. The Lam-Bremhorst low-Reynolds number k-e turbulence model was modified to also improve the predictions of airfoil heat transfer under transitional flows with both free-stream turbulence and pressure gradients.

9. A fully elliptic Navier-Stokes code was developed for turbine airfoils and includes turbulence modeling, an energy equation and improved user friendliness.

Frequently, heat transfer is a limiting factor in the performance and durability of an engine. However, as we continue to pursue higher and higher speeds, advancing technology becomes an interdisciplinary effort involving aerothermal loads definition and the structural response of advanced materials. This is especially true for hypersonic vehicles where the overall thermal management and design of the vehicle and the propulsion system become an integrated interactive entity. We now have, or are developing, tremendous analytical capabilities with which one can attack these very complex technology issues.

LOOK TO THE FUTURE

Many recent studies have been made to assess the aeropropulsion technology requirements into the 21st century. The consensus seems to suggest that significant technology advances are required to meet the goals of the future. Whether the goals are high speed sustained flight, single-stage-to-orbit or subsonic transport, the issues for the designer are improved fuel efficiency, high thrust-to-weight, improved component performance while maintaining component durability and reduced operating and maintenance costs. These issues will only serve to increase the "opportunities" available to the researcher in aerothermal loads and structures analysis. The verifiable predictions of unsteady flowfields with significant secondary flow phenomena and coupled thermal/velocity profiles is a fertile research area. Very little progress has been made to date in applying CFD techniques to the intricate and complex coolant channels required in the hot-section components. With the expected advances in high-temperature materials the components with significant aerothermal loads problems will expand beyond the airfoils and combustor liners to shrouds, rims, seals, bearings, compressor blading, ducting, nozzles, etc. The issues to be addressed and the technology advances required to provide the aeropropulsion systems of the 21st century are quite challenging.

REFERENCES

Anderson, O. L., 1985a, "Assessment of a 3-D Boundary Layer Analysis to Predict Heat Transfer and Flow Field in a Turbine Passage," NASA CR-174894.

Anderson, O. L., 1985b, "Calculation of Three-Dimensional Boundary Layers on Rotating Turbine Blades," Three Dimensional Flow Phenomena in Fluid Machinery, A. Hamed, J. Herring, and L. Povinelli, eds., ASME, New York, pp. 121-132.

Anderson, O. L., and Caplin, B., 1985c, "User's Manual for Three Dimensional Boundary Layer (BL3-D) Code," NASA CR-174899.

Blair, M. F., Dring, R. P., and Joslyn, H. D., 1988a, "The Effects of Turbulence and Stator/Rotor Interactions on Turbine Heat Transfer, Part II - Effects of Reynolds Number and Incidence," ASME Paper to be presented at the 33rd ASME Gas Turbine Conference, The Netherlands.

Blair, M. F., Dring, R. P., and Joslyn, H. D., 1988b, "The Effects of Turbulence and Stator/Rotor Interactions on Turbine Heat Transfer, Part I - Design Operating Conditions," ASME Paper to be presented at the 33rd ASME Gas Turbine Conference, The Netherlands.

Chyu, M. K., Metzger, D. E., and Hwan, C. L., 1987, "Heat Transfer in Shrouded Rectangular Cavities," Journal of Thermophysics and Heat Transfer, Vol. 1, No. 2, pp. 247-252.

Crawford, M.E., and Kay, W. M., 1976, "STAN5 - A Program for Numerical Computation of Two-Dimensional Internal and External Boundary Layer Flows," NASA CR-2742.

Crawford, R. A., et al, 1985, "Mean Velocity and Turbulence Measurements in a 90° Curved Duct With Thin Inlet Boundary Layer," NASA CR-174811.

Dring, R. P., Blair, M. F., and Joslyn, H. D., 1986a, "The Effects of Inlet Turbulence and Rotor Stator Interactions on the Aerodynamics and Heat Transfer of a Large-Scale Rotating Turbine Model. Vol. III, Heat Transfer Data Tabulation. 65% Axial Spacing," NASA CR-179468.

Dring, R. P., Blair, M. F., and Joslyn, H. D., 1986b, "The Effects of Inlet Turbulence and Rotor/Stator Interactions on the Aerodynamics and Heat Transfer of a Large-Scale Rotating Turbine Model. Vol. IV, Aerodynamic Data Tabulation," NASA CR-179469.

Dring, R. P., Blair, M. F., and Joslyn, H. D., 1986c, "The Effects of Inlet Turbulence and Rotor Stator Interactions on the Aerodynamics and Heat Transfer of a Large-Scale Rotating Turbine Model. Vol. II, Heat Transfer Data Tabulation. 15% Axial Spacing," NASA CR-179467.

Dring, R. P., et al, 1987, "The Effects of Inlet Turbulence and Rotor/Stator Interactions on the Aerodynamics and Heat Transfer of a Large-Scale Rotating Turbine Model, Vol. I," NASA CR-4079.

Florschuetz, L. W., and Isoda, Y., 1982a, "Flow Distributions and Discharge Coefficient Effects for Jet Array Impingement With Initial Crossflow," ASME Paper 82-GT-156.

Florschuetz, L. W., et al, 1982b, "Jet Array Impingement Flow Distributions and Heat Transfer Characteristics - Effects of Initial Crossflow and Nonuniform Array Geometry - Gas Turbine Engine Component Cooling," NASA CR-3630.

Florschuetz, L. W., Metzger, D. E., and Su, C. C., 1983, "Heat Transfer Characteristics for Jet Array Impingement with Initial Crossflow," ASME Paper 83-GT-28.

Florschuetz, L. W., and Tseng, H. H., 1984a, "Effect of Nonuniform Geometries on Flow Distributions and Heat Transfer Characteristics for Arrays of Impinging Jets," ASME Paper 84-GT-156.

Florschuetz, L. W., and Metzger, D. E., 1984b, "Effect of Initial Crossflow Temperature on Turbine Cooling With Jet Arrays," Heat and Mass Transfer in Rotating Machinery, D.E. Metzger and N. Afgan, eds., Hemisphere Publishing Corp., Washingotn, D.C., pp. 499-510.

Florschuetz, L. W., and Su, C. C., 1985, "Heat Transfer Characteristics Within an Array of Impinging Jets," NASA CR-3936.

Florschuetz, L. W., and Su, C. C., 1987, "Recovery Effects on Heat Transfer Characteristics Within an Array of Impinging Jets," Heat Transfer and Fluid Flow in Rotating Machinery, W.J. Yang, ed., Hemisphere Publishing Corp., Washington, D.C., pp. 375-387.

Gladden, H. J., Yeh, F. C., and Fronek, D. L., 1985a, "Heat Transfer Results and Operational Characteristics of the NASA Lewis Research Center Hot Section Cascade Test Facility," ASME Paper 85-GT-82. (NASA TM-86890).

Gladden, H. J., and Proctor, M. P., 1985b, "Transient Technique for Measuring Heat Transfer Coefficients on Stator Airfoils in a Jet Engine Environment," AIAA Paper 85-1471. (NASA TM-87005).

Gladden, H. J., Yeh, F. C., and Austin, P. J. Jr., 1987, "Computation of Full-Coverage, Film-Cooled Airfoil Temperatures by Two Methods and Comparison With High Heat Flux Data," ASME Paper 87-GT-213. (NASA TM-88931).

Hippensteele, S. A., Russell, L. M., and Torres, F. J., 1985, "Local Heat-Transfer Measurements on a Large Scale-Model Turbine Blade Airfoil Using a Composite of a Heat Element and Liquid Crystals," ASME Paper 85-GT-59. (NASA TM-86900).

Hylton, L. D., et al, 1983, "Analytical and Experimental Evaluation of the Heat Transfer Distribution Over the Surfaces of Turbine Vanes," NASA CR-168015.

Kopper, F.C., 1984, "Coolant Passage Heat Transfer With Rotation," Turbine Engine Hot Section Technology, NASA CP-2339, pp. 401-409.

Lord, W. K., Pickett, G. F., Sturgess, G. J., and Weingold, H. D., 1987, "Application of CFD Codes to the Design and Development of Propulsion Systems," Supercomputing in Aerospace, NASA CP-2454, P. Kutler and H.Yee, eds., NASA, Washington, D.C., pp. 139-148.

Nealy, D. A., et al, 1983, "Measurement of Heat Transfer Distribution Over the Surfaces of Highly Loaded Turbine Nozzle Guide Vanes," ASME Paper 83-GT-53,.

Nealy, D. A., Mihelc, M. S., Hylton, L. D., and Gladden, H. J., 1984, "Measurements of Heat Transfer Distribution Over the Surfaces of Highly Loaded Turbine Nozzle Guide Vanes," Journal of Engineering for Gas Turbines and Power, Vol. 106, No. 1, pp. 149-158.

Richards, D. R., and Florschuetz, L. W., 1984, "Forced Convection Heat Transfer to Air/Water Vapor Mixtures," NASA CR-3769.

Schmidt, R. C., and Patankar, S. V., 1987, "Prediction of Transition on a Flat Plate Under the Influence of Free-Stream Turbulence Using Low-Reynolds-Number Two-Equation Turbulence Models," ASME Paper 87-HT-32.

Stepka, F. S., 1980, "Analysis of Uncertainties in Turbine Metal Temperature Predictions," NASA TP-1593.

Sturgess, G. J., and Datta, P., 1987, "Calculation of Flow Development in Rotating Passages for Cooled Gas Turbine Blades," Computers in Engineering - 1987, Vol. 3, ASME, New York, pp. 149-158.

Thomas, P. D., 1979, "Numerical Method for Predicting Flow Characteristics and Performance of Nonaxisymmetric Nozzles Theory," NASA CR-3147.

Turner, E. R., et al, 1985, "Turbine Vane External Heat Transfer, Vol. I - Analytical and Experimental Evaluation of Surface Heat Transfer Distributions With Leading Edge Showerhead Film Cooling," NASA CR-174827.

Vatsa, V. N., 1985, "A Three-Dimensional Boundary Layer Analysis Including Heat-Transfer and Blade-Rotation Effects," 3rd Symposium on Numerical and Physical Aspects of Aerodynamic Flows, T. Cebeci, ed., California State University, pp. 10-45 to 10-59,

Weinberg, B. C., et. al, 1985 "Calculations of Two- and Three-Dimensional Transonic Cascade Flow Fields Using the Navier-Stokes Equations," ASME Paper 85-GT-66.

Yang, R. J., et al, 1985, "Turbine Vane External Heat Transfer, Vol. II - Numerical Solutions of the Navier-Stokes Equations for Two- and Three-Dimensional Turbine Cascades With Heat Transfer," NASA CR-174828.

TABLE I. - TURBINE HEAT TRANSFER SUBPROJECT SUMMARY

Figures 1 and 2	Work element	Results
Nonrotating experiments		
		Provide fundamental experimental data bases with focus on -
1	Airfoil with film cooling[a]	Film cooling
11	Curved duct	Secondary flows
3	Impingement cooling	Impingement pattern correlations
5	Large-scale, high-intensity turbulence	Combustor exit simulation
6	Real engine environment	The real environment
Rotating experiments		
8	Large low-speed turbine[a]	Rotor-stator interaction
2	Rotating coolant passage	Coriolis and buoyancy effects
4	Tip region simulator	Flow across moving airfoil tip
9	Warm core turbine	Vane and blade passage flow map fully scaled
Analyses		
		Enhance analytic tools for turbine application
1	STAN5 modifications[a]	Adapt boundary layer code to current airfoil data
10	Three-dimensional boundary layer	Zoom focus on Three-dimensional regions
8	Unsteady boundary layer[a]	Account for rotor-stator interaction effects
2	Teach code with rotation[a]	Three-dimensional Navier-Stokes with rotation terms
7	Low Reynolds number	Develop turbine airfoil specific turbulence model
12	Mint code[b]	Three-dimensional Navier-Stokes applied to turbine airfoil geometry

[a]Experiment and analysis in the same contract.
[b]Work done under two separate contracts.

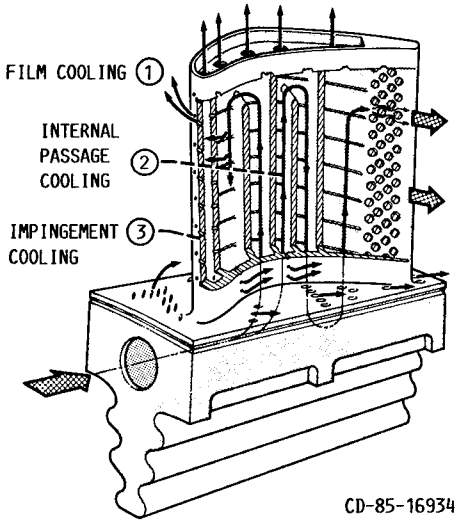

FIGURE 1. - TYPICAL COOLED AIRCRAFT GAS TURBINE BLADE. SEE TABLE I FOR DESCRIPTION OF NUMBERED FLOW PHENOMENA.

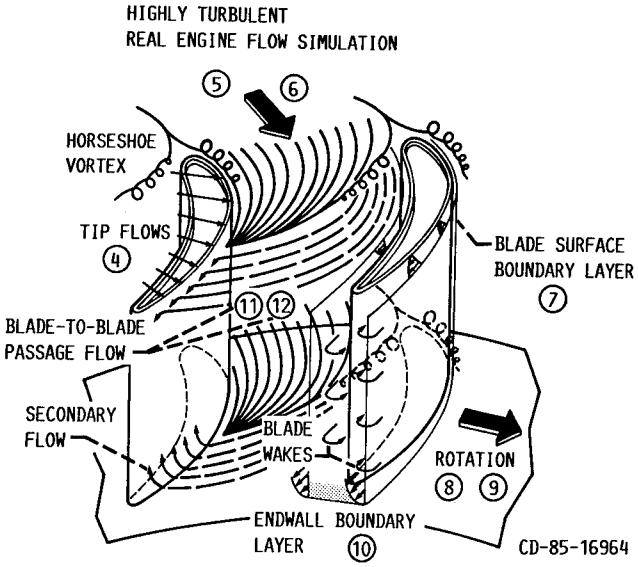

FIGURE 2. - COMPLEX FLOW PHENOMENA IN A TURBINE PASSAGE. SEE TABLE I FOR DESCRIPTION OF NUMBERED FLOW PHENOMENA.

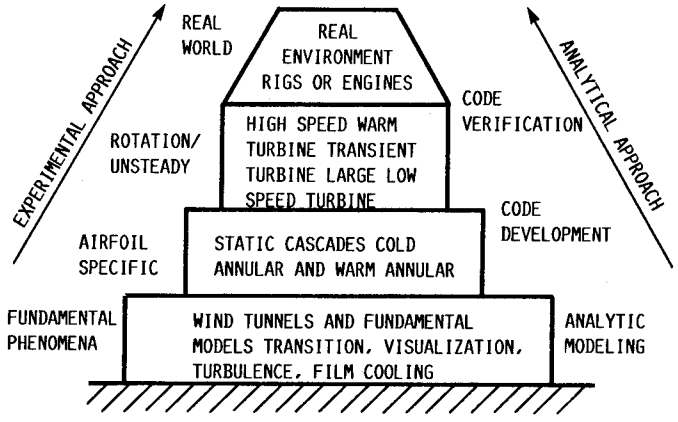

FIGURE 3.- BUILDING BLOCK APPROACH TO TURBINE AEROTHERMAL RESEARCH.

CD-85-16940

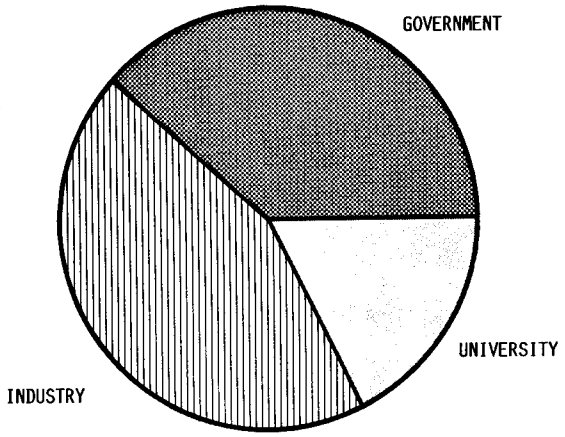

(A) BY LOCATION OF RESEARCH.

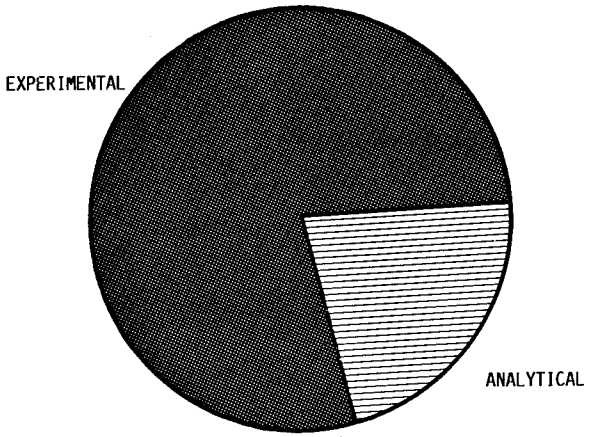

(B) BY TYPE OF RESEARCH.

FIGURE 4.- HOST TURBINE HEAT TRANSFER SUBPROJECT DISTRIBUTION OF RESOURCES.

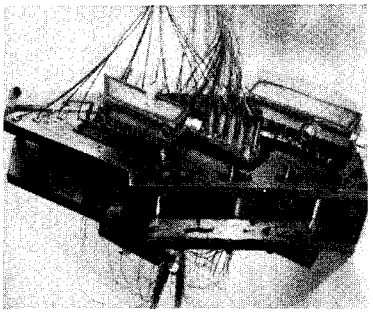

(A) THREE-VANE CASCADE.

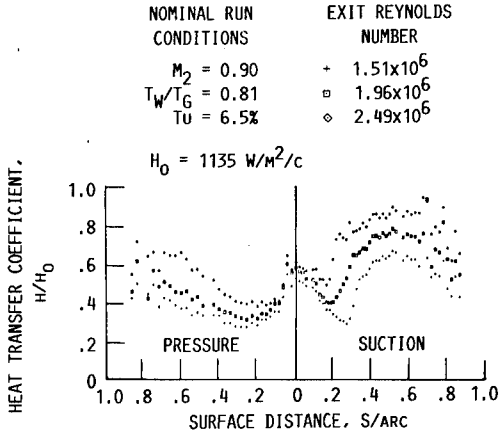

(B) NONFILM-COOLED AIRFOIL HEAT TRANSFER COEFFICIENTS.

DATA	M_2	RE_2	$P_{C,DS}/P_T$	$P_{C,LE}/P_T$	T_W/T_G
BASE	.75	2.00E6			
○	.75	2.05E6	1.10	1.10	.67
△	.74	2.00E6	1.10	1.05	.65
◇	.75	2.01E6	1.10	1.02	.65
□	.75	2.00E6	1.10	1.00	.66

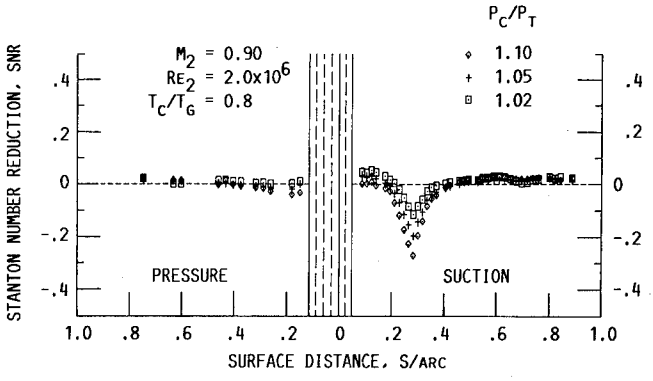

(C) INFLUENCE OF LEADING EDGE FILM-COOLING ON HEAT TRANSFER.

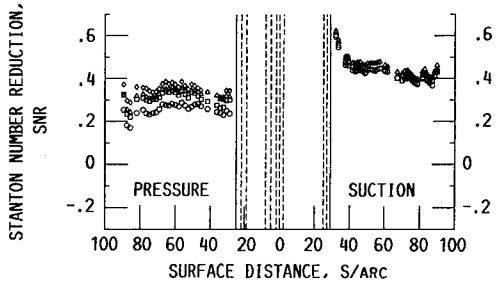

(D) COMBINED LEADING EDGE AND DOWNSTREAM FILM-COOLING.

FIGURE 5. - GAS-SIDE EXPERIMENTAL HEAT TRANSFER DATA FOR BOTH NON-FILM-COOLED AND FILM COOLED AIRFOILS. ALLISON GAS TURBINE DIVISION.

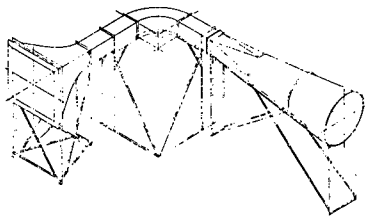

CURVED-DUCT FACILITY

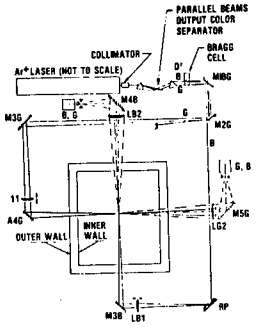

3-D LV OPTICAL SYSTEM

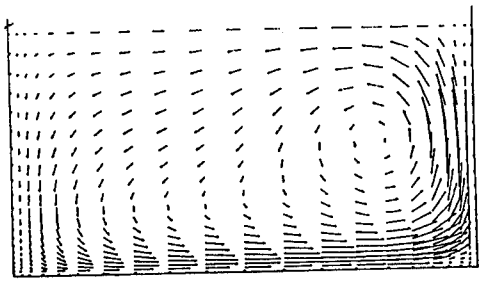

DUCT CROSS-FLOW PLOT P.D. THOMAS CODE
ANALYTICAL RESULTS

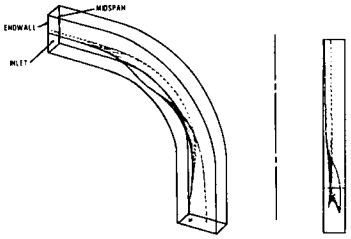

STREAM SHEET VELOCITY PATTERN THROUGH DUCT

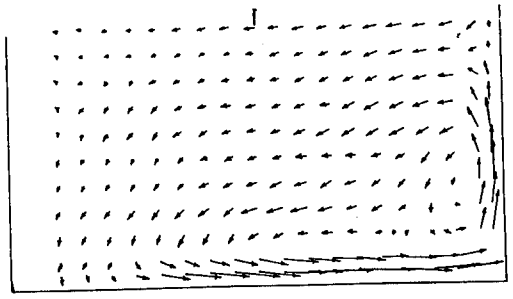

LOW REYNOLDS NUMBER DATA
EXPERIMENTAL RESULTS

FIGURE 6. - THREE-DIMENSIONAL FLOW-FIELD MEASUREMENTS IN A CURVED DUCT REPRESENTING AN AIRFOIL PASSAGE. UNIVERSITY OF TENNESSEE SPACE INSTITUTE.

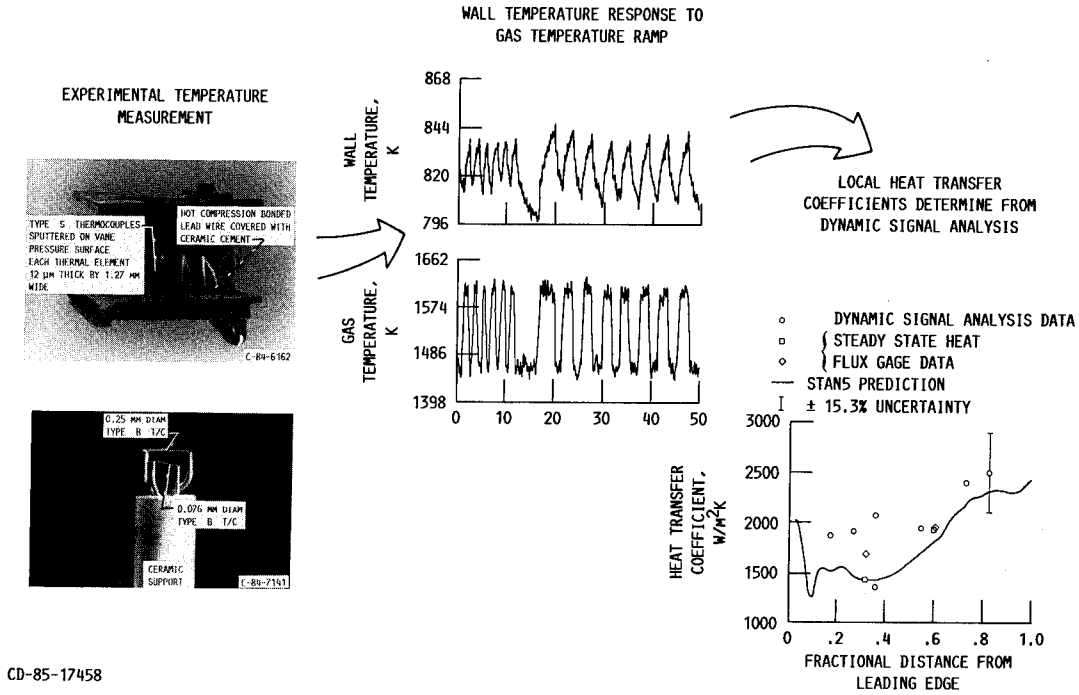

CD-85-17458

FIGURE 7. - HEAT FLUX MEASUREMENTS MADE IN A SIMULATED REAL ENGINE ENVIRONMENT ON STATOR AIRFOILS. LEWIS RESEARCH CENTER.

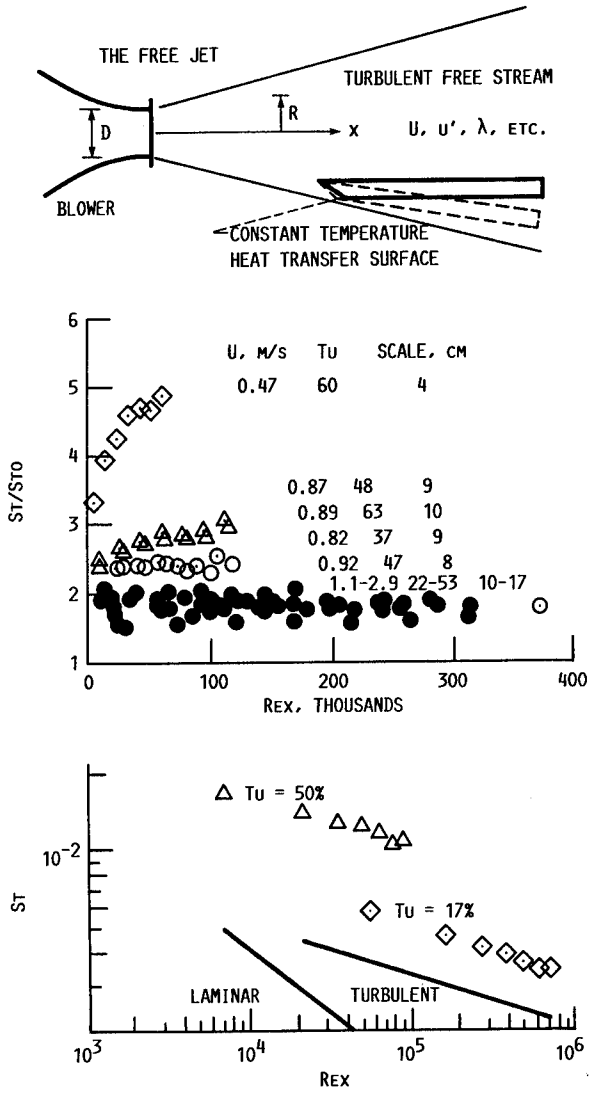

FIGURE 8. - HEAT TRANSFER AUGMENTATION RESULTING FROM HIGH FREE STREAM TURBULENCE AND SCALE. STANFORD UNIVESITY.

LARGE SCALE ROTARING RIG 1-1/2 STAGE TURBINE CONFIGURATION FIRST VANE AND ROTOR CASE REMOVED

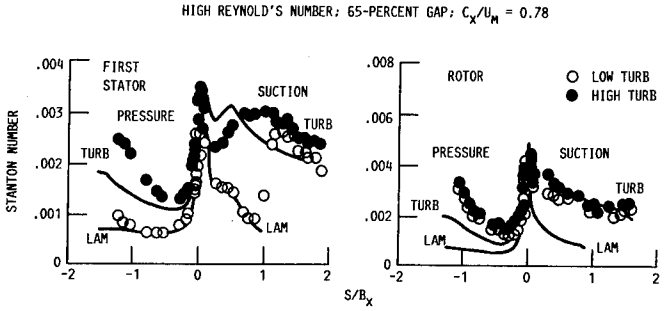

FIGURE 9. - ROTOR/STATOR INTERACTION AND THE AFFECT ON HEAT TRANSFER OF HIGH AND LOW FREESTREAM TURBULENCE. UNITED TECHNOLOGIES RESEARCH CENTER.

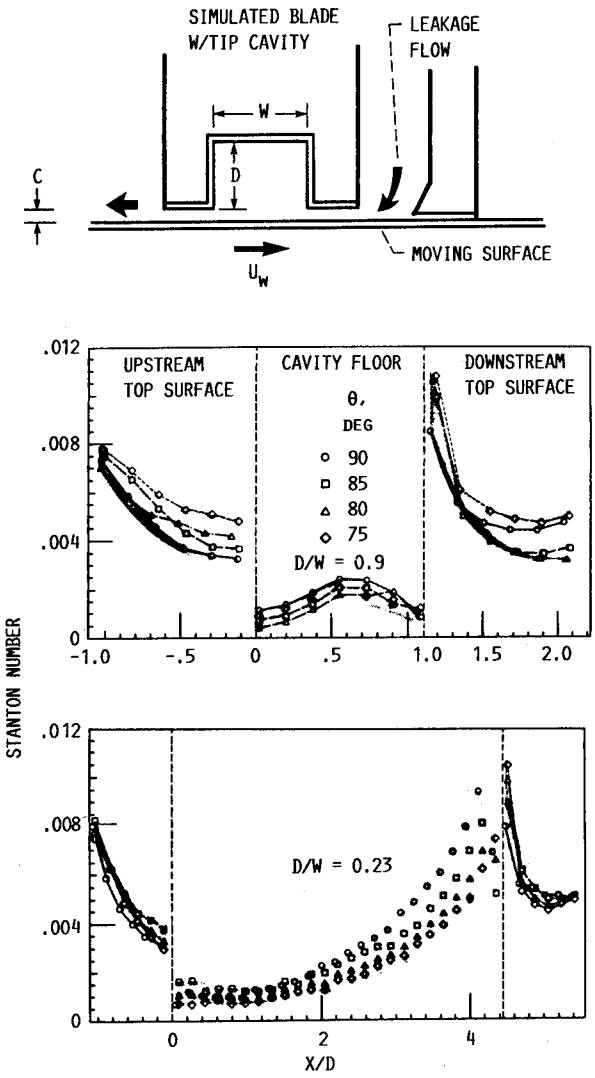

FIGURE 10. - EXPERIMENTAL HEAT TRANSFER RESULTS FOR A SIMULATED BLADE TIP CAVITY. ARIZONA STATE UNIVERSITY.

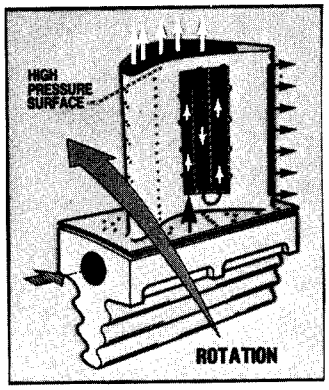

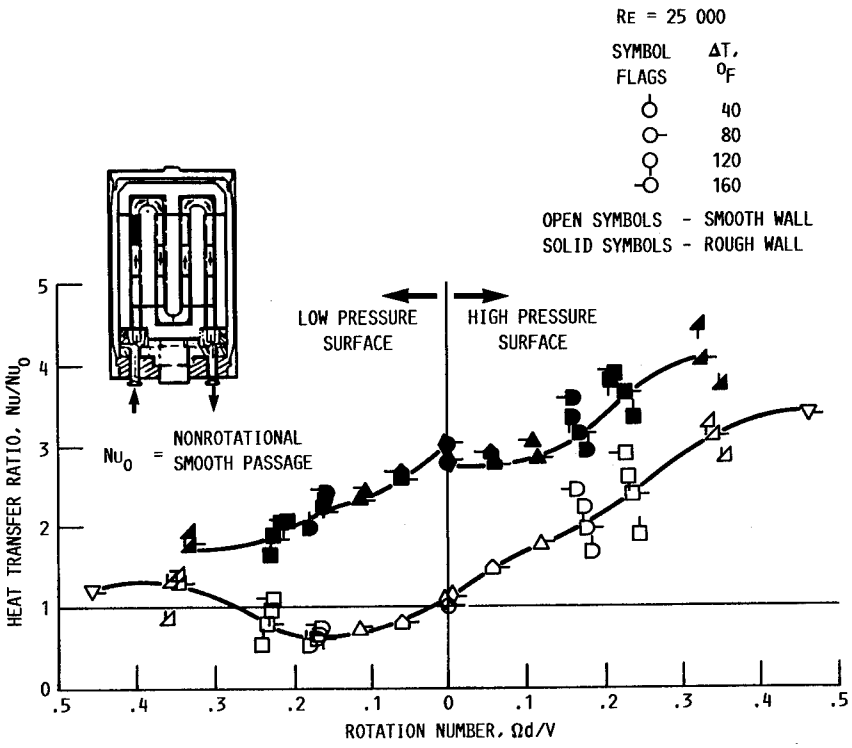

FIGURE 11. - THE EFFECTS OF ROTATION ON HEAT TRANSFER IN MULTIPASS COOLANT PASSAGES WITH AND WITHOUT TURBULATORS ARE SHOWN FOR AN OUTWARD FLOWING PASSAGE. PRATT AND WHITNEY AIRCRAFT.

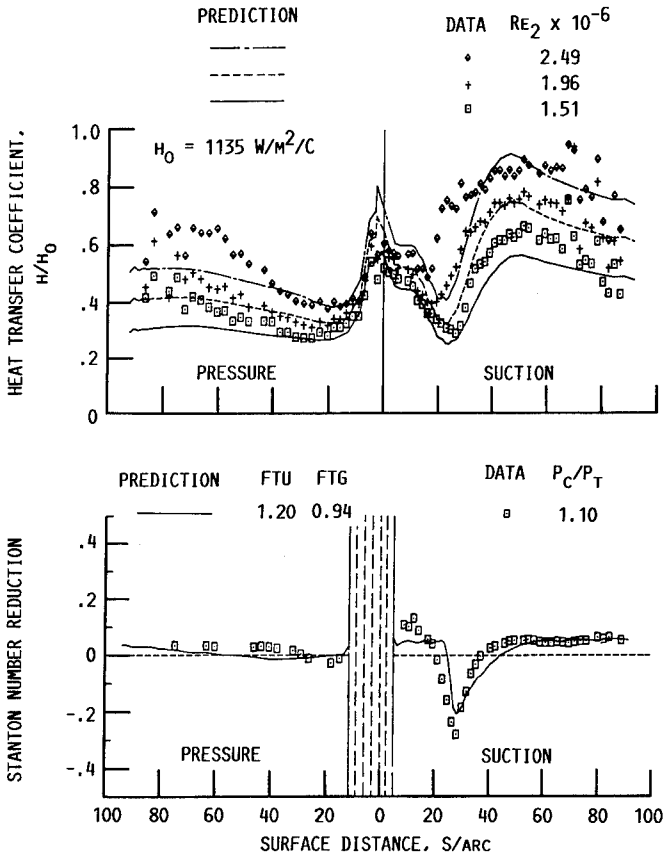

FIGURE 12. - A MODIFIED STAN-5 BOUNDARY LAYER ANALYSIS IS COMPARED WITH MEASUREMENTS FROM A NON-FILM-COOLED AIRFOIL AND THE SAME AIRFOIL GEOMETRY WITH A SHOWER-HEAD DESIGN. ALLISON GAS TURBINE DIVISION.

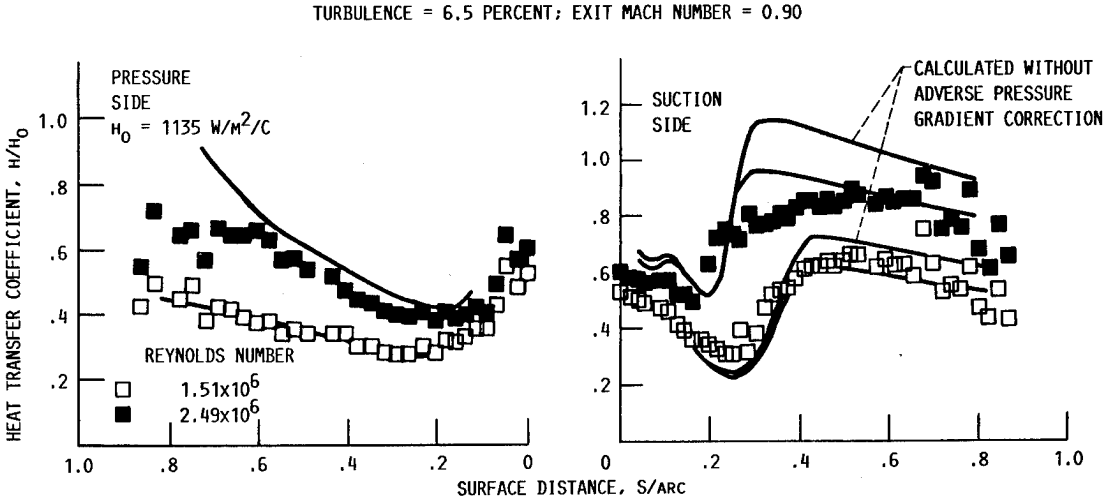

FIGURE 13. - A MODIFIED LOW REYNOLDS NUMBER K-ε TURBULENCE MODEL FOR A BOUNDARY LAYER ANALYSIS IS COMPARED WITH EXPERIMENTAL MEASUREMENTS. UNIVERSITY OF MINNESOTA.

CD-87-29102

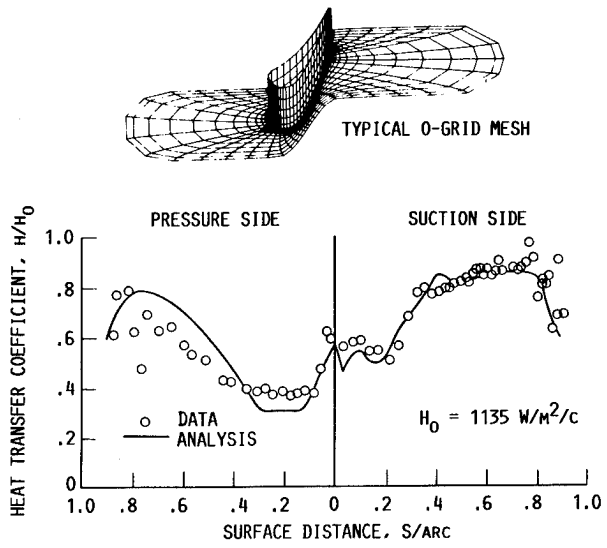

FIGURE 14. - A FULLY ELLIPTIC NAVIER-STOKES SOLUTION IS COMPARED WITH THE SAME EXPERIMENTAL MEASUREMENTS FOUND IN FIGURES 12 AND 13. SCIENTIFIC RESEARCH ASSOCIATE, INC.

STRUCTURAL ANALYSIS METHODS DEVELOPMENT FOR TURBINE HOT SECTION COMPONENTS

R. L. Thompson
National Aeronautics and Space Administration
Lewis Research Center
Cleveland, Ohio

ABSTRACT

This paper summarizes the structural analysis technologies and activities of the NASA Lewis Research Center's gas turbine engine Hot Section Technology (HOST) program. The technologies synergistically developed and validated include: time-varying thermal/mechanical load models; component-specific automated geometric modeling and solution strategy capabilities; advanced inelastic analysis methods; inelastic constitutive models; high-temperature experimental techniques and experiments; and nonlinear structural analysis codes. Features of the program that incorporate the new technologies and their application to hot section component analysis and design are described. Improved and, in some cases, first-time three-dimensional nonlinear structural analyses of hot section components of isotropic and anisotropic nickel-base superalloys are presented.

INTRODUCTION

Hot section components of aircraft gas turbine engines are subjected to severe thermal-structural loading conditions during the engine mission cycle. The most severe and damaging stresses and strains are those induced by the steep thermal gradients which occur during the startup and shutdown transients. The transient, as well as steady state, stresses and strains are difficult to predict, in part, because the temperature gradients and distributions are not well known or readily predictable and, in part, because the cyclic elastic-viscoplastic behavior of the materials at these extremes of temperature and strain are not well known or readily predictable.

A broad spectrum of structures related technology programs has been underway at the NASA Lewis to address these deficiencies at the basic as well as the applied levels, with participation by industry and universities. One of these programs was the structures element of the turbine engine Hot Section Technology (HOST) program. The structures element focused on three key technology areas: inelastic constitutive model development, three-dimensional nonlinear structural methods and code development, and experimentation to calibrate and validate the models and codes. These technology areas were selected not only because todays hot section component designs are materially and structurally difficult to analyze with existing analytical tools, but because even greater demands will be placed on the analysis of advanced designs. It is the need for improved engine performance (higher temperatures, lower cooling flows), lower engine weight, and improved engine reliability and durability which will require advanced analytical tools and expanded experimental capabilities.

Because materials used in today's turbine engine hot section components are operating at elevated temperature, time-independent (plastic) and time-dependent (creep and stress relaxation) material behavioral phenomena occur simultaneously, and these phenomena will be exacerbated in future component designs. Classical elastic-plastic theories, where creep and plasticity are uncoupled do not adequately characterize these interactive phenomena. These interactions are captured with inelastic (viscoplastic or unified) constitutive models. Under HOST, several viscoplastic models were developed for high-temperature isotropic and anisotropic nickel-base superalloys used in hot section components. These models were incorporated in several nonlinear three-dimensional structural analysis codes.

The analysis demands placed on hot section component designs result not only from the use of advanced materials and their characterization, but also from the use of new and innovative structural design concepts. There is an obvious need to develop advanced computational methods and codes, with the focus on improved accuracy and efficiency, to predict nonlinear structural response of advanced component designs. Under HOST, improved time-varying thermal-mechanical load models for the entire engine mission cycle from startup to shutdown were developed. The thermal model refinements are consistent with those required by the structural codes, including considerations of mesh-point density, strain concentrations, and thermal gradients. An automated component-specific geometric

modeling capability which will produce three-dimensional finite element models of the hot section components was also developed. Self-adaptive solution strategies were developed and included to facilitate the selection of appropriate elements, mesh sizes, etc. New and improved nonlinear three-dimensional structural analysis codes, including temporal elements with time-dependent properties to account for creep effects in the materials and components, were developed. A data transfer module was developed to automatically transfer temperatures from finite difference and finite element thermal analysis codes to finite element structural analysis codes.

Essential for the confident use of these models and structural analysis codes in the analysis and design of hot section components is their calibration and validation. Under HOST, experimental facilities were upgraded and experiments conducted to calibrate and validate the models and codes developed. Unique uniaxial and multiaxial high-temperature thermomechanical tests were conducted. In addition, unique thermomechanical tests on sections of conventional and advanced combustor liners were conducted in the Structural Component Response rig at NASA Lewis. Extensive, quality databases were generated. Advanced strain and temperature instrumentation was also evaluated.

Table I is a summary of the contracts and grants that were an integral part of the structures element under HOST. The research efforts of the grants and contracts, as well as in-house efforts, are described in the paper along with the most significant of the many accomplishments for each. Figure 1 summarizes the nonlinear structural analysis technologies and activities under HOST.

ISOTROPIC MATERIAL MODELING

Southwest Research Institute Contract

Unified constitutive models were developed for structural analysis of turbine engine hot section components under NASA/HOST contract NAS3-23925, "Constitutive Modeling for Isotropic Materials" (Chan et al., 1986). During this project, two existing models of the unified type were developed for application to isotropic, cast, nickel-base alloys used for air-cooled turbine blades and vanes. The two models are those of Walker (1981), and of Bodner and Partom (1975). Both models were demonstrated to yield good correlation with experimental results for two alloys: PWA alloy B1900+Hf and MAR-M247. The experimental correlations were made with testing under uniaxial and biaxial tensile, creep, relaxation, cyclic, and thermomechanical loading conditions over a range in strain rates and temperatures up to 1100 °C. Also, both models were implemented in the MARC nonlinear finite element computer code with test cases run for a notched round tensile specimen and an airfoil portion of a typical cooled turbine blade.

Typical results of thermomechanical strain cycling of B1900+Hf material are shown in Figs. 2 and 3. In Fig. 2, we show a single specimen cycled to saturation at 538 °C, a temperature increase to 982 °C with saturated loops achieved at that temperature, and a return to 538 °C, all under constant strain range control. Two observations evidence absence of thermal history effect. The high-temperature excursion resulted in no change in the hysteresis loop at 538 °C, and the cyclic stress range associated with a given cyclic strain was the same under this type of nonisothermal history as under strictly isothermal cycling, as shown in Fig. 3. Both types of cycling agree with the Bodner-Partom model prediction which is based on isothermal data only.

A second example is the analysis of an airfoil of a typical cooled turbine blade. Simulations were run in which a classical creep-plasticity model was compared with the Walker and Bodner-Partom models for B1900+Hf material. The airfoil was exercised through three full flight spectra of taxi, take off, climb, cruise, descent, taxi, and shutdown. Computational efficiency with the unified models was as good or better than with a more classical elasticplastic approach. The effective stress versus strain response at the airfoil critical location is compared in Fig. 4 for all three constitutive models. The unified models yield very similar results but substantially different from the classical creep-plasticity model. Unfortunately, no experimental results are available or easily obtainable for this complex problem.

In summary, the program has demonstrated that for the cast nickel-base alloys studied, B1900+Hf and MAR-M247, both isothermal and nonisothermal complex loading histories can be well predicted using the unified constitutive model approach with all necessary material constants derived solely from isothermal test data.

The program has also demonstrated rather conclusively that the unified constitutive model concept is a very powerful tool for predicting material response in hot section components under complex, time-varying, thermomechanical loadings. This confidence is gained from extensive correlations between two existing models and a large base of experimental data covering the range in stress, strain rate, and temperature of interest. The unified constitutive models have also been demonstrated to be computationally efficient when incorporated into a large finite element computer code (MARC).

General Electric Contract

Unified constitutive models were also developed and validated for structural analysis of turbine engine hot section components under NASA/HOST contract NAS3-23927, "Constitutive Modeling for Isotropic Materials," (Ramaswamy, 1986). As part of this effort, several viscoplastic constitutive theories were evaluated against a large uniaxial and multiaxial data base on René 80 material, which is a cast nickel-base alloy used in turbine blade and vane applications. Initially, it was the intent to evaluate only available theories; however, it was found that no available approach was satisfactory in modeling the high temperature time dependent behavior of René 80. Additional considerations in model development included the cyclic softening behavior of René 80, rate independence at lower temperatures, and the development of a new model for static recovery. These considerations were incorporated in a new constitutive model which was implemented into a finite element computer code. The code was developed as a part of the contract specifically for use with unified theories. The code was verified by a reanalysis of the turbine tip durability problem which was part of the pre-HOST activities at General Electric.

Typical of the many results obtained from this effort are the multiaxial thermomechanical comparisons shown in Figs. 5 and 6. Figure 5 shows that the new theory can predict 90° out-of-phase tension/torsion experimental results at elevated temperature with good accuracy. Figure 6 shows a comparison of prediction with experimental data from combined temperature and strain cycling tests. There is reasonably good agreement between predictions and experiment considering the predictions are based only on isothermal data.

The theory was implemented into a new three-dimensional finite element code which uses a 20-noded brick element. The program uses a dynamic time incrementing procedure to minimize cost while guaranteeing an accurate solution. The inelastic rate equations and state variable evolution equations are integrated using a second order Adams-Moulton predictor corrector technique. Piecewise linear load histories are modelled in order to simplify input. Further economics have been achieved by improving the stability of the initial strain method and further reducing the number of equilibrium iterations.

In summary, a new multiaxial constitutive model which can represent the complex nonlinear high temperature behavior of René 80 was developed. The model was extensively verified based on data at several temperatures. The thermomechanical proportional and nonproportional cyclic modeling capabilities of the model were demonstrated. The model was implemented in a three-dimensional structural analysis finite element code and a turbine blade was analyzed.

University of Akron Grant

Many viscoplastic constitutive models for high-temperature structural alloys are based exclusively on uniaxial test data, as previously discussed. Generalization to multiaxial states of stress is made by assuming the stress dependence to be on the second principal invariant (J_2) of the deviatoric stress, frequently called the "effective" stress. Testing other than uniaxial, e.g., shear, biaxial, etc., is generally done in the spirit of verification testing, not as part of the data base of the model. If such a J_2 theory, based on uniaxial testing, is called upon to predict behavior under conditions other than uniaxial, say pure shear, and it does so poorly, nothing is left to adjust in the theory. The exclusive dependence on J_2 must be questioned. For a fully isotropic material whose inelastic deformation behavior is relatively independent of hydrostatic stress, the most general stress dependence is on the two (nonzero) principal invariants of the deviatoric stress, J_2 and J_3. These invariants constitute what is known as an integrity basis for the material.

Under NASA Grant NAG3-379, "A Multiaxial Theory of Viscoplasticity for Isotropic Materials," (Robinson, 1984) a time-dependent description potential function based on constitutive theory with stress dependence on J_2 and J_3 that reduces to a known J_2 theory as a special case was developed. The characterization of viscoplasticity can be made largely on uniaxial testing but the "strength" of the J_3 dependence must be determined by testing other than uniaxial, e.g., pure shear.

Several calculations have been made using forms of the functions in the model and associated material parameters that are typical of ferritic chrome-based and austenitic stainless-steel alloys. Qualitatively similar results can be expected for nickel-based alloys. Figure 7 shows predicted hysteresis loops over a constant strain range ($\Delta\varepsilon$ = 0.6 percent) and strain rate ($\dot{\varepsilon}$ = 0.001/m). The curve labeled "uniaxial" can be thought of as having been carefully fit on the basis of uniaxial data. Predictions of pure shear response are also shown, corresponding to different values of C. A J_2, J_3 theory reduces to a J_2 theory for C = 0. Even after tedious fitting of uniaxial cyclic data, if the shear prediction does not correlate well with shear data, nothing can be done in a J_2 theory short of compromising the uniaxial correlations. The present J_2, J_3 theory allows some flexibility in accurately predicting response other than uniaxial through the parameter C. Note that the hysteresis loop labeled C = 10 indicates a cyclic response that is about 20 percent stronger than the J_2 response (C = 0).

Figure 8 shows predictions of creep response, i.e., behavior under constant stress. Here, the strain-time curve labeled "uniaxial and shear C = 0" represents both the uniaxial response (using the strain scale on the left) and the shear response for a J_2 material (using the strain scale on the right). Each shear response corresponding to a particular value of C is to be measured using the right-hand shear strain scale. In creep, the effect of the J_3 dependence appears to be more pronounced than for strain cycling. Here, for C = 10 the creep strain after 100 hr differs by a factor of 2 from that for the J_2 response (C = 0).

ANISOTROPIC MATERIAL MODELING

University of Connecticut Grant

Nickel-base monocrystal superalloys have been under development by turbine manufacturers for a number of years. Successful attempts have now been made under grant NAG3-512, "Constitutive Modeling of Single Crystal and Directionally Solidified Superalloys," (Walker, and Jordan, 1987) to model the deformation behavior of these materials based on both a macroscopic constitutive model and a micromechanical formulation based on crystallographic slip theory. These models have been programmed as FORTRAN subroutines under contract NAS3-23939 to Pratt and Whitney and included in the MARC nonlinear finite element program. They are currently being used to simulate thermal/mechanical loading conditions expected at the "fatigue critical" locations on a single crystal (PWA 1480) turbine blade. Such analyses form a natural precursor to the application of life prediction methods to gas turbine airfoils.

The difficulty in analyzing the deformation behavior of single crystal materials lies in their anisotropic behavior. Two separate unified viscoplastic constitutive models for monocrystal PWA 1480 have been completely formulated. In one model, the directional properties of the inelastic deformation behavior are achieved by resolving the summed crystallographic slip system stresses and strains onto the global coordinate system. In the other model, the required directional properties are achieved by operating on the global stresses and strains directly with fourth rank anisotropy tensors. The crystallographic slip based model is more accurate and has more physical significance than the macroscopic model, but is more computationally intensive than its macroscopic counterpart.

The material constants in both models can be obtained from uniaxial tests on <001> and <111> oriented uniaxial specimens, or from uniaxial and torsion tests on <001> orientated tubular specimens. Both models achieve good correlation with the experimental data in the <001> and <111> corners of the stereographic triangle, and both models correctly predict the deformation behavior of specimens orientated in the <011> direction. The tension-torsion tests on tubular specimens orientated in the <001> direction were carried out at a temperature of 870 °C (1600 °F) at the University of Connecticut. Further tests at temperatures ranging from room temperature to 1149 °C (2100 °F) have been carried out at Pratt and Whitney under contract NAS3-23939. Good correlations and predictions are uniformly achieved at temperatures above 649 °C (1200 °F), but further work appears to be necessary to correctly model the deformation behavior of PWA 1480 monocrystal material below 649 °C (1200 °F).

University of Cincinnati Grant

Nickel base single crystal superalloys have attracted considerable interest for use in gas turbine jet engine because of their superior high temperature properties. In polycrystalline turbine parts, rupture is usually due to crack propagation originating at the grain boundaries. Since single crystal alloys have no grain boundaries, use of the alloy has significant advantages for increased strength and longer life.

Under grant NAG3-511, "Anisotropic Constitutive Modeling for Nickel-Base Single Crystal Alloy René N4," an anisotropic constitutive model was developed based on a crystallographic approach. The current equations modified a previous model proposed by Dame and Stouffer (1986) where a Bodner-Partom equation with only the drag stress was used to model the local inelastic response in each slip system. Their model was considered successful for predicting both the orientation dependence and tension/compression asymmetry for tensile and creep histories for single crystal alloy René N4 at 760 °C (1400 °F). However, certain properties including fatigue were not satisfactorily modeled. A back stress state variable was incorporated into the local slip flow equation based on the observed experimental observations. Model predictability was improved especially for mechanical properties such as inelasticity and fatigue loops.

Figures 9 and 10 are typical of the numerous results obtained from this effort. Experimental data and predicted responses of tensile and cyclic conditions for different specimen orientations are compared. Shown in Fig. 9 are the experimental data in [100] and [111] orientations which were used to determine material constants. The response in [110] orientation is the predicted result. The model predicted very well the elastic moduli, hardening characteristics (the knee of the curves) and the saturated values. In Fig. 10, comparisons show the model predicts very well the cyclic tension/compression asymmetry, hardening characteristics and rate effect for the [100] orientation. The prediction of the hystersis loop was based solely on saturated constants determined from tensile tests.

University of Akron Grant

Structural alloys used in high-temperature applications exhibit complex thermomechanical behavior that is time-dependent and hereditary. Recent attention is being focused on metal-matrix composite materials for aerospace applications that, at high temperature, exhibit all the complexities of conventional alloys (e.g., creep, relaxation, recovery, rate sensitivity) and, in addition, exhibit further complexities because of their strong anisotropy.

Under grant NAG3-379, "A Continuum Deformation Theory for Metal-Matrix Composites at High Temperature," (Robinson et al., 1986) a continuum theory was developed for representing the high-temperature, time-dependent, hereditary deformation behavior of metallic composites that can be idealized as pseudo-homogeneous continua with locally definable directional characteristics. Homogenization of textured materials (molecular, granular, fibrous) and applicability of continuum mechanics in structural applications depends on characteristic body dimensions, the severity of gradients (stress, temperature, etc.) in the structure and on the relative size of the internal structure (cell size) of the material. Examination reveals that the appropriate conditions are met in a significantly large class of anticipated aerospace applications of metallic composites to justify research into the formulation of continuum-based theories.

The starting point for the theoretical development is the assumed existence of a dissipation potential function Ω for a composite material; that is a two constituent (fiber/matrix), pseudohomogeneous material.

The potential function is of the form

$$\Omega = \Omega(\sigma_{ij}, \alpha_{ij}, d_i d_j, T) \qquad (1)$$

in which σ_{ij} denotes the components of (Cauchy) stress, α_{ij} the components of a tensorial internal state variable (internal stress), $d_i d_j$ the components of a directional tensor, and T the temperature. The symmetric tensor $d_i d_j$ is formed by a self product of the unit vector d_i denoting the local fiber direction. Account can be taken of more than a single family of fibers inherent to the continuum element.

The present theory has been implemented into the commercial finite element code MARC. Several trial calculations have been made under uniaxial conditions using material functions and parameters that approximate a tungsten/copper composite material. A transversely isotropic continuum elasticity theory has been used in conjunction with the present viscoplastic theory. The results of the calculations show the expected responses of rate-dependent plasticity, creep, and relaxation as well as appropriate anisotropic features. Predictions of relaxation and hysteresis loops for different fiber orientation angles on a tungsten/copper like material are shown in Figs. 11 and 12.

COMPUTATIONAL METHODS AND CODE DEVELOPMENT

General Electric Contract

It has become apparent in recent years that there is a serious problem of interfacing the output temperatures and temperature gradients from either the heat transfer codes or engine tests with the input to the stress analysis codes. With the growth in computer postprocessors, the analysis of hot section components using hundreds and even thousands of nodes in the heat transfer and stress models has become economical and routine. This has exacerbated the problem of manual transfer of output three-dimensional temperatures from heat transfer codes to stress analysis input to where the engineering effort required is comparable to that required for the remainder of the analysis. Furthermore, a considerable amount of approximation has been introduced in an effort to accelerate the process. This tends to introduce errors into the temperature data which negates the improved accuracy in the temperature distribution achieved through use of a fine mesh. There is, then, a strong need for an automatic thermal interface module. A module was developed under contract NAS3-23272, "Burner Liner Thermal/Structural Load Modeling," (Maffeo, 1984).

The overall objectives of this thermal/structural transfer module were that it handle independent mesh configurations, finite difference and finite element heat transfer codes, perform the transfer in an accurate and efficient fashion and the total system be flexible for future applications. Key features of the code developed include: independent heat transfer and stress model meshes, accurate transfer of thermal data, computationally efficient transfer, user friendly program, flexible system, internal coordinate transformations, automated exterior surfacing techniques and geometrical and temporal windowing capability.

A schematic of the TRansfer ANalysis Code (TRANCITS) is shown in Fig. 13. The module can process heat transfer results directly from the MARC (finite

element) and SINDA (finite difference) programs and will output temperature information in the forms required for MARC and NASTRAN. The input and output routines in the module are very flexible and could easily be modified through a neutral file to except data from other heat transfer codes and format data to other stress analysis codes.

This thermal load transfer module has been shown to efficiently and accurately transfer thermal data from dissimilar heat transfer meshes to stress meshes. The fundamental part of the code, the three-dimensional search, interpolation and surfacing routines, have much more potential. They form an outstanding foundation for automatic construction of embedded meshes, local element mesh refinement, and the transfer of other mechanical type loading.

General Electric Contract

The overall objective of this program was to develop and verify a series of interdisciplinary modeling and analysis techniques specialized to address hot section components. These techniques incorporate data as well as theoretical methods from many diverse areas including cycle and performance analysis, heat transfer analysis, linear and nonlinear stress analysis, and mission analysis. Building on the proven techniques already available in these fields, the new methods developed through this contract were integrated into a system which provides an accurate, efficient, and unified approach to analyzing hot section structures. The methods and codes developed under this contract, NAS3-23687, "Component-Specific Modeling," (McKnight, 1985) predict temperatures, deformation, stress and strain histories throughout a complete flight mission.

Five basic modules were developed and then linked together with an executive module. They are:

(1) The Thermodynamic Engine Model (TDEM) which is the subsystem of computer software. It translates a list of mission flight points and delta times into time profiles of major engine performance parameters. Its present data base contains CF6-50C2 engine performance data. In order to adapt this system to a different engine requires only the restocking of this data base with the appropriate engine performance data.

(2) The Thermodynamic Loads Model (TDLM) which is the subsystem of computer software which works with the output of the TDEM to produce the mission cycle loading on the individual hot section components. There are separate segments for the combustor, the turbine blade, and the turbine vane. These segments translate the major engine performance parameter profiles from the TDEM into profiles of the local thermodynamic loads (pressures, temperatures, rpm) for each component. The formulas which perform this mapping in the TDLM models were developed for the specific engine components. To adapt these models to a different engine would require evaluating these formulas for their simulation capability and making any necessary changes.

(3) The Component Specific Structural Modeling which is the heart of the geometric modeling and mesh generation using the recipe concept. A generic geometry pattern is determined for each component. A recipe is developed for this basic geometry in terms of point coordinates, lengths, thicknesses, angles, and radii. These recipe parameters are encoded in computer software as variable input parameters. A set of default numerical values are stored for these parameters. The user need only input values for those parameters which are to have different values. These recipe parameters then uniquely define a generic component with the defined dimensions. The software logic then works with these parameters to develop a finite element model of this geometry consisting of 20-noded isoparametric elements. The user specifies the number and distribution of these elements through input control parameters. Figure 14 shows the generic geometry and recipe for a combustor liner panel.

(4) The subsystem which performs the three-dimensional nonlinear finite element analysis of the hot section component model and was developed under the NASA HOST contract NAS3-23698, "three-dimensional Inelastic Analysis Methods for Hot Section Structures." This software performs incremental nonlinear finite element analysis of complex three-dimensional structures under cyclic thermomechanical loading with temperature dependent material properties and material response behavior. The nonlinear analysis considers both time-independent and time-dependent material behavior. Among the constitutive models available is the Haisler-Allen classical model which performs plasticity analysis with isotropic material response, kinematic material response, or a combination of isotropic and kinematic material response. This is combined with a classical creep analysis formulation. A major advance in the ability to perform time-dependent analyses is a dynamic time incrementing strategy incorporated in this software.

(5) The COSMO system which consists of an executive module which controls the TDEM, TDLM, the geometric modeler, the structural analysis code, the file structure/data base, and certain ancillary modules. The ancillary modules consist of a band width optimizer module, a deck generation module, a remeshing/mesh refinement module and a postprocessing module. The executive directs the running of each module, controls the flow of data among modules and contains the selfadaptive control logic. Figure 15 is a flow chart of the COSMO system showing data flow and the action positions of the adaptive controls. The modular design of the system allows each subsystem to be viewed as a plug-in module. They can be abstracted and run alone or replaced with alternate systems.

The ideas, techniques, and computer software developed in the Component Specific Modeling program have proven to be extremely valuable in advancing the productivity and design-analysis capability for hot section structures.

General Electric Contract

Under NASA contract NAS3-23698, "Three-Dimensional Inelastic Analysis Methods for Hot Section Components," (McKnight et al., 1986), a series of three-dimensional inelastic structural analysis computer codes were developed and delivered to NASA Lewis. The objective of this program was to develop analytical methods capable of evaluating the cyclic time-dependent inelasticity which occurs in hot section engine components. Because of the large excursions in temperature associated with hot section engine components, the techniques developed must be able to accommodate large variations in material behavior including plasticity and creep. To meet this objective, General Electric developed a matrix consisting of three constitutive models and three element formulations. A separate program for each combination of constitutive model-element model was written, making a total of

nine programs. Each program was given a stand alone capability of performing cyclic nonlinear analysis.

The three constitutive models are in three distinct forms: a simplified theory (simple model), a classical theory, and a unified theory. In an inelastic analysis, the simplified theory uses a bilinear stress-strain curve to determine the plastic strain and a power law equation to obtain the creep strain. The second model is the classical theory of Haisler and Allen. The third model is the unified model of Bodner and Partom. All of the models were programmed for a linear variation of loads and temperatures with the material properties being temperature dependent.

The three element formulations used are an 8-node isoparametric shell element, a 9-node shell element, and a 20-node isoparametric solid element. The 8-node element uses serendipity shape functions for interpolation and Gaussian quadrature for numerical integration. Lagrange shape functions are used in the 9-node element. For numerical integration, the 9-node element uses Simpson's rule. The 20-node solid element uses Gaussian quadrature for integration.

For the linear analysis of structures, the nine codes use a blocked-column skyline, out-of-core equation solver. To analyze structures with nonlinear material behavior, the codes use an initial stress iterative scheme. Aitken's acceleration scheme was incorporated into the codes to increase the convergence rate of the iteration scheme.

The ability to model piecewise linear load histories was written into the codes. Since the inelastic strain rate can change dramatically during a linear load history, a dynamic time-incrementing procedure was included. The maximum inelastic strain increment, maximum stress increment, and the maximum rate of change of the inelastic strain rate are the criteria that control the size of the time step. The minimum time step calculated from the three criteria is the value that is used.

In dynamic analysis, the eigenvectors and eigenvalues can be extracted using either the determinant search technique or the subspace iteration method. These methods are only included with those finite-element codes containing the 8-node shell element.

Pratt and Whitney Aircraft Contract

The objective of the work done under contract NAS3-23697, "Three-dimensional Inelastic Analysis Methods for Hot Section Components," (Nakazawa, 1987; Wilson, and Banerjee, 1986) was to produce three new computer codes to permit accurate and efficient three-dimensional inelastic analysis of combustor liners, turbine blades, and turbine vanes. The three codes developed are called MOMM (Mechanics of Materials Model), MHOST (MARC-HOST) and BEST (Boundary Element Stress Technology). These codes embody a progression of mathematical models for increasingly comprehensive representation of the geometrical features, loading conditions, and forms of nonlinear material response that distinguish the three groups of hot section components.

Software in the form of stand-alone codes was developed by Pratt and Whitney Aircraft (PWA) with assistance from three subcontractors: MARC Analysis Research Corporation (MARC), United Technology Research Center (UTRC), and the State University of New York at Buffalo (SUNY-B).

Three increasingly sophisticated constitutive models were implemented in MOMM, MHOST, and BEST to account for inelastic material behavior (plasticity, creep) in the elevated temperature regime. The simplified model assumes a bilinear approximation of stress-strain response and glosses over the complications associated with strain rate effects, etc. The state-of-the-art model partitions time-independent plasticity and time-dependent creep in the conventional way, invoking the von Mises yield criterion and standard (isotropic, kinematic, combined) hardening rules for the former, and a power law for the latter. Walker's viscoplasticity theory which accounts for the interaction between creep/relaxation and plasticity that occurs under cyclic loading conditions, has been adopted as the advanced constitutive model.

MOMM - This is a stiffness method finite element code that utilizes one-, two- and three-dimensional arrays of beam elements to simulate hot section component behavior. Despite limitations of such beam model representations, the code will be useful during early phases of component design as a fast, easy to use, computationally efficient tool. All of the structural analysis types (static, buckling, vibration, dynamics), as well as the three constitutive models mentioned above, are provided by MOMM. Capabilities of the code have been tested for a variety of simple problem discretizations.

MHOST - This code employs both shell and solid (brick) elements in a mixed method framework to provide comprehensive capabilities for investigating local (stress/strain) and global (vibration, buckling) behavior of hot section components. Attention was given to the development of solution algorithms, integration algorithms for stiffness, strain recovery and residual terms, and modeling methods that permit accurate representations of thermal effects on structural loading and material properties, as well as geometrical discontinuities.

The three constitutive models implemented are the secant elasticity model, von Mise's plasticity model, and Walker's creep plasticity model. Temperature dependency and anisotropy can be obtained through user subroutines in MHOST. Nonlinear transient analysis and eigenvalue extraction for buckling and modal analyses are some of the other important features in the program. The improved algorithm models and finite elements implemented in the code significantly reduced CPU (Central Processing Units) time requirements for three-dimensional analyses.

To test the validity of the MHOST finite-element code, considerable efforts were made in applying the code in different cases with results compared to theoretical predictions or numerical values generated by other codes. For example, the code was used in-house to analyze a General Electric CF/6-50 engine blade and rotor model with data generated by a computational structural mechanics simulator system. The simulator system provided data, such as pressure and temperature distribution, centrifugal force, and time duration, at various stages of flight. Figure 16 shows the variation of the radical displacement of the leading edge tip in the static condition during the entire flight without consideration of the centrifugal force effect.

BEST3D - This is a general purpose three-dimensional structural analysis program utilizing the boundary element method. The method has been implemented for very general three-dimensional geometries, and for elastic, inelastic and dynamic stress analysis. Although the feasibility of many of the capabilities provided has been demonstrated in a number of individual prior research efforts, the present code is the first in which they have been made available for large scale problems in a single code. In addition, important basic advances have been made in a number of areas, including the development and implementation of a variable stiffness plasticity algorithm, the incorporation of an embedded time algorithm for elastodynamics and the extensive application of particular

solutions within the boundary element method. Major features presently available in the BEST3D code include: very general geometry definition, including the use of double curved isoparametric surface elements and volume cells, with provision of full substructuring capability; general capability for the definition of complex, time-dependent boundary conditions; capability for nonlinear analysis using a variety of algorithms, solution procedures and constitutive models; and a very complete elastodynamic capability including provision for free vibration, forced response and transient analysis.

The BEST3D code was validated by comparing predictions from BEST3D with those from theoretical and/or numerical predictions and some experimental data. For example, results from a benchmark notch test program were used. Finite element and boundary element meshes for one-quarter of a specimen gage section are shown in Fig. 17. Measurements of notch root stress-strain behavior for initial uploadings were compared with predictions (Fig. 18). Simulation of first-cycle notch root behavior with BEST3D was proven to be quite accurate.

EXPERIMENTAL FACILITIES AND DATA

Oak Ridge National Laboratory Interagency Agreement

An experimental effort was undertaken under Interagency Agreement Number 40-1447-84 and U.S. Department of Energy contract DE-AC05-840R 21400 with Martin Marietta Energy Systems Inc., "Determination of Surface of Constant Inelastic Strain Rate at Elevated Temperature," (Battiste, and Ball, 1986). Special exploratory multiaxial deformation tests on tubular specimens of type 316 stainless steel at 649 °C (1200 °F) were conducted to investigate time-dependent material behavior.

In classical plasticity the concept of yield surfaces in multiaxial stress space plays a central role, not only in the definition of initial yielding but in determining subsequent plastic flow. At high temperatures the deformation behavior of structural alloys is strongly time dependent. Consequently, the significance of yield surfaces breaks down, and it has been proposed that in their place the concept of surfaces of constant inelastic strain rate (SCISR) might be utilized. Such surfaces, called SCISRs, can be shown to have a potential nature and thus constitute the basis of a rational multiaxial viscoplastic constitutive theory.

A surface of constant inelastic strain rate was determined by loading the specimen at a constant effective stress rate in the two-dimensional axial/torsional stress state in various directions until a predetermined inelastic effective strain rate was reached. After each probe, the stress was returned to the initial starting point; thus a locus of points (surface of constant inelastic strain rate) was established.

Two types of tests were conducted. One test specimen was subjected to a time-independent torsional shear strain test history, and surfaces of constant inelastic strain rate (SCISRs) in an axial/torsional stress space were measured at various predetermined points during the test. A second specimen was subjected to a 14-week time-dependent (creep-recovery-creep periods) torsional shear stress histogram. SCISRs determinations were made at 17 points during the test. The tests were conducted in a high-temperature, computer-controlled axial/torsional test facility using an Oak Ridge National Laboratory developed high-temperature multiaxial extensometer.

A key result of this testing effort was that surfaces of constant inelastic strain rate exist and can be determined or measured at an elevated temperature, 650 °C. This is shown in Fig. 19. The conclusion is validated or deduced by the execution of the test programs and by the consistency of the surface results, especially the repeated surfaces. To our knowledge, this is the first successful determination of high-temperature surfaces of constant inelastic strain rate.

Although conclusions regarding the effect of these SCISRs data on different theories will be left to the constitutive equation developers, several results can be stated. First, the surfaces did not move or change shape in the axial/torsional stress state by any significant amount. Second, a deduction that plastic deformations have a larger effect than creep deformations can be stated. Third, SCISRs determined immediately after large plastic deformation show more inconsistent results than SCISRs which have not undergone immediate prior plastic deformations. Last, the extensometer system and software control system performed extremely well in a difficult application.

In-house Lewis Research Center Experimental Facilities and Data

Uniaxial Test Systems. Under HOST, recent expansion of the uniaxial testing capability of the fatigue and structures laboratory included the addition of four new test systems (Bartolotta, and McGaw, 1987). One of these systems is shown in Fig. 20. The load rating for two of the new systems is ±9072 kg (±20 000 lb), and the other two at ±22 680 kg (±50 000 lb). Each system is equipped with a state-of-the-art digital controller. The digital controllers have the ability to complete a smooth control mode transfer, which is accomplished either manually or electronically. This feature will make it possible to conduct some of the more complex tests that have been defined by the constitutive model developers at NASA Lewis and elsewhere. Specimen heat is provided by 5 kW radio frequency induction heaters. Axial strains are measured using an axial extensometer. To study the effects of the environment on creep-fatigue behavior, the two smaller load capacity test systems are equipped with environmental chambers capable of providing a vacuum and/or an inert environment. The environmental chamber is able to sustain a vacuum of 2.67×10^{-4} Pa (2×10^{-6} torr) with a specimen temperature of 1093 °C (2000 °F). All systems include water-cooled hydraulic grips for simple specimen installation. By the means of exchanging two collets these grips can be adapted to handle either flat bar, smooth shank, or threaded-end specimens. Each uniaxial system has its own minicomputer for experimental control and data acquisition. Preliminary software has been developed by the experimentalists to conduct tests as simple as a low cycle fatigue test, and as complicated as thermomechanical tests.

Biaxial Test Systems. In many life and material behavior models, multiaxial representations are formulated by modifying uniaxial criteria. Unfortunately, this method does not always achieve the accuracy needed to meet design goals of hot section components. In response to this need for better life and material behavior predictions under complex states of stress and strain, a multiaxial testing capability is being developed. As an evolutionary step from a uniaxial test capability, a decision was made to begin with biaxial (axial-torsion) test systems (Fig. 21) and

eventually progress to triaxial systems through the use of internal pressure. Under HOST, three new biaxial test systems were added to the laboratory (Bartolotta, and McGaw, 1987).

The load frames for each test system are rated for loads of ±22 948 kg (±50 000 lb) axial and ±2824 N-m (±25 000 in.-lb) torsional. Electronics for these systems consist of two servocontrollers, two data display units, function generators, and an oscilloscope. The two servocontrollers allow for both independent and combined control of axial and torsional loading. Each servocontroller can control specimen loading in one of three modes: load, strain or stroke for axial loading and torque, torsional strain or angular displacement for torsional loading. Data display units are used to monitor analog data signals, and provide an important interface between the test system and the computer system. These units can be programmed to perform a variety of signal processing operations.

The heating system for each biaxial test system consists of an audio frequency induction generator, an induction coil fixture, and a PID controller for closed-loop temperature control. Each generator has a power output of 50 kW at an operating frequency of 9.6 kHz. Audio frequency generators were chosen because of their ability to operate with minimal electrical interference to instrumentation signals.

Each axial-torsional test system is interfaced with its own minicomputer. These minicomputers, along with the data display units, are used for experimental control and data acquisition. Preliminary software is being used to conduct simple tests, while more complicated test programs are still in their developmental stages.

A thin-walled tube was chosen as the basic specimen geometry. This type of geometry has the following advantages: (a) easy decomposition of axial-torsional components of stress and strain, (b) at high temperatures thermal gradients across the diameter are minimal, and (c) for thermomechanical testing, cooling rates are higher.

Uniaxial Experimental Results. Extensive databases for several materials have been generated under the grants and contracts previously discussed. In the Lewis Fatigue and Structures Laboratory, a uniaxial database on Hastelloy-X, a nickel-base superalloy used in hot section component applications, was generated (Bartolotta, 1985; Ellis et al., 1986; Bartolotta, and Ellis, 1987). These data are being used in the development and calibration of constitutive models. In addition, some of the data generated was used to address a number of questions regarding the validity of methods adopted in characterizing the constitutive models for particular high-temperature materials. One area of concern is that the majority of experimental data available for this purpose are determined under isothermal conditions. This is in contrast to service conditions which almost always involve some form of thermal cycling. The obvious question arises as to whether a constitutive model characterized using an isothermal data base can adequately predict material response under thermomechanical conditions. Described here is an example of results of the most recent isothermal and thermomechanical experiments conducted on Hastelloy-X to address this concern.

Results obtained from two uniaxial isothermal (205 and 425 °C) and one out-of-phase uniaxial thermomechanical (200 to 400 °C) experiments are presented in Fig. 22. The thermomechanical test was conducted in such a way that the mechanical strain range and mechanical strain rate were similar to what was used for the isothermal experiments. Because of the temperature response limitations of the experiment itself, it should be noted that at the tensile peaks of each thermomechanical cycle, the temperature undershot its lower bound by -5 °C (195 °C instead of 200 °C).

From Fig. 22 it can be observed that at the tenth cycle of the isothermal tests the stress - inelastic strain responses are similar. As for the thermomechanical test, the stress - inelastic strain response is slightly different compared to the isothermal data. This is probably due to the difference in mechanical strain range caused by the temperature overshoot. As can be seen, the stress - inelastic strain response for the thermomechanical experiments seems to follow more closely that of the lower temperature isothermal test. As cycling continues, the thermomechanical material response seems to start following that of the higher temperature isothermal experiment. This observation was also observed in another thermomechanical experiment (400 to 600 °C), which suggests that this trend is a general material hardening characteristic, but further investigation will have to be conducted before this can be confirmed.

Preliminary inelastic strain comparisons between isothermal and thermomechanical experimental data have proven useful in developing a better understanding of thermomechanical material response for Hastelloy-X. From these types of comparisons it appears that general thermomechanical material behavior can be extracted from isothermal experimental data, but information concerning changes in material strain hardening behavior must come from thermomechanical test data.

Tests on Haynes 188, a cobalt-based superalloy used in hot section component applications were also conducted in the laboratory (Ellis et al., 1987). An example of the test results obtained is presented. In this example we are concerned with determining the stress levels or "thresholds" at which creep deformations first become significant in Haynes 188 over a temperature range of interest. A second series of experiments was conducted to establish whether the thresholds determined under monotonic conditions also apply in the case of thermomechanical loading.

As shown in Table II, the threshold experiments showed the expected result that early creep response is strongly temperature dependent. It can be seen that at 649 °C, stress levels must exceed 207 MPa (30 ksi) before creep strains become significant during the 1.5 hr hold periods. At temperatures of 760 and 871 °C, the corresponding values of stress are 75.9 MPa (11 ksi) and 27.6 MPa (4 ksi), respectively. One important point to be noted about this result is that it would not have been predicted by inspection of handbook data. This is because material handbooks provide little or no information regarding the early stages of creep. It follows that problems can arise if decisions regarding the need for inelastic analysis are based on casual inspection of handbook data. The present study clearly indicated that some form of inelastic analysis is necessary for components operating at temperatures as high as 871 °C if stress levels are expected to exceed 27.6 MPa (4 ksi).

Turning to the results of the thermomechanical experiments on Haynes 188, ratchetting behavior can be observed in the data shown in Fig. 23 for a mean stress of 42.5 MPa (6.17 ksi). In this case, the creep strain accumulated during cycle (1) was about 100 με. On subsequent cycles, the creep occurring per

cycle was 50 με or less and the data exhibited considerable scatter. The reason for the scatter is the electrical noise which complicated interpretation of the 42.5 MPa (6.17 ksi) mean stress data.

The material exhibited creep ratchetting during simulated service cycles. This result was not predicted by analysis using current constitutive models for Haynes 188.

Lewis Annular Combustor Liner Test Facility Structural Component Response Rig

Segments, or cylindrical sections of gas turbine engine combustor liners were radiantly heated in the Structural Component Response rig shown in Fig. 24. Quartz lamps were used to cyclically heat the 20-in (0.5 m) diameter test liners. This resulted in axial and circumferential temperature variations as well as through-the-thickness temperature gradients in the test liner similar to those of in-service liners, and thus similar thermally induced stresses and strains. A typical engine mission cycle (take-off, cruise, landing, and taxi) of 3 to 4 hr was simulated in 2 to 3 min. The simulated cyclic temperatures and temperature gradients were felt to be adequate to capture the time-independent and time-dependent interactions resulting in deformation as well as the low-cycle thermal fatigue phenomena of in-service liners. The primary purpose of the rig was to generate large quality thermomechanical databases on combustor liners (Thompson, and Tong, 1986).

The test program was a cooperative effort with Pratt and Whitney Aircraft (PWA), a division of United Technologies Research, East Hartford, Connecticut. PWA supplied the test rig, which included the quartz lamp heating system and several test liners. Lewis provided the test facility and had the responsibilities from integrating the test rig into the test facility up to and including conducting the tests and acquiring the data. Lewis and PWA personnel developed automated computer control strategies, data acquisition systems, and methods for efficient data reduction and analysis.

The quartz lamp heating system consists of 112-6-kVA lamps configured circumferentially in 16 sectors, each having 7 lamps. This system, in addition to drawing up to 672 kVA of 480-V power, requires 3.5 lb/sec of ambient temperature air at 5 psig, 1.5 lb/sec ambient temperature air at 1 psig and 80 gal/min of specially treated water for cooling the rig.

A natural-gas and air mixture is burned in a combustor can upstream of the test section to provide preheated cooling air to the test liner. Cooling air temperatures are controllable from 205 to 316 °C (400 to 600 °F) by varying the fuel/air mixture ratio. The test liner cooling airflow rate is variable from about 4.0 to 7.5 lb/sec at 35 psig. Both the cooling-air temperature and flow rate can be varied to obtain the desired cyclic temperatures on the test liner.

The annular rig has six 5-in. diameter quartz window viewports, three of which are spaced at 120° apart and are used to view the middle section of the test liner. The other three, also spaced at 120° apart, are used to view the upstream portion of the liner and its attachment piece. These windows are rotated 45° from the liner windows. The quartz windows are air and water cooled. Through these windows television, infrared, and high resolution cameras are used to monitor liner condition, temperature, and deformation, respectively.

A microprocessor with a dual-loop programmable controller is used to control the power to the lamps. A specified power-time history is programmed into the microprocessor, and the cooling air temperature and flow rate are appropriately set so that when combined, the desired thermal cycle is imposed on a test liner.

Thermocouples and an infrared thermovision system are used to obtain surface temperatures on the test liner. There are provisions for having a total of 140 thermocouples on the test liner. Both thermocouple and thermal image data are obtained on the cool side of the test specimen. Only thermocouple data are obtained on the hot side (facing the quartz lamps) of the test liner. The thermocouple data provide temperatures at discrete points, while the infrared system provides detailed maps of cool-side thermal information.

The thermal images obtained from the infrared camera are stored on a VHS tape recorder, with the clock time superimposed on each image. Images of the test specimen of from about 4 to about 1 in. in diameter (for finer resolution of temperatures) can be obtained with the zooming capability of the infrared system. Thirty thermal images are captured on tape every second. A computer system is then used to process, reduce, enhance, and analyze the transient temperature information. These data are also compared with the thermocouple data. Thermocouple data are used in the calibration of the infrared system.

During a test run both the facilities data (pressures flows, power, etc.) and the research data (primarily temperature) are acquired for each thermal cycle using the ESCORT II data acquisition system at Lewis. These data are stored automatically once every second on a mainframe computer for later reduction and analysis.

Liner Tests and Results

Two combustor liner segments were tested in the Structural Component Response Rig. First, a conventional liner of sheet metal seam-welded louver construction from Hastelloy-X material (Fig. 25) was tested. Second, an advanced paneled liner (Fig. 25) was tested.

A large, quality (thermocouple (96 TC's) and IR) temperature database was obtained on the conventional liner. Some typical thermocouple data are shown in Fig. 26. The corresponding power history for the thermal cycle is shown in Fig. 27. Figure 26 shows the transient temperature response at three locations on louver 5. The temperature measurements are used in the heat transfer/structural analysis of the liner.

The liner was thermally cycled for almost 1800 cycles. Between 1500 and 1600 cycles an axial crack about 0.2 in. in length developed in the liner. This crack occurred at a hot spot which developed because of closure of several cooling holes. There was no thermocouple right at the hot spot, but surrounding TC's indicated the maximum temperature was at least 937 °C (1720 °F) and could have been over 976 °C (1890 °F).

A composite photograph of the liner after 1782 cycles is shown in Fig. 28. This shows that most of the distortion occurred in louvers 4 to 7, particularly in the bottom (180°) and left (270°) views. The top (0°) and right (90°) views show less distortion.

The test program was terminated after 1782 cycles because the distortion of the louvers became severe enough to contact the frame of one of the quartz lamp banks. Measurements of the crack from the initial observation at 1600 to 1728 cycles indicated 2 percent increase in length.

The distortion of the louvers is typical of liners run in service. The distortion shows some symmetry to the heat pattern of the lamps in that the peaks

of distortion are at the longitudinal center of a lamp bank where the maximum heat flux occurred. It should be noted that a distortion peak was not formed at every bank of lamps.

Similarly, a large quality data base on the advanced combustor liner is being obtained. This liner, consisting of small panels and an outer support shell to which the panels are attached, is instrumented with 125 thermocouples, 73 on the hot side of the panels and 52 on the support shell. A grid system of lines of temperature-sensitive paints was applied to over half of the panels in the liner to increase the area in which we could observe temperature changes. An infrared camera system is being used to obtain temperature maps of a portion of the outer shell of the liner through a quartz viewing window. Over the same field of view, high-resolution photographs of the outer shell are also being taken to determine the total strain during cycling.

Figure 29 is representative of the data obtained on the advanced liner. It is an isometric plot of the thermocouple temperature measurements of the hot side of the liner panels (which shows the cylindrical liner as if it were cut upon and flattened out) and shows a maximum temperature of 760 °C (1400 °F) at the maximum quartz lamp power (cruise condition). A similar plot of the outer shell shows the maximum temperature to be about 316 °C (600 °F). These temperatures were obtained for a heat flux equivalent to that applied to the conventional liner. Transient data are also being obtained. The thermal paint did not indicate a maximum temperature of more than about 649 °C (1200 °F). The infrared data and the high-resolution photographs are being reduced and analyzed.

After 1500 thermal cycles the advanced liner is operating at much lower temperatures than the conventional liner (about 205 °C (400 °F) lower) for the same heat flux. At the lower temperature and low thermal gradients, little distortion to the panels has been observed. Based on the test results and analyses, the operating conditions are not severe enough to distort or damage the advanced liner.

Thermal/Structural/Life Analyses of the Test Liners

The liner surface temperature measurements obtained from the thermocouples and the infrared thermovision system were used to obtain the film coefficients on the cool and hot surfaces. Based on these coefficients, a heat transfer analysis of each liner was performed using MARC, a general purpose nonlinear finite-element heat-transfer and structural-analysis program.

Eight-node three-dimensional solid elements were used to construct the liner heat transfer models. The conventional liner model had 546 elements and 1274 nodes, and the advanced liner model had 536 elements and 1117 nodes. Comparisons between predicted and measured transient temperatures showed good agreement.

The temperature (or thermal loads) are input to the structural analysis program. The MARC program was used to perform the structural analysis. The stress models were identical to the heat transfer models.

The Walker and Bodner viscoplastic models, which were described earlier, were used in the structural analysis. Representative results are the hysteresis loops shown in Fig. 30 for three locations on the conventional liner. Similarly, Fig. 31 is representative of a stress plot of a symmetrically heated panel.

Based on the nonlinear structural analyses of the two liners, it was determined that the critical stress-strain location in the advanced liner was at the retention loop. For the conventional liner, the critical location was at the seam weld.

Based on the stress-strain and temperature at the critical locations, cyclic life of the two liners was assessed. The results are summarized and compared in Table II. The estimated life of the conventional liner (400 to 1000 cycles) is based on limited cyclic life data. Tests showed liner cracking at the seam weld after 1500 cycles. The advanced liner will have a much longer life than the conventional liner because it has a lower average temperature (about 215 °C (440 °F)) and no structural constraint in the circumferential direction. After 1500 cycles the advanced liner shows little distortion and no cracking. The predicted life is greater than 10^6 cycles. These comparisons show there is good agreement between predicted life and measured life.

CONCLUSIONS

The broad scope of structural analysis activities carried out under the HOST project, by the combined efforts of industry, government and universities has resulted in numerous significant accomplishments and, in some cases, major breakthroughs in the nonlinear three-dimensional structural analyses of turbine engine hot section components. The major accomplishments in the three areas of technology addressed synergistically, namely, inelastic constitutive model development, nonlinear three-dimensional structural analysis methods and code development, and experimentation to calibrate and validate the codes are summarized below:

(1) New types of multiaxial viscoplastic constitutive models for high-temperature isotropic and anisotropic (single crystal) superalloys, and metal matrix composites have been developed, calibrated, and validated.

(2) New and improved nonlinear structural analysis methods and codes, in which the viscoplastic constitutive models were incorporated have been developed and, to some extent, validated.

(3) Extensive quality databases, including uniaxial and multiaxial thermomechanical data, were generated for René N4, René 80, Hastelloy-X, MAR M247, B-1900+Hf, PWA1480 and Haynes 188 materials for the purpose of calibrating and validating the constitutive models.

(4) Extensive quality databases have been generated for conventional and advanced combustor liner segments and compared with detailed thermal/structural analyses of these liners using many of the analytical tools developed under HOST.

(5) Advanced instrumentation to measure temperature, displacement and strain have been evaluated.

(6) High temperature laboratories and facilities at universities, other governmental agencies, and industry have been modified and upgraded, and at NASA Lewis, a unique high-temperature fatigue and structures research laboratory has been implemented.

(7) At NASA Lewis, a high-temperature structural component response research facility for testing large diameter combustor liner segments has been implemented.

While the structural analysis capabilities and accomplishments described in this paper are a good beginning, there is much room for improvement. It is expected that these capabilities and future improvements will grow rapidly in their engineering applications and have a major impact and payoff in the analysis and design of the next generation aeronautic and aerospace propulsion systems.

REFERENCES

Chan, K.S., Lindholm, U.S., Bodner, S.R., Hill, J.T., Weber, R.M., and Meyer, T.G., 1986, NASA CR-17922.

Walker, K.P., 1981, "Research and Development Program for Non-Linear Structural Modeling With Advanced Time-Temperature Dependent Constitutive Relationships," NASA CR-165533.

Bodner, S.R. and Partom, Y., 1975, "Constitutive Equations for Elastic-Viscoplastic Strain-Hardening Materials," Journal of Applied Mechanics, Vol. 42, No. 2, pp. 385-389.

Ramaswamy, V.G., 1986, "A Constitutive Model for the Inelastic Multiaxial Cyclic Response of a Nickel Base Superalloy RENE 80," NASA CR-3998.

Robinson, D.N., 1984, "Constitutive Relationships for Anisotropic High-Temperature Alloys," Nuclear Engineering and Design, Vol. 83, No. 3, pp. 389-396.

Walker, K.P., and Jordan, E.H., 1987, "Constitutive Modelling of Single Crystal and Directionally Solidified Superalloys," Turbine Engine Hot Section Technology 1987, NASA CP-2493, pp. 299-301.

Dame, L.T., and Stouffer, D.C., 1986, "Anisotropic Constitutive Model for Nickel Base Single Crystal Alloys: Development and Finite Element Implementation," NASA CR-175015.

Robinson, D.N., Duffy, S.F., and Ellis, J.R., 1986, "A Viscoplastic Constitutive Theory for Metal Matrix Composites at High Temperature," NASA CR-179530.

Maffeo, R., 1984, "Burner Liner Thermal-Structural Load Modeling," NASA CR-174892.

McKnight, R.L., 1985, "Component-Specific Modeling," NASA CR-174925.

McKnight, R.L., Chen, P.C., Dame, L.T., Holt, R.V., Hugny, H., Hartle, M., Gellin, S., Allen, D.H., and Haisler, W.E., 1986, "On 3D Inelastic Analysis Methods for Hot Section Components," Turbine Engine Hot Section Technology 1986, NASA CP-2444, pp. 257-268.

Nakazawa, S., 1987, "On 3D Inelastic Analysis Methods for Hot Section Components, Vol. 1 - Special Finite Element Models," NASA CR-179494.

Wilson, R.B. and Banerjee, P.K., 1986, "On 3D Inelastic Analysis Methods for Hot Section Components, Vol. 2 - Advance Special Function Models," NASA CR-179517.

Battiste, R.L. and Ball, S.J., 1986, "Determination of Surfaces of Constant Inelastic Strain Rate at Elevated Temperature," Turbine Engine Hot Section Technology 1986, NASA CP-2444, pp. 307-325.

Bartolotta, P.A. and McGaw, M.A., 1987, "A High Temperature Fatigue and Structures Testing Facility," NASA TM-100151.

Bartolotta, P.A., 1985, "Thermomechanical Cyclic Hardening Behavior of Hastelloy-X," NASA CR-174999.

Ellis, J.R., Bartolotta, P.A., Allen, G.P., and Robinson, D.N., 1986, "Thermomechanical Characterization of Hastelloy-X Under Uniaxial Cyclic Loading," Turbine Engine Hot Section Technology 1986, NASA CP-2444, pp. 293-305.

Bartolotta, P.A., 1987, "Use of Inelastic Strain as a Basis for Analyzing Thermomechanical Test Data," Turbine Engine Hot Section Technology 1987, NASA CP-2493, pp. 303-315.

Ellis, J.R., Bartolotta, P.A., and Mladsi, S.W., 1987, "Preliminary Study of Creep Thresholds and Thermomechanical Response in Haynes 188 at Temperatures in the Range 649 to 871 °C," Turbine Engine Hot Section Technology 1987, NASA CP-2493, pp. 317-334.

Thompson, R.L. and Tong, M.T., 1986, "Unified Constitutive Materials Model Development and Evaluation for High-Temperature Structural Analysis Applications," 15th Congress of the International Council of the Aeronautical Sciences, Vol. 2, AIAA, New York, pp. 1505a-1505s.

TABLE I. - HOST STRUCTURAL ANALYSIS PROGRAMS

NAS3-23925, Southwest Research Institute (U.S. Lindholm), Constitutive Modeling for Isotropic Materials.

NAS3-23927, General Electric (V.G. Ramaswamy), Constitutive Modeling for Isotropic Materials.

NAS3-379, University of Akron (D.N. Robinson), Multiaxial Theories of Viscoplastic for Isotropic and Anisotropic Materials.

NAG3-512, University of Connecticut (E.H. Jordan), Constitutive Modeling of Single Crystal and Directionally Solidified Superalloys.

NAG3-511, University of Cincinnati (D.C. Stouffer), Anisotropic Constitutive Modeling for Nickel-Base Single Crystal Superalloy René N4.

NAS3-23272, General Electric (R. Maffeo), Burner Liner Thermal/Structural Load Modeling.

NAS3-23687, General Electric (R.L. McKnight), Component-Specific Modeling.

NAS3-23698, General Electric (R.L. McKnight), Three-Dimensional Inelastic Analysis Methods for Hot Section Components I.

NAS3-23697, Pratt and Whitney Aircraft (E.S. Todd), Three-Dimensional Inelastic Analysis Methods for Hot Section Components II.

IAN 40-1447-84 and DE-AC05-840R 21400, Oak Ridge National Laboratory (J.R. Corum), Determination of Surface of Constant Inelastic Strain Rate at Elevated Temperature.

NASA Lewis Research Center (J.R. Ellis and P.E. Moorhead), High-Temperature Fatigue and Structures Laboratory/Structural Component Response Facility.

TABLE II. - CREEP THRESOLDS DETERMINED FOR HAYNES 188 AT TEMPERATURES IN THE RANGE 649 TO 871 °C

Temperature, °C	Creep thresold,[a] ksi
649	30
760	11
871	4

TABLE III. - SUMMARY OF STRUCTURAL-LIFE ANLAYSES OF COMBUSTOR LINERS AT A CRITICAL LOCATION

(a) Conventional liner

Analytical method	Temperature range, °F	Strain range, με		Mean stress, psi	Predicted life, cycles
		Mechanical	Inelastic		
Unified (Walker)	950 to 1630	5870	3150	-35 000	400 to 1000
Unified (Bodner)	950 to 1630	5800	2700	-28 000	400 to 1000

(b) Segmented liner

Analytical method	Temperature range, °F	Strain range, με		Mean stress, psi	Predicted life, cycles
		Mechanical	Inelastic		
Unified (Walker)	755 to 1180	810	10^{-1}	10 000	$>10^6$
Unified (Bodner)	755 to 1180	820	10^{-1}	15 000	$>10^6$

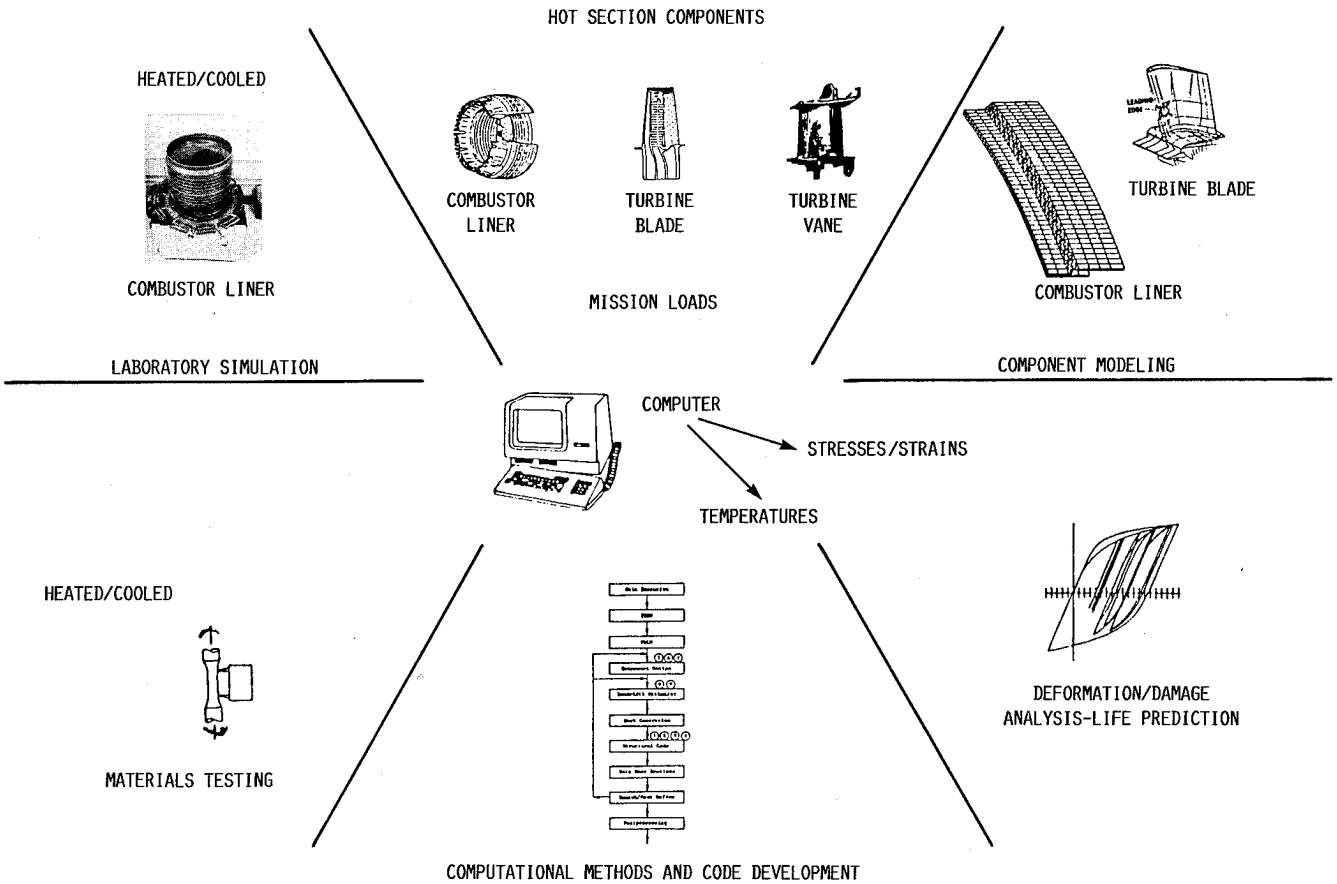

FIGURE 1. - NONLINEAR STRUCTURAL ANALYSIS TECHNOLOGIES AND ACTIVITIES UNDER HOST.

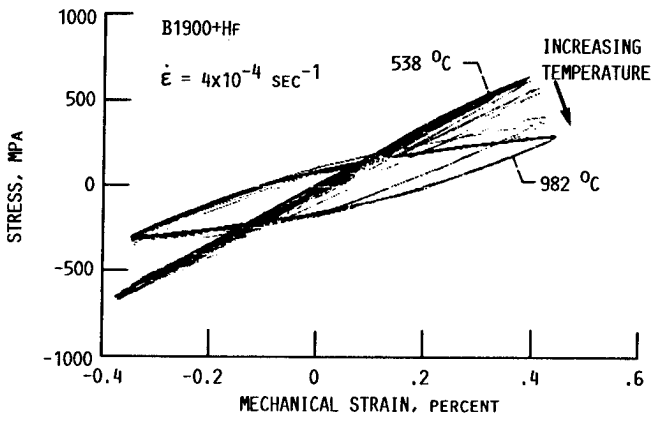

FIGURE 2. - CONTROLLED STRAIN CYCLING WITH TEMPERATURE CHANGE FROM 538 °C TO 982 °C.

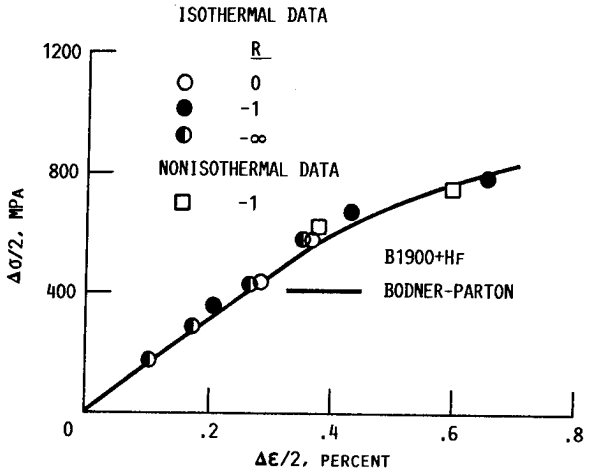

FIGURE 3. - COMPARISON OF ISOTHERMAL AND NON-ISOTHERMAL CYCLIC DATA OF B1900+Hf AT 760 °C.

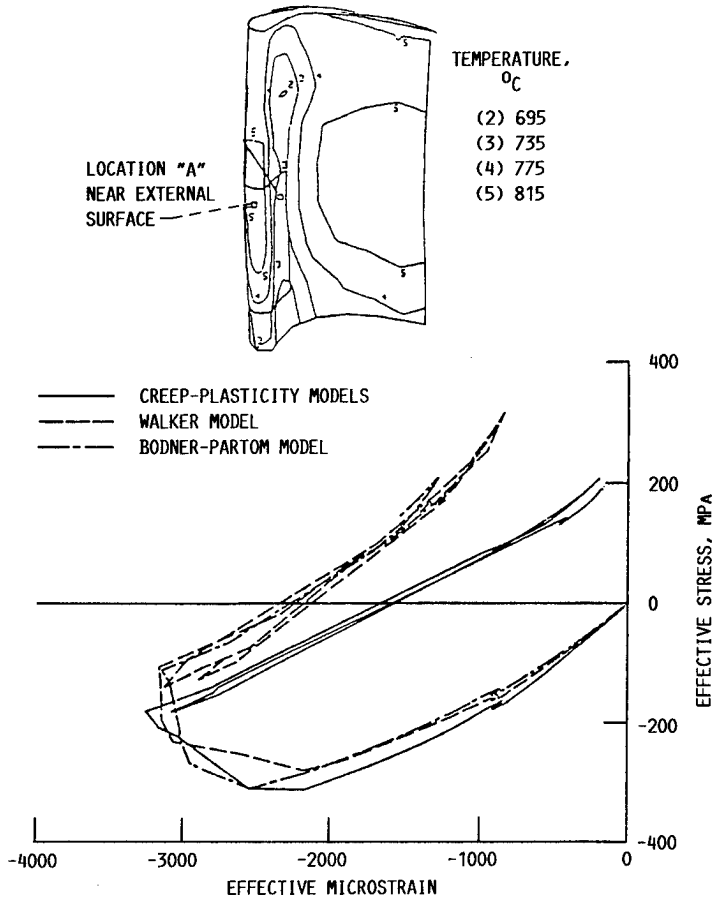

FIGURE 4. - AIRFOIL CALCULATIONS AT LOCATION "A" USING THE MARC FINITE ELEMENT ANALYSIS CODE.

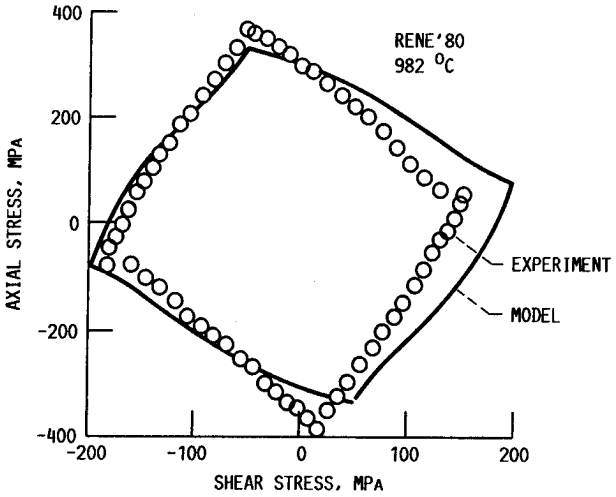

FIGURE 5. - RENE'80 RESPONSE TO 90° OUT-OF-PHASE TENSION/TORSION CYCLIC LOADING.

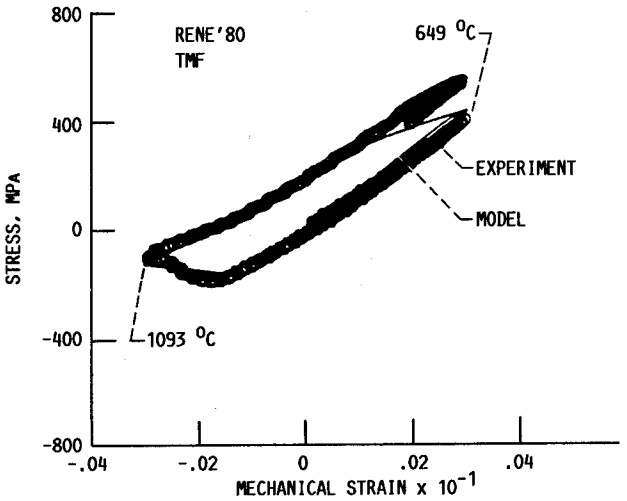

FIGURE 6. - RENE'80 TMF RESPONSE (649-1093 °C OUT-OF-PHASE).

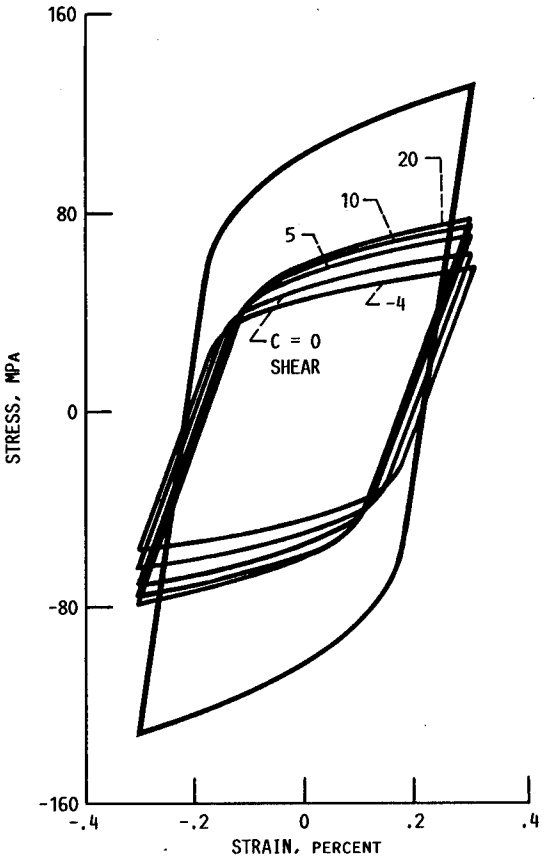

FIGURE 7. - SATURATED HYSTERESIS LOOPS FOR $\Delta\epsilon$ = 0.6 PERCENT AND $\dot{\epsilon}$ = .001/M. SHOWN IS UNIAXIAL RESPONSE AND SHEAR RESPONSES FOR SEVERAL VALUES OF C.

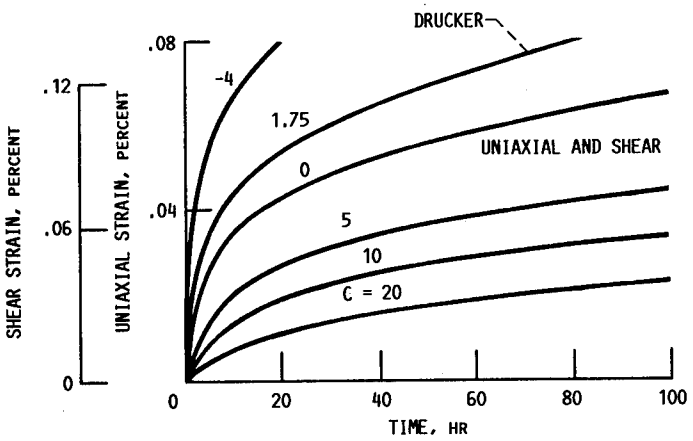

FIGURE 8. - CREEP RESPONSE IN UNIAXIAL TENSION AND SHEAR FOR SEVERAL VALUES OF C.

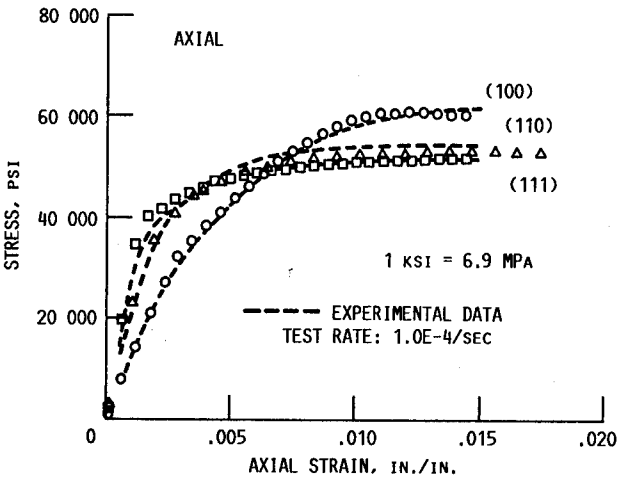

FIGURE 9. - RENE N4 PREDICTED TENSILE RESPONSE AND EXPERIMENTAL DATA FOR SPECIMEN ORIENTATIONS OF [100], [110], AND [111] AT 982 °C (1800 °F).

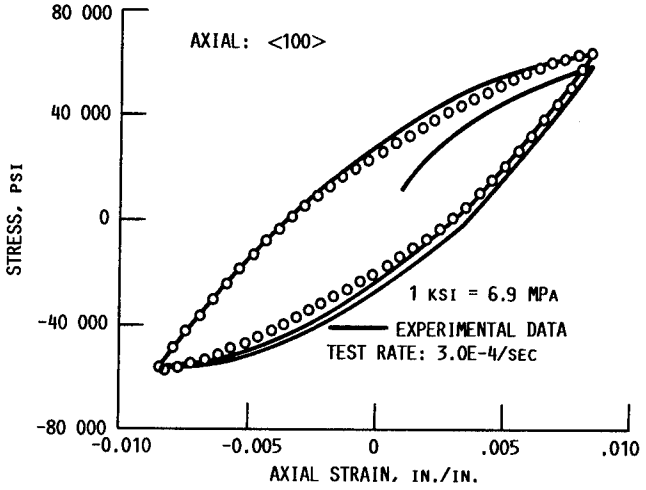

FIGURE 10. - RENE N4 PREDICTED CYCLIC RESPONSE AND EXPERIMENTAL DATA FOR SPECIMEN ORIENTATION OF [100] AT 982 ^{o}C (1800 ^{o}F).

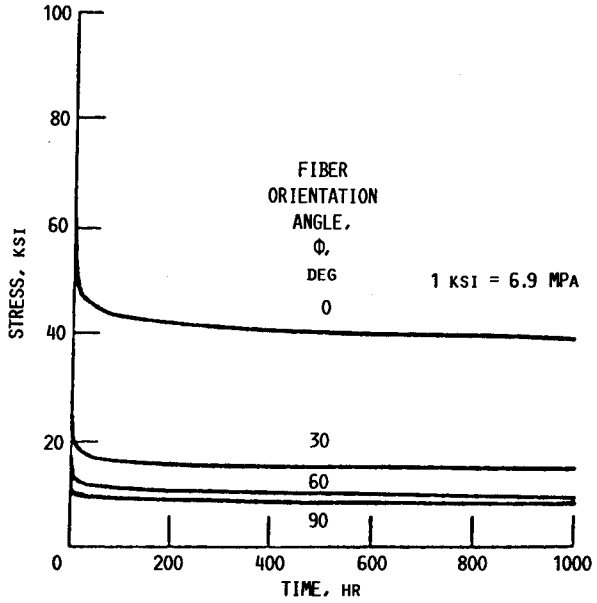

FIGURE 11. - RELAXATION CURVES FOR DIFFERENT FIBER ORIENTATION ANGLES.

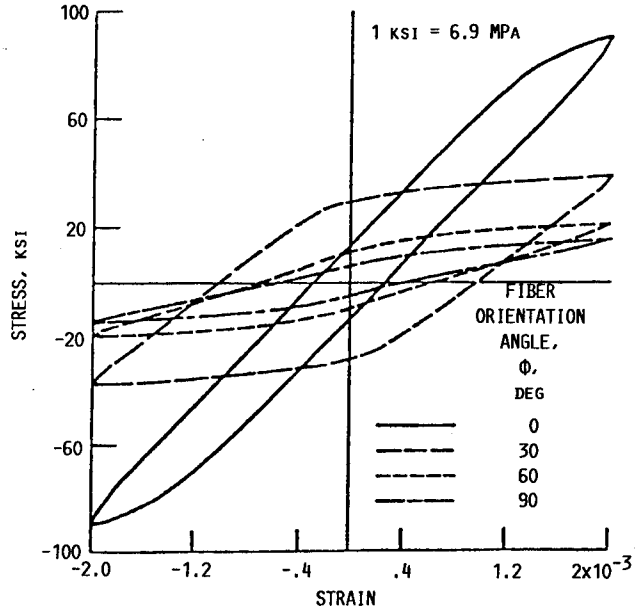

FIGURE 12. - HYSTERESIS LOOPS FOR DIFFERENT FIBER ORIENTATION ANGLES; STRAIN RATE = 0.001/MIN.

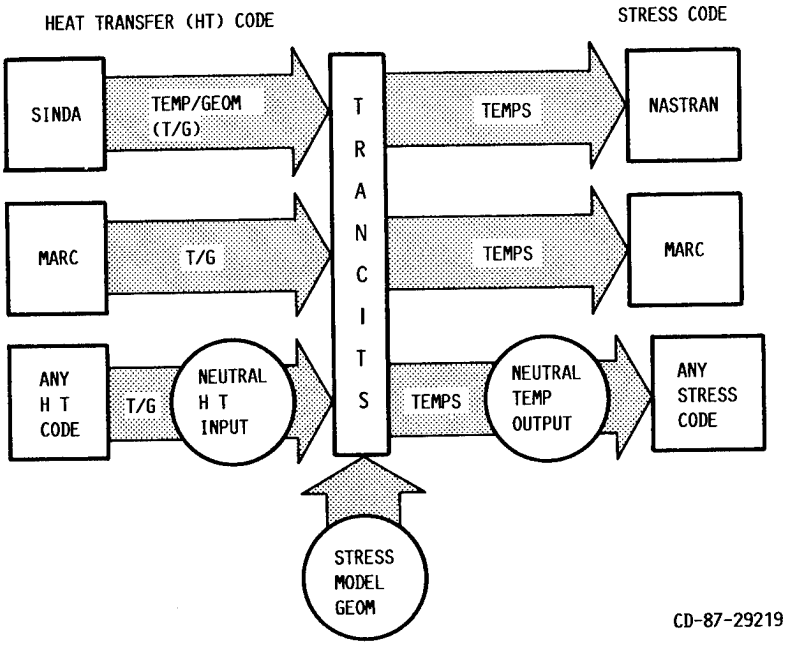

FIGURE 13. - SCHEMATIC FOR THREE-DIMENSIONAL TRANCITS COMPUTER PROGRAM.

COMBUSTOR LINER PARAMETER LIST

CODE	NAME	DEFAULT	CODE	NAME	DEFAULT
1	X_1	0.0	2	Y_1	0.0
3	σ_1	0.0	4	L_1	10.5
5	L_2	2.0	6	L_3	0.5
7	L_4	6.0	8	L_5	0.8
9	L_6	1.0	10	L_7	2.0
11	T_1	0.5	12	T_2	0.7
13	T_3	0.5	14	T_4	0.65
15	T_5	0.5	16	θ_1	90.0
17	θ_2	90.0	18	R_1	1.0
19	R_2	1.0	20	R_3	0.75
21	R_4	1.5	22	R_5	1.5
23	R_6	1.5			

X = COORDINATE
Y = COORDINATE
σ = ANGLE WRT. x - AXIS
L = LENGTH
T = THICKNESS
θ = ANGLE OF ROTATION
R = RADIUS OF CURVATURE
(N) = PARAMETER CODE NUMBER

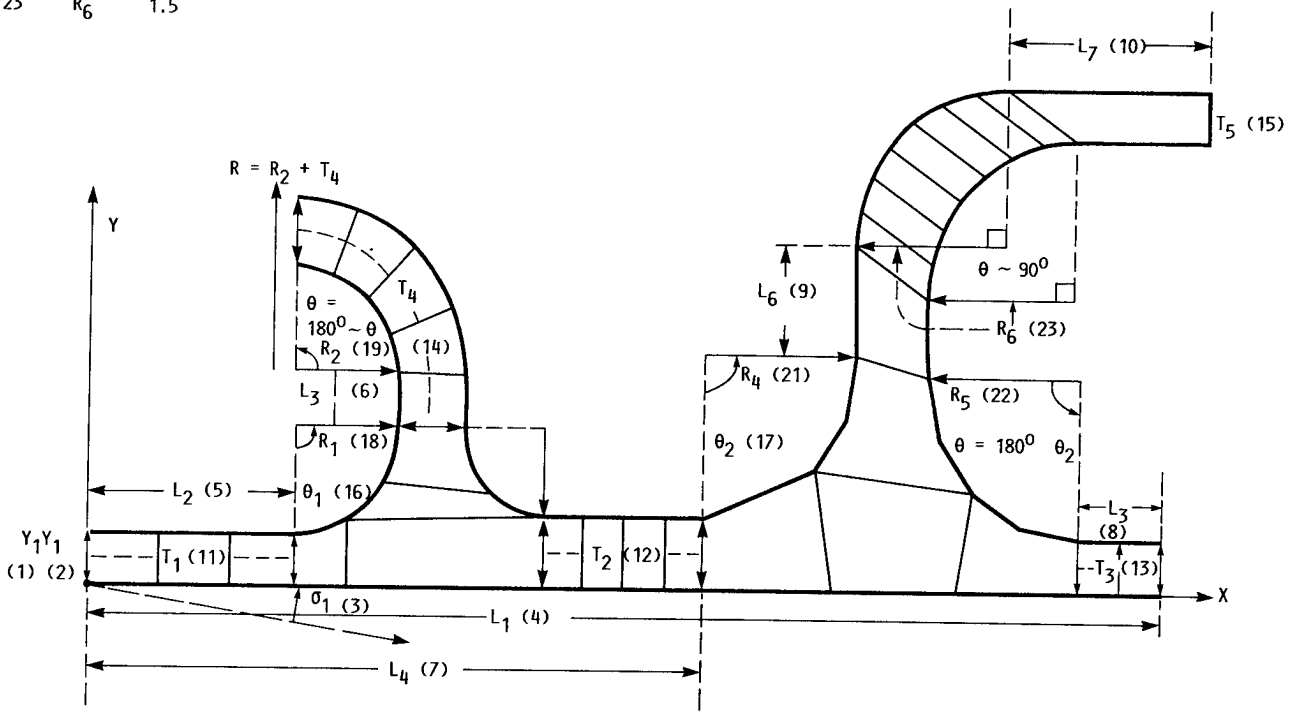

FIGURE 14. - COMBUSTOR LINER PARAMETERS.

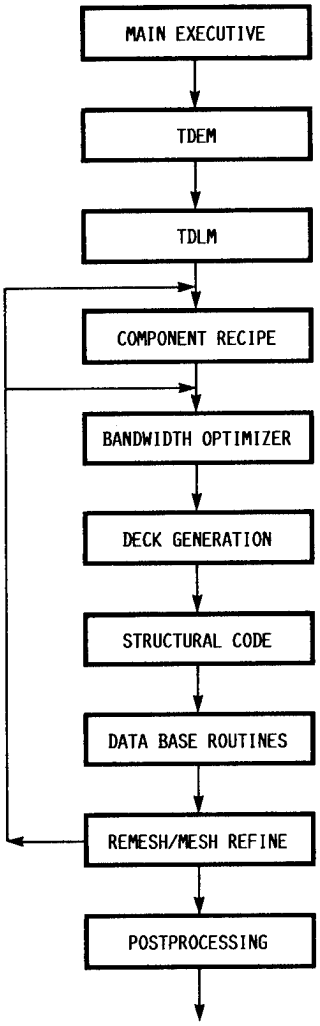

FIGURE 15. - SYSTEM FLOW CHART FOR COSMO.

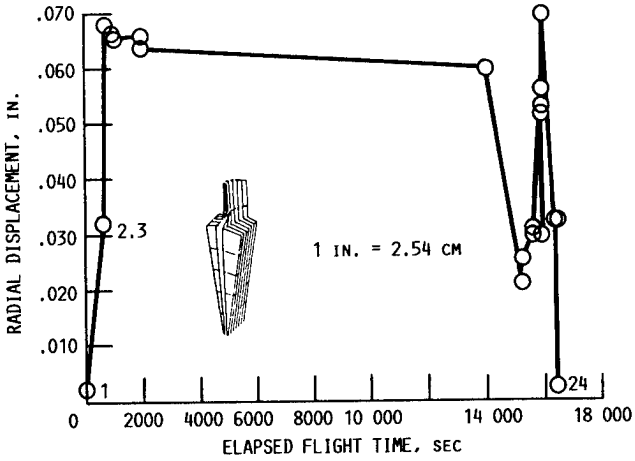

FIGURE 16. - RADIAL DISPLACEMENT OF LEADING EDGE TIP, STATIC.

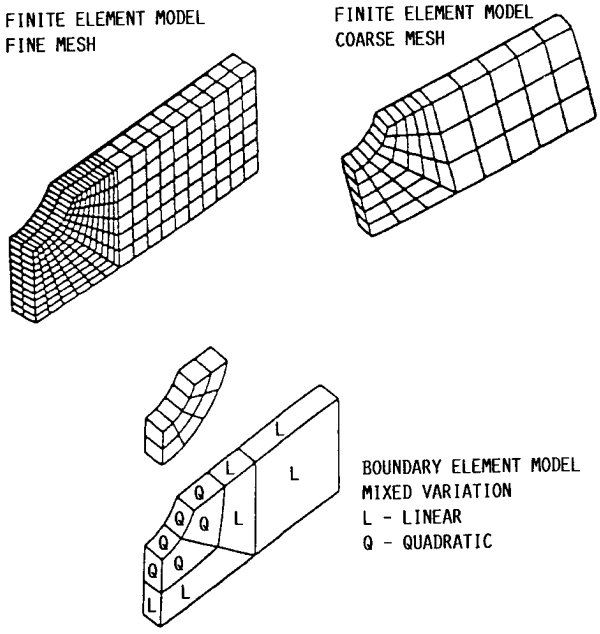

FIGURE 17. - MESHES USED IN BENCHMARK NOTCH ANALYSIS.

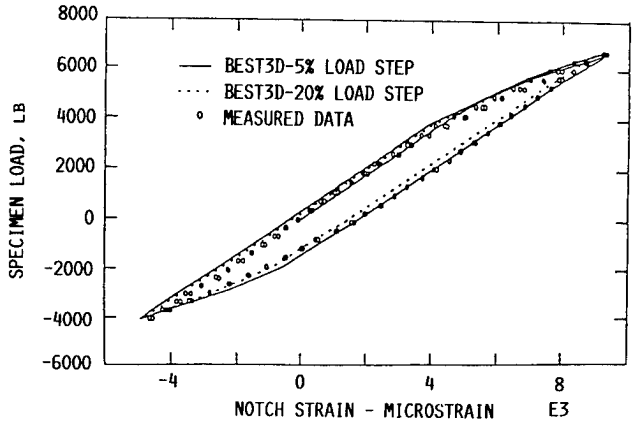

FIGURE 18. - CYCLIC BEHAVIOR AT ROOT OF SPECIMEN NOTCH.

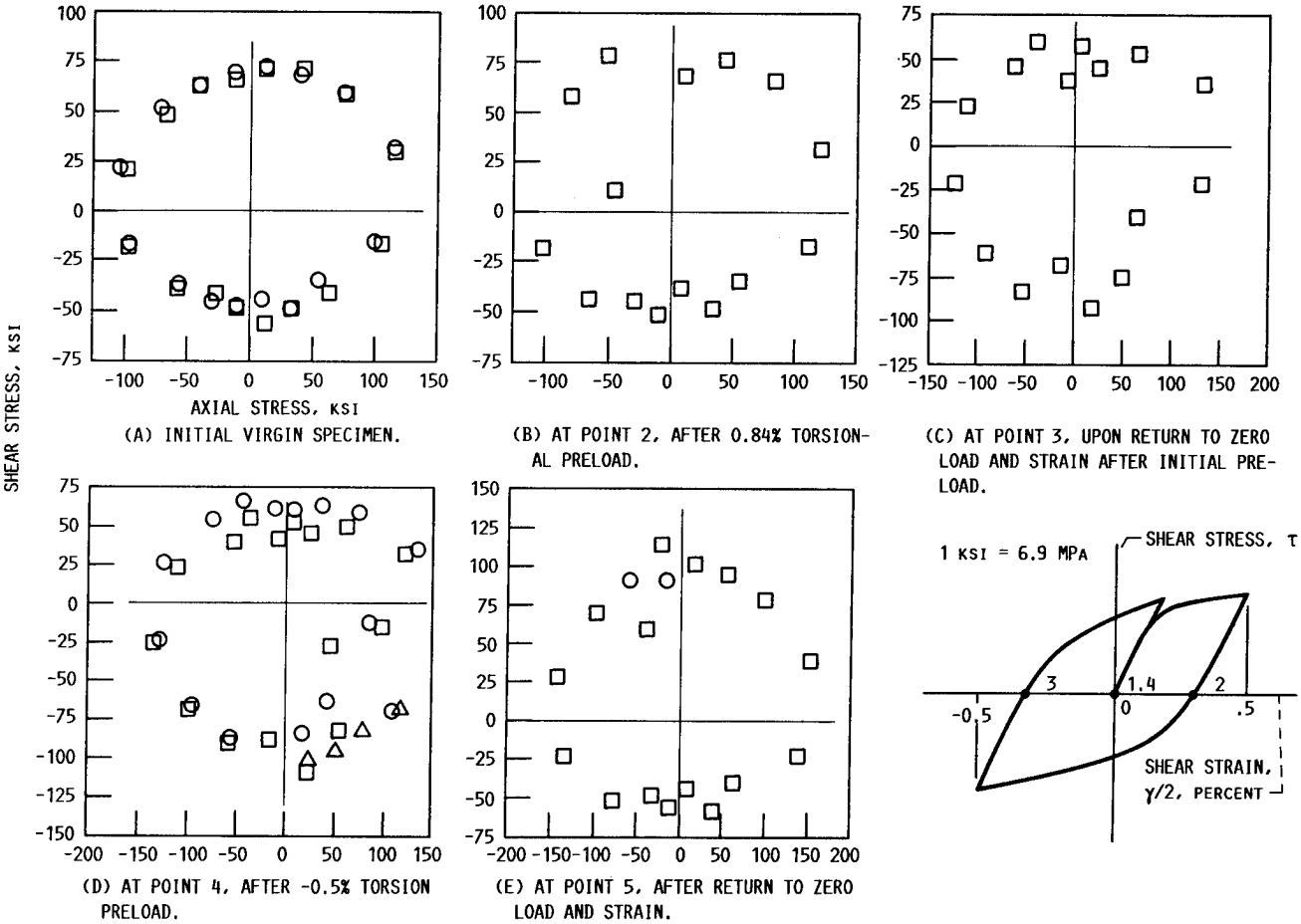

FIGURE 19. - MEASURED 650 ^{o}C SURFACES OF CONSTANT INELASTIC STRAIN RATE FOR REFERENCE SCISRs TEST PROGRAM.

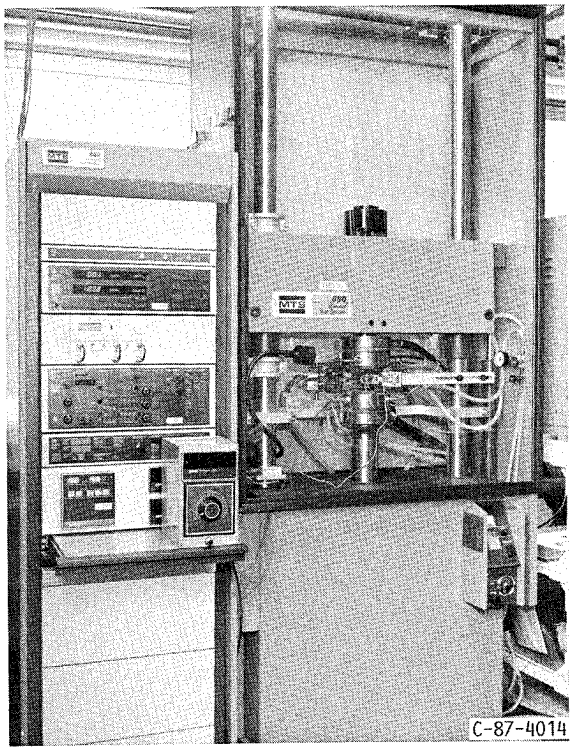

UNIAXIAL TEST SYSTEM

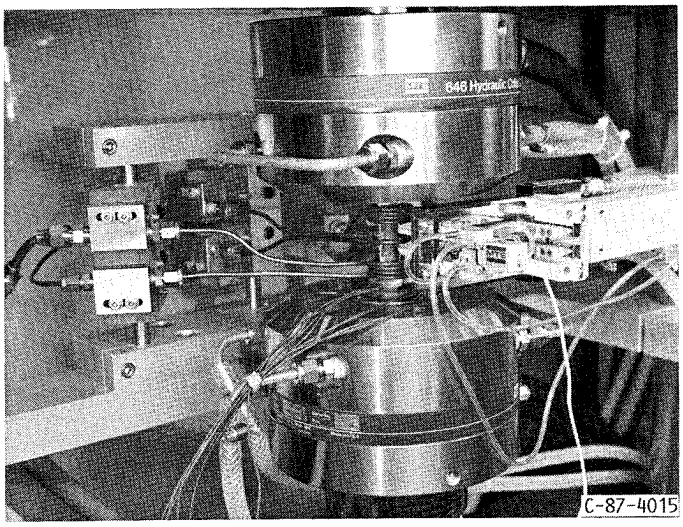

UNIAXIAL LONGITUDINAL EXTENSOMETER IN TEST SETUP

FIGURE 20. - UNIAXIAL TEST SYSTEM.

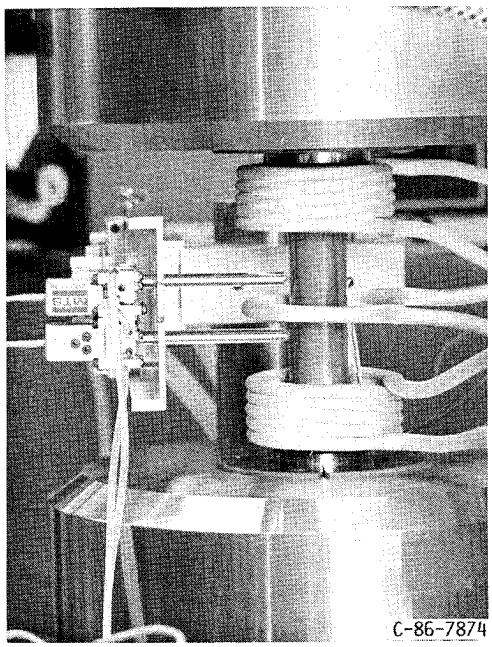

COMMERCIALLY AVAILABLE BIAXIAL EXTENSOMETER

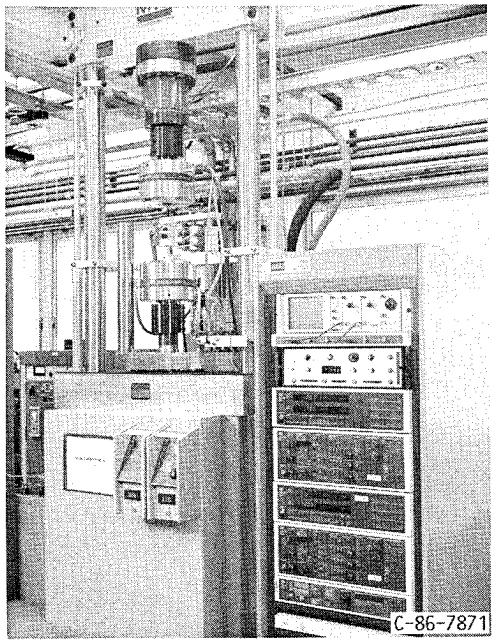

BIAXIAL MATERIAL TEST SYSTEM

FIGURE 21. - BIAXIAL MATERIAL TEST SYSTEM.

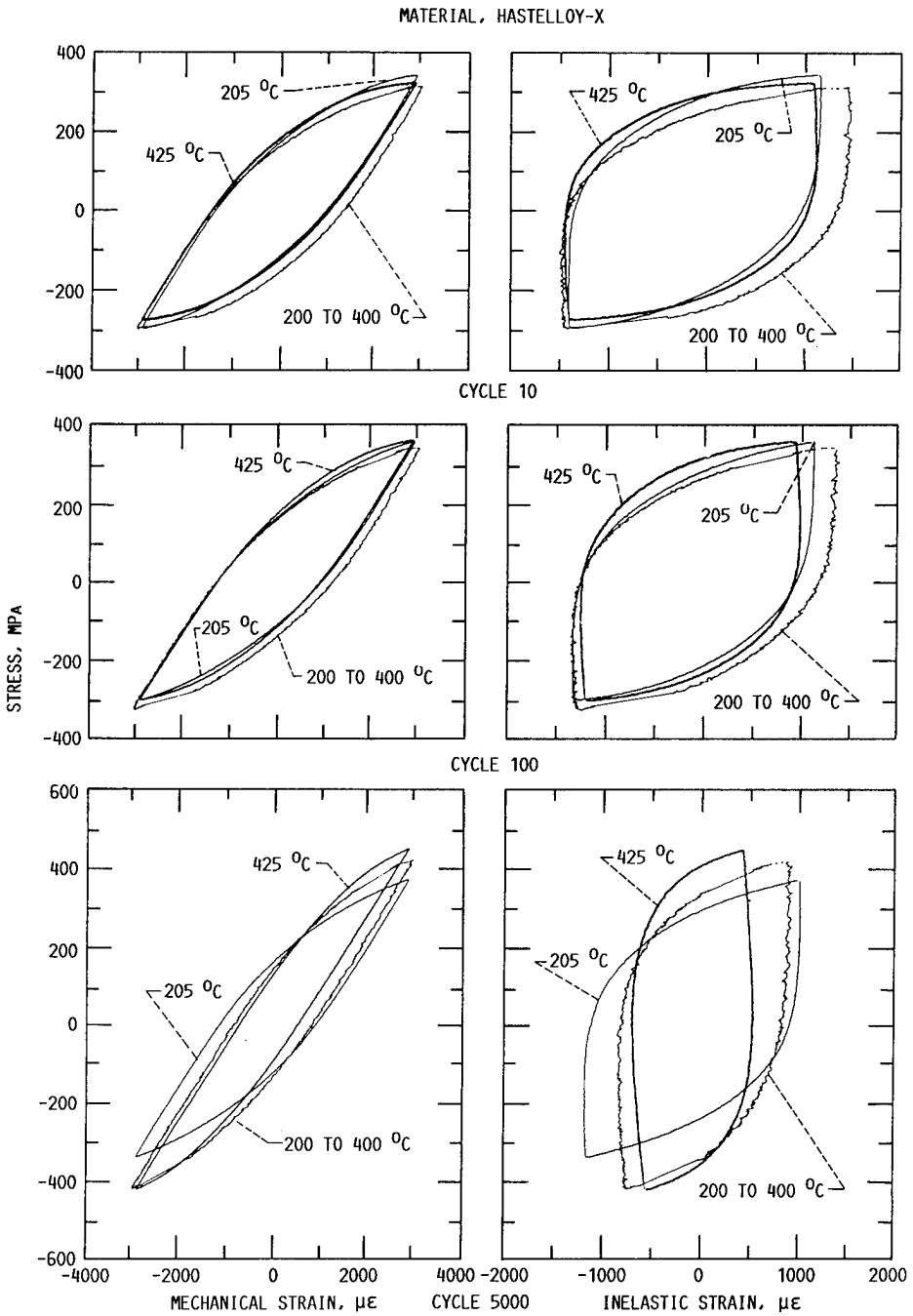

FIGURE 22. - COMPARISON OF MATERIAL RESPONSE DETERMINED UNDER ISOTHERMAL AND THERMO-MECHANICAL CYCLIC LOADING.

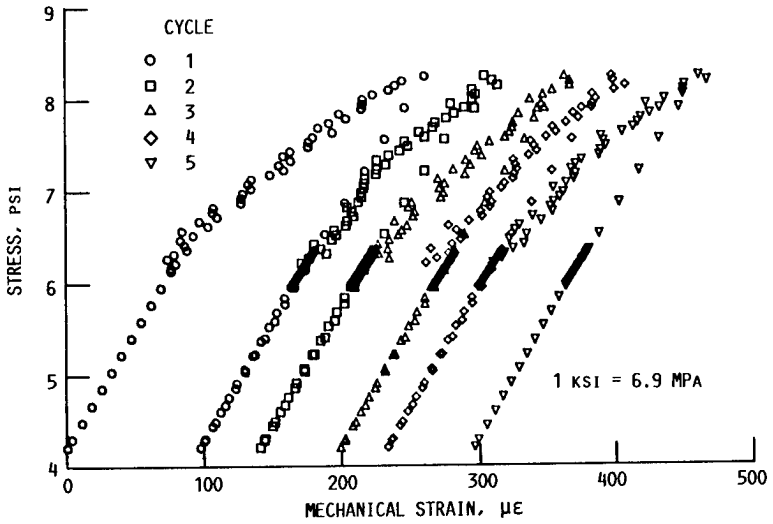

FIGURE 23. - CREEP RATCHETTING RESULTING FROM THERMOMECHANICAL CYCLING FOR 6.17 KSI MEAN STRESS.

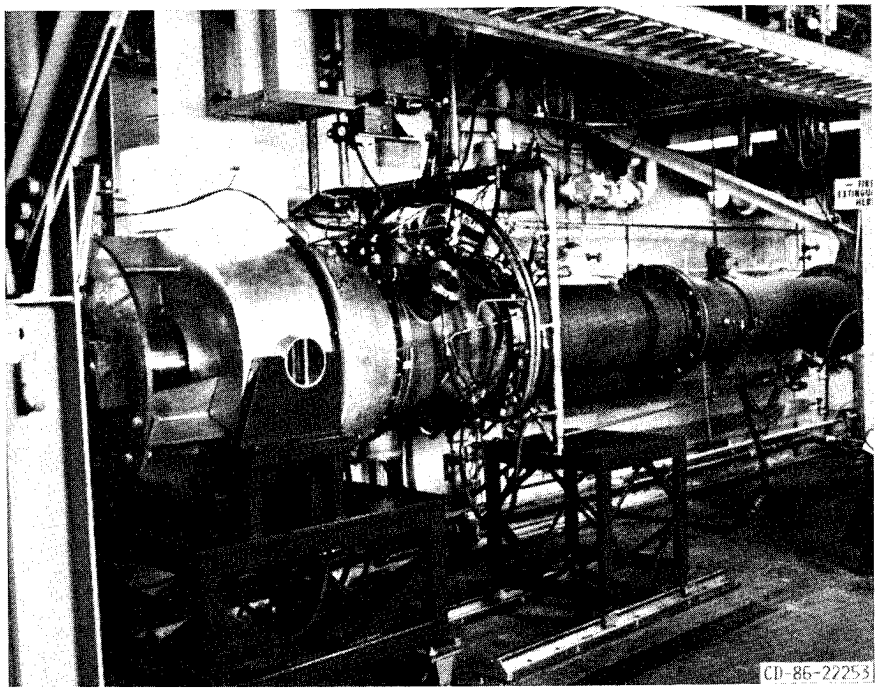

FIGURE 24. - STRUCTURAL COMPONENT RESPONSE RIG.

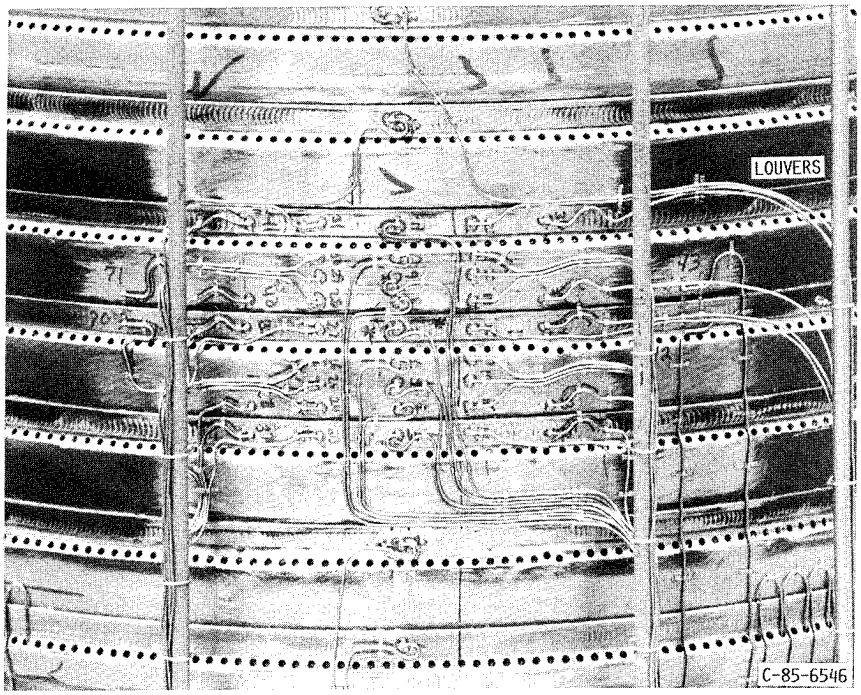

CONVENTIONAL

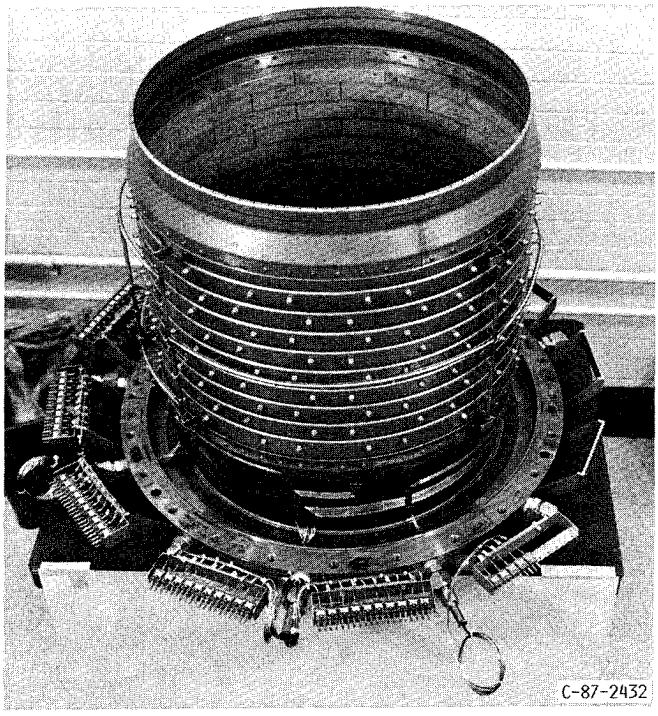

ADVANCED (SEGMENTED)

FIGURE 25. - CONVENTIONAL AND SEGMENTED COMBUSTOR LINERS INSTRUMENTED FOR TESTING.

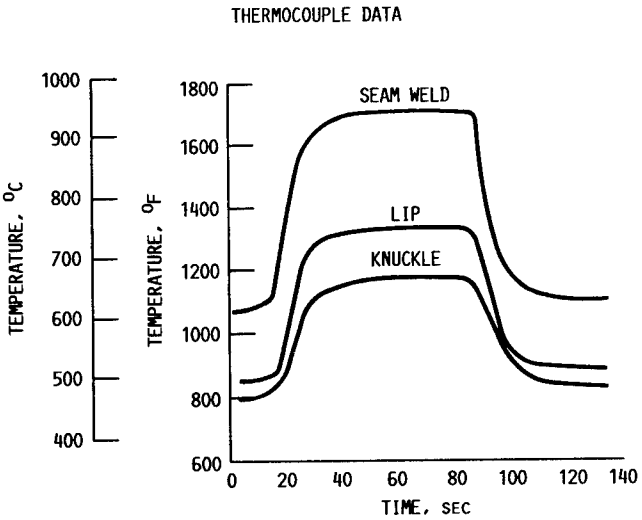

FIGURE 26. - CYCLIC SURFACE LINER TEMPERATURES AT THREE LOCATIONS ON LOUVER 5.

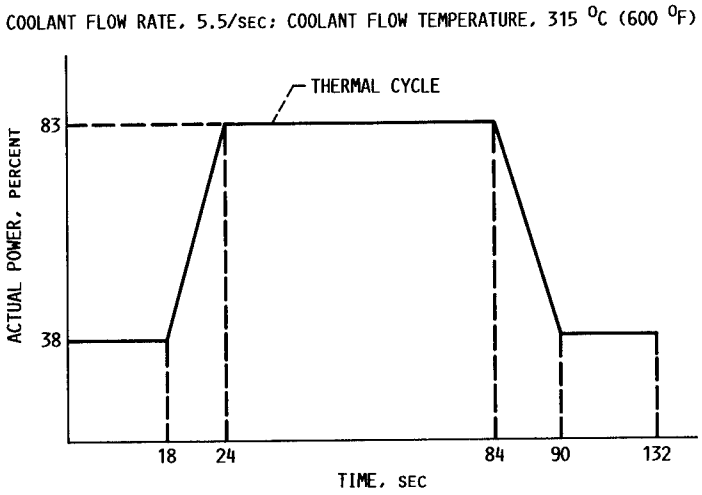

FIGURE 27. - POWER HISTORY FOR THERMAL CYCLE.

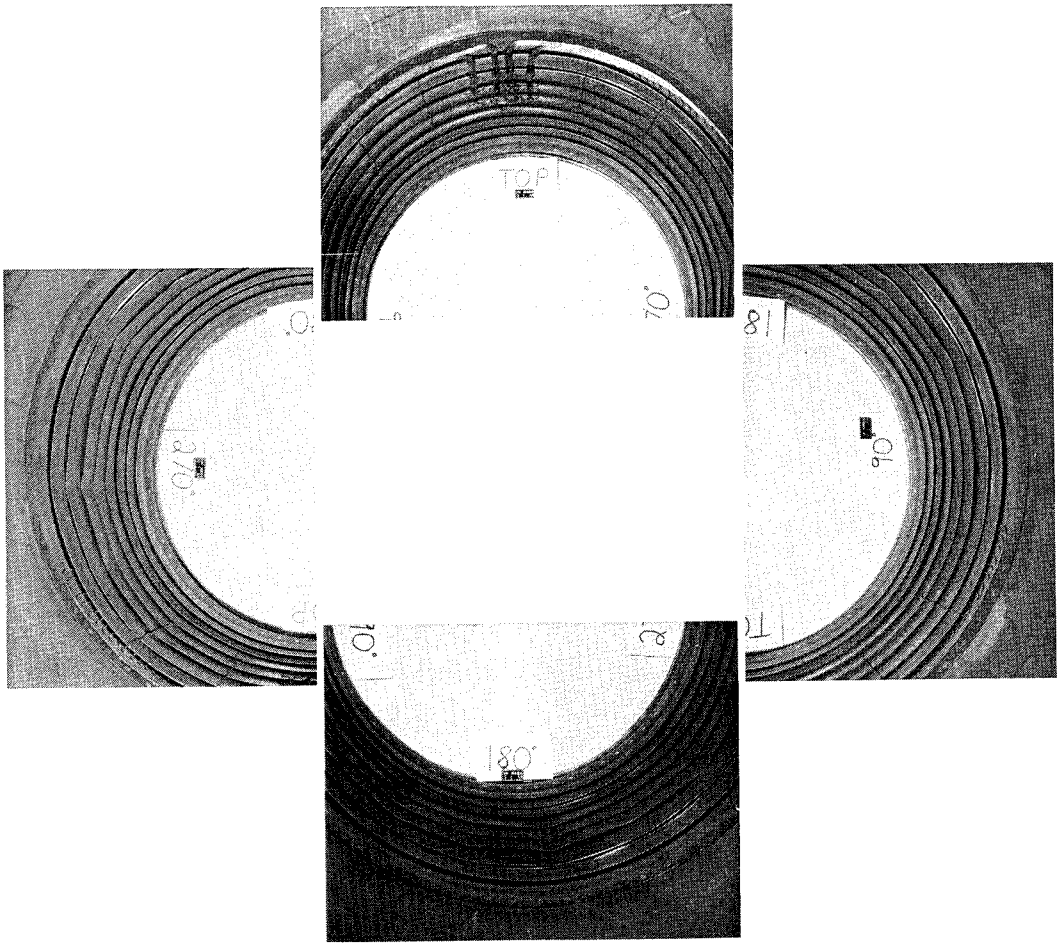

FIGURE 28. - COMPOSITE PHOTOGRAPH OF HOT SIDE CONVENTIONAL LINER DISTORTION AFTER 1782 THERMAL CYCLES.

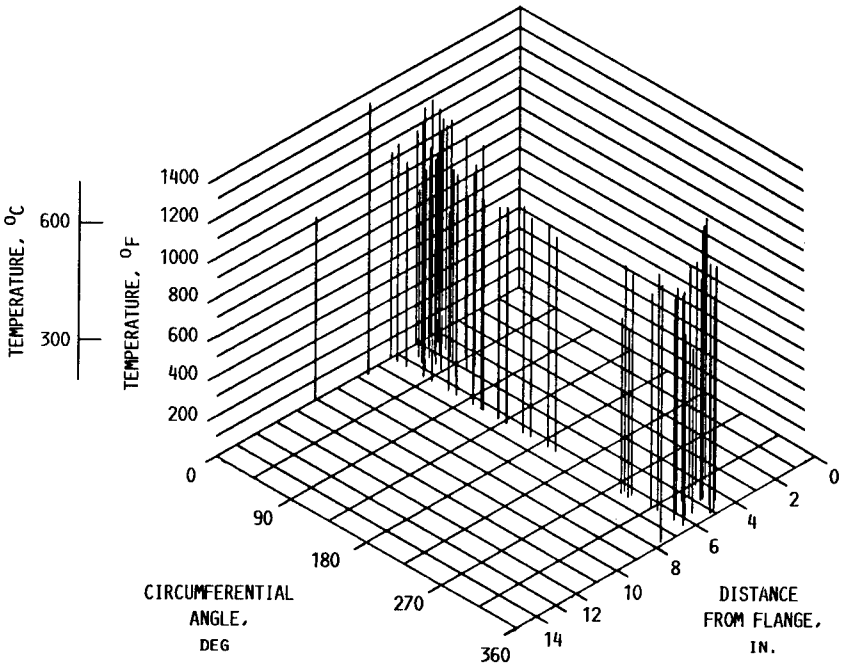

FIGURE 29. - ISOMETRIC PLOT OF TEMPERATURE ON INSIDE OF SEGMENTED COMBUSTOR LINER.

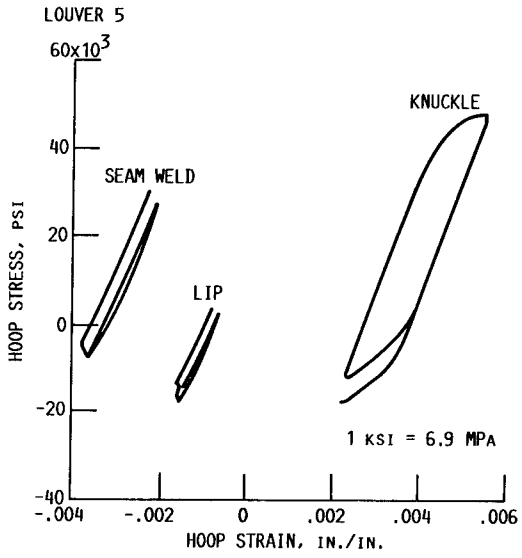

FIGURE 30. - REPRESENTATIVE STRESS-STRAIN PREDICTIONS AT THREE LOCATIONS ON THE CONVENTIONAL LINER.

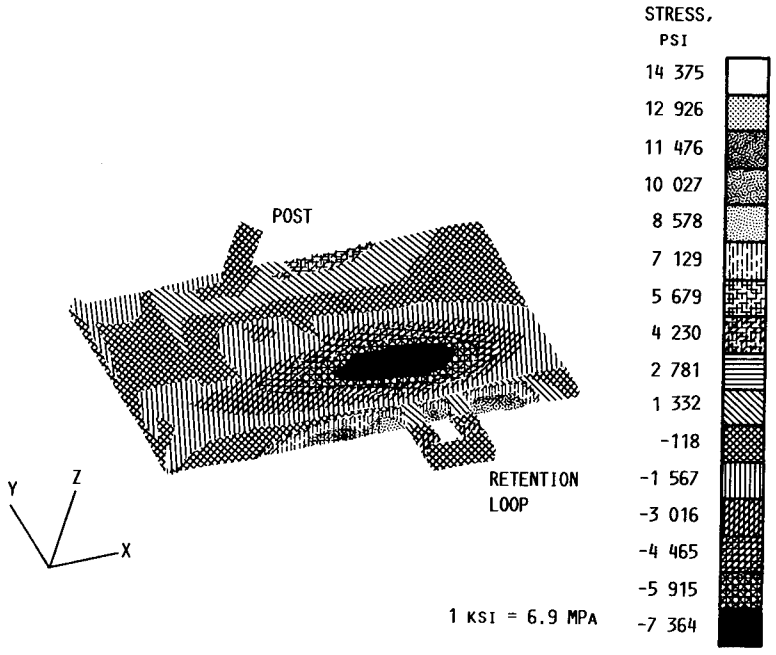

FIGURE 31. - ADVANCED COMBUSTOR LINER STRESS DISTRIBUTION ON SYMMETRICAL PANEL AT AN 83 PERCENT POWER LEVEL (X-DIRECTION).

STRUCTURAL ANALYSIS APPLICATIONS

R. L. McKnight
General Electric AEBG
Cincinnati, Ohio

ABSTRACT

The programs in the structural analysis area of the HOST program emphasized the generation of computer codes for performing three-dimensional inelastic analysis with more accuracy and less manpower. This paper presents the application of that technology to Aircraft Gas Turbine Engine (AGTE) components; combustors, turbine blades, and vanes. Previous limitations will be reviewed and the breakthrough technology highlighted. The synergism and spillover of the program will be demonstrated by reviewing applications to thermal barrier coatings analysis and the SSME HPFTP turbine blade. These applications show that this technology has increased the ability of the AGTE designer to be more innovative, productive, and accurate.

INTRODUCTION

The activities of the NASA Turbine Engine Hot Section Technology Project were directed toward functionality and durability needs of AGTE hot section components - the combustor, turbine vanes, and turbine blades. The overall approach of this program was to assess the existing analysis methods for strengths and deficiencies, and then to conduct supporting analytical and experimental research to rectify those deficiencies and, at the same time, incorporate state-of-the-art improvements into the analysis methods.

Structural analysis has two major objectives in the design of AGTE's. The first major objective is to generate and verify a functional design. The second major objective is to quantify the durability/reliability of these designs. The first objective can be accomplished by analyzing candidate designs for a simplified mission cycle - the maximum envelope of the technical requirements. Evaluations are made by comparing the code outputs - displacements, stresses, and strains - against technical requirements and design practices. The second objective requires that the entire mission cycle be analyzed and the code output be combined with durability/reliability technology in a postprocessing operation.

For both of these types of analyses, some portion of the airframe-engine system is mathematically simulated and a history of the operating environment and interaction effects of the remainder of the system imposed as loads and boundary conditions. For functionality the simpler-maximum history can be imposed on a larger portion of the overall system. Since durability/reliability is a point function, smaller portions of the system must be run through the total complex history of loading. For both of these analyses, the loading, environment, and interactions are provided to the analyst from other "expert" groups.

A deficiency common to both types of analyses is that of economy/productivity as measured by the total period of time, number of man-hours, and the computer resources required to complete a design analysis. For functional analyses, the second major deficiency was due to the combination of the formulation models (Finite-Element Model, Finite Difference Model, Boundary Element Model) and the numerical accuracy of the computer. These limitations affected the ability to accurately simulate large systems with their complex interactions without exceptionally fine modeling. For durability/reliability analyses, the second major deficiency was the inability of the combination of the formulation models, constitutive models, and the numerical accuracy of the computer to accurately simulate the local inelastic material behavior. This deficiency was particularly evident in the hot section components exposed to the severe thermal and mechanical operating environments of the AGTE. The local, durability limiting, areas of these structures are exposed to time varying temperature distribution which affect both the material properties and the thermal and mechanical stresses in a complex three-dimensional manner.

The HOST program successfully accomplished its goals by attacking the above deficiencies. This was done through a series of programs in which were developed constitutive models, three-dimensional inelastic structural analysis codes, a three-dimensional thermal

transfer code, and a component specific modeling system. The application of these advanced tools was almost simultaneous with their development. The remainder of this paper will present selective applications of these technologies.

Combustor Design and Analysis

The combustor is one of the most challenging and complex components of the AGTE. Its design involves many "expert" groups; controls, fuel nozzles, chemical combustion kinetics, heat transfer, and structures. It presents one of the major productivity drains in AGTE designs, both for initial design and for subsequent tuning for mission variations. HOST attacked all aspects of this problem, economy/productivity as well as accuracy, in the component specific modeling effort. In this program the many diverse disciplines which impact on a combustor liner design were integrated into a component specific system utilizing the HOST technologies.

The COSMO computer system consists of a Thermodynamic Engine Model (TDEM), a Thermomechanical Load Model (TDLM), and Combustor Structural Model. The TDEM generates the engine internal flow variables for any point in the operating mission by the specification of three variables, altitude (h), Mach number (M), and power level (PL) for the allowed flight map of an engine, as shown in Fig. 1. Additional control variables are ambient temperature deviations from the standard atmosphere, airframe bleed air requirements, and engine deterioration. For each input condition, specified by h, M, and PL the TDEM calculates gas weight flow (w), temperature (t), and pressure (p) for the combustor.

The TDEM technique is shown in Figs. 2 to 4. The engine to be analyzed must have its aerodynamic stations (Fig. 2) defined thermodynamically by an engine cycle deck (computer program) which can be run to generate the internal flow variables at chosen aerodynamic stations (Fig. 3). In COSMO the complete engine operating map (Fig. 1) is encompassed by selecting 148 operating points for which w, t, p as well as N_1 and N_2, the fan and core speeds, are calculated for the stations pertinent to the COSMO components.

From this station data an Engine Performance Cycle Map is constructed. This is essentially a set of three-dimensional data arrays which map the station data (w, t, p, n_1, and N_2) on to the engine operating map (Fig. 1). Given an arbitrary operating point defined by h, M, and PL it is then, in principle, possible to interpolate on the engine performance cycle map to determine station data. These station parameters are nonlinear functions of the input parameters and much effort went into the development of these multidimensional interpolation techniques.

The functioning of the TDEM is shown in Fig. 4. Given an engine mission, as shown schematically in Fig. 5, it can be defined by values of the input variables h, M, and PL at selected times through the mission. Using these input variables and the Engine Performance Cycle Map the interpolation program calculates engine station parameters throughout the mission (Fig. 4). These are then used to define the station mission profiles of w, t, p, N_1, and N_2 as functions of time at each aerodynamic station. These station mission profiles then become the input to the TDLM.

The TDLM is the computer program which works with the output of the TDEM to produce the mission cycle loading on the individual hot section components, in this case the combustor. This software translates the major engine performance parameter profiles from the TDEM into profiles of the components thermodynamic loads (pressures, temperatures, rpm). The formulas which perform this mapping in the TDLM models were developed for the specific engine components of the CF6-50C engine. To adapt these models to a different engine would require the evaluation of these formulas for their simulation capability and reformulating where necessary.

The heart of the component specific structural modeling is geometric modeling and mesh generation using the recipe concept. A generic geometry pattern is determined for each component. A recipe is developed for this basic geometry in terms of point coordinates, lengths, thicknesses, angles, and radii. Figures 6 to 8 show this process for a rolled ring combustor. These recipe parameters are encoded in computer software as variable input parameters with a set of default numerical values defined. Figure 9 defines the recipe which generates the combustor structural model.

A snapshot of a typical run of the combustor model is shown in Fig. 10. As indicated, the model contains a default set of recipe parameters, only changes to this list need be given. After the recipe parameters have been set, only five parameters need be specified to generate a three-dimensional sector model of a combustor to perform a hot streak analysis. The first parameter (shown as the number of exhaust nozzles) is required to divide the 360° combustor into the proper number of sectors. The next parameter (shown as the number of circumferential elements) is used by the analyst to split up the circumferential sector into a number of slices, NS, for the three-dimensional elements and bias these slices by specifying NS-1 percents.

For the particular case involved three exhaust nozzles are specified with four circumferential elements. These circumferential elements are then biased, starting at the hot streak, as 5, 15, and 30 percent. This leaves the final slice to be 50 percent. This is all the information required to generate a three-dimensional finite-element model consisting of 20-noded isoparametric finite elements. In this case the model consists of 648 elements, 3192 nodes, and has 768 element faces with pressure loading. Figures 11 and 12 are graphical depictions of this three-dimensional model. The temperatures and pressures from the TDLM are mapped onto this model and the necessary data files are generated for a nonlinear structural analysis.

The subsystem which performs the three-dimensional nonlinear finite-element analysis of the combustor model was that developed in the HOST program, "Three-dimensional Inelastic Analysis Methods for Hot Section Structures." This software performs incremental nonlinear finite-element analysis of complex three-dimensional structures under cyclic thermomechanical loading with temperature dependent material properties and material response behavior. The nonlinear analysis considers both time independent and time dependent material behavior. Among the constitutive models available are a simplified model, a classical model, and a unified model. A major advance in the ability to perform time dependent analyses is the dynamic time incrementing strategy incorporated in this software.

The COSMO system consists of an executive module which controls the TDEM, TDLM, the geometric modeler, the structural analysis code, the file structure/data base, and certain ancillary modules. These ancillary modules consist of a bandwidth optimizer module, a deck generation module, a remeshing/mesh refinement module, and a postprocessing module. The executive directs the running of each module, controls the flow of data among modules and contains the self-adaptive control logic. Figure 13 is a flow chart of the COSMO system showing the data flow and the action positions of the adaptive

controls. The modular design of the system allows each subsystem to be viewed as a plug-in module which can be replaced with alternates.

The ideas, techniques, and computer software contained in COSMO have proven to be extremely valuable in advancing the productivity and design analysis capability of combustors. This software in conjunction with modern supercomputers is able to reduce a design task which previously required man-months of effort over a time period of months to a one-man, less than a day effort. Along with this time compression comes increased accuracy from the advanced modeling and analysis techniques. As a result of this, more analytical design studies can be performed, reducing the chances for field surprises and the amount of combustor testing required.

Turbine Blade Analysis

The analysis of turbine blades is an excellent barometer of the improvements brought about by the HOST program. There was a pre-HOST program called, "Turbine Blade Tip Durability Analysis," which established the state-of-the-art prior to HOST. A commercial air-cooled turbine blade with a well-documented history of cracking in the squealer tip region was subjected to cyclic nonlinear analysis by a commercially available computer program, ANSYS. This three-dimensional problem had previously been analyzed, elastically, by an in-house computer program. At the end of the HOST program, this problem was once again used to establish the changes brought about by HOST.

The problem involved was the significant creep-fatigue encountered in a Stage-1 high-pressure turbine blade. These blades are hollow, air-cooled, and paired together on a single three-tang dovetail. Figure 14 shows one such blade and indicates the region of analysis. The three-dimensional finite-element model of the component blade tip above the 75-percent span was constructed of 580 eight-noded isoparametric brick elements with 1119 nodes. A detailed, exploded view of this model depicting the squealer tip, tip cap, and spar as discrete three-dimensional components is shown in Fig. 15.

This ANSYS model was exercised on the CDC-7600 computer. This model had previously been run on the TAMP-MASS computer program and the Honeywell 6000 computer. In 1986, this model was converted to 580, 20-noded isoparametric finite elements and run on one of the codes developed under, "Three-Dimensional Inelastic Analysis Methods for Hot Section Structures." Table 1 shows the times and costs experienced under the various conditions. The impact of the advancements in technology and computer hardware is apparent from this table.

Thermal Barrier Coating Analysis

Another technological area in the HOST program was that of "Surface Protection." Programs were developed under this area to produce an understanding and to generate theories and computer tools for the design, analysis, and life prediction of Thermal Barrier Coatings (TBC). Figure 16 shows one type of test specimen involved in this effort. Figure 17 shows the axisymmetric finite-element model used to simulate these test specimens. Figure 18 is a furnace thermal test cycle these specimens were cycled through. Figures 19 and 20 are representative analytical results for the critical life locations.

Without the developments in the structural analysis area of HOST this test simulation would not have been attempted because of the excessive amounts of computer time that would have been required. This problem is highly time dependent and numerically sensitive. The material properties and the creep properties differ greatly among the three constituents of this material system. An added nonlinearity occurs due to the growth of an oxide scale between the bond coat and the top coat. The dynamic time incrementing algorithm developed under the three-dimensional inelastic HOST program made the analysis of this nonlinear system possible.

SSME HPFTP Turbine Blade

One final example of the application of HOST technology is the NASA program with the acronym - SADCALM. This stands for, "Structural Analysis Demonstration of Constitutive and Life Models." Under this program, coated single crystal turbine blades such as the one indicated in Fig. 21 will be analyzed by the most advanced technology developed under HOST. This includes the 20-noded isoparametric finite element and the constitutive models developed in the three-dimensional inelastic programs. The single crystal-crystallographic constitutive model developed under the anisotropic constitutive modeling programs, and three HOST life theories, "Cyclic Damage Accumulation," "Total Strain-Strain Range Partitioning," and "Hysteretic Energy," will be used. This program involves testing, analysis, and correlation and will provide an excellent opportunity for demonstrating the benefits of the HOST program.

CONCLUSIONS

The ideas, techniques, and computer software developed under the NASA HOST program have proven to be extremely valuable in advancing the productivity and design analysis capability for hot section structures of AGTE's. This software in conjunction with modern supercomputers is able to reduce a design task significantly. These ideas are amenable to further generalization/specialization and extension to all areas of the engine structure. These techniques will have their major payoff in the next generation of aerospace propulsion systems with their increasingly large number of parametric variations.

REFERENCES

Maffeo, R., 1985, "Burner Liner Thermal/Structural Load Modeling, TRANCITS Program User's Manual," NASA CR-174891.

McKnight, R.L., 1983, "Component Specific Modeling; First Annual Status Report," NASA CR-174765.

McKnight, R.L., 1985, "Component Specific Modeling; Second Annual Status Report," NASA CR-174925.

McKnight, R.L., Laflen, J.H., Halford, G.R., and Kaufman, A., 1983, "Turbine Blade Nonlinear Structural and Life Analysis," Journal of Aircraft, Vol. 20, No. 5, pp. 475-480.

McKnight, R.L., Laflen, J.H., and Spamer, G.T., 1981, "Turbine Blade Tip Durability Analysis," NASA CR-165268.

TABLE 1. - TURBINE BLADE TIP MODEL HISTORY

Year	Computer program	Finite element	Computer	Wall time	Computer time
1975	TAMP-MASS	8-noded isoparametric	Honeywell 6000	60 hr	20 hr
1981	ANSYS	8-noded isoparametric	CDC-7600	24 hr	3 hr
1986	HOST three-dimensional inelastic	20-noded isoparametric	CRAY-1	115 sec	114 sec

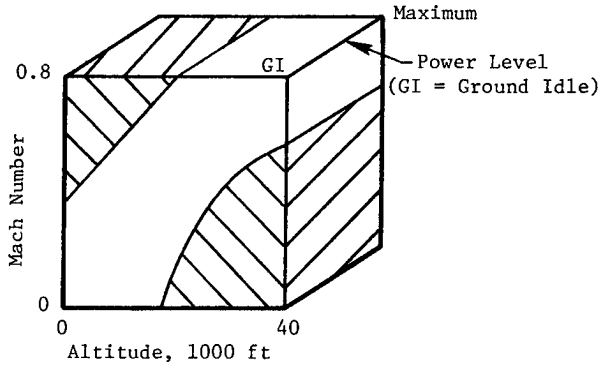

Figure 1. Engine Operating Map.

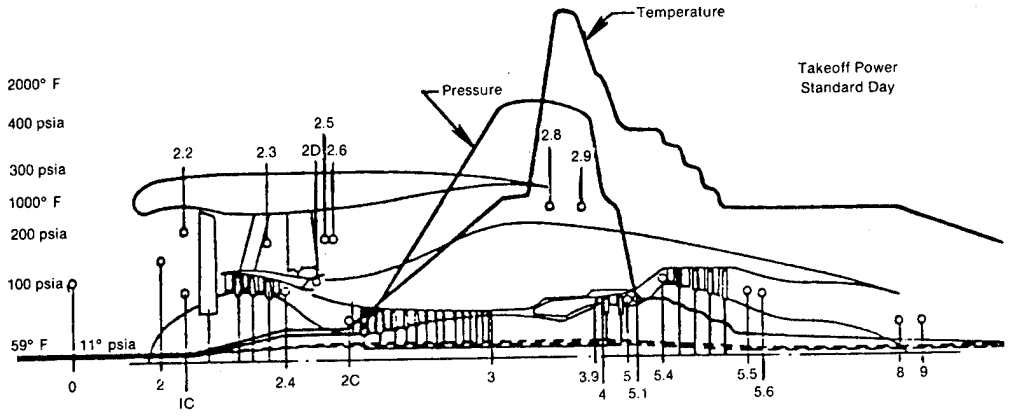

Legend

0 Ambient	2C HP Compressor Inlet
2 Engine Inlet	3 HP Compressor Discharge
2.2 Fan Tip (Bypass) Stream Inlet	3.9 HP Turbine First-Stage Nozzle Inlet (Without Cooling Flow)
1C Fan Hub (LP Compressor) Stream Inlet	4 HP Turbine Rotor Inlet (With Cooling Flow)
2.3 Fan Discharge	5 HP Turbine Discharge (Without Cooling Flow)
2.4 LP Compressor Discharge	5.1 HP Turbine Discharge (With Cooling Flow)
2.5 Bypass Stream Mixing Plane	5.4 LP Turbine Inlet (With Cooling Flow)
2.6 Bypass Duct Inlet (After Mixing)	5.5 LP Turbine Discharge (Without Cooling Flow)
2.8 Bypass Duct Jet Nozzle Throat	5.6 LP Turbine Discharge (With Cooling Flow)
2.9 Bypass Duct Nozzle Exit (Complete Expansion)	8 Primary Jet Nozzle Throat
	9 Primary Jet Nozzle Exit (Complete Expansion)

Temperature Fan - - - - - -
Core ——————
Pressure Fan — — — — —
Core ——————

Figure 2. Aerodynamic Stations.

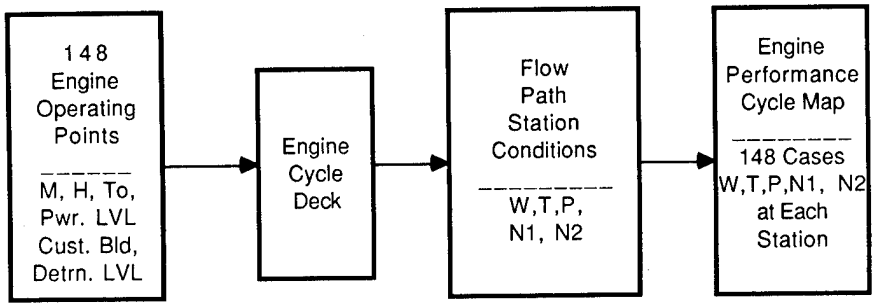

Figure 3. Thermodynamic Engine Model Cycle Map Generation.

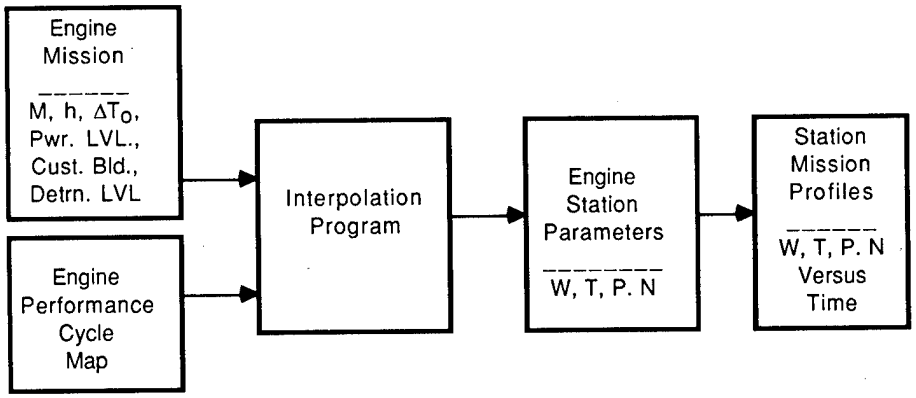

Figure 4. Thermodynamic Engine Model.

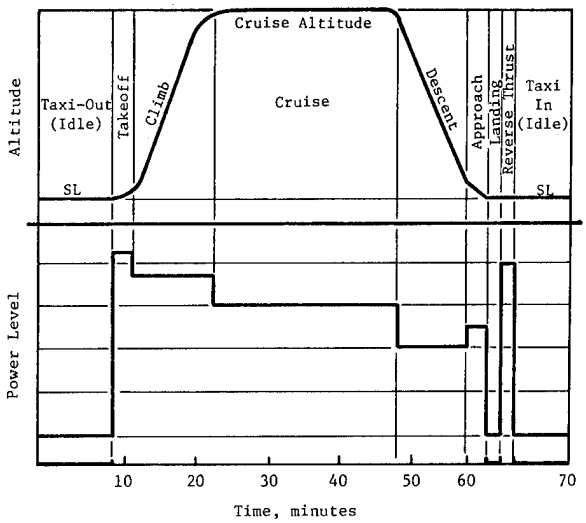

Figure 5. Typical Flight Cycle.

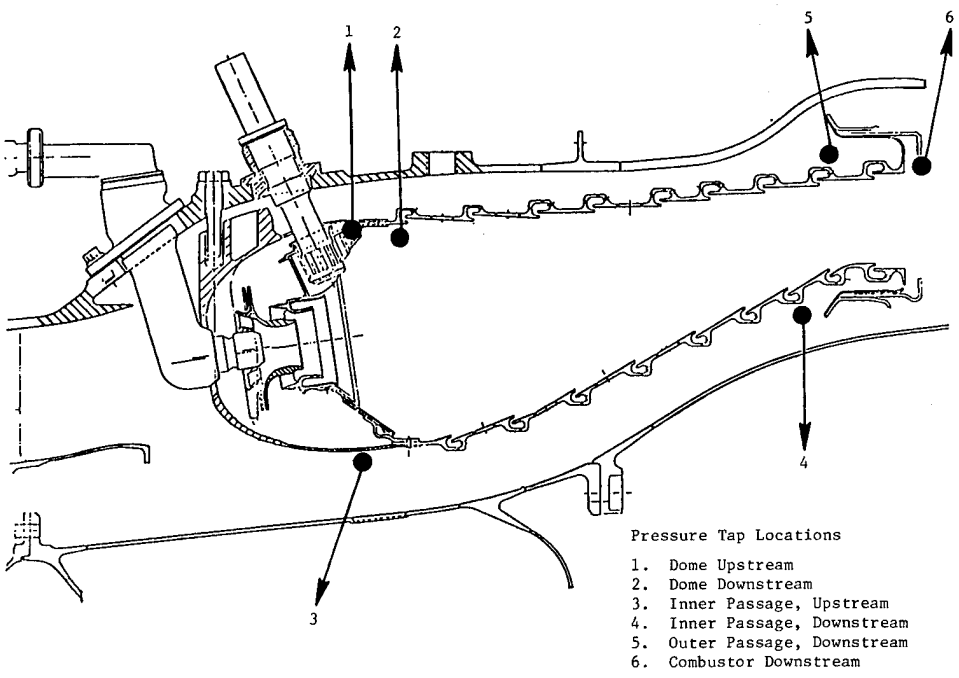

Figure 6. Rolled Ring Combustor.

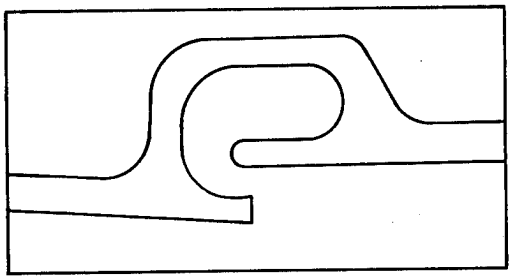

Typical Nugget

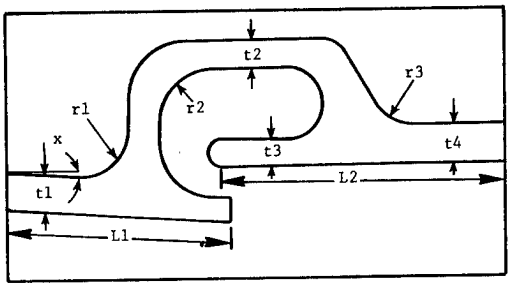

Physical Input Parameters

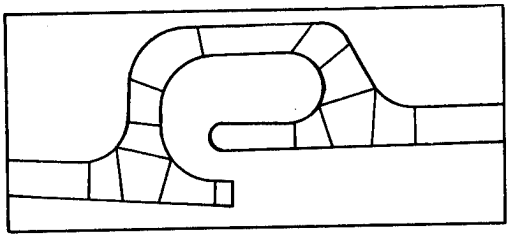

Master Region Definition

Figure 7. Combustor Recipe Process.

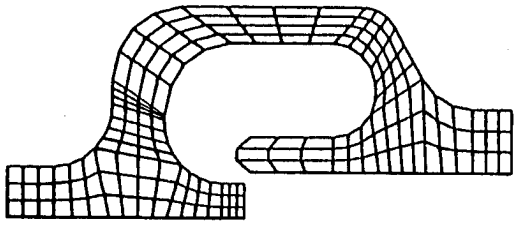

2D Model

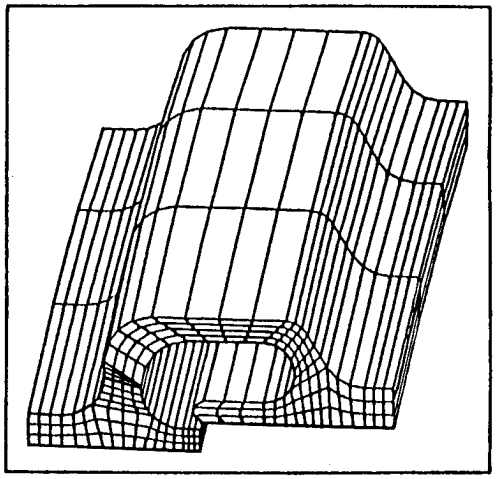

3D Model

Figure 8. Combustor Nugget Finite Element Models.

Combustor Liner Parameter List

Code	Name	Default	Code	Name	Default
1	X_1	0.0	2	Y_1	0.0
3	α_1	0.0	4	L_1	10.5
5	L_2	2.0	6	L_3	0.5
7	L_4	6.0	8	L_5	0.8
9	L_6	1.0	10	L_7	2.0
11	T_1	0.5	12	T_2	0.7
13	T_3	0.5	14	T_4	0.65
15	T_5	0.5	16	θ_1	90.0
17	θ_2	90.0	18	R_1	1.0
19	R_2	1.0	20	R_3	0.75
21	R_4	1.5	22	R_5	1.5
23	R_6	1.5			

X = Coordinate
Y = Coordinate
α = Angle Wrt, x - Axis
L = Length
T = Thickness
θ = Angle of Rotation
R = Radius of Curvature
(n)= Parameter Code Number

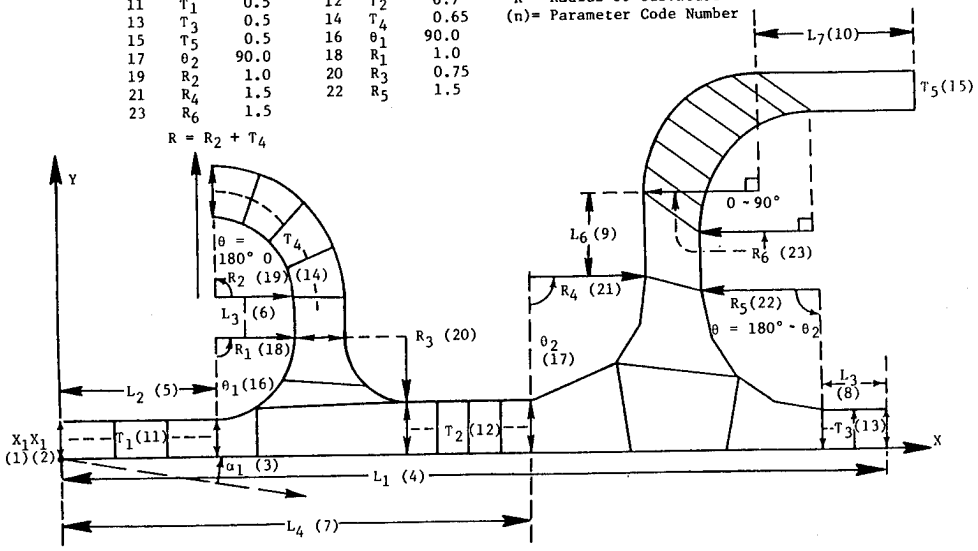

Figure 9. Combustor Liner Parameters.

```
$;RN /GN/NUGPRO

      NUGGET RECIPE    VERS.II 8/29/85

DO YOU HAVE A PARAMETER FILE 21? (0/1)
-
```

CODE	VALUE	CODE	VALUE
1	0.	2	0.
3	0.	4	1.16700
5	0.19200	6	0.04500
7	0.81000	8	0.06800
9	0.10000	10	0.20000
11	0.06000	12	0.08000
13	0.06000	14	0.06800
15	0.06800	16	110.00000
17	90.00000	18	0.06000
19	0.06700	20	0.12000
21	0.12500	22	0.08300
23	0.09500		

```
  ENTER PARAMETER CHANGES (ENTRY CODE, NEW VALUE)
      WHEN DONE ENTER     0 0

-0 0
```

CODE	VALUE	CODE	VALUE
1	0.	2	0.
3	0.	4	1.16700
5	0.19200	6	0.04500
7	0.81000	8	0.06800
9	0.10000	10	0.20000
11	0.06000	12	0.08000
13	0.06000	14	0.06800
15	0.06800	16	110.00000
17	90.00000	18	0.06000
19	0.06300	20	0.12000
21	0.12500	22	0.08300
23	0.09500		

```
 DO YOU WANT TO CHANGE PARAMETERS? (0/1)
-
READING FILE NUGCON
READING DONE
              27 ELEMENTS READ

ENTER ENGINE TEMPERATURE AND PRESSURE FILE NAME
-/GN/NUGINF
READING FILE /GN/NUGINF
READING DONE
              36 CENTROIDS READ


ENTER THE NUMBER OF EXHAUST NOZZLES
  AND THE NO. OF CIRCUMFIRENTIAL ELEMENTS
  BETWEEN T-AVE AND T-HOT (MAX NO.=10)
-3 4

ENTER THE  3 CIRCUMFIRENTIAL BIASING PARAMETERS
 -- ENTER AS PERCENTS, THE SUM BEING LESS THAN 100% --
-5 15 30

********  3192 NODES IN 3-D MODEL     ********
********   648 ELEMENTS IN 3-D MODEL  ********
********   768 FACES WITH PRESSURES   ********

 ### 2-D NODE  FILE IS TEMP FILE 20 ###
 ### PARAMETER FILE IS TEMP FILE 21 ###
 ### 3-D  UIF  FILE IS TEMP FILE 26 ###

-
```

Figure 10. Typical Program Run.

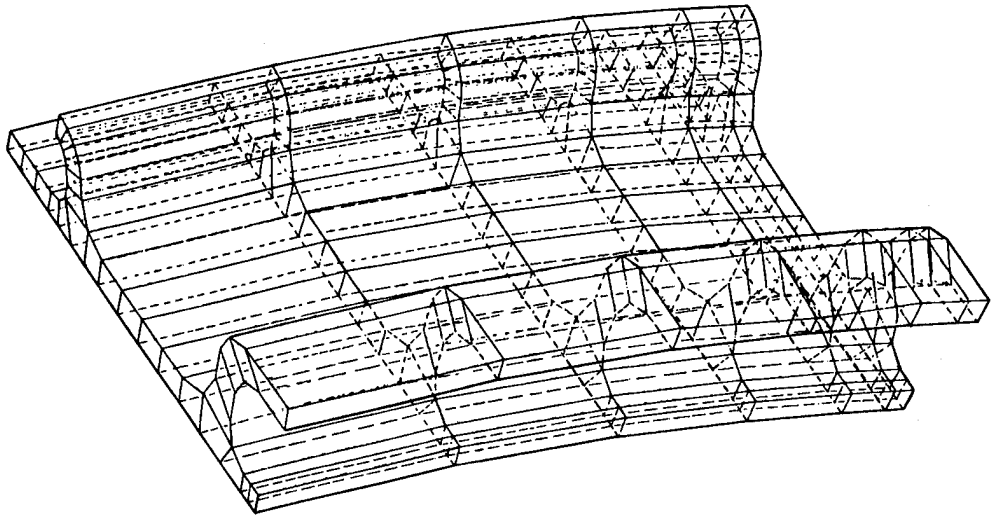

Figure 11. 3D Model Layout.

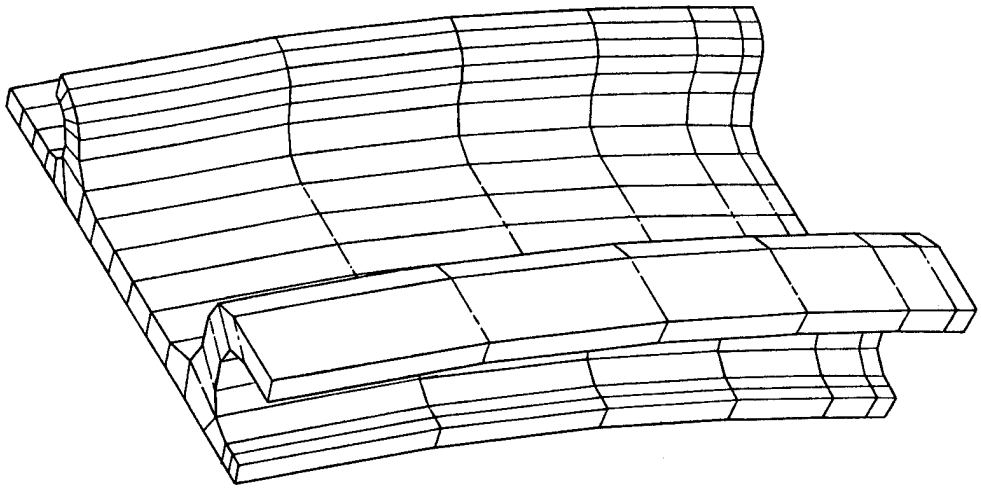

Figure 12. Hidden Line Plot of 3D Model.

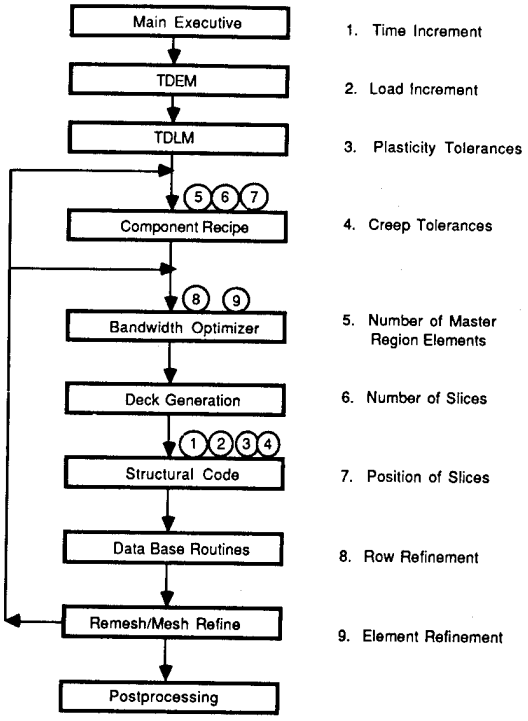

Figure 13. System Flowchart Showing Adaptive Control Positions.

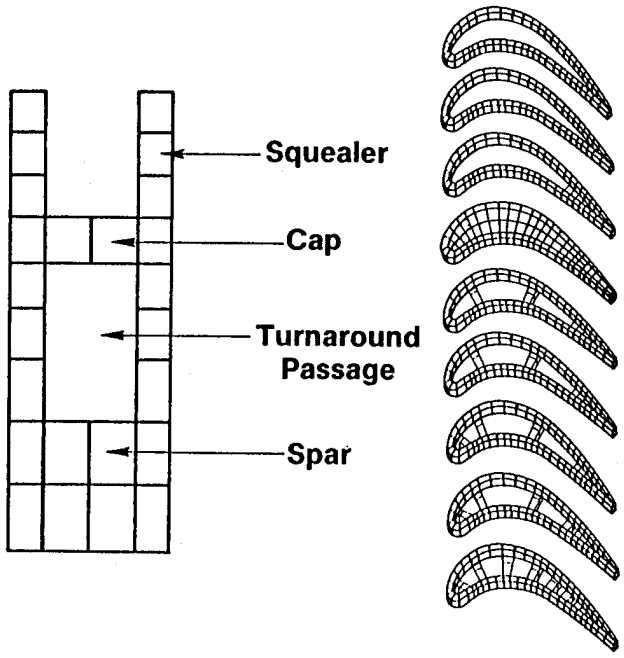

Figure 15. Finite Element Model of Blade Tip.

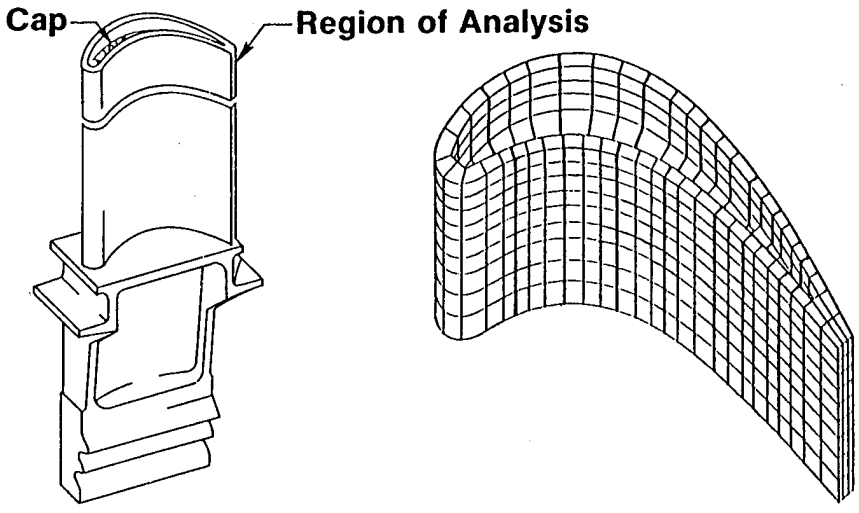

Figure 14. Stage 1 High Pressure Turbine Blade and Finite Element Model.

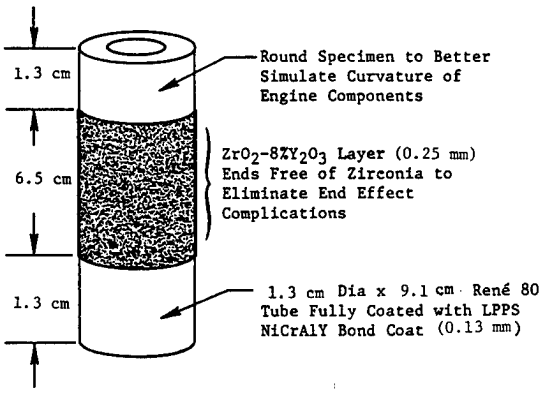

(a) Test Specimen Configuration

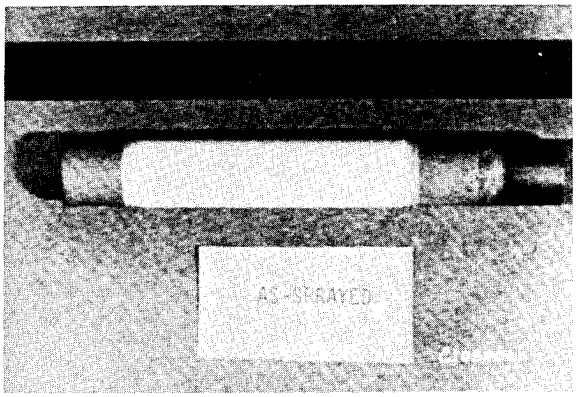

(b) As-Sprayed Specimen

Figure 16. Thermal Barrier Coated Tubular Specimen.

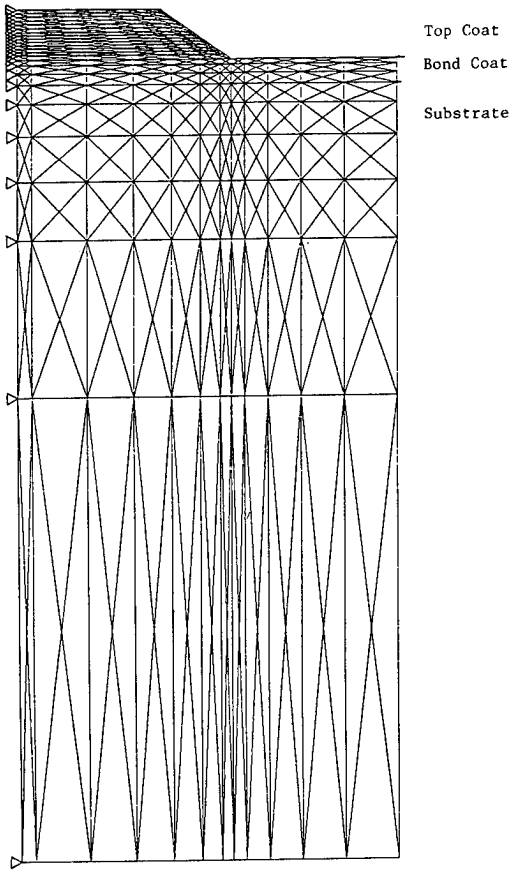

Figure 17. Finite Element Mesh for Thermal Barrier Coated Tubular Specimens.

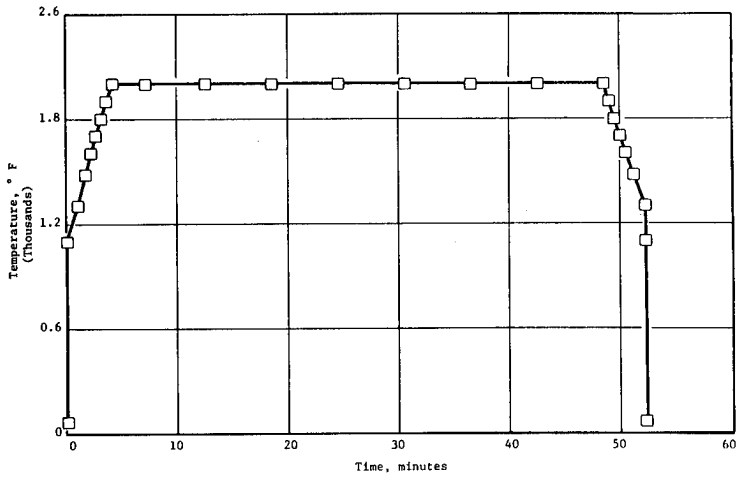

Figure 18. Thermal Loading Cycle.

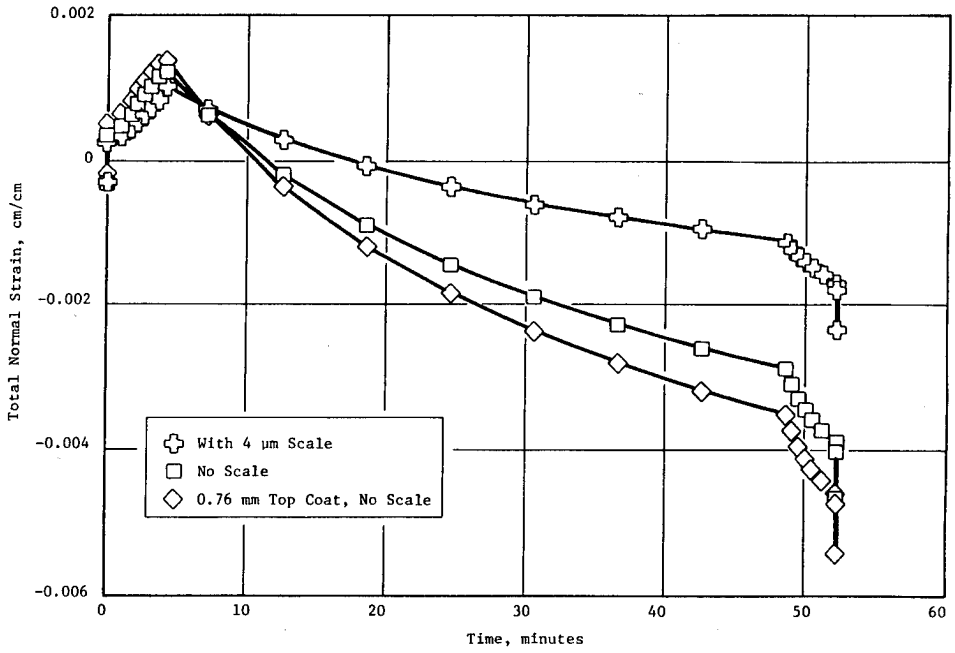

Figure 19. Calculated Total Normal Strain in Top Coat at Top Coat/Bond Coat Interface of Thermal Barrier Coated Tubular Specimen During Thermal Cycle. Bond Coat Thickness 0.13 mm; Top Coat Thickness 0.254 mm Unless Indicated Otherwise.

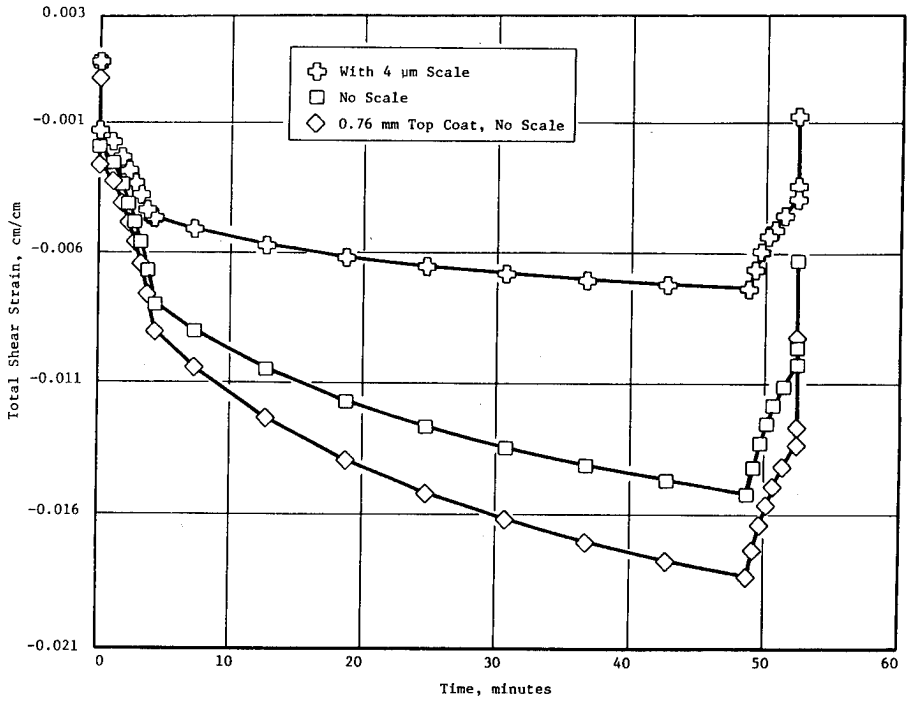

Figure 20. Calculated Total Shear Strain in Top Coat at Top Coat/Bond Coat Interface of Thermal Barrier Coated Tubular Specimen During Thermal Cycle. Bond Coat Thickness 0.13 mm; Top Coat Thickness 0.254 mm Unless Indicated Otherwise.

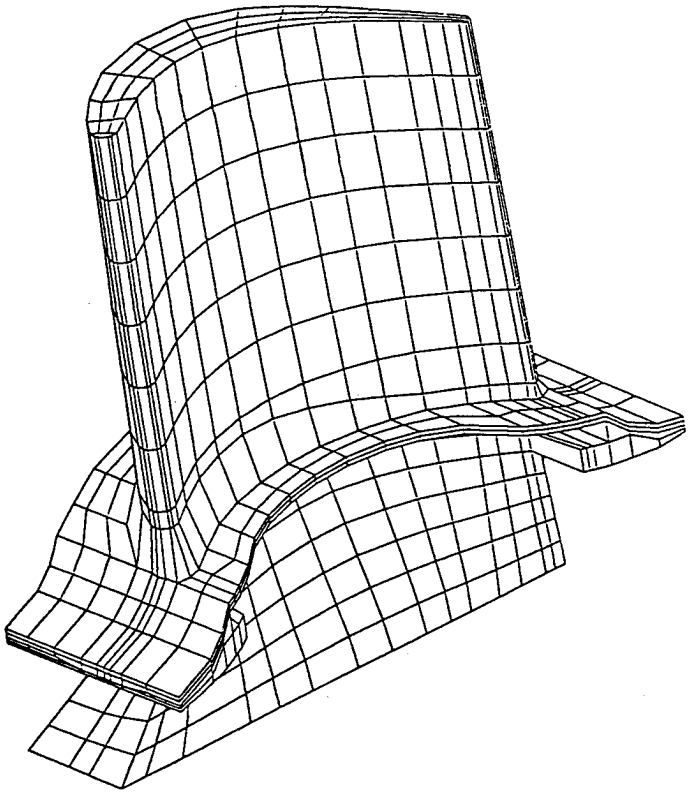

Figure 21. SIESTA Plot of Converted NASA Blade Model.

FATIGUE LIFE PREDICTION MODELING FOR TURBINE HOT SECTION MATERIALS

G. R. Halford
National Aeronautics and Space Administration
Lewis Research Center
Cleveland, Ohio

T. G. Meyer, R. S. Nelson, D. M. Nissley, and G. A. Swanson
United Technologies
Pratt and Whitney
East Hartford, Connecticut

ABSTRACT

This paper presents a summary of the life prediction methods developed under the NASA Lewis Research Center's Hot Section Technology (HOST) program. A major objective of the fatigue and fracture efforts under the HOST program was to significantly improve the analytic life prediction tools used by the aeronautical gas turbine engine industry. This has been achieved in the areas of high-temperature thermal and mechanical fatigue of bare and coated high-temperature superalloys. Such technical improvements will eventually reduce life cycle costs.

The cyclic crack initiation and propagation resistance of nominally isotropic polycrystalline alloys and highly anisotropic single crystal alloys has been addressed. A sizeable data base has been generated for three alloys [cast PWA 1455 (B-1900 + Hf), wrought Inconel 718, and cast single crystal PWA 1480] in bare and coated conditions. Two coatings systems, diffusion aluminide (PWA 273) and plasma sprayed MCrAlY overlay (PWA 286) were employed.

Life prediction modeling efforts were devoted to creep-fatigue interaction, oxidation, coatings interactions, multiaxiality of stress-strain states, mean stress effects, cumulative damage, and thermomechanical fatigue. The fatigue crack initiation life models developed to date include the Cyclic Damage Accumulation (CDA) Model of Pratt & Whitney and the Total Strain Version of Strainrange Partitioning (TS-SRP) of NASA Lewis for nominally isotropic materials, and the Tensile Hysteretic Energy Model of Pratt & Whitney for anisotropic superalloys. The fatigue model being developed by the General Electric Company is based upon the concepts of Path-Independent Integrals (PII) for describing cyclic crack growth under complex nonlinear response at the crack tip due to thermomechanical loading conditions. A micromechanistic oxidation crack extension model has been derived by researchers at Syracuse University. The models are described and discussed in the paper. Only limited verification has been achieved to-date as several of the technical programs are still in progress and the verification tasks are scheduled, quite naturally, near the conclusion of the program.

To-date, efforts have concentrated on development of independent models for cyclic constitutive behavior, cyclic crack initiation, and cyclic crack propagation. The transition between crack initiation and crack propagation has not been thoroughly researched as yet, and the integration of these models into a unified life prediction method has not been addressed.

INTRODUCTION

Background

Life cycle costs ranging from initial design costs to field replacement costs of limited durability component parts are the driving elements for improved analytic life prediction capability. Since life cycle costs are the highest for hot section gas turbine engine components, our efforts have concentrated on the problems in this area. Accurate calculation of expected service lifetimes, is crucial to the final judgment to proceed with a particular design. Inaccurate life calculations result in overly expensive designs--either from an under utilization of potential or a lack of adequate life. The fatigue and fracture portion of the HOST program was initiated to reduce life cycle costs through improved accuracy of analytic life predictive models. The specific areas of primary concern are very high-temperature cyclic crack initiation and propagation in both isotropic and anisotropic superalloys used in hot section turbine engine components.

HOST Life Prediction Program

Table I lists the specific programs that have supported the fatigue and fracture life prediction efforts. Each will be discussed and the most significant of the numerous accomplishments will be pointed out. Space does not permit elaboration of the numerous methods nor of the experimental details. The reader is referred to the more thoroughly documented original references.

In addition to the Industrial Contracts and University Grants supported by the the HOST program, some funding was set aside to rejuvenate aging test facilities in the the area of fatigue and fracture. The advanced, high-temperature fatigue and structures research laboratory at Lewis (McGaw and Bartolotta, 1987) is now operational, and in fact has grown to the point of requiring further expansion. The facility is equipped with the very latest closed-loop, servo-controlled machinery, and most importantly boasts a unique computerized nerve center for programmed test control; data taking, storage and retrieval; and data reduction and plotting.

ISOTROPIC MATERIAL MODELING

Cyclic Crack Initiation

The majority of usable cyclic lifetime of turbine engine hot section components is usually spent in what is called the "cyclic crack initiation" portion of the fatigue life. Strictly speaking, crack initiation does indeed contain a considerable amount of cyclic crack growth, although the physical size of the cracks is quite small. From an engineering point of view, any crack growth below a crack size of approximately 0.8 mm (1/32 in.) typically is included in the "initiation" portion of the life. Justification for this definition is based upon: (a) the inability to reliably detect cracks of smaller size, and (b) the inability of cyclic crack growth laws to adequately model cyclic extension of cracks smaller than this size. Such a definition of cyclic crack initiation is used in the development of the Pratt & Whitney Cyclic Damage Accumulation Model addressed in the next section.

Pratt & Whitney Cyclic Damage Accumulation (CDA) model. The interaction of creep with fatigue at high temperatures is being studied in detail under NASA/HOST Contract NAS3-23288, "Creep-Fatigue Life Prediction for Engine Hot Section Materials (Isotropic)" (Moreno, 1983, Moreno et al., 1986, and Nelson et al., 1986). This effort has investigated fundamental approaches to high temperature crack initiation life prediction using a cast nickel-base alloy, PWA 1455 (B1900 + Hf) as the base material. During the program, over 157 specimen tests were completed under loading conditions which consisted of monotonic tensile and creep tests as well as continuously cycled fatigue tests. A review of existing fatigue models was conducted, and desirable features of each of these were identified. A new method of high temperature fatigue life prediction called Cyclic Damage Accumulation (CDA) was subsequently developed which incorporates many of these features.

Complex loadings were introduced during the latter stages of the program to study the effects of thermomechanical fatigue, multiaxial loading, cumulative damage, environment, mean stress, and coatings. An additional 160 strain-controlled fatigue tests have been conducted as a part of these tasks. Three different surface treatments were utilized for the TMF and coated tests: bare (no coating), overlay NiCoCrAlY coated, and diffusion aluminide coated. Several refinements have been incorporated into the CDA life prediction model based on the results of these complex tests. The current form of the model for accumulated transgranular damage is given by Eq. (1).

$$1 = \int_0^{N_i} \left(\frac{1}{\bar{\varepsilon}_p}\right)\left(\frac{1}{G_{NL}}\right)\left(\frac{dD}{dN}\right)_R\left[\left(\frac{\Delta\sigma}{\Delta\sigma_R}\right)\left(\frac{\sigma_T}{\sigma_{TR}}\right) + D_{TD}\left(\frac{f_{ox}}{f_{ox_R}}\right)\right] dN \qquad (1)$$

where

N_i initiation life, transgranular mode

$\bar{\varepsilon}_p$ primary creep ductility

G_{NL} nonlinear damage accumulation function

$\left(\frac{dD}{dN}\right)_R$ reference cyclic damage rate

σ_T maximum tensile stress in current cycle

σ_{TR} reference maximum tensile stress

$\Delta\sigma$ stress range of current cycle

$\Delta\sigma_R$ reference stress range

D_{TD} time-dependent damage rate modifier

f_{ox} cyclic oxidation rate for current fatigue cycle

f_{ox_R} reference fatigue/cyclic oxidation rate

The basis for Eq. (1) is explained by Moreno (1983), Moreno et al. (1984), and Nelson (1986). A goal of the program to develop the CDA model was to limit the complexity of the experiments to determine the material behavior constants. For example, only monotonic creep tests and continuous cycling fatigue experiments are required to evaluate the constants in the first term of the CDA expression. The second term requires that cyclic oxidation measurements be made during fatigue testing.

Nonlinear damage accumulation calculations are now possible for both cycle-dependent and time-dependent, cases. Modular terms which capture the effects of multiaxiality, coatings, and intergranular cracking are currently under development. The ability of the model to correlate thermomechanical fatigue data is shown in Fig. 1 for bare and coated material, respectively. Complete details of test conditions employed are given by Nelson (1986). Most of the thermomechanical fatigue (TMF) tests were performed at temperatures between 538 and 871 °C at one CPM with total mechanical strain ranges between 0.4 and 0.5 percent. The dog-leg experiments utilized 54 sec hold periods in either tension or compression. Work continues on a refined version of the model which will attempt to capture all the important life trends seen during the latter stages of the contract.

The final task under the program is to perform a similar series of tests on an alternate alloy, wrought Inconel 718. A total of 55 of these specimen tests have now been completed, including isothermal, thermomechanical fatigue, and multiaxial strain-controlled tests. It is expected that the final form of the CDA model may include additional refinements required to predict properly the life trends for forged alloys.

Lewis Research Center Total Strain Version of Strainrange Partitioning. The Strainrange Partitioning (SRP) method for characterizing and predicting creep-fatigue behavior of alloys has long been associated with using inelastic strains to relate to cyclic life. Recent advances by Halford and Saltsman (1983) and Saltsman and Halford (1985) now permit the approach to be expressed in terms of total strain range versus cyclic life. These developments make the SRP method more attractive for application to life prediction of aeronautical gas turbine hot section components.

Here, materials and loading conditions result in strain levels that, while they are severe and produce low-cycle fatigue cracking, involve only small amounts of inelastic deformation within nominally elastic strain fields. The limited inelasticity produced locally may exert a significant influence on life. The type of inelastic strains present (time-dependent creep and time-independent plasticity) and the direction of the strains (tension or compression) can be quite important in governing the resultant cyclic crack initiation life. The total strain based SRP approach (TS-SRP) has been developed to deal explicitly with the above conditions. A brief description is given below to show how the procedures are employed.

The total strain range, $\Delta\varepsilon_t$, is the sum of two terms, the elastic, $\Delta\varepsilon_{el}$, and the inelastic, $\Delta\varepsilon_{in}$, strain ranges. Each strain range is related to cyclic life by a power law relation as shown in Eq. (2) and Fig. 2.

$$\Delta\varepsilon_t = \Delta\varepsilon_{el} + \Delta\varepsilon_{in} = B(N_f)^b + C'(N_f)^c \qquad (2)$$

To apply Eq. (2) at high temperatures requires the evaluation of the coefficients, B and C', and the exponents, b and c. It is assumed, initially, that b and c are constants for all conditions at a given temperature, i.e., they are time- and waveshape-independent, and that B and C' are time- and cycle waveshape-dependent.

To determine C', as many of the four basic SRP inelastic strain range versus life relations, PP, CC, PC, and CP, as are required for the cycle of interest must be known. How the inelastic strains are partitioned within the cycle must also be known, i.e., how much of each type of PP, CC, PC, or CP strain range is present in the hysteresis loop. Experimental procedures for establishing the four inelastic SRP life relations, techniques for approximating them, and experimental partitioning procedures are given by Hirschberg and Halford (1976), Halford et al. (1977), and Manson et al. (1975), respectively.

In principle, the partitioning and thus the determination of C' could be accomplished analytically using advanced cyclic constitutive equations such as those developed under the NASA/HOST Program by Lindholm (1984) and Ramaswamy et al. (1985). Advanced cyclic constitutive models are capable of computing the exact details of a stress-strain hysteresis loop, knowing only the imposed temperature, total mechanical strains, and how they vary with time for a representative cycle. Details of the inelastic straining rates are also computable, and hence creep strains (time-dependent) and plastic strains (time-independent) can be separated, i.e., partitioned. If a constitutive model is not available, the empirical approach presented by Saltsman and Halford (1988) can be used to determine C' and B. The required equations are summarized below.

$$C' = \left[\sum F_{ij}(C_{ij})^{1/c}\right]^c \qquad (3)$$

$$B = K_{ij}(C')^n \qquad (4)$$

$$F_{ij}/(\Delta\varepsilon_t)^\alpha = A(t)^m \qquad (5)$$

$$K_{ij} = A_i(t)^{m_i} \qquad (6)$$

where ij = pp, cc, pc, or cp

The cyclic strain hardening exponent, n, in Eq. (4) is obtained from completely reversed rapid strain-cycling PP results,

$$\Delta\varepsilon_{el,pp} = K_{pp}(\Delta\varepsilon_{pp})^n \qquad (7)$$

For cycles involving creep,

$$\Delta\varepsilon_{el,ij} = K_{ij}(\Delta\varepsilon_{ij})^n \qquad (8)$$

A complete nomenclature for TS-SRP is given by Saltsman (1988).

To apply the TS-SRP approach, the specific mission cycles of interest are identified and the cyclic stress-strain-temperature-time history is determined at the critical location in the structural component. Then, the appropriate elastic and inelastic strain range versus life relations are calculated and added together to obtain the desired total strain range versus cyclic life diagram. Entering the diagram with the known total strain range, the cyclic life is determined directly without having to calculate the magnitude of the inelastic strain range. Example life prediction calculations by the TS-SRP approach have been reported by Halford and Saltsman (1983), Moreno et al. (1985), and Saltsman and Halford (1988). The degree of success of the method is shown in Fig. 3. Here, the TS-SRP method was applied by Moreno et al. (1985) to a series of five different types of complex verification experiments performed on the nickel-base superalloy, B1900 + Hf. A direct comparison of the TS-SRP approach with the CDA model also was made by Moreno et al. (1985), wherein the principal features of each method were emphasized. The TS-SRP model and the Pratt & Whitney CDA model were both designed for application to strain-driven fatigue loading conditions in the nominally elastic regime. Both methods are currently being adapted for application to TMF problems.

Cyclic Crack Propagation

Cyclic growth of cracks and defects in turbine engine hot section components is of considerable concern because of the lack of structural redundancy in the construction of these components. As such, crack growth to a critical fracture size must by avoided to prevent catastrophic fast fracture and subsequent loss of engine function. Typically, concern for fast fracture is associated more with rotating components than with static structures. For combustor liners, guide vanes, stationary spacers, and other nonrotating components, concern for cyclic crack growth is more economic in nature than safety-related. In the HOST fatigue and fracture program, two approaches to crack growth were taken. An engineering methodology was applied in an attempt to develop directly useful design tools, and a scientific approach examined the micromechanisms of crack extension at the crystallographic level and the interaction with oxidation phenomena.

General Electric Path-Independent Integral model. A major goal of the contract program with the General Electric Company is to develop reliable and accurate engineering life prediction capabilities to deal with cyclic crack growth at elevated temperatures. Several of the Path-Independent Integrals, Jx, that have been proposed over the past few years have been shown to be

applicable to fracture mechanics calculations of cyclic crack growth under uniform and nonuniform thermal gradients and thermomechanical loadings. Specifically, the various Jx integrals proposed by Tada et al. (1973), Ainsworth et al. (1978), Blackburn et al. (1977), Kishimoto et al. (1980), and Atluri (1982) have been found suitable for analysis of crack stress fields involving nonlinear and time-dependent thermomechanical response (Kim and Orange, 1988). The traditional Rice J-integral (Rice, 1968), however, becomes path dependent and loses its physical significance for thermomechanical loadings. Figure 5 compares the results of a series of calculations applied to an instrumented single edge notch specimen of Inconel 718 with a linear thermal gradient. The current program with the General Electric Company will continue into 1989, during which time one of the path-independent integrals will be selected for further verification under realistic thermomechanical loading conditions found in the hot section of gas turbine engines.

Syracuse University oxidation crack extension model. Liu and Oshida (1986) and Oshida and Liu (1988) have taken a micromechanistic approach to dealing with crack propagation in superalloys. A model of intermittent micro-rupture of grain boundary oxide has been proposed for high temperature fatigue crack extension. The model is outlined briefly below for the case of a trapezoidal waveform.

Oxygen arriving at a grain boundary crack tip must diffuse into the region ahead of the crack in order to form oxide along the grain boundary. When the crack tip grain boundary oxide, at a given stress level, reaches a critical size, δa, the oxide will rupture and the crack will grow by the amount, δa. The critical size, δa, depends on the stress intensity level during the holding period. Once the crack tip has advanced to its new position, the process of grain boundary diffusion, grain boundary oxidation, and micro-rupture of the oxide is repeated. This process of micro-rupture of a crack tip grain boundary can recur intermittently during a fatigue cycle, and in fact, many micro-ruptures can take place. After each micro-rupture, the penetration of grain boundary oxide must start all over again from a "time" zero. The time interval, δt, necessary to reach the critical size, δa, is given by,

$$\delta t = (B/D_{gb})(\delta a/\beta B)^{1/n} \qquad (9)$$

where

B magnitude of the diffusion jumping vector or interatomic spacing

D_{gb} grain boundary diffusion coefficient

β, β' proportionality constants

n positive exponent (less than unity)

The number of micro-ruptures during the holding period, Δt_H, is,

$$m = \Delta t_H/\delta t = (\Delta t_H D_{gb}/B)(\beta B/\delta a)^{1/n} \qquad (10)$$

m is linearly proportional to the holding period and is inversely proportional to the frequency.

Fatigue crack growth per cycle is the sum of the micro-ruptures during the holding period,

$$da/dN = m\,\delta a \qquad (11)$$

From Eqs. (9) to (11) we obtain,

$$da/dN = \beta' \Delta t_H D_{gb} (B/\delta a)^{1-n/n} = \beta' (D_{gb}/f)(B/\delta a)^{1-n/n} \qquad (12)$$

Note that da/dN is inversely proportional to frequency, f. Figure 5 taken from Liu and Oshida (1986) illustrates the success the approach has had in correlating crack growth under high temperature environments. The experimental results shown in the figure were obtained from the open literature.

ANISOTROPIC MATERIAL MODELING

Pratt & Whitney single crystal constitutive model. Because of the exceptionally strong link between the cyclic deformation mechanisms in single crystal alloys and the fatigue crack initiation process, it was deemed advisable to develop both the cyclic constitutive and cyclic crack initiation life prediction models within a single program. Furthermore, since single crystal alloys invariably require a protective coating for successful high-temperature applications, it was also necessary to develop a cyclic constitutive and life model for the coating systems. The constitutive models will be discussed in the following section.

A unified constitutive model has been formulated for PWA 1480 single crystal material and is currently in the final stages of development. The model uses the unified approach for computing all inelastic strain rather than the conventional approach of treating creep and plasticity separately. The model assumes that all inelastic behavior results from shear strains on each of the twelve octahedral and six cube slip systems and that the global inelastic strains are simply the sum of these slip systems strains. Slip system inelastic shear strain rates are governed by a set of viscoplastic equations which involve the slip system stresses and two evolutionary state variables. The general form of the equation governing inelastic shear strain on the rth slip system as given by Swanson (1987) is,

$$\dot{\gamma}_r = \frac{(\pi_r - \omega_r)\,|\pi_r - \omega_r|^{P-1}}{K^P} \qquad (13)$$

where

$\dot{\gamma}_r$ inelastic shear strain rate on the slip system

π_r effective stress acting on the slip system

ω_r back stress acting on the slip system

K drag stress acting on the slip system

The model has been formulated to include several effects that have been reported to influence deformation. These include contributions from slip system stresses other than the Schmid shear stress, latent hardening due to simultaneous straining on all slip systems, and cross-slip from the octahedral to the cube slip systems.

A large body of isothermal constitutive data has been obtained at temperatures ranging from 427 to 1149 °C using uniaxial specimens oriented in the

<001>, <011>, <111>, <123> crystal orientations. The constitutive model constants have been determined from these isothermal tests. Figures 6 and 7 show the measured stress strain behavior and the calculated constitutive model behavior at 871 °C. The model is currently being evaluated against the stress-strain response of thermomechanical fatigue (TMF) tests which were conducted for life modeling. The single crystal constitutive model as well as the coating constitutive model reported below are compatible with a commercially available finite element computer code.

Pratt & Whitney coating constitutive model. Thermomechanical fatigue (TMF) cracks in turbine airfoils of PWA 1480 material generally originate from a coating crack. Thus, for airfoil life prediction, it is important to model the coating mechanical behavior as well as that of the PWA 1480. In this program, viscoplastic constitutive models are being developed for two fundamentally different coating types which are commonly used in gas turbines to provide oxidation protection: (1) a plasma sprayed NiCoCrAlY overlay coating, and (2) a pack-cementation-applied NiAl diffusion coating.

The isotropic formulation of Walker (1981) was chosen as the overlay coating constitutive model, based on its ability to reproduce isothermal and thermomechanical hysteresis loop data reported by Swanson et al. (1987). The predicted overlay coating response of an out-of-phase thermomechanical cycle is compared to data in Fig. 8. For these purposes, solid cylindrical specimens of coating material were cut from a billet prepared by hot isostatic pressing of material powder. The aluminide diffusion coating constitutive model is currently under development, and will be more difficult to determine owing to the fact that it will be impossible to make solid specimens of stand-alone coating material.

Cyclic Crack Initiation

Directionally cast, anisotropic, nickel-base superalloys (particularly single crystals) exhibit greater creep-fatigue resistance than their conventionally cast polycrystalline counterparts. To take full advantage of these improved material properties, however, requires the development of accurate cyclic constitutive and life prediction models for these highly directional alloys. Direct modification of polycrystalline behavior models is inadequate, and a new approach that recognizes the micromechanisms of crystal response is necessary. Unfortunately, the program was able to address only the crack initiation aspects of single crystal superalloys. Cyclic crack growth life prediction modeling must await future efforts.

Pratt & Whitney coating and single crystal life prediction model. Generally, all coated PWA 1480 orientations (i.e., <001>, <011>, <111>, and <123>) which were tested in thermomechanical fatigue initiated cracks in the metal at sites where coating cracking had occurred. Isothermal tests of coated <001> PWA 1480 also typically initiated cracks first in the coating layer. However, many coated non- <001> isothermal fatigue tests initiated cracks underneath the specimen outer surface in either the PWA 1480 or the coating/PWA 1480 interfacial region. Initiation occurred predominately at porosity sites.

The following life prediction approach was developed to account for the observed specimen cracking modes,

$$N_f = N_c + N_{sc} + N_{sp}$$

or (14)

$$N_f = N_{si} + N_{sp}$$

whichever is the smallest.

where

N_c cycles to initiate a crack through the coating

N_{sc} cycles for coating initiated crack to penetrate a small distance into the substrate

N_{si} cycles to initiate a substrate crack due to macroscopic slip, oxidation effects, or defects

N_{sp} cycles to propagate substrate crack to failure

N_f total cycles to fail specimen or component

The following modified tensile hysteretic energy model was developed for the overlay coating,

$$N_c = C(\Delta W_t)^{-b} \nu^m \qquad (15)$$

where

$$\nu = \frac{1}{\sum_{\text{cycle}} \frac{r(T_i)}{r(T_o)} t_i - D_o} \; ; \; \nu \leq 1.0 \qquad (16)$$

$r(T)$ $r_o \exp(-Q/T)$ temperature- and time-dependent damage rate

ΔW_t tensile hysteretic energy, N-m/m^3 (in-lbf/in.^{3})

T_i individual temperature levels in the the cycle, K (°R)

t_i time (min) at T_i, including 100 percent of tensile hold and 30 percent of compressive hold times in the cycle, if any

To threshold temperature for temperature dependent damage, assumed to be 1088 K (1960 °R)

D_o "incubation damage"

Q effective activation energy for temperature- and time-dependent damage.

The term, ν, is an extension of the Ostergren (1976) time-dependent damage frequency term. As used herein, it includes both temperature- and time-dependent damage functions to model thermally activated processes.

Model constants were determined from isothermal tests conducted at 427, 760, 927, and 1038 °C (800, 1400, 1700, and 1900 °F). Coating hysteresis loops were predicted using the PWA 286 constitutive model incorporated into a one-dimensional model. This model determines the stress-strain of the substrate and coating by imposing an equivalent displacement history. Differences in coefficients of thermal expansion are included in the model.

The model unifies isothermal and TMF predicted lives within a factor of about 2.5, as seen in Fig. 9. Generally, the worst predicted test lives were limited to 1149 °C (2100 °F) maximum temperature TMF tests.

Prediction of these test results should improve when 1149 °C (2100 °F) isothermal tests are included in the data set used to determine model constants.

Additional model modification will be necessary to include the effect of biaxial coating loads introduced by the thermal growth mismatch between the coating and the substrate during uniaxial TMF tests and engine transients.

PWA 273 aluminide coating and PWA 1480 crack initiation model development for calculating N_{sc}, N_{sp}, and N_{si} is currently in process. At present, based on isothermal fatigue correlations, the most promising candidate models for these materials are also derived from an approach based on hysteretic energy.

CONCLUDING REMARKS

In conclusion, we would like to emphasize that significant accomplishments have been achieved in the fatigue and fracture arena through the atmosphere created by the HOST Project. We are now much better able to deal with durability enhancement in the aeronautical propulsion industry through theoretical, analytical, and experimental approaches. Given the ability to complete the tasks we have started, we expect to reap even greater rewards in the near future.

The major accomplishments to-date are summarized below:

1. An advanced high-temperature fatigue and structures research laboratory has been implemented at the NASA Lewis.

2. Two new crack initiation life prediction methods have been developed for application to complex creep-fatigue loading of nominally isotropic superalloys a high temperatures.

3. Cyclic constitutive models for oxidation protective coatings and for highly anisotropic single crystal turbine blade alloys have been developed and verified.

4. A preliminary cyclic crack initiation life prediction model for coated single crystal superalloys has been proposed and is undergoing continued evaluation. The model utilizes tensile hysteretic energy and frequency as primary variables.

5. Two high temperature cyclic crack growth life prediction models have been proposed: micromechanistic and phenomenological engineering approaches have been taken. The micromechanistic approach is based upon oxidation interactions with mechanical deformation at the crack tip, while the engineering approach has its origins in the use of Path-Independent Integrals to describe the necessary fracture mechanics parameters.

REFERENCES

Ainsworth, R.A., Neale, B.K., and Price, R.H., 1978, "Fracture Behavior in the Presence of Thermal Strains," Tolerance of Flaws in Pressurized Components, Institution of Mechanical Engineers, London, pp. 171-178.

Atluri, S.N., 1982, "Path-Independent Integrals in Finite Elasticity and Inelasticity, with Body Forces, Inertia, and Arbitrary Crack-Face Conditions," Engineering Fracture Mechanics, Vol. 16, No. 3, pp. 341-364.

Blackburn, W.S., Jackson, A.D., and Hellen, T.K., 1977, "An Integral Associated with the State of a Crack Tip in a Nonelastic Material," International Journal of Fracture, Vol. 13, No. 2, pp. 183-200.

Halford, G.R., Saltsman, J.F., and Hirschberg, M.H., 1977, "Ductility Normalized-Strainrange Partitioning Life Relations for Creep-Fatigue Life Prediction," Environmental Degradation of Engineering Materials, M.R. Louthan and R.P. McNitt, eds., Virginia Tech. Printing Dept., V.P.I. and State University, Blacksburg, VA, pp. 599-612. (NASA TM-73737).

Halford, G.R. and Saltsman, J.F., 1983, "Strainrange Partitioning - A Total Strainrange Version," Advances in Life Prediction Methods, D.A. Woodford and J.R. Whitehead, eds., ASME, New York, pp. 17-26.

Hirschberg, M.H. and Halford, G.R., "Use of Strainrange Partitioning to Predict High-Temperature Low-Cycle Fatigue Life," NASA TN D-8072, 1976.

Kim, K.S., and Orange, T.W., 1988, "A Review of Path-Independent Integrals in Elastic-Plastic Fracture Mechanics," Fracture Mechanics: 18th National Symposium, ASTM STP-945, ASTM, Philadelphia, PA, In Press. (See also NASA CR-174956).

Kishimoto, K., Aoki, S., and Sakata, M., 1980, "On the Path Independent Integral-J," Engineering Fracture Mechanics, Vol. 13, No. 4, pp. 841-850.

Lindholm, U.S., Chan, K.S., Bodner, S.R., Weber, R.M., Walker, K.P., and Cassenti, B.N., 1984, "Constitutive Modeling for Isotropic Materials (HOST)," NASA CR-174718.

Liu, H.W. and Oshida, Y., 1986, "Grain Boundary Oxidation and Fatigue Crack Growth at Elevated Temperatures," Theoretical and Applied Fracture Mechanics, Vol. 6, No. 2, pp. 85-94.

Manson, S.S., Halford, G.R., and Nachtigall, A.J., 1975, "Separation of the Strain Components for Use in Strainrange Partitioning," Advances in Design for Elevated Temperature Environment, S.Y. Zamrik and R.I. Jetter, eds., ASME, New York, pp. 17-28.

McGaw, M.A. and Bartalotta, P.A., 1987, "A High Temperature Fatigue and Structures Testing Facility," 4th Annual Hostile Environments and High Temperature Measurements Conference Proceedings, Society for Experimental Mechanics, Bethel, CT, pp. 12-29. (See also, NASA TM-100151).

Moreno, V., 1983, "Creep Fatigue Life Prediction for Engine Hot Section Materials (Isotropic)," NASA CR-168228.

Moreno, V., Nissley, D.M., and Liu, L.S., 1985, "Creep Fatigue Life Prediction for Engine Hot Section Materials (Isotropic)," NASA CR-174844.

Moreno, V., Nissley, D.M., Halford, G.R., and Saltsman, J.F., 1985, "Application of Two Creep-Fatigue Life Models for the Prediction of Elevated Temperature Crack Initiation of a Nickel-Base Alloy," AIAA Paper 85-1420.

Nelson, R.S., Schoendorf, J.F., and Lin, L.S., 1986, "Creep Fatigue Life Prediction for Engine Hot Section Materials (Isotropic)," NASA CR-179550.

Oshida, Y. and Liu, H.W., 1988, "Grain Boundary Oxidation and an Analysis of the Effects of Oxidation on Fatigue Crack Nucleation Life," Low Cycle Fatigue--Directions for the Future, ASTM STP-942, ASTM, Philadelphia, PA, pp. 1199-1217.

Ostergren, W.J., 1976, "A Damage Function and Associated Failure Equations for Predicting Hold Time and Frequency Effects in Elevated-Temperature, Low-Cycle Fatigue," Journal of Testing and Evaluation, Vol. 4, No. 5, pp. 327-339

Ramaswamy, V.G., Van Stone, R.H., Dame, L.T., and Laflen, J.H., 1985, "Constitutive Modeling for Isotropic Materials," NASA CR-175004.

Saltsman, J.F. and Halford, G.R., 1988, "An Update of the Total Strain Version of SRP," Low Cycle Fatigue--Directions for the Future, ASTM STP-942, ASTM, Philadelphia, PA, pp. 329-341.

Swanson, G.A., Linask, I., Nissley, D.M., Norris, P.P., Meyer, T.G., and Walker, K.P., 1987, "Life Prediction and Constitutive Models for Engine Hot Section Anisotropic Materials," NASA CR-179594.

Tada, H., Paris, P.C., and Irwin, G.R., 1973, The Stress Analysis of Cracks Handbook, Del Research Corporation, Hellertown, PA.

Walker, K.P., 1981, "Research and Development Programs for Nonlinear Structural Modeling with Advanced Time-Temperature Dependent Constitutive Relationships," NASA CR-165533.

TABLE I. - HOST FATIGUE AND FRACTURE PROGRAMS

- NAS3-23288, Pratt & Whitney (R.S. Nelson)
  Creep-Fatigue Crack Initiation--Isotropic
- NAS3-23940, General Electric (J.J. Laflen)
  Elevated Temperature Crack Growth--Isotropic
- NAS3-23939, Pratt & Whitney (G.A. Swanson)
  Life Prediction/Constitutive Modeling--Anisotropic
- NAG3-348, Syracuse University (H.W. Liu)
  Crack Growth Mechanisms--Isotropic
- Lewis (M.A. McGaw)
  High-Temperature Fatigue and Structures Laboratory

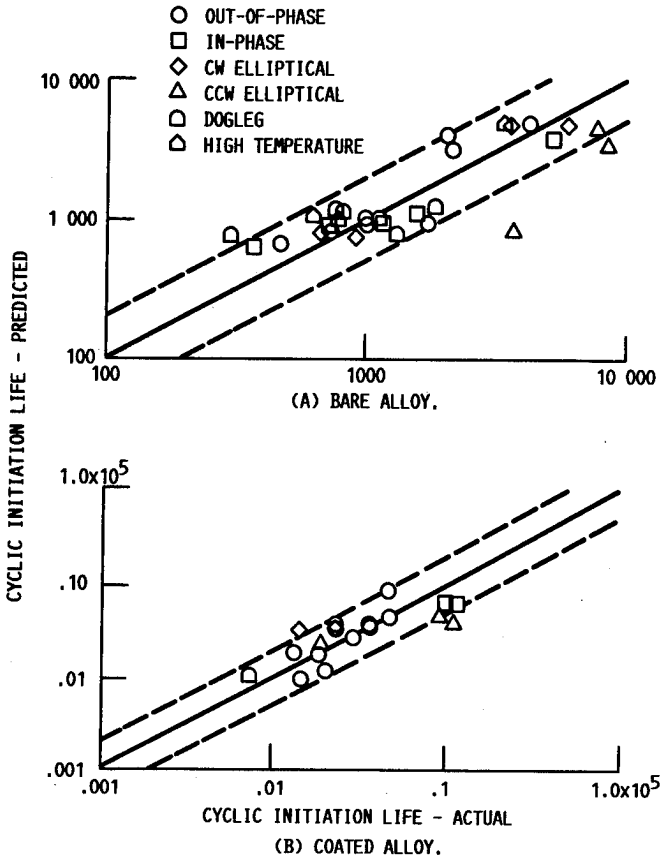

FIGURE 1. - APPLICATION OF PRELIMINARY CDA MODEL TO TMF LIFE PREDICTION FOR THE CAST NICKEL-BASE ALLOY, PWA 1455 (B1900 + Hf), AFTER MORENO (1986).

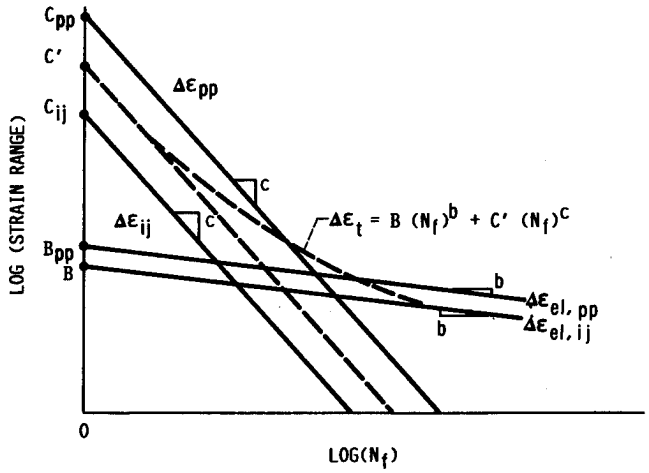

FIGURE 2. - SCHEMATIC REPRESENTATION OF TOTAL STRAIN-STRAINRANGE PARTITIONING (TS-SRP).

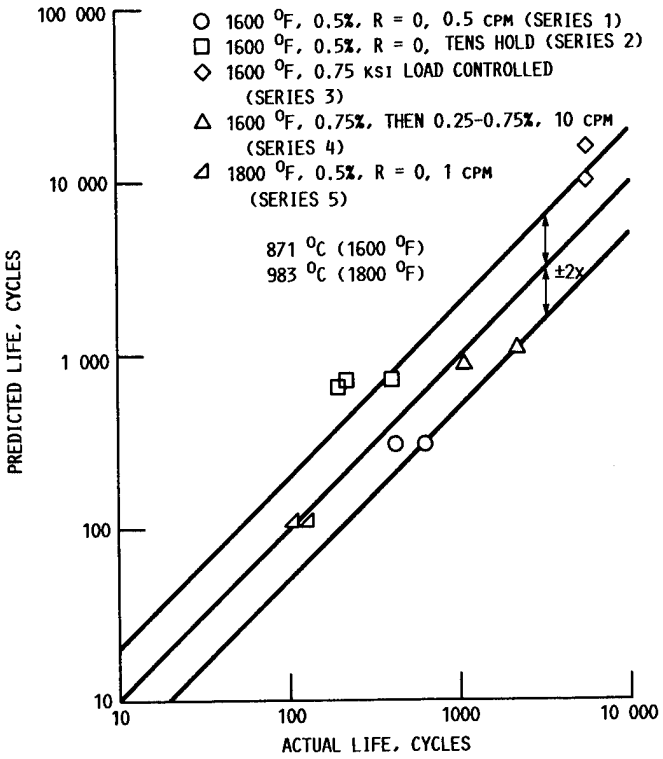

FIGURE 3. - PREDICTION OF COMPLEX VERIFICATION EXPERIMENTS USING TS-SRP, AFTER MORENO (1985).

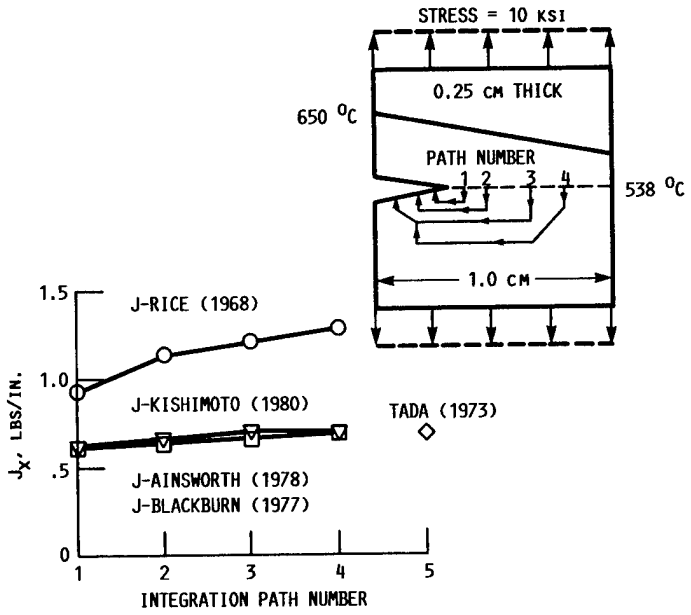

FIGURE 4. - EVALUATION OF PATH-INDEPENDENT INTEGRALS UNDER LINEAR TEMPERATURE GRADIENT IN SINGLE EDGE NOTCH SPECIMENS OF INCONEL 718, AFTER KIM AND ORANGE (1988).

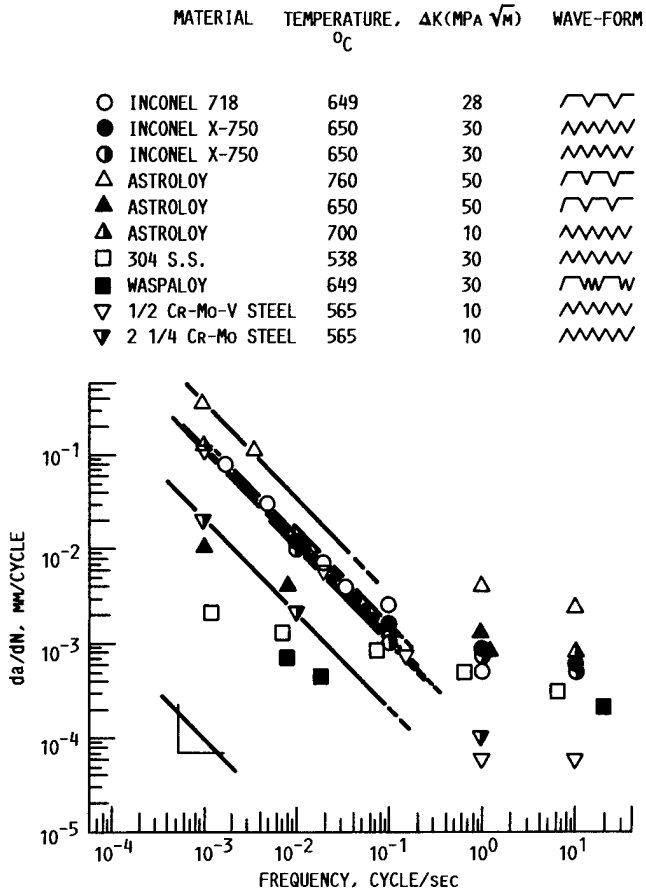

FIGURE 5. - EVALUATION OF THE MICROMECHANISTIC OXIDATION CRACK EXTENSION MODEL OF LIU AND OSHIDA (1986).

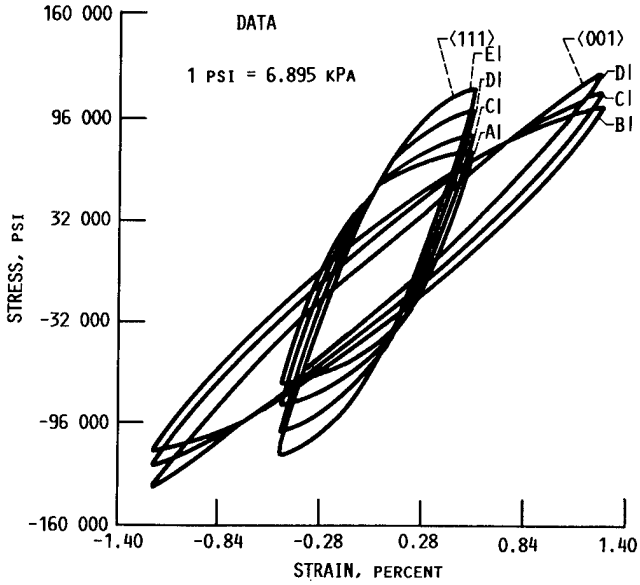

FIGURE 6. - EXPERIMENTAL LOOPS IN ⟨001⟩ AND ⟨111⟩ DIRECTIONS AT 871 C(1600 °F) AT STRAIN RATES OF: (A) 0.001% PER SECOND, (B) 0.0025% PER SECOND, (C) 0.01% PER SECOND, (D) 0.1% PER SECOND, AND (E) 0.5% PER SECOND.

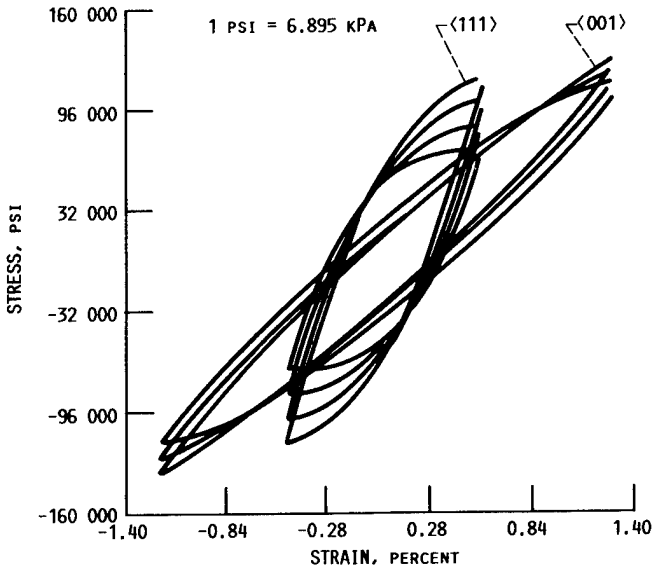

FIGURE 7. - MICRO MODEL WITH BOTH OCTAHEDRAL AND CUBE SLIP TERMS CORRELATED TO ⟨111⟩ AND ⟨001⟩ DATA.

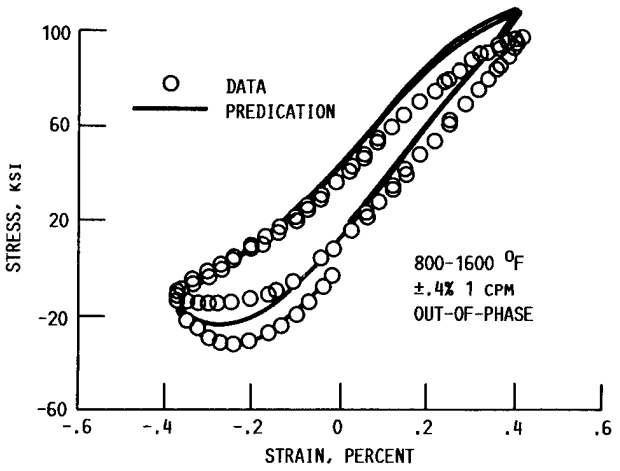

FIGURE 8. - OVERLAY COATING CONSTITUTIVE MODEL PREDICTION OF THERMAL MECHANICAL CYCLE AND COMPARISON WITH DATA.

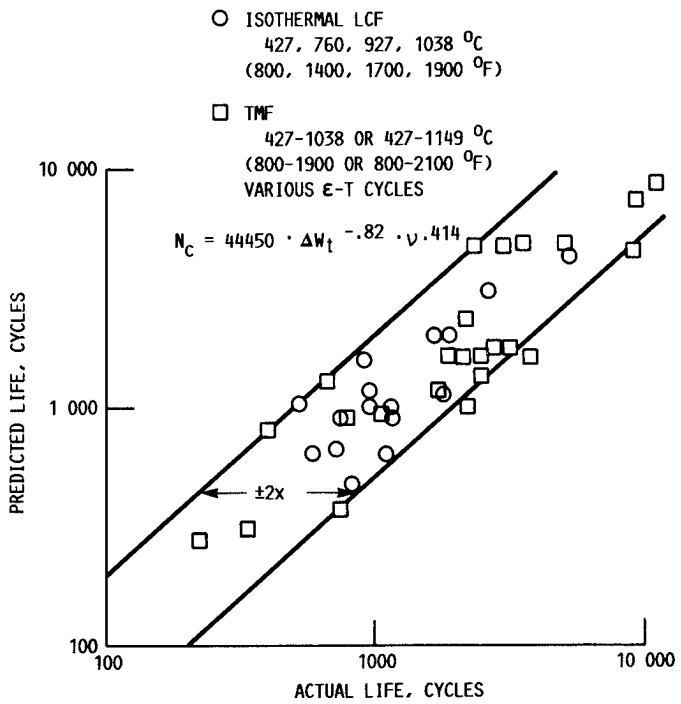

FIGURE 9. - OVERLAY COATING LIFE MODEL CORRELATION OF OF ISOTHERMAL LIFE DATA AND PREDICTION OF THERMAL MECHANICAL FATIGUE LIFE DATA.

LIFE MODELING OF THERMAL BARRIER COATINGS FOR AIRCRAFT GAS TURBINE ENGINES

R. A. Miller
National Aeronautics and Space Administration
Lewis Research Center
Cleveland, Ohio

ABSTRACT

Thermal barrier coating life models developed under the NASA Lewis Research Center's Hot Section Technology (HOST) program are summarized. An initial laboratory model and three design-capable models are discussed. Current understanding of coating failure mechanisms are also summarized.

INTRODUCTION

Thermal barrier coatings are being developed for protecting air-cooled turbine blades and vanes in aircraft gas turbine engines. The current state-of-the-art coating system consists of about 0.25 mm of a zirconia-yttria ceramic over 0.13 mm of an MCrAlY alloy bond coat. Both layers are applied by plasma spraying. The benefits arise from the insulation provided by the ceramic layer. This insulation allows higher gas temperatures, lower component temperatures, reduced cooling air requirements, moderation of thermal transients, and/or a decrease in the severity of hot spots. This yields improvements in performance, efficiency, and component durability. Future engine designs are expected to rely heavily on thermal barrier coatings. Thus life models are required to assess the risks associated with any given design and to insure that these coatings can be exploited fully. Further details may be found in Miller (1987), DeMasi et al., (1988), Strangman et al., (1987), and Hillery (1987).

The NASA thermal barrier coating life model development program consisted initially of an in-house program designed to improve understanding and to develop a model suitable for treating laboratory life data (Miller, 1987). This work was then extended via three contracts under the HOST program to the development of design-capable models (DeMasi et al., 1988; Strangman et al., 1987; Hillery et al., 1987). These contracts were devised determine thermomechanical properties, to analyze coating stresses and strains, and to develop life models. Phase I of each contract has now been successfully completed, and the results will be summarized in this paper.

COATING FAILURE MECHANISMS

A basic understanding of coating failure mechanisms is a prerequisite to the development of life prediction models. Failure mechanisms in gas turbine engines and in laboratory simulations have been discussed in detail elsewhere (e.g., Miller, 1987; DeMasi et al., 1988; Strangman et al., 1987, Hillery et al., 1987). There is now general agreement that these coatings fail primarily as a result of stresses induced by the thermal expansion mismatch between the ceramic and metallic layers, and that these stresses are greatly influenced by time-at-temperature processes such as oxidation and possibly sintering. The stress state in the ceramic layer which leads to crack propagation and eventual spalling is one of biaxial compression in the plane of the coating and radial tension. These stresses are further complicated by the wavy and irregular interface between the ceramic and metallic layers. In fact, HOST-sponsored calculations indicate that the radial stresses above a wavy interface may actually alternate between regions of compression and tension as illustrated in Fig. 1 (Chang et al., 1987). Figure 2 illustrates that the behavior of plasma sprayed zirconia-based thermal barrier coatings differs significantly from the behavior of conventional ceramics. This behavior, which is believed to result from the splat structure, includes very low thermal conductivity and very high compressive strain tolerance. In-plane tensile strain tolerance of the coating system is also very high because such loading may lead to segmentation cracking in the ceramic with no degradation to the attachment strength. Plasma sprayed zirconia-yttria also exhibits creep-like behavior, presumably as a result of sliding at the splat boundaries, and fatigue-like behavior, presumably as a result of slow crack growth. Experimental evidence of slow crack growth (or microcrack link up), creep, and fatigue are presented in DeMasi et al., (1988).

INITIAL LABORATORY MODEL DEVELOPMENT

A preliminary life prediction model has been described (Miller, 1987; Miller, 1984; Miller et al., 1984). This model assumed that the complex state of

stress and strain imposed on the coating system by the thermal loads could be expressed in terms of a single parameter. This parameter was labelled ε_r -- which was taken to be the radial component of the thermal expansion mismatch strain. Next it was assumed that the time-at-temperature effects could be treated in terms of oxidation alone and that oxidation could be characterized by the weight gain at the conclusion of each cycle w_N. Then, weight gain and strain were related using either of two alternate approaches. In the first case, depicted in Fig. 3(a), an oxidized coating is assumed to behave as if an effective strain ε_e is increasing. At zero weight gain this effective strain equals the radial strain ε_r. At a critical weight gain w_c -- defined as the weight gain required to fail the coating in a single cycle -- the effective strain equals a failure strain ε_f. This leads to the expression

$$\varepsilon_e = \varepsilon_f - \varepsilon_r \left(\frac{w_N}{w_c}\right)^m + \varepsilon_r \qquad (1)$$

where the exponent m has been added to allow the curve in Fig. 3(a) to be nonlinear. The alternate assumption (Miller, 1987) is to assume that the failure strain degrades from an initial value ε_{f0} to a final value equal to ε_r. This case, illustrated in Fig. 3(b) leads to the expression

$$\frac{\varepsilon_f}{\varepsilon_r} = \left(1 - \frac{\varepsilon_{f0}}{\varepsilon_r}\right)\left(\frac{w_N}{w_c}\right)^m + \frac{\varepsilon_{f0}}{\varepsilon_r} \qquad (2)$$

Cracks in the ceramic layer may be assumed to grow according to a crack growth law of the form

$$\frac{dA}{dN} = A\varepsilon_e{}^b a^c \qquad (3)$$

where da/dN is the incremental crack growth per cycle, A is a constant, b and c are exponents related to the subcritical crack growth exponent, and a is the crack length. The model resulting from expression 1 is

$$\sum_{N=1}^{N_f} \left[\left(1 - \frac{\varepsilon_r}{\varepsilon_f}\right)\left(\frac{w_N}{w_c}\right)^m + \frac{\varepsilon_r}{\varepsilon_f}\right]^b = 1 \qquad (4)$$

and the alternative model resulting from expression 2 is

$$\sum_{N=1}^{N_f} \left[\left(1 - \frac{\varepsilon_{f0}}{\varepsilon_r}\right)\left(\frac{w_N}{w_c}\right)^m + \frac{\varepsilon_{f0}}{\varepsilon_r}\right]^{-b} = 1 \qquad (5)$$

These models may also be derived from the familiar fatigue expression (Miller et al., 1984; Manson, 1966).

$$N_f = \left(\frac{\varepsilon_e}{\varepsilon_f}\right)^{-b} \qquad (6)$$

and Miner's Law

$$\sum_{N=1}^{N_f} \left(\frac{1}{N_{fN}}\right) = 1 \qquad (7)$$

where N_{fN} is the apparent number of cycles remaining after cycle N and weight gain w_N.

Figure 4 illustrates the fits obtained using expression 4 and applying it to life data collected at 1100 °C for three different cycle lengths. It should be mentioned that the set of parameters given in the figure are not unique. Numerous other sets provide equally good fits. For example raising the assumed value of b while lowering the strain ratio produces an equally good fit. Also, the life data can be fit equally well using expressions 4 or 5.

DESIGN-CAPABLE LIFE MODELING

While the above model represented a first step it was not in a form which would be of use to an engine designer. Therefore three contracts were instituted under the HOST program which were aimed at the development of design-capable models.

Pratt & Whitney Aircraft (DeMasi et al., 1988), along with subcontractor Southwest Research Institute, developed a fatigue-based coating life model which uses Miner's Law (expression 7) along with expression 6 rewritten as

$$N_f = \left(\frac{\Delta\varepsilon_i}{\Delta\varepsilon_f}\right)^{-b} \qquad (8)$$

where $\Delta\varepsilon_i$ is the inelastic strain range defined by

$$\Delta\varepsilon_i = \Delta(\alpha\,\Delta T) + \Delta\varepsilon_h + \Delta\varepsilon_c - \frac{2\sigma_{ys}}{E} \qquad (9)$$

The term $\Delta(\alpha\,\Delta T)$ in the above expression is the thermal expansion mismatch strain (which was expressed in terms of ε_r in the previous section), $\Delta\varepsilon_h$ is the strain resulting from the heating transient, $\Delta\varepsilon_c$ is the strain resulting from the cooling transient, and σ_{ys}/E is the elastic strain at yielding. The assumed relationship between oxidation and strain, analogous to expression 2, was

$$\Delta\varepsilon_f = \Delta\varepsilon_{f0}\left(\frac{1-\delta}{\delta_c}\right)^c + \Delta\varepsilon_i\left(\frac{\delta}{\delta_c}\right)^d \qquad (10)$$

where oxidation has been expressed in terms of the oxide layer thickness δ rather than the specific weight gain w. The inelastic strain range was calculated using finite element techniques which employed a time dependent inelastic model developed by Walker (1983). Figure 5 shows an example of the use of this model to calculate compressive and tensile strains which may be compared with experimental data. In Fig. 6 the ceramic stress-strain behavior is calculated for a single cycle. This figure displays the large amount of reversed inelastic strain produced by thermal cycling. Figure 7 shows a plot of observed versus calculated lives for a wide range of test conditions. As shown in the figure the model is accurate to plus or minus a factor of 3, which is considered adequate.

The model developed by the Garrett Turbine Engine Company (Strangman et al., 1987) may be expressed as

$$\text{TBC LIFE} = \frac{1}{\left[\dfrac{\text{HEATING CYCLE LENGTH FACTOR}}{(\text{OXIDATION LIFE})^{-1} + \dfrac{\text{ZIRCONIA DENSIFICATION}}{\text{PLUS OXIDATION LIFE}}}\right]^{-1} + \left[\dfrac{\text{SALT FILM}}{\text{DAMAGE LIFE}}\right]^{-1}} \qquad (11)$$

Equation 11 is expressed schematically in Fig. 8 which shows that the model considers bond coat oxidation, zirconia toughness reduction, and damage due to molten salt deposits. The model is driven by the thermal analysis of the component of interest for its anticipated mission. The left side of the denominator in expression 11 as determined from test data calibrations is

$$\frac{(t^{0.25} + 0.181)\ MTBREF}{\{\exp[-0.015(T + 273) + C_1]\}^{-1} + \{\exp[-0.041(+273) + C_2]\}^{-1}} \qquad (12)$$

where MTBREF is a multitemperature burner rig experience factor which forces predictions and experiment into agreement. The right side of the denominator in expression 11 is calculated using a Garrett-developed model (Strangman, 1984; Strangman et al., 1987). In practice, the model is driven by thermal analysis of the component of interest. An example of the application of the thermal barrier coating life model to laboratory test data is shown in Fig. 9, and mission analysis predictions are shown in Fig. 10.

The approach used by the General Electric Company (Hillery et al., 1987) employed time-dependent, nonlinear finite element modeling of the stresses and strains present in the thermal barrier coating system, followed by the correlation of these stresses and strains with test lives. The life model developed using this approach may be expressed as

$$\Delta\varepsilon_{RZ} + 0.4\ \Delta\varepsilon_{R} = 0.121\ N_f^{-0.486} \qquad (13)$$

where $\Delta\varepsilon_{RZ}$ is the shear strain range, $\Delta\varepsilon_{R}$ is the normal strain range, and N_f is the number of cycles to failure. The above model is the only one to consider failure induced by edges and hence is the only one to consider shear strain. Expression 13 is illustrated graphically in Fig. 11

CONCLUDING REMARKS

In conclusion, the materials and structural aspects of thermal barrier coatings have been successfully integrated under the NASA HOST program to produce models which may now or in the near future be used in design. Efforts on this program continue at Pratt & Whitney Aircraft where their model is being extended to the life prediction of physical vapor deposited thermal barrier coatings.

While the HOST program has been quite successful it should also be noted that many new and unanswered questions have been raised by this work. For example, the effects of creep and inelasticity in both the ceramic and bond coat layers are poorly understood. The role of shearing stresses, including the role that shearing at an edge may play in reducing the fatigue exponent, is not well understood. The detailed mechanism by which oxidation controls coating system life is not well understood either. Also, it is not known whether the assumption of a smooth interface, commonly employed to simplify finite element analyses can lead to inaccurate or even misleading results. Other areas of uncertainty involve the importance of sintering at high temperatures and hot corrosion at relatively low temperatures.

REFERENCES

Chang, G.C., Phucharoen, W., and Miller, R.A., 1987, Behavior of Thermal Barrier Coatings for Advanced Gas Turbine Blades," Surface and Coatings Technology, Vol. 30, pp. 13-28.

DeMasi, J.T., Ortiz, M., and Sheffler, K.D.,1988, "Thermal Barrier Coating Life Prediction Model Development", NASA Contractor Report, to be published (Pratt & Whitney Aircraft)

Hillery, R.V., Pilsner, B.H., McKnight, R.L., Cook, T. S., and Hartle, M. S., 1987, "Thermal Barrier Coating Life Prediction Model, Final Report," NASA CR-180807.

Manson, S.S., 1966, "Thermal Stress and Low Cycle Fatigue," McGraw-Hill Book Company, New York, 1966.

Miller, R.A., 1984, "Oxidation-Based Thermal Barrier Coating Life Prediction Model" Journal of the American Ceramic Science, Vol. 67, No. 8, pp. 517-521.

Miller, R.A., Agarwal, P., and Duderstadt, E.C., 1984, Life Modeling of Atmospheric and Low Pressure Plasma Sprayed Thermal Barrier Coating," Ceramic Engineering Science Procedings, Vol 5, No. 7-8, pp. 470-478.

Miller, R.A., 1987, "Current Status of Thermal Barrier Coatings - An Overview," Surface and Coatings Technology, Vol. 30, No. 1, pp. 1-11.

Strangman, T.E., 1984, "Life Prediction and Development of Coatings for Turbine Airfoils," Workshop on Gas Turbine Materials in a Marine Environment, Bath, U. K.

Strangman, T.E., Neumann, J., and Liu, A., 1987, "Thermal Barrier Coating Life Prediction Model Development, Final Report," NASA CR-179648.

Walker, K.P., 1983, "Research and Development Program for Non-Linear Structural Modeling with Advanced Time-Temperature Dependent Constituitive Relationships," NASA CR-165533.

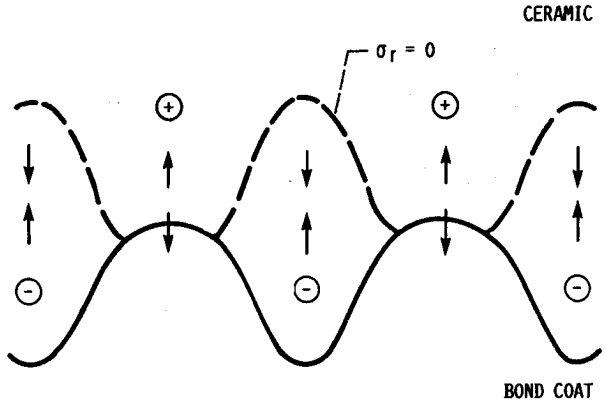

FIGURE 1. - SCHEMATIC REPRESENTATION OF CALCULATED RADIAL THERMAL EXPANSION MISMATCH STRESS ABOVE A WAVY INTERFACE.

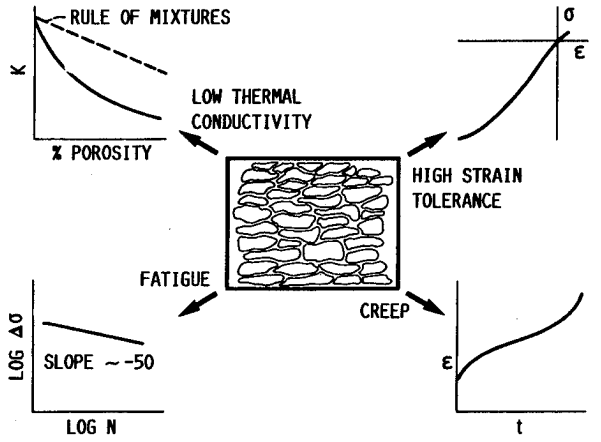

FIGURE 2. - SCHEMATIC REPRESENTATION OF THERMAL MECHANICAL PROPERTIES RESULTING FROM COATING SPLAT STRUCTURE.

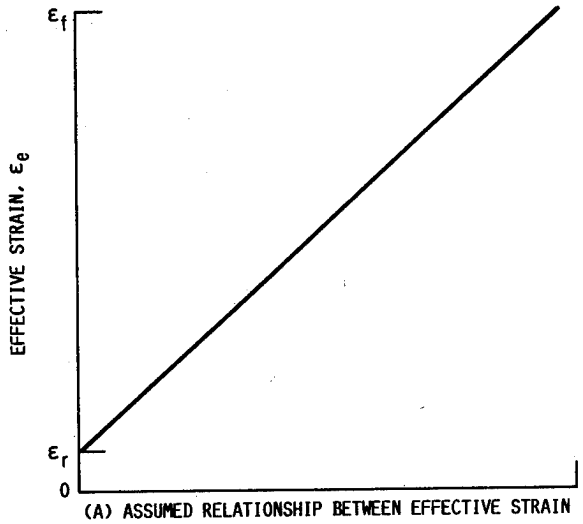

(A) ASSUMED RELATIONSHIP BETWEEN EFFECTIVE STRAIN AND OXIDATIVE WEIGHT GAIN.

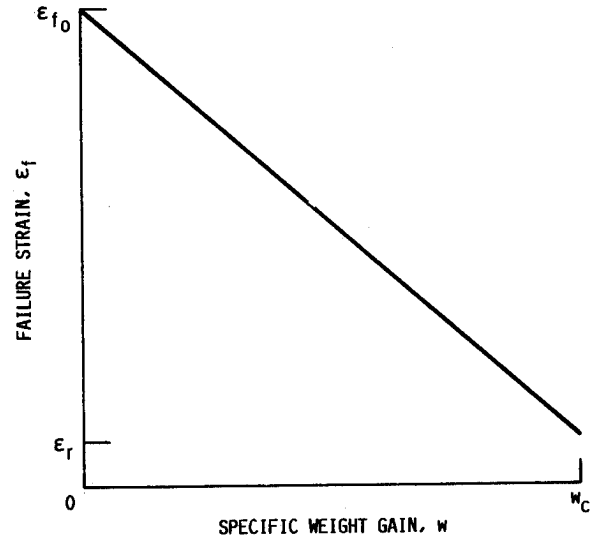

(B) ASSUMED ALTERNATE RELATIONSHIP BETWEEN FAILURE STRAIN AND OXIDATIVE WEIGHT GAIN.

FIGURE 3. - ASSUMED WEIGHT GAIN/STRAIN RELATIONSHIPS.

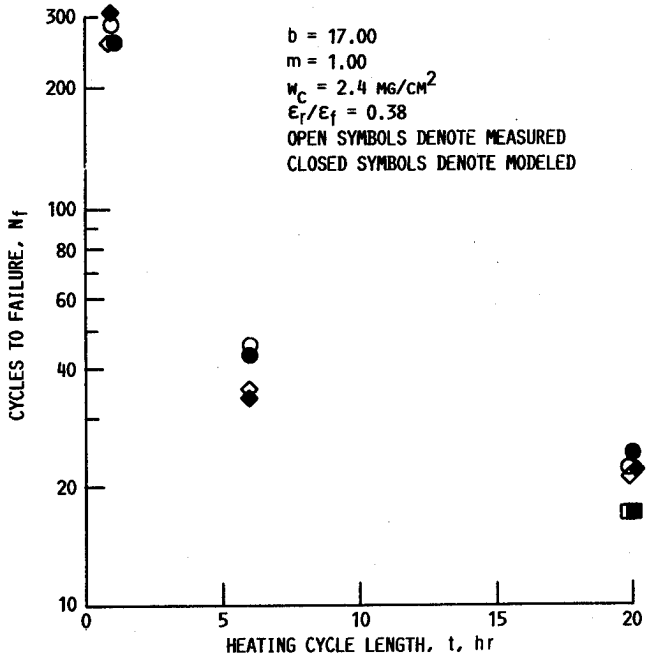

FIGURE 4. - COMPARISON OF CALCULATED AND MODELED LIFE AS A FUNCTION OF HEATING CYCLE DURATION ACCORDING TO NASA LABORATORY MODEL.

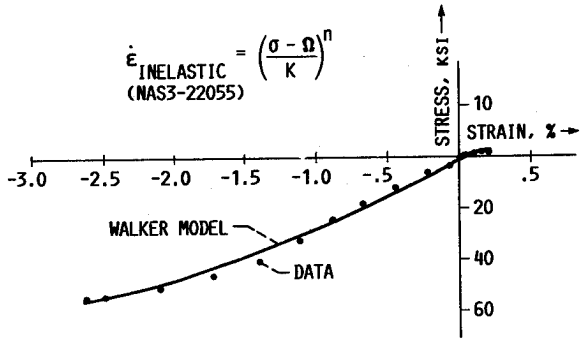

FIGURE 5. - CERAMIC BEHAVIOR MODELED WITH WALKER EQUATION ACCORDING TO THE PRATT & WHITNEY MODEL.

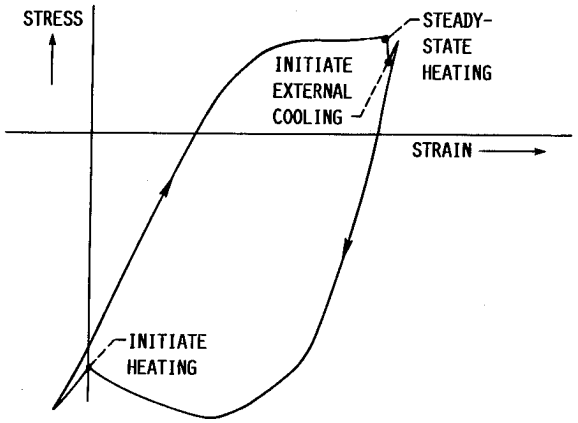

FIGURE 6. - SCHEMATIC OF STRAINS CALCULATED FOR A TYPICAL CYCLE ACCORDING TO THE PRATT & WHITNEY MODEL.

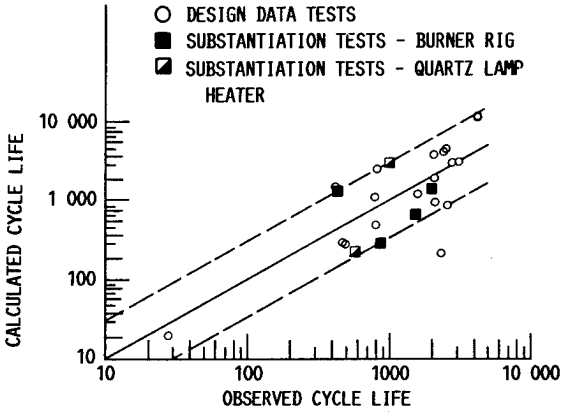

FIGURE 7. - COMPARISON OF CALCULATED AND MODELED LIVES ACCORDING TO THE PRATT & WHITNEY MODEL.

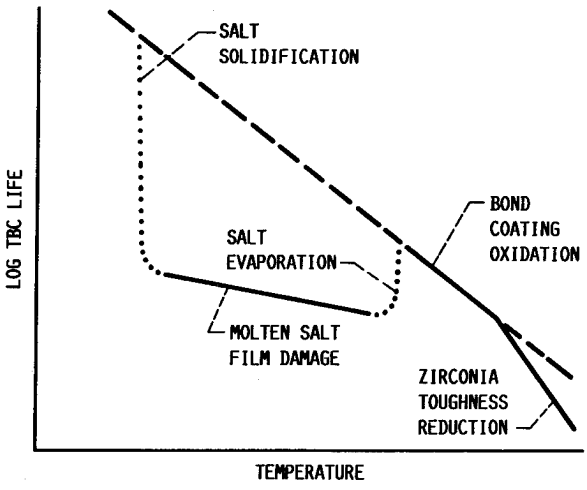

FIGURE 8. - SCHEMATIC OF PROCESSES CONSIDERED IN THE GARRETT MODEL.

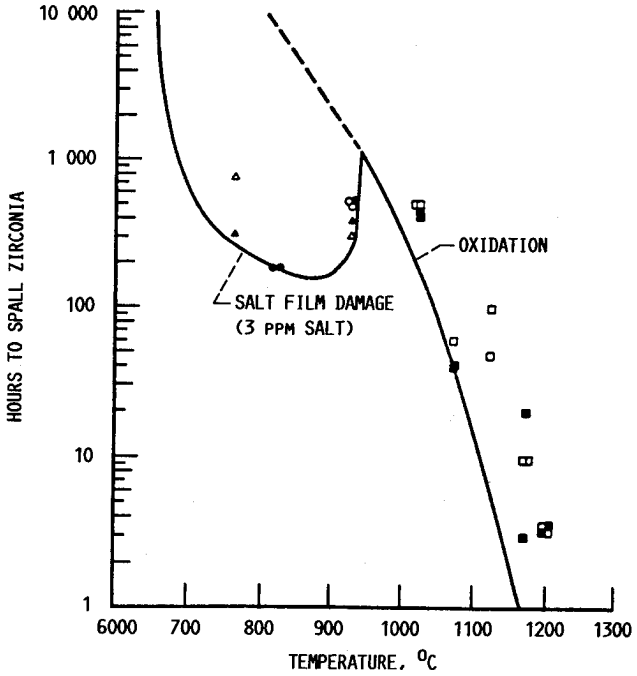

FIGURE 9. - CONSERVATIVE FIT OF LABORATORY LIFE DATA TO THE GARRETT MODEL.

TBC SYSTEM	BUSINESS JET, HR	MARITIME SURVEILLANCE, HR
PLASMA SPRAY		
CHROMALLOY	16 517	9 843
UNION CARBIDE	6 656	5 207
KLOCK	49 644	29 973
EB-PVD		
TEMESCAL	55 607	2 106

FIGURE 10. - MISSION ANALYSIS PREDICTIONS BY THE GARRETT MODEL.

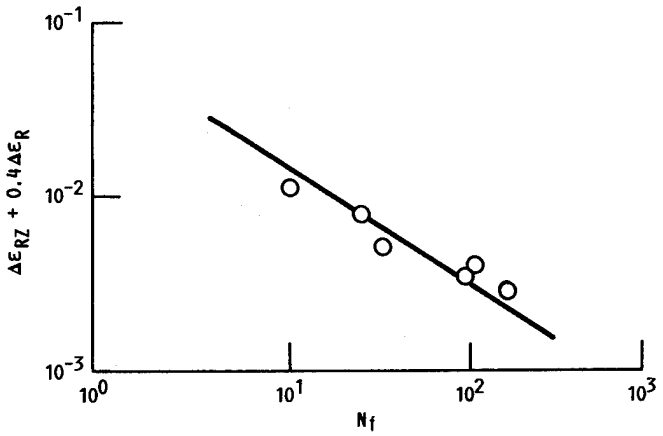

FIGURE 11. - CORRELATION BETWEEN CALCULATED STRAIN RELATIONSHIP AND EXPERIMENTAL CYCLES TO FAILURE ACCORDING TO THE GENERAL ELECTRIC MODEL.

VIEWS ON THE IMPACT OF HOST

J. B. Esgar
Sverdrup Technology, Inc.
Lewis Research Center
Cleveland, Ohio

D. E. Sokolowski
National Aeronautics and Space Administration
Lewis Research Center
Cleveland, Ohio

ABSTRACT

The Hot Section Technology (HOST) Project, which was initiated by NASA Lewis Research Center in 1980 and concluded in 1987, was aimed at improving advanced aircraft engine hot section durability through better technical understanding and more accurate design analysis capability. The project was a multidisciplinary, multiorganizational, focused research effort that involved 21 organizations and 70 research and technology activities and generated approximately 250 research reports. No major hardware was developed. To evaluate whether HOST had a significant impact on the overall aircraft engine industry in the development of new engines, interviews were conducted with 41 participants in the project to obtain their views. The summarized results of these interviews are presented.

SUMMARY

The NASA-sponsored HOST Project addressed durability needs in advanced aircraft engine combustors and turbines by developing improved methods for design analysis and life prediction of critical parts. Providing technology to improve engine durability should, in turn, reduce maintenance costs and improve flight safety. Because of the nature of challenges in developing durable structures, the project was multidisciplinary and multiorganizational involving 70 research and technology activities. While most projects result in a deliverable piece of major hardware, the HOST Project instead generated approximately 250 research reports that cover results from analytical modeling, highly controlled small-scale experiments, and numerous computer codes that were developed. HOST Annual Workshops brought together representatives from all major U.S. gas turbine manufacturers and from a significant number of universities and research institutes in an effective forum to discuss and critique recent research findings. To better understand the impact of the HOST Project, its cost effectiveness, and benefits derived by organizations having association with it, numerous interviews were conducted with key program participants, primarily from industry and academia, to determine their viewpoints. This paper summarizes results from the interviews.

INTRODUCTION

The Hot Section Technology Project, which has the acronym HOST, was initiated by NASA Lewis Research Center in the Fall of 1980 to address the need for improving durability of advanced aircraft turbine engines. Near the conclusion of the project in the Fall of 1987 a survey of knowledgeable participants was conducted to assess the impact and value of HOST to industry, to academia, and to the government. This paper summarizes the results of the survey.

The HOST Project was unique in several ways. Its focus on durability was in contrast to other recent NASA-sponsored programs that focused primarily on performance improvements. Those programs included the Energy Efficient Engine (EEE), Engine Component Improvement (ECI), and Advanced Turboprop Program (ATP) and involved only a portion of the aircraft engine industry. The HOST Project complemented such programs on performance improvement, which often tend to aggravate engine hardware durability. In addition the 70 major research and technology activities initiated under HOST drew on researchers from three work sectors--industry (including all the large U.S. engine manufacturers), academia, and government--to work jointly toward common goals.

Another unique feature of HOST was its focused and integrated research encompassing six engineering disciplines that addressed critical technology needs in the engine hot section--the combustor and turbine components. The disciplines are instrumentation, combustion, turbine heat transfer, structural analysis, fatigue and fracture, and surface protection. HOST acted as a keystone that helped bridge the gap between these sometimes diverse groups and provided mutual support in helping them work together.

While the program was justified for civil aircraft needs, military needs were equally satisfied because the same design analysis systems are used by

manufacturers in developing both civil and military engines.

Finally, no major hardware, such as an engine prototype, was developed. Instead technical understanding and design analysis capability were improved and documented in approximately 250 published research reports and in numerous computer codes that were developed. Technology was further identified and transferred in a timely manner through six major annual workshops, which had a total attendance of 1500 people. Using the research presented in the reports and at the workshops, a move was started to change development of advanced engines from the historical experimental testing approach of "build 'em and bust 'em" to a more analytical approach in which component hardware designs are analyzed with much more accurate data bases and mathematical models before testing is begun. Testing is then more for design verification than for experimental development.

A total of 40 separate activities were competitively contracted with aircraft engine manufacturers and research institutes plus 13 grants to universities. Seventeen major activities were supported at the NASA Lewis Research Center. A total of 21 organizations were represented in the effort. In addition to the above mentioned university grants, several manufacturers subcontracted parts of their work to university researchers, who may or may not also have had direct NASA HOST grants. The 40 contracts were generally multiyear and often multiphased. This approach provided a greater opportunity for interaction between various organizations represented than is normally encountered in government short-term contracted efforts.

To evaluate and report the impact of the HOST Project, 41 individuals from participating organizations were interviewed. These interviews, plus some results from a 1984 mid-project assessment that also involved industry and academia participants, are summarized in this paper to provide written testimony on the HOST Project. Further, the findings may provide guidance in planning future government-sponsored research programs.

APPROACH

The goal of this study was to determine the HOST Project's impact by obtaining views from a representative number of key participants. Efforts were made to avoid biases, if any, of the interviewer. The authors of this paper include the NASA manager of the HOST Project, who conceived and guided the study, and a support service contractor, who conducted the study and who had considerable airbreathing engine background prior to this project. The support service contractor had no prior knowledge of the HOST Project and entered the study with no biases regarding HOST. The project manager made suggestions as to appropriate HOST participating organizations and people to contact. The contractor contacted these organizations, made arrangements for visits, and conducted interviews both with people suggested by the project manager and with others suggested by some of those interviewed. Throughout the duration of the interview period some HOST participants called and volunteered unsolicited comments. By means of this approach the co-author most familiar with the project provided leads of organizations and/or personnel who had been active in the overall program, and the other author conducted the interviews and gathered data presented herein without preconceived ideas on the impact of HOST.

Approximately 90 percent of the interviews were conducted in person, with the remainder conducted by telephone. A total of 41 interviews were conducted with the following breakdown by organization: 26 from engine manufacturers, 5 from universities, 4 from research institutions, and 6 from government (NASA and U.S. Air Force). Personal interviews were conducted with key participants from the four major aircraft engine manufacturers in the program, namely Pratt and Whitney, General Electric Company, Allison Gas Turbine Division of General Motors Corporation, and Garrett Turbine Engine Company. The approach was to first call the organization and tell them the subject to be discussed. Visits then were made and those interviewed were given the opportunity to state their views on both positive and negative aspects of the project. Efforts were made to solicit individual views, either pro or con, and to avoid questions or comments seeking praise for the program. No set questions were asked in the interviews. Instead, individuals were asked a few general questions and then given the opportunity to express whatever opinions they had. Active listening was used to encourage discussion and to avoid guiding answers. If there were questions concerning the interpretation of comments given, follow-up telephone calls were made for clarification. In several cases the interviewer's written summary of comments was sent to the organizations interviewed to determine if the individuals concurred with the interviewer's interpretation. It is the belief of the interviewing author that the appraisals given were spontaneous and honest. This report does not identify individuals or organizations other than listing the four engine manufacturers and the government organizations from whom comments were solicited.

FINDINGS

There was unanimous agreement from everyone interviewed that the HOST Project was highly effective and to the mutual benefit of all participants. NASA was lauded for the conception, advocacy, and management of the program. There was agreement that without HOST many of the important research programs, which are needed to advance technology in the hot section of gas turbine engines, would have been delayed for years or never undertaken. Elements of HOST which were particularly emphasized as being beneficial by a number of those interviewed included: (1) three-dimensional inelastic structural analysis, (2) thermomechanical fatigue testing, (3) constitutive modeling, (4) combustor aerothermal modeling, (5) turbine heat transfer, and (6) protective coatings. Instrumentation research was also emphasized as being beneficial, primarily by the single organization conducting that research. Other organizations were less enthusiastic because the developed instrumentation was not commercially available to them. In a somewhat similar manner computer codes developed in the HOST Project were generally more useful to the organization developing the codes than to others, particularly for the longer, more complex codes.

Two areas, that were not research in nature, received near unanimous approval. The first was the annual workshops where current research results were presented and discussed, and the second was the improved industry-university-NASA relationships.

Discussion of comments received on the above mentioned areas plus other benefits or comments for improvement follow.

Impact on Technical Understanding and Predictive Capability

Three-dimensional inelastic structural analysis. Inelastic or nonlinear structural analyses have limited, but very important, applications. These analyses are used primarily for short-life cyclic applications where it may be acceptable to exceed the elastic limit for a few cycles. For long-life applications, however, hardware generally should be designed for operation within the elastic range. But even for long-life applications based on elastic design, there are occasions when three-dimensional (3-D) inelastic analysis may be needed. One occasion is when a shorter than predicted life is encountered. In this case an inelastic analysis can often pinpoint the problem area. In addition a 3-D inelastic analysis can be useful for determining stress redistribution when local yielding occurs. Thus for such special cases, 3-D inelastic analysis can be a very important design tool.

True three-dimensional analytical methods have only become available to engine design analysts within the last few years--after the HOST Project was initiated. Several approaches to 3-D inelastic analysis were pursued in the project. The best approach may not be known for some time. Currently 3-D inelastic design analyses are cumbersome, complicated, and require a great deal of computer time. Consequently there is some reluctance on the part of analysts to use 3-D inelastic analysis unless absolutely necessary. With time, however, as design analysts become more comfortable with this analysis approach, it should be used more extensively. Its use is both for problems that occur early during engine development and later for pinpointing the cause and cure for field problems, when local yielding is suspected to be occurring. As a result, 3-D inelastic structural analysis has been reported by participants to be a significant advancement that resulted from HOST.

Thermomechanical fatigue testing. In the past, mechanical properties of metallic materials have been determined experimentally using simpler mechanical and thermal load variations than the complex variations experienced in many engine applications. The need to improve engine durability requires evaluation of material behavior and life under more realistic conditions. In the HOST program, contracts, grants, and NASA in-house research were conducted on evaluating material behavior, including both crack propogation and material deformation, as a function of time, under cyclic biaxial mechanical loads, and in numerous atmospheric and cyclic temperature environments. Cyclic mechanical loadings have included high frequency loads superimposed on lower frequency loads.

The key objective of this research was to gain a better understanding of how and why cracks develop in different types of materials exposed to cyclic temperature and mechanical loading conditions. These data can be the basis of engineering life predictions methods that can be applied to the severe conditions in the engine hot section. The deformation testing portion of the research supports the development of viscoplastic constitutive models for structural analysis.

These mechanical property data are obtained under more realistic conditions and with greater precision than were heretofore possible. According to some of those interviewed, the data base of thermomechanical material properties plus experimental data from other phases of HOST program may be one of the most useful aspects of the HOST Project.

Constitutive modeling. Constitutive modeling is an analytical approach for predicting stresses and strains as a function of time under complex cyclic biaxial mechanical loading and temperature variations. The modeling is based on experimental thermomechanical deformation data. Prior to the HOST Project research on constitutive modeling was done primarily at universities, and not at aircraft engine manufacturers. HOST provided a team approach of industry, universities, and NASA working together to develop a capability that did not exist previously. The aerospace industry now has the capability to use nonlinear constitutive models of both isotropic and anisotropic metallic materials in inelastic structural analysis. This research has provided a base to further extend constitutive modeling to more complex materials such as metal matrices. As a result of the HOST Project NASA Lewis Research Center has become an important center, worldwide, for constitutive modeling. HOST has not only introduced constitutive modeling to engine companies, it has resulted in a closer working relationship between them and academia.

Combustor aerothermal modeling. Research had been conducted prior to HOST on combustor modeling aimed at predicting dilution jet airflow mixing with combustion gases. Those modeling studies were based on bulk average temperature measurements from jet mixing experiments. Such research had greatly diminished by the time of HOST initiation. In the HOST Project all four engine manufacturing companies were awarded contracts to assess the state of the art in combustor aerothermal modeling. As a result of this assessment and additional research with nonreacting flows, aerothermal modeling is much better understood and is being used throughout the aerospace industry. This is not to say, however, that all problems have been solved. The accurate prediction of combustor aerothermal performance along with prediction of wall temperature levels and gradients will require further improvement in numerical schemes with input from experimental, fully-specified reacting flow data that is not yet available. HOST was terminated before reacting gas flow and fuel swirl characterization data could be obtained. However, analytical procedures have improved to the point that one organization indicated the use of three-dimensional fluid flow analysis in the design of combustors that required a minimum of testing.

There was an almost unanimous opinion of those commenting on combustor modeling that the HOST program was long overdue, and it spearheaded the move toward an analytic capability in combustor understanding and design analysis.

Turbine heat transfer. The HOST-sponsored activities in turbine heat transfer encompassed nearly all aspects of internal and external heat transfer in turbine airfoils. Some of the research contracts and grants in the overall program included external airfoil heat transfer with and without film cooling, impingement cooling, interaction of rotor and stator in a large low speed turbine, coriolis and buoyancy effects on heat transfer in coolant passages, heat transfer with flow across a moving airfoil tip, and end wall boundary layer studies. As a result of this research correlations have been developed that have resulted in significant improvement in accuracy of calculated blade metal temperatures. Also quality experimental data sets, along with good documentation, were developed that will find widespread use by heat transfer analysts in the future. It is now possible

as a result of HOST to better control local temperatures, which in turn, result in better control of blade life and surface oxidation.

Protective coatings. Protective coatings include both thermal barrier coatings, to reduce heat transfer, and oxidation resistant coatings. Progress has been made on improving coatings and a better understanding of interactions between coatings and structural base materials. In addition, thermomechanical fatigue testing has been conducted on materials having oxidation and thermal barrier coatings. Life prediction models are being developed. A side benefit of this research was development of an awareness that designers and materials research personnel must work more closely together in improving life prediction models.

Computer codes from the HOST Project. The output from HOST was technical information in the form of research reports, experimental data sets, and computer codes. A requirement in the development of computer codes was installation and operation of the codes on one or more of the following NASA Lewis Research Center computers: Cray X-MP/2-4 with COS operating system, Amdahl 5840 with VM operating system, or VAX 11-750. This requirement was aimed at making the codes more generally available and usable. In some cases the original code development was on a more advanced computer model than the one at NASA Lewis. Modification to make the code run at NASA Lewis would have the advantage of making it workable on a wider range of computers.

In practice the above described concept has not worked as well as hoped. In some cases codes developed by one organization have been readily used by other organizations. These have generally been the simpler codes. In other cases, however, the codes from HOST have been of only limited benefit to the nondeveloper of the code. For the more complicated codes, it has been the experience of NASA personnel that it takes from 3 to 12 months to debug and become familiar with codes supplied by HOST contractors for the NASA computers. A similar period of time is expected to be needed by other users of the code even though considerable debugging was accomplished at NASA. A shortcoming with these codes is that support service cannot be provided by the developer or NASA in the manner available for commercial codes.

A comment made by one of those interviewed might solve this problem of computer code support. In future programs funding should be allocated for a commercial software company to adequately debug and document the more complicated computer codes. Further, by permitting the software company to market the code they would be in a position to provide a continuing support and updating function. In this manner codes developed could be made available and usable by interested parties over an extended period of time.

Most of those interviewed stated that without code support they could make only limited use of codes from HOST that they themselves did not develop. Some organizations did state, however, that they expected to rewrite portions of some of the codes of interest. Another interviewer stated that although a code may not be directly usable as developed by another organization, it can be rewritten in about one-half the time originally required to write the code. It also is possible to capitalize on problems that may have been experienced by the original programmer so that the rewritten code will be superior to the original.

Impact on Engine Development Process

Improved engine design capability. Both computer codes and experimental data bases developed under the HOST Project have already been of value in engine design. The impact is expected to be felt for years to come. While there are certain reservations relating to the extent of code development, the overall technology generated by HOST will continue to be useful throughout the aircraft engine industry. It is clear that the value of research that has developed both computer codes and experimental data bases has been greatest to those conducting the research, but other organizations are certainly making use of the research results to varying degrees.

Design analysis capabilities have been improved in the combustor and turbine. As a result of these capabilities less experimentation is required in development of the components. It is expected that reliability will be improved because of improvements in the prediction of temperatures and stresses from heat transfer, fluid flow, and inelastic stress analyses. At this time there has not been enough history generated to determine if HOST has resulted in reduced maintenance costs, one of the goals of the project. But it is reasonable to expect that if durability and reliability are improved, maintenance costs will be reduced.

Comments received from a number of those interviewed indicated that data bases generated from experiments in fluid flow in the combustor and turbine, turbine heat transfer, and thermomechanical fatigue will be at least as important to analysts as the computer codes generated from HOST contracts. As mentioned earlier in this paper, it will probably be some time before designers are comfortable with, and will routinely use, some of the advanced computer codes that have been developed in HOST.

Reduced engine development costs. Reduction in engine development costs was not one of the original goals of the HOST Project, but it has become a possible significant side benefit. The computer codes and data bases developed in HOST have improved design capabilities to the extent that less development testing is expected for new engines. However, reduced experimental test costs are counterbalanced by increased computer costs in the design analysis process. A completely clear picture has not emerged in all cases. Part of this lack of clarity results from several factors: (1) HOST has played a significant part in improving technology in engine hot sections, but it is not a sole player. Other in-house, Independent Research and Development (IR&D), and government sponsored programs are also resulting in improved technology. It is generally difficult to quantitatively define the contributions of HOST to overall improvements in technology; (2) Each new engine development program utilizes advances in technology compared to the last engine developed, often with increased complexity and/or designs to higher limits of temperature, pressure, stress, etc. This "moving target" makes comparisons of development costs with previous engines difficult; (3) Computer capabilities are constantly improving and costs to accomplish computing tasks are decreasing.

Consideration of all these factors makes it difficult to draw definitive conclusions as to whether, or how much, HOST has actually reduced engine development costs. However, the following are informed opinions that were presented by some of those interviewed:

1. Computing methods that have been developed under HOST have resulted in annual savings of several millions of dollars in reduced computer time for the required number of computer runs in engine development programs.

2. A HOST-developed computer code that transforms temperatures from the output of course-grid finite element heat transfer analyses to the input of fine-grid finite element structural analyses has reduced engineering labor by 26 man-years per year for one company.

3. Increased computer costs using three-dimensional fluid flow and inelastic stress analyses that result in more refined designs are just about balanced by reduced experimental testing costs for these designs at the present time. But the analytical costs are dropping rapidly, so cost savings are expected soon.

4. It is estimated that if development of new engines had to use 1975 vintage design and testing technology, the cost of engine development would be approximately three times as high as presently experienced when using advanced technology in which HOST has been a significant contributor. The overall savings are measured in billions of dollars.

5. It is reasonable to expect that improved predictive capability in engine design can reduce testing requirements. If this improvement can eliminate just one design or test-build iteration during a development or demonstrator program, savings of $250,000 or more can be reasonably claimed. Moreover, the cost savings by eliminating one service-revealed deficiency could be an order of magnitude greater.

From the above comments it is obvious that in some cases hard numbers can be generated for cost savings resulting from HOST. In other cases savings can be inferred but not necessarily firmly documented. However, engine manufacturing company personnel comments which relate to engine development cost reductions and savings resulting from reducing service-revealed deficiencies provide reasonable certainty that projected savings arising from HOST-generated technology will be orders of magnitude greater than the cost of the project itself.

Impact on Technology Transfer

Approximately 250 technical research reports have been written in the HOST Project and numerous computer codes have been generated. In addition six annual major workshops were held as well as a number of mini-workshops devoted to a single area of research. Because of the large attendance of 250 to 300 at each annual workshop, which had both formal presentations and informal discussions, there was a maximum opportunity for information exchange and technology transfer. Since representatives from all large U.S. engine manufacturers, as well as many from academia, research institutes, and government, attended these workshops, there was probably a better transfer of technology than from any other NASA-sponsored aircraft engine research or development project.

There was a unanimous opinion of those interviewed that the two-day workshops were highly successful. Not only were the presentations useful, but the informal discussions that occurred during breaks in the presentations and during the evening after the presentations were deemed extremely beneficial. Some comments made by those interviewed include:

1. "There hasn't been another forum in the U.S. to compare to the HOST Annual Workshops that has brought together the right mix of people to discuss research of common interest."

2. "Workshops provide an annual update in the thinking and planning by both NASA and industry. This once-a-year contact between industry and academia is of great value."

3. "The casual conversations with other participants that take place at the coffee breaks are of such significant benefit that NASA should consider increasing the number of coffee breaks and providing more informal get-togethers."

4. "HOST workshops have provided an excellent forum for probing discussions and the "give and take" necessary to generate useful knowledge and understanding for all participants of the advantages and disadvantages of various approaches. These discussions have aided companies to evaluate the directions of their own research."

5. "The workshops are useful in providing and developing relationships with peers from other organizations, including NASA."

6. "The HOST workshops are extremely effective because the technical community is better represented than at society meetings."

From the above sampling of comments it is evident that one of the big strengths of the HOST Project was not only the research and technology generated, but the timely dissemination of this information through formal presentations and informal discussions in the workshops.

Impact on Industry-University-Government Partnership

Improved relationships. There was a consensus that the HOST Project, largely through the workshops, substantially improved relationships of personnel in industry, academia, and government. The program also provided opportunities for university professors to work directly with engine manufacturers. This arrangement was a double barrelled benefit; the companies were able to capitalize on present and previous university research, and the professors developed a better understanding of the environment and problems of engine manufacturers which they could pass on to their students.

One university professor stated that he, along with others, had held discussions for a number of years on how to get better interaction between industry and universities. He then said, "HOST did it!" As a result, he feels that companies and universities are now working together better.

Although most of those interviewed emphasized the improved relations between industry and universities, several also commented that the HOST program improved their relationship with NASA. In addition several were very complementary about the NASA organization and management of the HOST program. They felt that the program was well conceived, and the NASA managers were both knowledgeable and helpful in overcoming problems that developed during the course of investigations.

Enthusiasm of participants. Essentially everyone interviewed showed enthusiasm for the HOST Project, but the degree of enthusiasm differed both by

organization and individual. Among the larger organizations there appeared to be a general correlation between enthusiasm and the degree of participation (number of contracts) in HOST. There is some indication that the organizational enthusiasm also may be significantly influenced by the degree of enthusiasm of the HOST coordinator for that organization. It has been indicated by NASA personnel that the same organizational enthusiasm was evident prior to award of contracts. It seems that enthusiasm by a leader is contagious.

It appeared that those interviewed from universities, on the average, showed a greater degree of enthusiasm than those from industry, possibly because university personnel less often have the opportunity to be involved with a project of the magnitude of HOST. Other reasons for their enthusiam were expressed in their interviews. For some it was the first opportunity for the results of their research to be used directly by an industrial concern. To find that what you are doing is useful to a large organization certainly can be exhilarating. HOST also permitted some researchers from universities to depart somewhat from their more academic activities and work on real problems relevant to industrial concerns. This type of work and interaction with engine manufacturers has the added benefit of bringing "the real world" into the classroom to guide students in the directions of problems presently facing at least one segment of the industrial world. Another benefit included guiding some graduate students towards employment in the aircraft engine industry because of this exposure.

A factor influencing the enthusiasm of university professors has been the workshops. At these annual meetings there has been opportunity for interaction with appropriate quality and quantity of industrial personnel. For some this has been a new experience. Previous relations with industrial personnel had been on a more limited basis to a few people they have met at society meetings, or to a few engineers in an industry where they have had a contract. Generally, they never have had the opportunity to interact with so many quality people from industry having interests similar to theirs.

Considerations for Future Contract Efforts

Although most comments received in the interviews were favorable on how the HOST Project was conducted and on the results obtained, some comments received could possibly provide some improvements relative to HOST in future contract efforts.

An often expressed comment from those interviewed concerned the earlier-than-expected termination of the HOST Project because of NASA budgetary considerations. Because of this early termination some programs were not able to be completed. The main concerns expressed were (1) experimental verification of computer codes is incomplete, and (2) reaction kinetics was not investigated in the combustor aerothermal modeling programs as originally planned. At this time it is uncertain when this added research can be completed. It may take years before funds are available to conduct the research. It would certainly be beneficial in future programming efforts to try to avoid early termination of successful projects.

As mentioned earlier, concern was expressed by some of the nonparticipants in instrumentation research. This research was deemed to be of little value to those except for the developer because the instruments developed were not available for purchase. Consideration should be given in program planning to evaluate the probable benefits to all participants or to encourage third-party manufacturing of such developing technology.

The following comments expressed by only one or two individuals may not be a consensus of those interviewed, but many have merit and require consideration for future contract efforts:

1. Rather than fund so many research areas as in HOST, fewer areas should be more generously funded.

2. HOST was worthwhile, but from the company standpoint the benefit would have been greater with a hardware-oriented program that would have resulted in an advanced engine that could be marketed. (It should be pointed out that this was a minority comment. Many more of those interviewed stressed the value of a research-oriented program.)

3. More funds should have been made available in HOST for technology transfer from the organization doing the research to other organizations. As stated earlier in this paper, funding of an organization to provide support and updating of computer programs would be extremely beneficial.

4. Small organizations could not participate to any great extent in HOST unless they teamed with a larger organization.

5. Some contracts were awarded based upon estimated costs rather than on the organization's capabilities and expectations of producing all that was promised in the proposal.

6. Building NASA in-house facilities was overdone, particularly for thermomechanical fatigue testing.

Although not all of the above comments may be of a positive nature, there may be merit to many, and all should be given consideration.

SUMMARY OF FINDINGS

From interviews conducted with 41 industry, university, and government personnel soliciting their views on the impact of HOST the major findings can be summarized as follows:

1. There was 100 percent agreement that the HOST Project was highly successful and worthwhile.

2. The HOST approach for expending research funds was very effective. The emphasis on research rather than hardware development was viewed by several interviewed as the role NASA research centers should take to provide long lasting benefits to the aircraft industry. Having many organizations working to a common goal and many of the organizations having similar programs led to "cross fertilization" that improved the research for each organization.

3. HOST yielded advantages over traditional research and technology contracted efforts by providing a focus and acceleration to problems involving the entire hot section of engines. In addition HOST resulted in a working relationship between industry, academia, and government not previously experienced.

4. The annual workshops were a major contributor to the success of HOST. Critiques of the results presented were an aid in developing improved programs.

The information was distributed to all concerned in a more timely manner than waiting until reports were completed and distributed. The large gatherings of highly qualified research personnel from all major organizations having a common goal of improved engine reliability provided a timely interchange of information.

5. The computer codes and data bases that were generated will be useful to analysts for years to come. However, some of the larger codes may not be used by organizations which did not develop then because of lack of code support. These computer codes could have been made more useful by bringing in commercial software companies to provide code support, to keep the codes updated, and to market them for general use.

6. NASA was lauded for program concept and management. The program managers were deemed to be technically competent and helpful in overcoming problems that developed in various contracts.

7. While most of the comments on the HOST Project were favorable, comments critical of the project also may have merit and should be given consideration in future government sponsored projects.

8. A side benefit of HOST has been the potential for significantly reducing the cost of engine development using advanced design techniques developed by HOST-sponsored research.

9. The cost reductions in engine development plus savings from reducing service-revealed deficiencies (a result of better predictive capability in engine design) are projected to be orders of magnitude greater than the cost of the HOST Project.

10. At the present time there are not definitive answers to the question of whether the goals of the HOST Project of improved engine reliability and reduced maintenance costs have been met because engines have not yet been produced that utilize the improved technology resulting from HOST. There is reason to believe, however, that the superior design techniques coming from HOST research can result in better engine reliability, improved flight safety, and ultimately reduced maintenance costs.

CONCLUDING REMARKS

The HOST Project activities encompassed researchers from industry, academia, and government. Perhaps due to the size and visibility as well as the difficult technical challenges of the project, high-caliber people were involved, including leading experts in each discipline. This quality of the researchers was always apparent in the technology developed.

The approach to addressing durability challenges can include one or more of the following: higher-temperature materials, more effective cooling techniques, advanced structural design concepts, and improved design analysis tools. Because of the potential gains and perhaps because of the timely growth in computer hardware and availability, the HOST Project's approach was on improved design analysis tools. To better understand the physics involved in the development of these design analysis tools for combustors and turbines, high-quality experiments were often conducted. Early project plans included significant testing in the new High Pressure Facility at NASA Lewis Research Center. However, technical problems that limited full testing capability, limited operating funds, and a move toward less component testing at Lewis led to mothballing of the facility early in 1986. This had a significant impact on HOST, first, in greatly reducing model/code verification testing and, second, in reducing immediate use of HOST-developed instrumentation for hot section research.

Most research results from HOST were generic. They were applied to both large and small turbine engines. In addition certain codes were used outside of the HOST Project for durability improvements in the Space Shuttle Main Engine as well as design analysis of an advanced communications technology satellite. There are, however, unique durability challenges in small turbine engines which could not be addressed in HOST because of funding constraints. These challenges include higher turbine blade attachment stresses, faster thermal transients, and different materials. Such challenges in today's small engines are believed to be the challenges in tomorrow's large engines.

Experience has shown that, in general, development of new design analysis tools is followed by slow user acceptance. This slow acceptance has appeared in some aspects of the HOST Project. Sometimes acceptance time is reduced during a crisis, such as in-service engine problems.

While a return on the investment in HOST has already been realized, additional return lies in the future as analysts use HOST codes more, and as such codes are used as the basis for developing new codes for design analysis applicable to high-temperature composite and structural ceramic materials. Technology development for these materials was outside the scope of the HOST Project.

NASA
National Aeronautics and Space Administration

Report Documentation Page

1. Report No.	2. Government Accession No.	3. Recipient's Catalog No.
NASA TM-4087		

4. Title and Subtitle	5. Report Date
Toward Improved Durability in Advanced Aircraft Engine Hot Sections	April 1989
	6. Performing Organization Code

7. Author(s)	8. Performing Organization Report No.
D. E. Sokolowski, Editor	E-4468
	10. Work Unit No. 505-63-1B

9. Performing Organization Name and Address	11. Contract or Grant No.
National Aeronautics and Space Administration Lewis Research Center Cleveland, Ohio 44135-3191	
	13. Type of Report and Period Covered: Technical Memorandum

12. Sponsoring Agency Name and Address	14. Sponsoring Agency Code
National Aeronautics and Space Administration Washington, D.C. 20546-0001	

15. Supplementary Notes

Also printed as a compilation of papers presented at the 33rd ASME International Gas Turbine and Aeroengine Congress and Exposition, Amsterdam, The Netherlands, June 5-9, 1988 (IGTI—Vol. 2).

16. Abstract

Advanced aircraft turbine engine durability needs were addressed in the NASA sponsored Hot Section Technology (HOST) Project. The seven year project, which was concluded in late 1987, involved representatives from six engineering disciplines who were spread across three work sectors. To address more fully the technology needs resulting from durability challenges, the NASA Lewis Research Center encouraged researchers from the disciplines of instrumentation, combustion, turbine heat transfer, structural analysis, fatigue and fracture, and surface protection to work together, and prompted both basic and applications-oriented research within each of the six disciplines. This involved scientists and engineers from three work sectors: academia, where significant basic research usually is performed; industry, where research as well as applications work is addressed; and NASA, which supports both basic and applications research and has the resources to link the other two sectors. Research results from the HOST project have been reported in approximately 250 technical reports. The ASME 33rd International Gas Turbine and Aeroengine Congress and Exposition, conducted in June 1988, provided a timely and most appropriate forum in which to summarize such research results. The one-day session entitled "Toward Improved Durability in Advanced Aircraft Engine Hot Sections" and this volume of the session's papers is the result.

17. Key Words (Suggested by Author(s))	18. Distribution Statement
Turbine engine; Combustor; Turbine; Durability; Instrumentation; Combustion; Heat transfer; Structural analysis; Fatigue and fracture; Thermal barrier coating	Unclassified – Unlimited Subject Category 07

19. Security Classif. (of this report)	20. Security Classif. (of this page)	21. No of pages	22. Price*
Unclassified	Unclassified	128	A07

NASA FORM 1626 OCT 86

*For sale by the National Technical Information Service, Springfield, Virginia 22161

NASA-Langley, 1989